UNCLASSIFIED
SECURITY CLASSIFICATION OF THIS PAGE

AD-A199 593

REPORT DOCUMENTATION PAGE

Form Approved
OMB No 0704-0188
Exp Date Jun 30, 1986

1a. REPORT SECURITY CLASSIFICATION: UNCLASSIFIED	1b. RESTRICTIVE MARKINGS
2a. SECURITY CLASSIFICATION AUTHORITY	3. DISTRIBUTION/AVAILABILITY OF REPORT: Approved for public release; distribution unlimited.
2b. DECLASSIFICATION/DOWNGRADING SCHEDULE	
4. PERFORMING ORGANIZATION REPORT NUMBER(S): NATICK/TR-87/042	5. MONITORING ORGANIZATION REPORT NUMBER(S)
6a. NAME OF PERFORMING ORGANIZATION: U.S. Army Natick Research, Development and Engineering Center* — 6b. OFFICE SYMBOL (If applicable): STRNC-UE	7a. NAME OF MONITORING ORGANIZATION
6c. ADDRESS (City, State, and ZIP Code): Kansas Street, Natick, MA 01760-5017	7b. ADDRESS (City, State, and ZIP Code)
8a. NAME OF FUNDING/SPONSORING ORGANIZATION — 8b. OFFICE SYMBOL (If applicable)	9. PROCUREMENT INSTRUMENT IDENTIFICATION NUMBER
8c. ADDRESS (City, State, and ZIP Code)	10. SOURCE OF FUNDING NUMBERS: PROGRAM ELEMENT NO. 62210; PROJECT NO. 1L162210D283; TASK NO. 01; WORK UNIT ACCESSION NO DA0K4250

11. TITLE (Include Security Classification)

DESIGN, FABRICATION AND TESTING OF AN AIRDROP PLATFORM UTILIZING AIRBAGS AS SHOCK ABSORBERS

12. PERSONAL AUTHOR(S)
Timothy Fredrick Patterson

13a. TYPE OF REPORT	13b. TIME COVERED	14. DATE OF REPORT (Year, Month, Day)	15. PAGE COUNT
Final	FROM Mar 84 TO May 85	1985 September	222

16. SUPPLEMENTARY NOTATION
Fr. p. 1
* Formerly known as the U.S. Army Natick Research and Development Center (NRDC)

17. COSATI CODES			18. SUBJECT TERMS (Continue on reverse if necessary and identify by block number)
FIELD	GROUP	SUB-GROUP	AIRDROP PLATFORM, IMPACT SHOCK, ENERGY DISSIPATION, AERIAL DELIVERY, AIR DROP OPERATIONS, GROUND SHOCK, LANDING IMPACT, AIRBAGS, PLATFORMS, (SDW)

19. ABSTRACT (Continue on reverse if necessary and identify by block number)

This technical report was prepared as part of project no. 1L162210D283AA48. The feasibility of an airdrop platform, which utilizes airbags for impact energy dissipation is studied. A computer program that was written to simulate ground impact is used to evaluate potential platform configurations. The goal is to limit total platform accelerations to less than 15G, for a ground impact occurring at 10 m/s (32.8 ft/s) horizontal velocity and 6 m/s (19.2 ft/s) vertical velocity. It is desired that the platform be reusable.

Based on the results of a computer study, the most promising design was fabricated and tested. Twenty-six test drops were conducted with a simulated payload and impact velocities ranging from 0 m/s horizontal and 3 m/s vertical to 10 m/s horizontal and 6 m/s vertical. Platform accelerations, airbag pressures and various other parameters were

20. DISTRIBUTION/AVAILABILITY OF ABSTRACT: ☒ UNCLASSIFIED/UNLIMITED ☐ SAME AS RPT. ☐ DTIC USERS	21. ABSTRACT SECURITY CLASSIFICATION: UNCLASSIFIED
22a. NAME OF RESPONSIBLE INDIVIDUAL: Timothy Fredrick Patterson	22b. TELEPHONE (Include Area Code): (617) 651-5264 — 22c. OFFICE SYMBOL: STRNC-UE

DD FORM 1473, 84 MAR — 83 APR edition may be used until exhausted. All other editions are obsolete.

SECURITY CLASSIFICATION OF THIS PAGE
UNCLASSIFIED

19. ABSTRACT (cont'd)

recorded versus time; high speed motion picture coverage was provided for selected drops. Ground impact conditions increased in severity as the test progressed. The platform was not damaged. Peak vertical accelerations were generally under 10G, but during a small number of maximum velocity drops, impact accelerations exceeded 10G; these drops are discussed in detail. The accuracy of the computer simulation as compared to the experimental results and the suitability of the platform for airdrop are also discussed. The computer simulation accurately predicted the times at which the acceleration peaks occurred, but did not always accurately predict the magnitudes.

PREFACE

The present system of airdropping military vehicles and equipment utilizes a standard parachute canopy. Paper honeycomb is used to mitigate ground impact shock. This system has a number of drawbacks. A proposed system consisting of a gliding parachute canopy and an airbag landing platform has the potential to replace the current system for some applications. In order to investigate the feasibility of utilizing an airbag landing platform with a gliding parachute canopy, a prototype airbag landing platform was designed and built by personnel of the Aero-Mechanical Engineering Laboratory (AMEL) at the U.S. Army Natick Research and Development Center (NRDC).* The airbag landing platform was tested to determine the ability of the platform to dissipate the impact shock associated with the landing of a gliding parachute delivered payload. This project served both to provide necessary information to the U.S. Army on the performance of airbag landing platforms, under Project No. 1L162210D283AA048, and as the subject of a Master's thesis submitted to Northeastern University, Boston, Massachusetts.

The author wishes to acknowledge the invaluable advice and assistance offered by William Nykvist of AMEL, NRDC; Thomas Goodrick of AMEL, NRDC; and Dr. John Dunn of Northeastern University; the drafting work done by James Fairneny, and the computer graphing routines done by Mike Johnson, both Northeastern University co-op students working at NRDC. The author also wishes to acknowledge the test work done by the

*AMEL and NRDC have recently been renamed Aero-Mechanical Engineering Directorate (AMED) and Natick Research, Development and Engineering Center (NRDEC), respectively.

Experimental Analysis and Design Division of AMEL, NRDC. The skilled efforts of John Doucette, John Lanza, Richard Erickson, and Mike Ferriera in gathering the test data that is the foundation of this report, are appreciated as well as the incredibly patient and expert word processing work done by June Hanlon and Joyce Koshivas of the Engineering Technology Division, AMEL, NRDC.

TABLE OF CONTENTS

TABLE OF CONTENTS (Cont.)

LIST OF FIGURES

LIST OF FIGURES (Cont.)

LIST OF FIGURES (Cont.)

LIST OF FIGURES (Cont.)

LIST OF TABLES

DESIGN, FABRICATION, AND TESTING OF AN AIRDROP PLATFORM UTILIZING AIRBAGS AS SHOCK ABSORBERS

INTRODUCTION

The subject of this paper is an airdrop platform being developed at the US Army Natick Research, Development and Engineering Center in Natick, Massachusetts. The platform is a prototype, utilizing airbags for ground impact energy dissipation. The prototype was developed to assess the feasibility of using the proposed arrangement to cushion the impact of gliding parachute delivered cargos. The platform will be referred to as the Airbag Gliding Airdrop Reusable Platform (AGARP).

The prototype airdrop platform consists of four cylindrical airbags sandwiched between upper and lower plates.* The ends of the airbags are fastened to the plates ~~as shown~~ in Fig. 1. Air from the bags is exhausted through orifice holes which are an integral part at the lower plate. Foam cushions, referred to as bump stops, are mounted on the upper surface of the lower plate. Motion of one plate with respect to the other is constrained by a number of straps.

The platform is part of an airdrop landing system which consists of a large gliding parachute canopy, a guidance package, a servo mechanism, and the airbag platform. The platform is suspended beneath the parachute canopy. The canopy is steerable and the guidance package and servo-mechanism are used for the active control of the canopy flight.

The airbag landing system is intended to be deployed from an aircraft some distance from its intended landing point and with sufficient altitude to glide to that point. Because of the difficulty in determining the exact

*The term "plate" is used as a convenience; the construction of the two plates is more elaborate than the name implies.

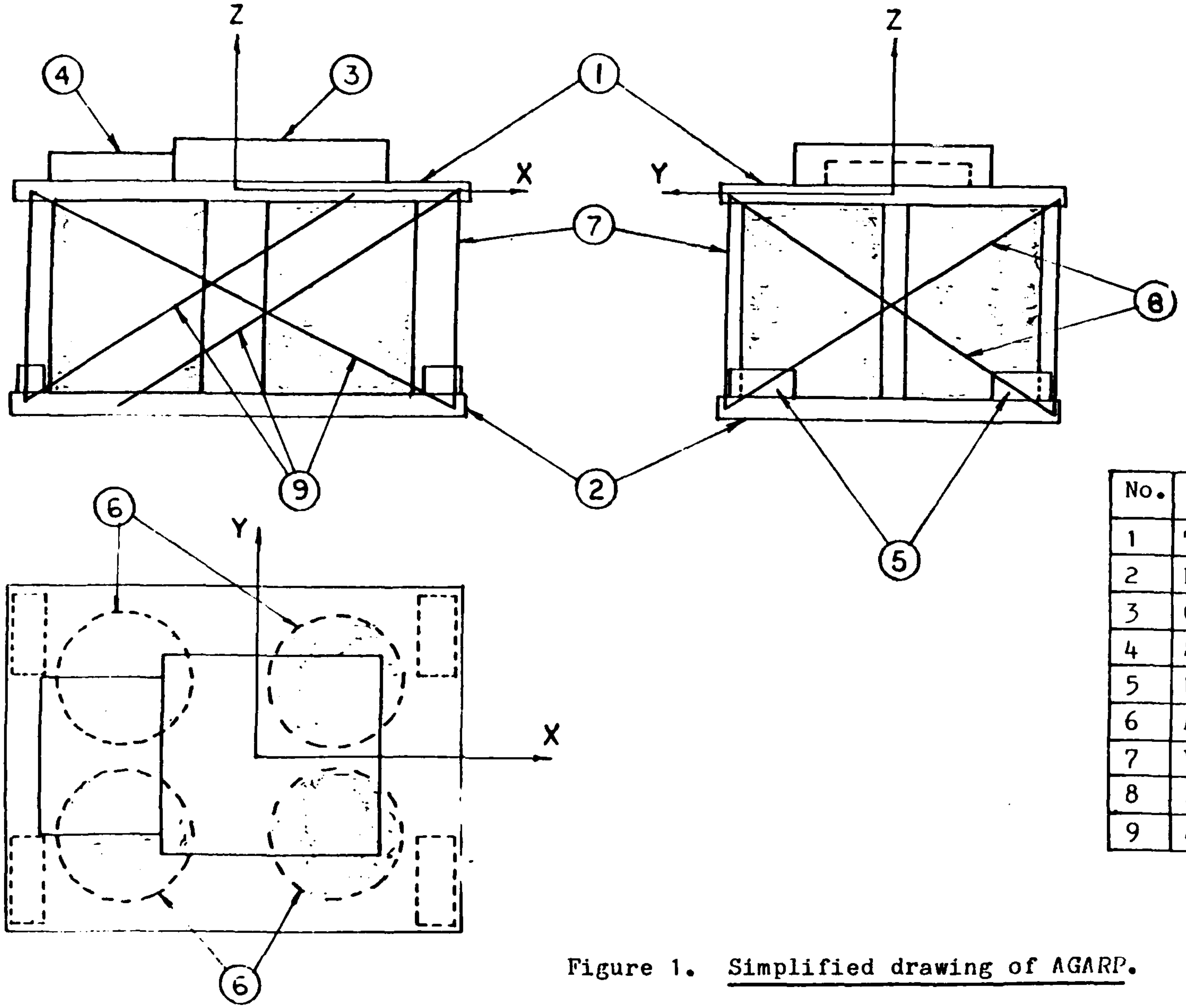

No.	Part
1	Top Plate
2	Bottom Plate
3	Guidance Package
4	Servo Mechanism
5	Bump Stop
6	Airbag
7	Vertical Strap
8	End Diagonal Strap
9	Side Diagonal Strap

Figure 1. Simplified drawing of AGARP.

moment of ground impact, flaring the canopy just prior to impact, to reduce the impact velocities, is impractical. Consequently, it must be expected that impact will occur while the canopy is moving at its maximum flying speed, which is approximately 10 m/s (32.8 ft/s) forward velocity and 6 m/s (19.7 ft/s) vertical velocity.

The primary objective of the AGARP is to protect the payload, the guidance package, and the servo-mechanism during landing. It is necessary that the platform dissipate, in a controlled manner, the kinetic energy of a landing occurring at the maximum canopy flying speed. The airbag platform studied dissipates energy through airbag crush, through friction with the ground, and through bump stop deflection. The bump stops are positioned to prevent the upper plate from hitting the lower plate. The goal was to develop a system that satisfies the following requirements:

(1) payload accelerations must not exceed 15 G
(2) the relative displacement of one plate with respect to the other must be limited to avoid damaging the airbags
(3) strap forces that tend to compress the airbags must be limited to avoid excessively high airbag crush rates
(4) the forces applied by the straps at any one point must be limited to avoid damaging the platform.

Presently, paper honeycomb is used to cushion the impact of airdropped payloads. The paper honeycomb is crushed during impact and discarded afterwards. Rigging and derigging of the payload is a complicated process as the payload must be hoisted up onto carefully positioned stacks of paper honeycomb. All cargo airdrop systems currently in use utilize

conventional parachute canopies and are not capable of being controlled in flight. The airbag landing system, of which the AGARP is an integral part, incorporates capabilities that present systems do not possess. These capabilities are:

(1) vehicle roll-on/roll-off capability

(2) greatly simplified rigging and derigging

(3) reusable

(4) low c.g. in the aircraft -- airbags are folded

(5) unaffected by moisture or rain.

The prototype configuration was established as follows: First a computer program was developed to simulate ground impact of the airbag platform. This computer program was used to study various platform configurations for a variety of impact conditions. Input parameters were further varied in an attempt to determine the best possible combination of platform components. Based on the results of this study, the AGARP was then designed, built and tested under conditions as close as possible to those expected in actual use.

This paper details the above procedures, presents an analysis of the test results, and draws conclusions from those results.

COMPUTER PROGRAM- LAND3

The first step in developing the AGARP was to develop a computer program to simulate the platform's ground impact. Simple models for each of the platform's major elements (i.e. plates, straps, airbags, and bump stops) were devised. The intent was to resort to more complicated representations only if the simple ones proved inadequate. The

program's intended use was as a design tool; it was therefore made as flexible as possible. A large number of parameters, both system physical characteristics, as well as initial impact conditions, were included in the program as input variables (see Appendix A). In its final form the program was called LAND3.

The starting point for the development of the program was a similar type of program written by Thomas Goodrick of the U.S. Army Natick Research, Development and Engineering Center.[1] Goodrick's program simulates the six degree of freedom (6 DOF) motion of a single plate having up to 14 legs attached to its sides. A simple diagram is shown in Fig. 2. This system impacts on a rigid surface. The plate is modeled as a rigid body and the legs are modeled as damped springs. A modified representation of this system was utilized to simulate contact between the ground and the bottom plate of the airbag platform.

Other elements of Goodrick's program that were retained intact or with modifications for use in LAND3 included:

a. method of displaying line drawings of the system

b. method of displaying output parameters in a graphical format

c. method of calculating ground friction and reaction forces

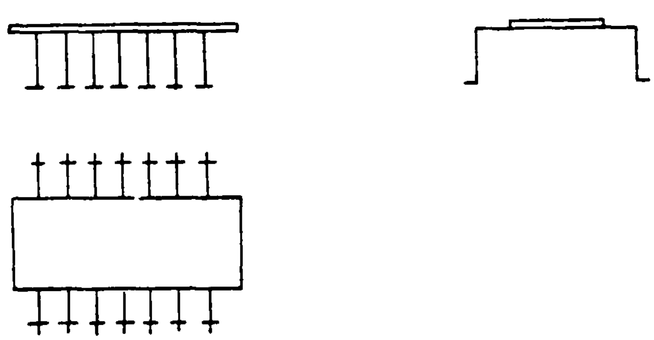

Figure 2. Goodrick's multi-legged lander.

d. direction cosine calculations

e. calculation of Euler angles and method of resolution of rotational motion (angles are calculated twice and the results averaged, lines 1150-1168 and 1200-1218 of LAND3, see Appendix B).

f. method of calculating new positions and velocities based on accelerations caused by applied forces.

Although the two systems have considerable differences, Goodrick's program served as an invaluable guide in writing the new program.

The airbag landing platform program, LAND3, can accommodate a variety of different platform configurations. Platforms consisting of two to eight airbags, up to sixteen straps, and four bump stops can be simulated by the program. One configuration with four airbags and fourteen straps is shown in Fig. 3.

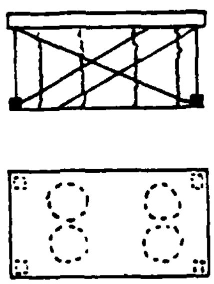

Figure 3. One possible LAND3 simulated platform configuration.

A listing of the program and an explanation of both the input and output variables are given in Appendices A, B, and C. A general description of how each system component is modeled and how the components interact is given below. Fig. 4 illustrates the description.

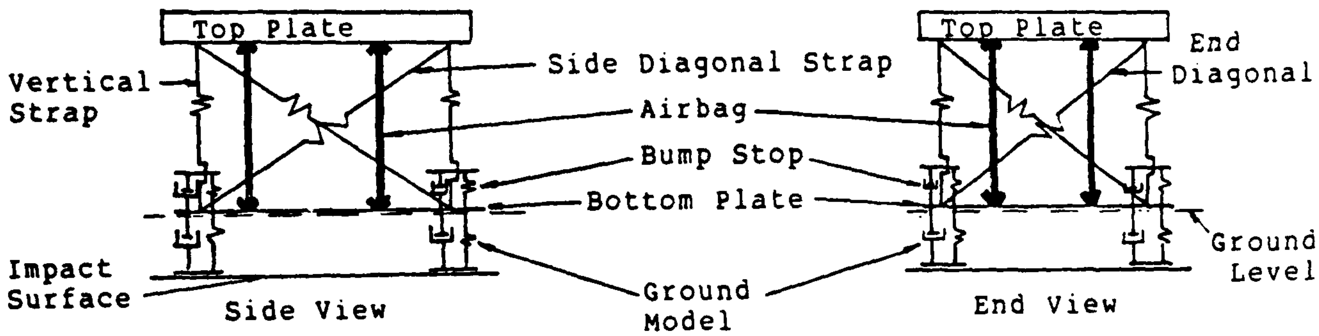

Figure 4. Schematic representation of platform component models used in LAND3.

Component	Model
Top plate	Modeled as a rigid body. The plate's thickness, width, length, mass, and mass moments of inertia are all input variables. A payload can be included in the upper plate by combining the masses and moments of inertia of the payload and the plate. The plate is free to move in the X, Y, and Z directions, as well as roll, pitch, and yaw (6 DOF).
Bottom plate	Modeled as a rigid body. The plate's width, length, mass, and mass moments of inertia are all input variables. In the simulation the plate is treated as a plate of zero thickness for ease of handling [coordinate system transformations are greatly simplified]; the plate is free to move in the X, Y, and Z directions as well as roll, pitch, and yaw (6 DOF). Bottom plate motion is specified independently of the top plate motion.
Straps	There are three types of straps, all are modeled as springs, although there is a provision in the program for modeling them as damped springs. The end points of the springs are attached between the upper and lower plate. The 4 end diagonal straps (2 at each end of the platform) and the 4 vertical straps (1 at each corner) are standard. Near the corners of each plate is a single point—the attachment point for the vertical and end diagonal straps terminating at that corner. The exact positions of the end points are specified by input variables. The side diagonal straps are optional. There can be zero to four straps per side. The points to which the ends of these straps are attached are also specified by input variables. Stiffnesses of the straps are specified by input variables.

Bump stops	Modeled as damped springs. The bump stops are attached to points on the upper surface of the bottom plate. The attachment points are the same as those used for the end diagonal and vertical straps. The initial height of the bump stops is an input variable. Bump stop compression is calculated by comparing the distance between the attachment points of the vertical straps to the initial height of the bump stops.
Airbags	Modeled according to equations developed by A. C. Browning.[2] Performance is a function of bag height, bag diameter, orifice diameter (input variables) and airbag compression rate. Airbags are arranged in pairs with uniform separation between them. It is assumed the airbags maintain a cylindrical shape at all times. The points at the centers of either end of the bags are used for height and compression rate calculations and are also the points at which forces are applied.
Ground	Modeled as damped springs, which are attached to the four corners of the bottom plate. Ground slide is accommodated by having the springs act against a rigid unmoving impact surface. The impact surface is defined as being below the level of the ground. In this way the spring damper combination does not begin to act until the bottom plate reaches the level of the ground. The points these spring damper combinations are attached to are the same as the end points of the vertical straps. Stiffness and damping coefficients are input variables. Both the ground and the bump stops exert friction forces when they come into contact with either the impact surface or the upper plate. The friction coefficients are specified by input variables. The frictional force is based on the normal forces exerted at the appropriate spring-damper combination.

The two main components of the simulation are the top and bottom plates. On each plate are a number of fixed points to which the other platform components are attached. Three coordinate systems are used to keep track of the motions of the two plates and the attachment points. The first coordinate system is an inertial coordinate system. The origin of this system is positioned at "ground level". The Z-axis is perpendicular to

the "ground", with the positive direction being upward. The X and Y axes are in the plane of the ground. The other two coordinate systems are body axis coordinate systems. One of these coordinate systems has its origin located at the c.g. of the top plate. The Z-axis of this system is perpendicular to the upper surface of the plate, with the positive Z-direction being upward. The X and Y axes are in the plane of the plate, with the positive X-direction being towards the front of the plate. The other body axis coordinate system has its origin located at the c.g. of the bottom plate. The Z-axis of this system is perpendicular to the upper surface of the plate, with positive Z-direction being upward. The X and Y axes are in the plane of the plate, with the positive X-direction being towards the front of the plate. Direction cosines are used to convert displacements, velocities, and forces from one coordinate system to another. Direction cosines are based on the orientation of the plates relative to the inertial system and are continuously recalculated.

The computer program, LAND3, was not written using structured programming techniques. However, the flow of the program does proceed in a logical manner. A general description is given below.

In the first program step the user is asked to define the physical parameters of the platform configuration to be simulated. This is done by choosing appropriate values for the input parameters that specify the platform's physical characteristics. Input parameters are listed in Appendix A. At the beginning of the simulation, it is assumed that the airbags are fully extended, the straps connecting the two plates are not slack, and that the top and bottom plates are parallel to each other.

The next step involves defining the initial conditions for the computer run. Standard practice was to use those conditions which would exist just prior to ground impact. Input variables are used to specify the position (X, Y, Z), velocity (X, Y, Z directions), orientation (roll, pitch, yaw) and angular rates (roll rate, pitch rate, yaw rate) of the top plate c.g. relative to the inertial coordinate system. After these parameters are specified, the position, velocity, orientation, and angular rates of the bottom plate c.g. are calculated, and the two moving coordinate systems are initialized.

Once the above steps have been completed, the program asks the user to specify the number of iteration cycles to be performed, the Δt to be used for iteration cycle, the format of the line drawings, and the variables that will be output at the end of the program. These are the last of the input variables.

A series of calculations are then made, the results of which are used to display a pictorial line drawing of the platform. The program periodically returns to this program step. Thus, platform pictorials are generated at equal time intervals during the course of the computer run, allowing the motion of the platform to be observed.

The iteration cycle follows the above-mentioned display calculations. The first step in this cycle is the determination of the position and velocity of each plate relative to the inertial coordinate system. The next step is to calculate the position and velocity of the attachment points on each plate relative to one another and relative to the ground. These values are used to determine strap stretch, airbag height, airbag compression, bump stop deflection, bump stop

deflection rate, ground deflection, and ground deflection rate. The resulting forces are calculated and then converted to the moving coordinate system of the affected plate. Individual forces and resultant moments are summed and the total is converted back to the inertial coordinate system. By using the inertia properties of the plates, the linear and angular accelerations are determined. The new positions, orientations, velocities, and angular rates of each plate and the corresponding component attachment points are calculated using these accelerations and the previously specified Δt. After each pass through the iteration cycle, control is transferred to the beginning of the cycle, the direction cosines are recalculated, and the cycle is restarted. Every time a prespecified number of iterations have been completed, control is transferred to the program step that does the calculations for the platform pictorials. When the drawings are complete, control returns to the iteration cycle. This process continues until the total number iterations specified by input variable have been completed. A listing of the FORTRAN statements comprising the LAND3 Program is shown in Appendix B.

When the iteration process is complete, various parameters are made available for output. The output is in graphical form, with each parameter plotted vs time. As many parameters as desired can be plotted on one graph. There are 98 that can be selected for output; all are listed in Appendix C.

This completes the general description of the workings of the airbag landing simulation program, LAND3. In the following section, the method by which the program was used to find a satisfactory system configuration will be discussed.

COMPUTER STUDY

A study of various airbag landing platform configurations was made using the computer program LAND3. The objective of the study was to find the arrangement of platform elements that best satisfied the stated performance requirements. This configuration would then be used as a guide in designing the actual platform.

Procedures

At the beginning of the computer study, the materials to be used in the construction of the platform were unknown. Therefore, an iterative process was used to arrive at a satisfactory platform configuration. Initially, typical values were assumed for the properties and/or dimensions of each platform element. The values were selected to be representative of possible construction materials. The computer program, LAND3 was then run using various "worst case" impact conditions. The resultant forces exerted on or by each of the platform components were recorded as output variables from the program. Given these resultant forces, the properties and/or dimensions of individual components were modified to correct for any deficiencies in the platform performance. The modified properties were then incorporated into the appropriate component model and the computer program rerun using the same "worst case" impact conditions. Further modifications were made as required. Attention was focused on one component at a

time. The study continued until a satisfactory configuration was determined.

Limitations

The computer study was limited in scope by a numer of factors. Available time, available construction materials, and acceptable platform size and weight all combined to restrict the study to a reasonable size. The specific limitations imposed and their effect on the study are outlined below.

Testing of the completed platform was scheduled for the fall of 1984. This time frame was selected to avoid the problems of testing outdoors during the winter months. Construction of the platform had to be completed by early fall to meet this schedule. This time limit, as well as procurement restrictions, dictated that only easily available materials or those materials already at Natick RD&E Center be considered as possible materials for platform construction.

Restrictions on the overall size and weight of the AGARP placed additional limitations on the extent of the computer study. If the platform proved successful it was to be used in actual airdrops to test the guidance package, servo-mechanism and the performance of a prototype gliding parachute. The weight of the AGARP was limited to about 273 kg (600 lb) by the maximum load limitations of the prototype parachute. During the test drops the guidance package and servo-mechanism were to be the only payloads mounted on the platform. Given the known sizes and weights of the guidance package and servo-mechanism, and a desire to keep the AGARP about half the size of the standard 2.7 m x 3.6 m (9-ft x 12-ft) platform; a platform size of 1.22 m x 1.82 m (4 ft x 6 ft) was chosen.

The computer study was not required to address the question of platform size (a detailed description of the final AGARP configuration is given in the CONSTRUCTION section of this paper).

The determination of the overall dimensions of the two plates imposed limitations on the diameter and number of airbags that could be used. According to A. C. Browning[3] and Tomcsak,[4] when using airbags as decelerators, the ideal is to use large diameter bags and to use as many of them as possible. Using large diameter airbags gives the optimum load distribution. Using a large number of airbags results in the most stable configuration. These are conflicting goals given the limited plate size. Therefore, a compromise configuration of four airbags with a diameter of 0.483 m (19 in) was chosen. Airbags with a larger diameter could not be used because allowance had to be made for attaching the airbags to the plates, folding of the crushed airbags and for orifice holes. Limiting the airbag diameter placed further limitations on the extent of the computer study. The study need only to evaluate variations in airbag height and orifice size when determining the most satisfactory airbag configuration.

Results

The platform elements evaluated during the computer study were: the geometry and material properties of the restraining straps, the height of the airbags, the size of the airbag orifices, and the properties of the bump stops. The characteristics of these components were major factors in determining the performance of the platform.

One additional factor affecting platform performance was the ground. The properties of the ground were kept constant throughout the computer study. In the real world the properties of the ground

vary considerably from place to place. The methods used to characterize the response of the ground to impact or to dynamic loading are not always simple or extremely accurate (see M. G. Bekker).[5] However, the exact nature of the ground response is masked by properly functioning airbags. Therefore, all that is required of the simulated ground force is that it stop the vertical motion of the bottom plate in a short distance. A one-inch ground deflection resulting from a maximum vertical velocity platform impact, was considered to be representative of a typical ground impact surface by Natick RD&E Center engineers.[6] The spring-damper combination used to model the ground was given the following characteristics:

spring constant	1 459 000 N/m (99973 lbf/ft)
damping coefficient	14 593 N-sec/m (999 lbf-sec/ft)

Given AGARP's mass the above values will yield proper results.

The coefficient of friction assigned to the ground has a much greater effect on platform performance than the exact characteristics of the spring-damper combination. When the study began, the bottom surface of the lower plate had not been designed. However, plywood was considered the most likely construction material. Natick RD&E Center engineers had previously determined the coefficient of friction of plywood on various surfaces; these values are shown in Table 1.[7]

TABLE 1: Friction Coefficients for Plywood*

Surface	Normal Force (N)	Friction Force (N)	Friction Coefficient
Gravel	511.5	222.4	0.435
Sand	511.5	266.8	0.522
Short Grass	511.5	329.2	0.643
Long Grass	511.5	311.4	0.609

*Source: N. Rosato, Unpublished notes on soil deformation, NRDC, 1983

A value of 0.7, which would represent one of the more severe impact conditions possible was chosen for use during the computer study. The value of 0.7 provides a significant horizontal retardation force on the bottom plate. A high horizontal retardation force causes greater displacement of one plate relative to the other and higher forces in the restraining straps. A friction coefficient which causes the lower platform to stop immediately on ground impact (i.e. similar to hitting a large rock) would be the worst case. However, during such an impact, even the best designed platform would sustain heavy damage.

The restraining straps were the first platform component evaluated using the computer program LAND3. Before evaluation of the straps began, a number of preliminary computer runs were made to determine the initial properties of the airbags and bump stops. These properties did not result in the best possible platform performance, but rather performance that was realistic for the evaluation of the restraining straps. As a result of these preliminary computer runs the following values were assigned:

Airbag Height	=	0.508 m (20 in)
Airbag Orifice Size	=	0.0054 m (8.40 in)
Airbag Diameter	=	0.483 m (19 in)
Bump Stop Height	=	0.08 m (3.15 in)
Bump Stop Spring Constant	=	729650 N/m (4997 lbf/in)
Bump Stop Damping Coefficient	=	7296 N-sec/in (499 lbf-sec/in)

Straps with breaking strengths from 100 lb to 15,000 lb were available at Natick RD&E Center. Since, a strap of almost any strength was available, the spring constant of each of the restraining straps was set up as a variable parameter. The following formula was used by the computer program to calculate the various spring constants:

$$K = \frac{(\#\ \text{Plies of strap})\ (\text{Break Strength})}{(\%\ \text{Elongation at Break})} \quad \frac{1}{(\text{Length})}$$

The assumptions involved in the formula were:

1. Spring constant decreases with increasing length.
2. The percentage elongation of a strap under a particular load is a characteristic of the strap material.

   An increase in the number of plies increases the spring constant.
4. The relation between strap load and strap elongation is linear.

Assumption number 4 was not entirely correct (see Fig. 5). However, given the alternative of attempting to model the nonlinearities of each strap or accepting the inaccuracies of a linear model, the linear model was chosen.

The selection of strap materials and geometries was based on four factors:

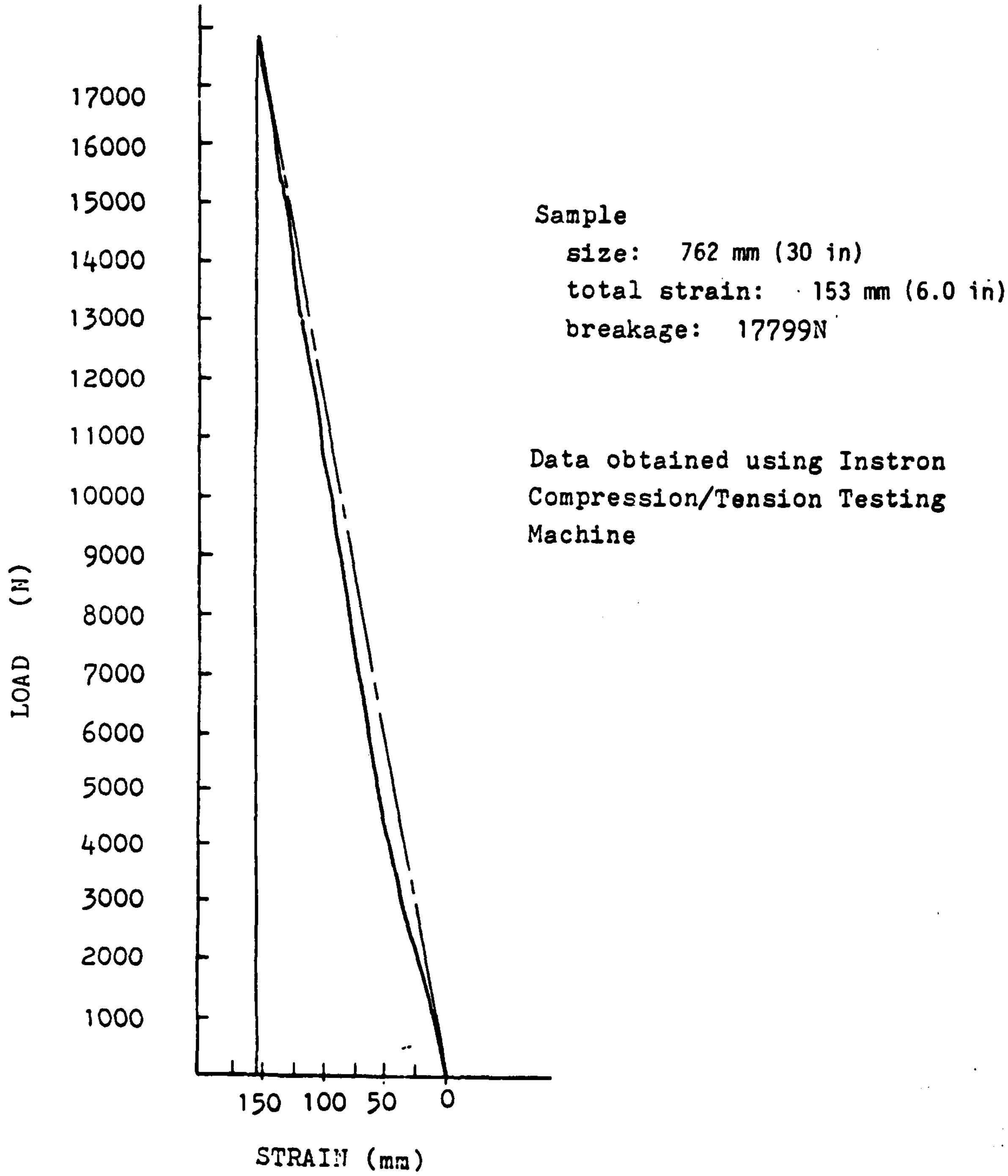

Figure 5. Sample load vs deflection curve for 2.54-cm (1-in) tubular nylon strap.

1. Forces exerted by each strap

2. Accelerations of the top plate

3. Airbag pressures

4. Displacement of one plate with respect to the other

Initially, two materials, nylon and Kevlar®,* were considered for use as restraining straps. Kevlar was eliminated as a possible strap material during the preliminary computer runs. The material is non-yielding and caused excessively high accelerations in the horizontal direction. Nylon was the only material subjected to a more extensive evaluation.

Four strap geometries were considered (see Fig. 6). Each of these geometries employed multiple straps to restrain the forward motion of the top plate. The multiple straps were used to reduce the load applied by individual straps. Preliminary computer runs had shown that when only one strap was used to restrain forward motion, that strap exerted excessively high forces. Configurations 1 and 2 were chosen to evaluate the effect of strap placement on the accelerations of the top plate. There was a trade-off to be considered. Configuration 2 would yield less relative motion (see Fig. 7), but it was not known if the more forward placement of the strap end points would cause excessive angular accelerations. Configurations 3 and 4 were included to determine if the additional side strap would improve the performance of Configurations 1 and 2.

*Product of E I du Pont de Nemours & Co.

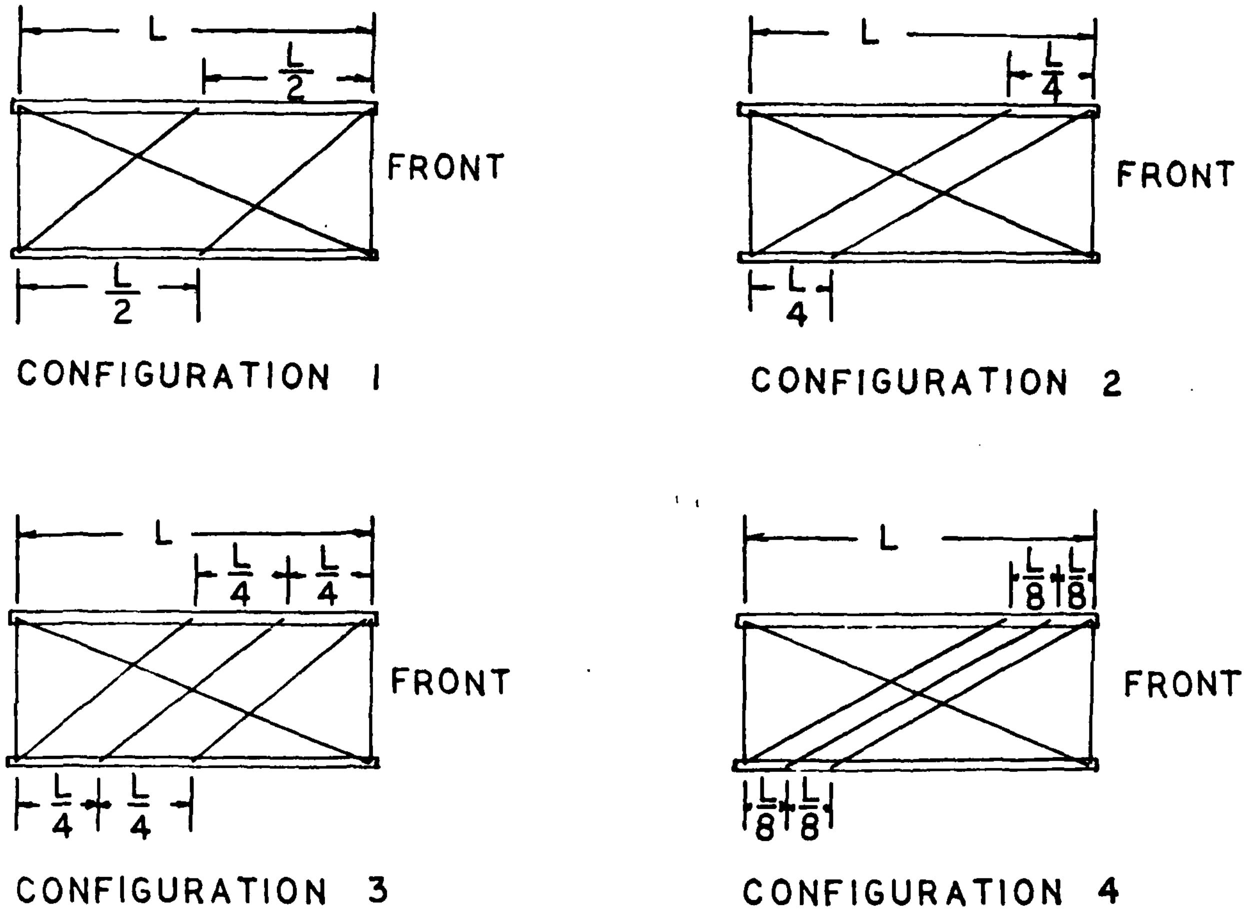

Figure 6. Four restraining strap configurations evaluated using LAND3.

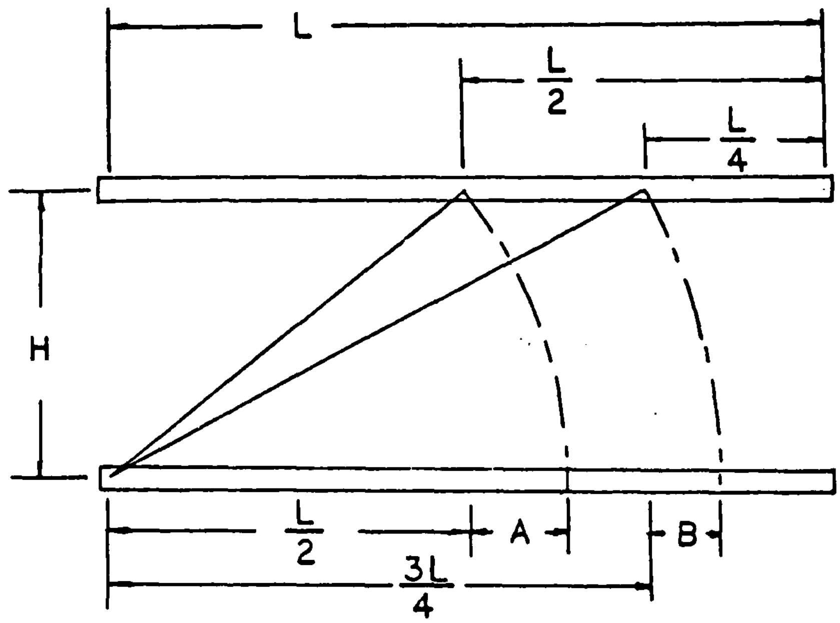

Legend:

$$A = (H^2+(L/2)^2)^{1/2}-L/2$$

$$B = (H^2+(3L/4)^2)^{1/2}-3L/4$$

Where

H = 0.609 m
L = 1.828 m
A = 0.015 m
B = 0.011 m

Figure 7. Comparison of plate motion due to restraining strap rotation.

Table 2 summarizes the results of the computer runs made to evaluate the various strap configurations. Three "worst case" impact conditions were used for the evaluation. In all cases the impact velocities were: 10 m/s (32.8 ft/s) forward, 6 m/s (19.2 ft/s) vertical, and 2.0 m/s (6.6 ft/s) to the left (port). Impact orientations are shown in Table 2. Pitch and Roll rotations of 10° were chosen because under most landing conditions a properly rigged payload will not impact with greater than 10° of rotation. The 30° yaw was chosen to simulate a sideways impact. The same strap material properties were used for all runs and proved to be strong enough in all cases.

In comparing the results for strap Configurations 1 & 2, it can be seen that Configuration 2 yielded less displacement of the top plate relative to the bottom plate, lower side strap forces, and, for the no-yaw impacts, slightly lower accelerations. The nose-up impact showed the greatest differences between the two configurations. The difference in relative motion of the plates was expected. The airbag pressures and the vertical accelerations indicated that strap Configuration 2 and strap Configuration 1 produced similar downward forces on the top plate. Strap Configuration 2 did not cause excessive vertical or angular accelerations.

Configuration 4 was evaluated to see if it was an improvement over Configuration 2. The first and only run made was the nose up impact. The outcome of this simulation run was that the strap forces were not significantly reduced, the horizontal accelerations were higher and the displacement of the plates relative to one another was less. The additional side strap had increased the total strap stiffness. Over

TABLE 2. SUMMARY OF COMPUTER RUNS MADE TO EVALUATE VARIOUS RESTRAINING STRAP CONFIGURATIONS

Run #	Strap Config.	Velocities (m/s)			Orientation (deg)*			Peak Strap Forces (KN)					Max. Relative Displacement (cm)		Max. Acceleration (G) at Top Plate c.g.			Max Airbag Gas Press (Pa 1x10^5)
		Vx	Vy	Vz	Roll	Pitch	Yaw	Side 1	Side 2/3	Side 4	End	Vert	Forward	Side	X	Y	Z	
62802	1	10	2	-6	10	-10	0	9.87	10.00/-	4.36	4.36	6.58	19.5	11.9	-17	-3.5	17	1.74
70501	1	10	2	-6	-10	10	0	5.78	6.58/-	0	4.98	3.74	16.7	11.9	-11	-3.1	12	1.25
70601	1	10	2	-6	0	0	-30	5.20	4.80/-	0	8.76	0	20.1	20.1	-9.5	-9	11	
62801	2	10	2	-6	10	-10	0	6.89	7.43/-	4.80	4.58	6.67	16.0	12.4	-12	-3	16	1.43
62902	2	10	2	-6	-10	10	0	6.00	6.09/-	0	4.80	4.00	14.5	12.4	-11	-3.3	10	1.75
62901	2	10	2	-6	0	0	-30	4.98	4.89/-	0	9.25	0	18.3	9.9	-9	-9	11	1.24
62803	4	10	2	-6	10	-10	0	6.76	6.49/6.98	5.25	3.82	6.81	12.9	10.5	-17	-3	16	1.80

*positive pitch: nose pitch down
negative pitch: nose pitch up

positive roll: roll right (starboard)
negative toll: roll left (port)

positive yaw: yaw clockwise
negative yaw: yaw counterclockwise

all, Configuration 2 had yielded more satisfactory results and additional runs were not made. The increased complication of rigging an additional strap on an actual platform was also a factor in this decision. Configuration 3 was not considered for test as the results would show an increase in horizontal accelerations similar to Configuration 4, and would yield no improvement over Configuration 1. Strap Configuration 2 was considered to have the best overall performance and was used for all future computer runs. It was eventually incorporated into the platform design.

The airbags were the next platform component to be studied using the computer program LAND3. The airbags were modeled using equations developed by A. C. Browning. Browning developed the equations using basic principles of fluid mechanics and thermodynamics. Browning's equations are shown in Appendix E.

Two groups of computer runs were made to evaluate airbag characteristics and performance. The purpose of the first group was to study only the airbags. The purpose of the second group was to study both the airbags and the bump stops. During both sets of computer runs airbag performance was evaluated by comparing the following factors:

1. Accelerations of the top plate
2. Airbag pressure
3. Peak forces exerted by the bump stops

The peak bump stop forces were used as an indication of how well the airbags dissipated the kinetic energy of the top plate.

During the first group of computer runs the initial height of the bump stops was changed to 0.1524 m (6 in), a height which better

represented the anticipated actual height. Two airbag heights were evaluated, 0.584 m (23 in) and 0.635 m (25 in). These heights allowed for 0.432 m (17 in) and 0.483 m (19 in) of airbag crush respectively (see Fig. 8). Previous computer runs used airbag and bump stop heights that allowed for slightly less than 0.432 m (17 in) of airbag crush. A number of different orifice sizes were tried with each airbag height. The results for this group of computer runs are summarized in Table 3. As can be seen from the Table, better performance was obtained from the taller airbag. Both peak bump stop forces and vertical accelerations of the top plate were lower with the 0.635 m (25-in) airbag. In two out of four cases, the 0.584 m (23-in) bag allowed the top plate to hit the bump stops at a velocity that resulted in the bump stops causing much greater decelerations than those caused by the airbags. This occurred in only one out of the six cases for the 0.635 m (25-in) bag. In that one case the accelerations caused by the bump stops were lower than in any of the 0.584-m (23-in) bag cases. Peak airbag pressures for both airbag heights were similar when the same orifice diameters were used. The larger orifice sizes resulted in higher compression rates and lower pressures.

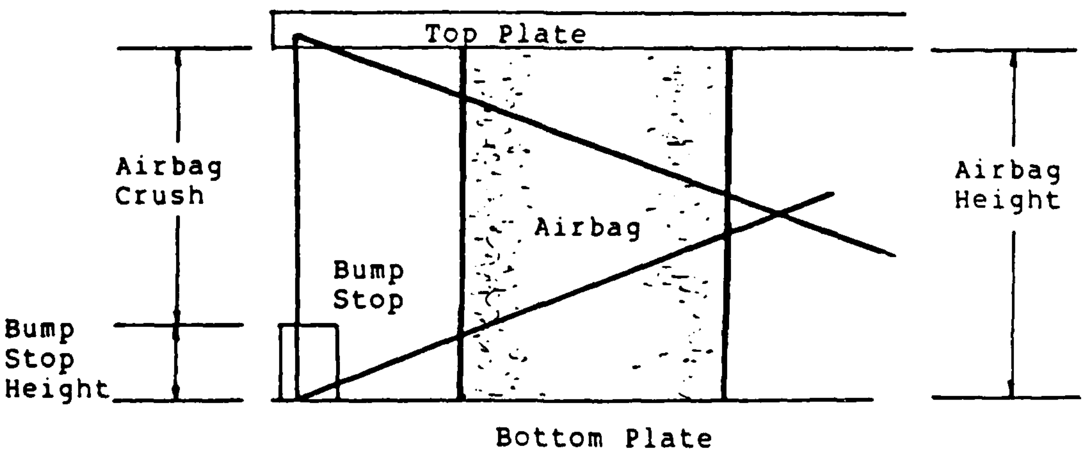

Figure 8. Amount of airbag crush as compared to airbag height.

TABLE 3. SUMMARY OF COMPUTER RUNS MADE TO EVALUATE AIRBAG HEIGHT AND ORIFICE DIAMETER

Run #	Airbag[a] Height (m)	Orifice Size (m^2)	Velocities (m/s) Vx	Vy	Vz	Orientation (deg)[b] Roll	Pitch	Yaw	Acceleration of Top Plate c.g. (G) X	Y	Z	Bump Accel. (G) Z	Max. Bump Stop Force (KN)	Max. Airbag Gage Press. (Pa 1×10^5)
71201	0.584	0.00541	10	2	-6	10	-10	0	-17	-2.6	14	-	10.34	1.56
71301	0.584	0.00541	10	2	-6	-10	10	0	-8	-3.5	10	15	12.01	1.42
71601	0.584	0.00433	10	2	-6	10	-10	0	-18	-3	15	-	10.50	1.62
71302	0.584	0.00433	10	2	-6	-10	10	0	-7.5	-3.7	11	14	9.96	1.45
71602	0.635	0.00541	10	2	-6	10	-10	0	-18	-2.5	14	-	7.78	1.56
71603	0.635	0.00541	10	2	-6	-10	10	0	-7.5	-3.5	9.7	11	11.47	1.41
71801	0.635	0.00456	10	2	-6	10	-10	0	-18	-3	15	-	11.47	1.62
71802	0.635	0.00456	10	2	-6	-10	10	0	-7.5	-4	11	-	8.50	1.44
71901	0.635	0.00483	10	2	-6	10	-10	0	-18	-2.7	15	-	9.61	1.39
71902	0.635	0.00483	10	2	-6	-10	10	0	-7.5	-3.8	10.5	-	5.52	1.43

[a] 0.584 m (23 in) airbag height - 0.432 m (17 in) airbag crushable height
0.635 m (25 in) airbag height - 0.483 m (19 in) airbag crushable height

[b] positive pitch - nose pitch down
positive roll - roll right (starboard)
positive yaw - yaw clockwise

Although, the bump stops were not the platform element being studied during the drops summarized in Table 3, some useful information was obtained. Accelerations caused by the bump-stops during these computer runs were rather high. It was thought that these accelerations could be reduced by selecting a material that was less stiff than that used in the bump-stop model during this group of computer runs. In addition to the bump-stop forces, the velocities at which the top plate hit the bump stops were also obtained from these computer runs. Using this information, a number of materials were studied to determine whether or not they were suitable for use as bump stops. Two materials, Scott 900-4 and Scott 900-8 foams, were the final candidates. Both foams possessed the required resilence and lack of permanent set (i.e. after an initial deflection, the foam quickly returned to its original shape). These two foams had been tested previously on an impact testing machine at Natick RD&E Center. Data for various impact velocities were available for both foams. The data indicated that the Scott 900-8 foam would be the best choice. The impact crush data for the Scott 900-8 foam, which most closely approximated the impact velocity of the top plate on the bump stops, was linearized and incorporated into the bump stop model. Appendix F details the selection and linearization process. The second group of computer runs utilized this modification to the bump stop model.

Table 4 summarizes the results from the second group of computer runs. This group of computer runs was made to optimize the airbag orifice size and to verify that the bump stop performance was adequate. The following factors were used to evaluate bump stop performance:

TABLE 4. SUMMARY OF COMPUTER RUNS MADE TO EVALUATE AIRBAG AND BUMP STOP CONFIGURATIONS

Run #	Airbag Height (m)[a]	Orifice Size (m^2)	Velocities (m/s) Vx	Vy	Vz	Orientation (deg)[b] Roll	Pitch	Yaw	Acceleration of Top Plate c.g. (G) X	Y	Z	Max. Bump Stop Force (KN)	Deflection (mm)	Max. Airbag Gage Press. (Pa 1×10^5)
81402	0.635	0.00541	10	2	-6	-10	10	0	- 7.5	-3.5	9.7	2.42	30.5	1.41
81301A	0.635	0.00541	10	2	-6	10	-10	0	-18	-2.5	14	2.83	37.3	1.56
81702	0.635	0.00603	10	2	-6	-10	10	0	- 7.5	-3.1	8.5	5.10	42.4	1.37
81701	0.635	0.00603	10	2	-6	10	-10	0	-17.5	-2.4	13	2.97	37.3	1.46
81401	0.635	0.00636	10	2	-6	-10	10	0	- 7.5	-3.1	8.5	5.10	42.4	1.37
81304	0.635	0.00636	10	2	6	10	-10	0	-17.5	-2.4	12	2.95	37.3	1.51
81303	0.635	0.00709	10	2	-6	-10	10	0	- 8	-3	10	9.25	61.5	1.34
81301	0.635	0.00709	10	2	-6	10	-10	0	-17	-3	11	5.05	42.4	1.46
80801	0.584	0.00483	10	2	-6	-10	10	0	- 7.5	-3.8	11	10.14	-	1.48
81001A	0.584	0.00541	10	2	-6	-10	10	0	- 7.7	-3.4	10	13.21	-	1.42
81001	0.584	0.00541	10	2	-6	10	-10	0	-17.5	-2.6	14.0	12.32	-	1.57

[a] 0.584m (23 in) airbag height - 0.432m (17 in) airbag crushable height
0.635m (25 in) airbag height - 0.483m (19 in) airbag crushable height

[b] positive pitch - nose pitch down
positive roll - roll right (starboard)
positive yaw - yaw clockwise

[c] peak caused by bump stop

1. Top plate accelerations

2. Bump stop deflection

Airbag performance was evaluated using the previously defined criteria.

The data from Table 4 indicate that the 0.635-m (25-in) airbag with the 0.00636-m^2 (9.86-in^2) area orifice provided the best performance. Using this airbag configuration and the Scott 900-8 bump stop foam model, the vertical accelerations of the top plate were kept to a reasonable level. Absorption of the top plate's kinetic energy occurred in a manner that did not require the bump stops or the airbags to exert excessive forces. If higher pressures and greater bump stop deflections are acceptable, a shorter bag with a smaller orifice could be used. This can be seen in Table 4, as shown by computer runs 80801, 81001, and 81001A.

All airbag configurations produced similar horizontal accelerations. These accelerations were higher than what was desired. It was assumed that the horizontal accelerations could be reduced by using less stiff restraining straps.

In summary, the computer study showed that the best AGARP configuration used airbags that allowed 0.483 m (19 in) of airbag crush [airbag height: 0.635 m (25 in)]; had a 0.00636-m^2 (9.86-in^2) orifice area; 0.524-m (6-in) Scott 900-8 foam bump stops; and restraining straps arranged as shown in Configuration 1 (see Fig. 6).

CONSTRUCTION

Methods

The results of the computer study were used as a guide to designing the AGARP. The AGARP is not an exact duplicate of the platform con-

figuration used during the final runs of the computer study. Real world circumstances forced compromises and modifications to be made.

The top and bottom plates of the AGARP were approximately 1.22 m x 1.82 m (4 ft x 6 ft). The top plate measured 1.14 m x 1.82 m and the bottom plate measured 1.29 m x 1.79 m. The airbags were 0.483 m (19 in) in diameter and 0.635 m (25 in) tall. Each airbag had four orifice holes for a total orifice area of 0.00713 m^2 (11.04 in^2). The airbag height allowed for 0.444 m (17.5 in) of airbag crush before bump stop contact occurred. The bump stops had a total height of 0.190 m (7.5 in). The restraining straps were arranged in a manner similar to that shown in Configuration 2 of Figure 6 (i.e. two straps on each side of the platform restraining forward motion of the top plate; one strap on each side restraining rearward motion of the top plate; one vertical strap at each of the four corners; and two diagonal straps at either end of the platform). Details of airbag construction and installation for a single airbag are shown in Fig. 9. Engineering drawings of the AGARP are shown in Fig. 10 through 17.

In constructing the platform it was required that the use of metal beneath the lower surface of the top plate be kept to an absolute minimum. If the platform successfully completed its testing, it would be used for actual airdrop tests of the parachute control system. The control system measures direction to the target using an antenna mounted in the lower surface of the top plate. Any metal between the antenna and the target will adversely affect the measurement accuracy.

The airbags were fabricated using an on-hand Neoprene coated Nylon material made by Reeves Brothers. It is a three-ply material; the outer layers are Neoprene and the interior layer is nylon fabric. The

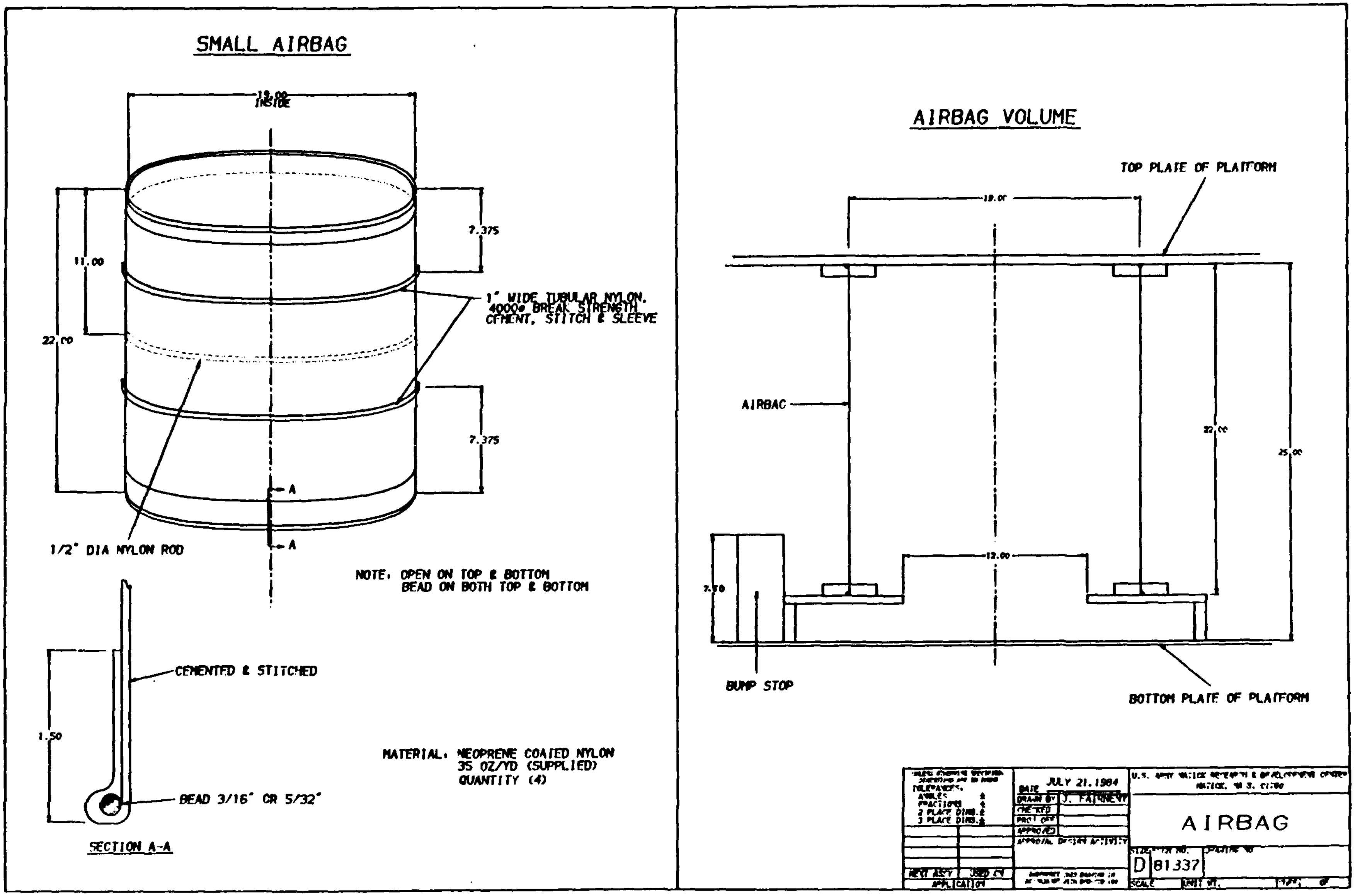

Figure 9. Airbag Construction.

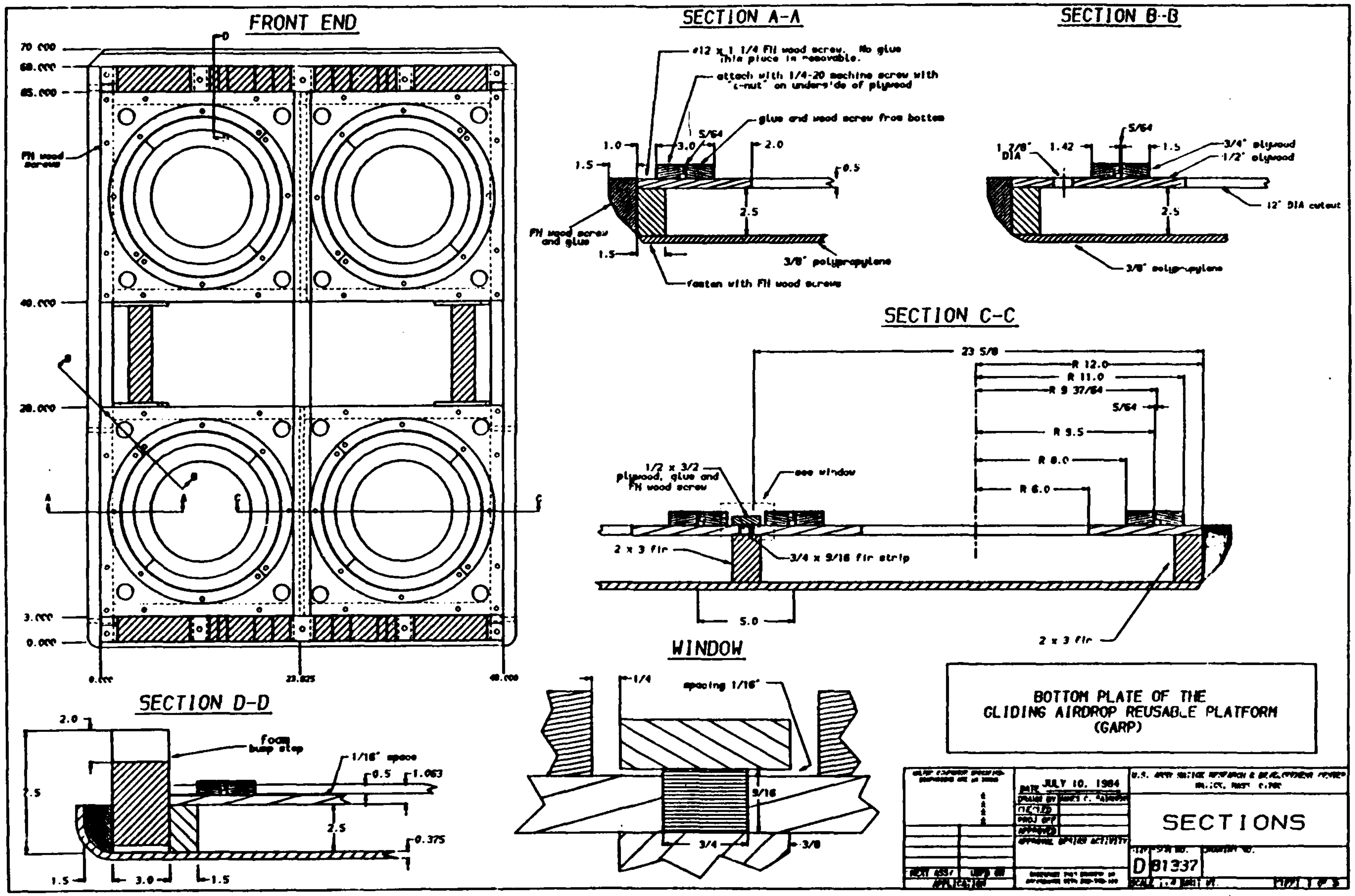

Figure 10. SECTIONS.

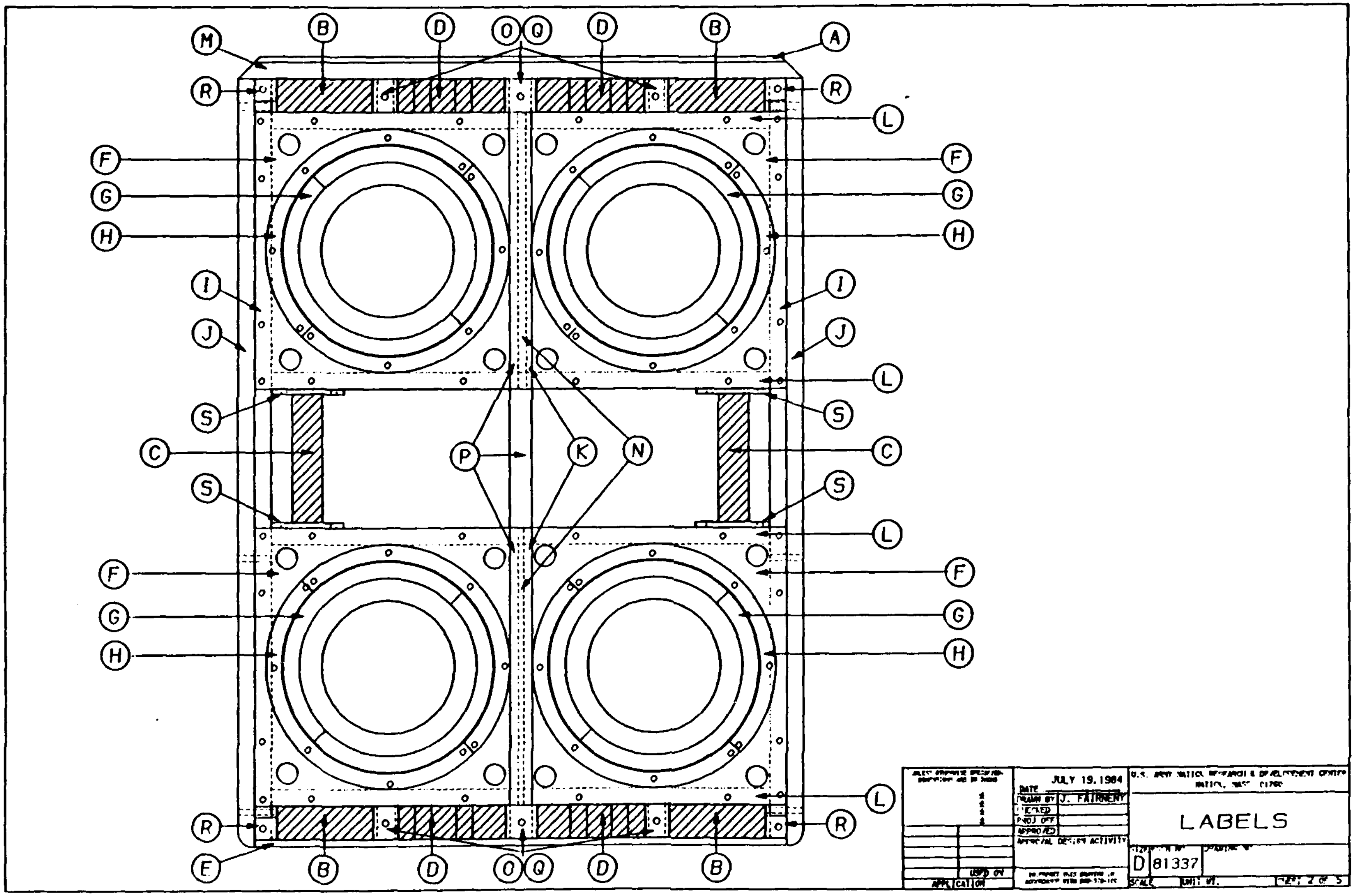

Figure 11. LABELS.

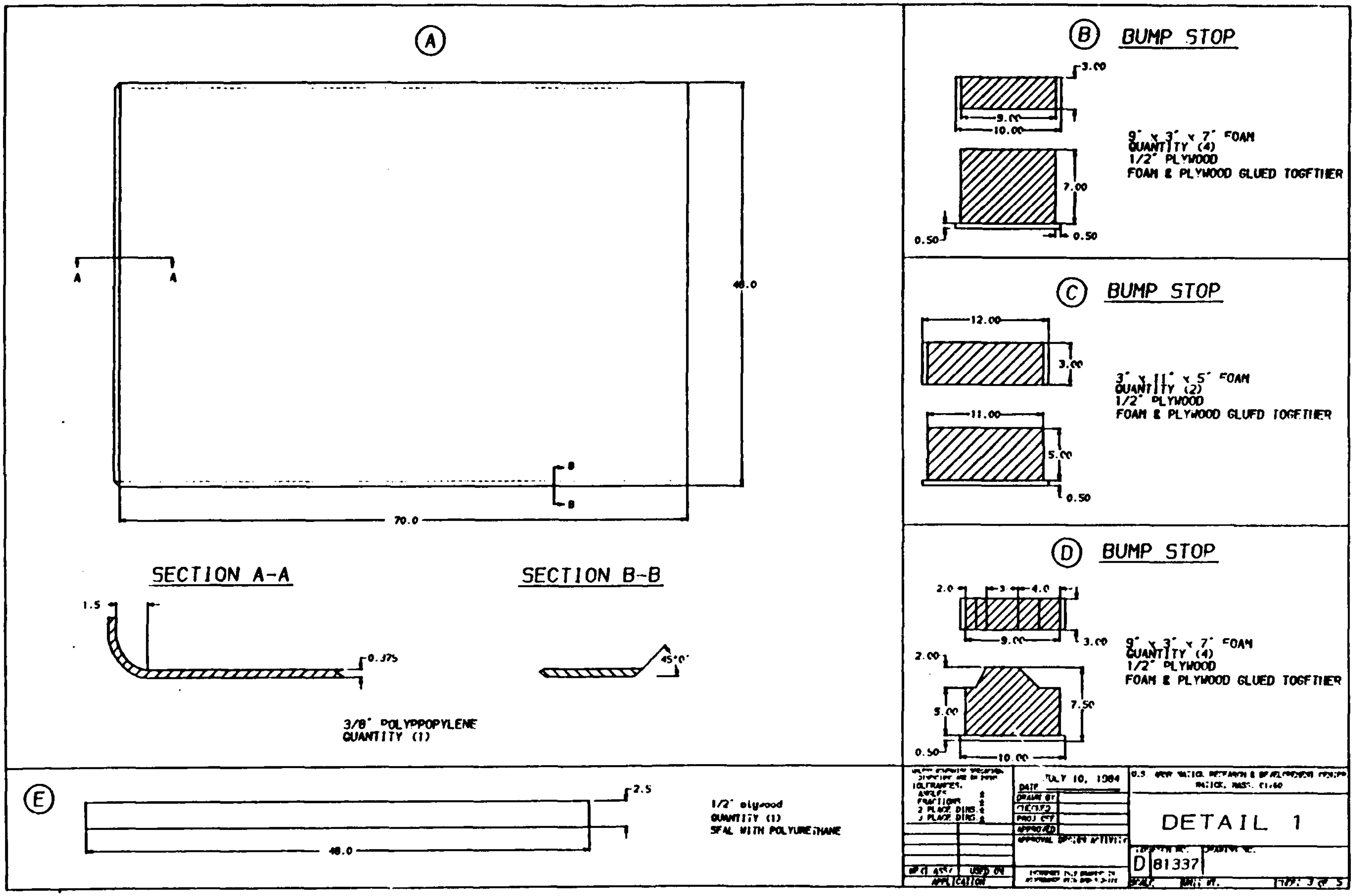

Figure 12. DETAIL 1.

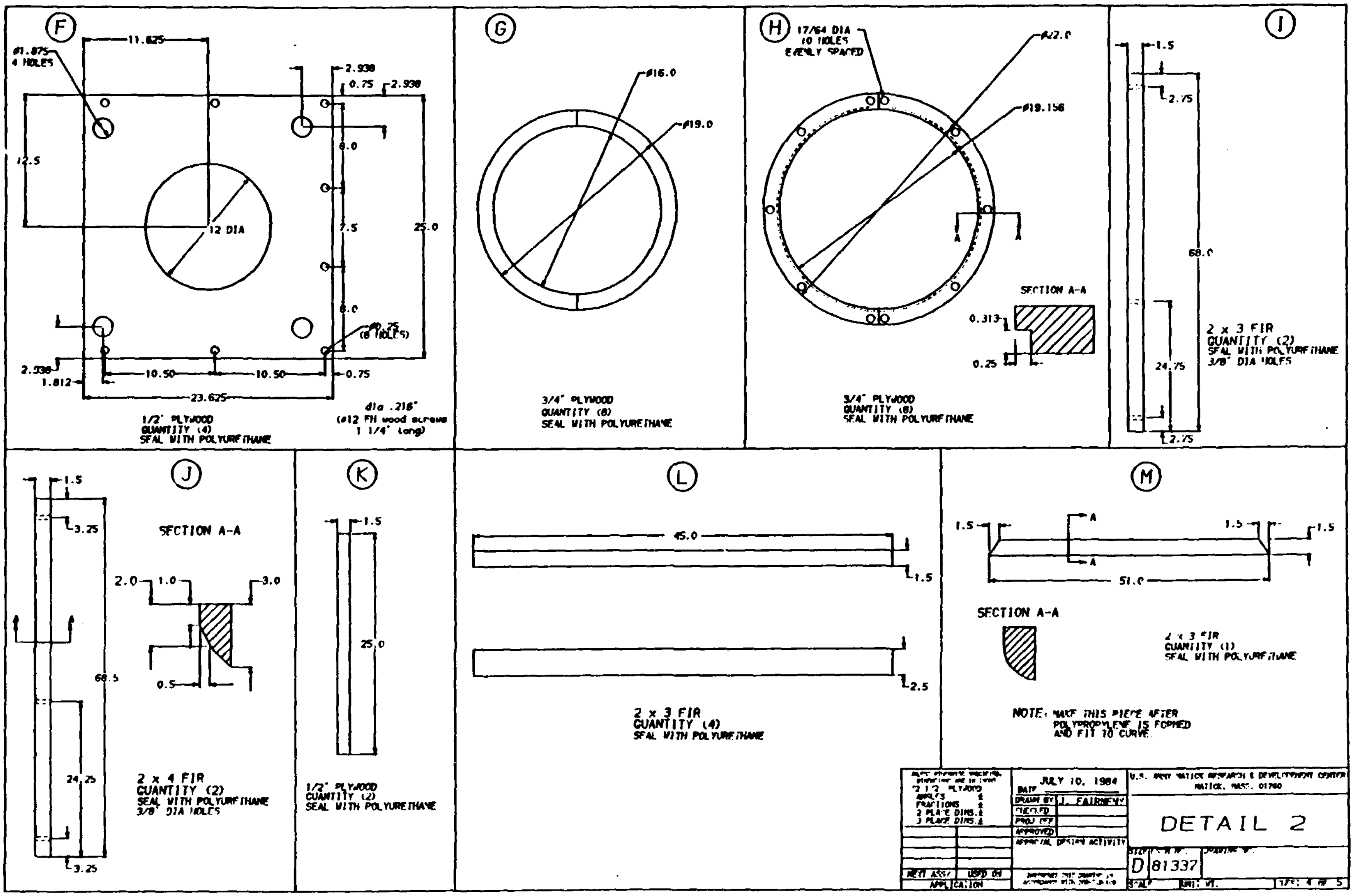

Figure 13. DETAIL 2.

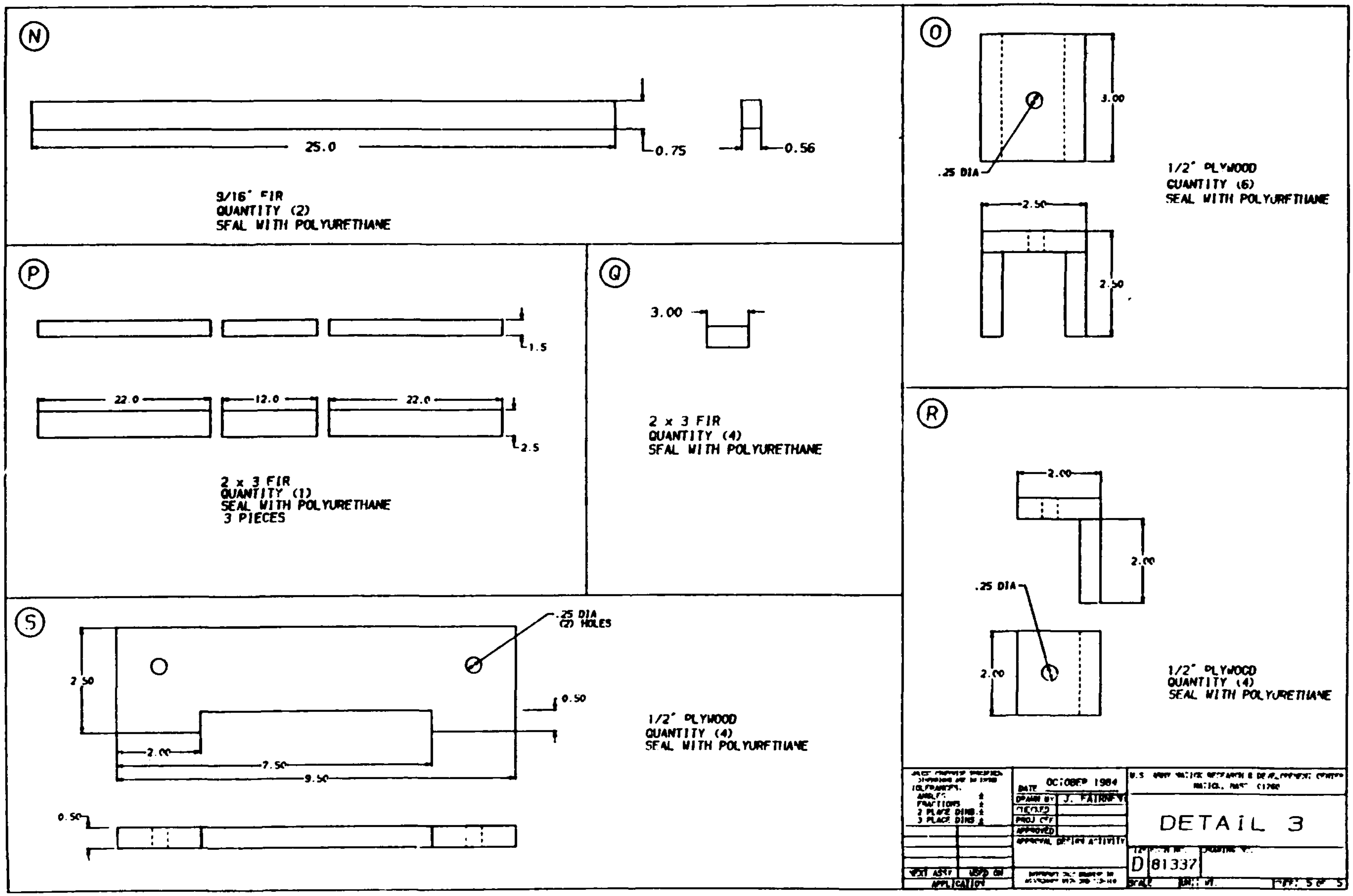

Figure 14. DETAIL 3.

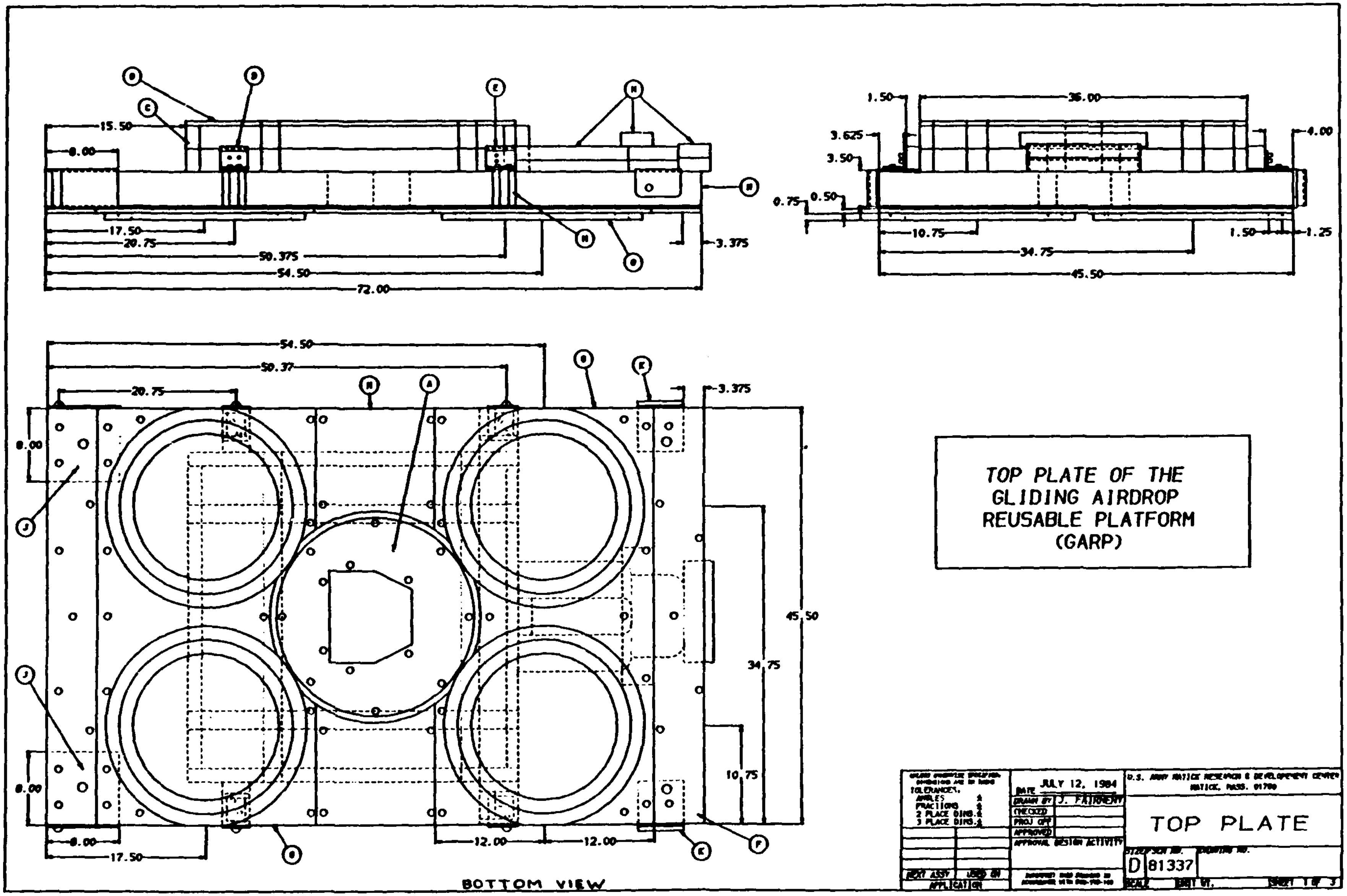

Figure 15. TOP PLATE.

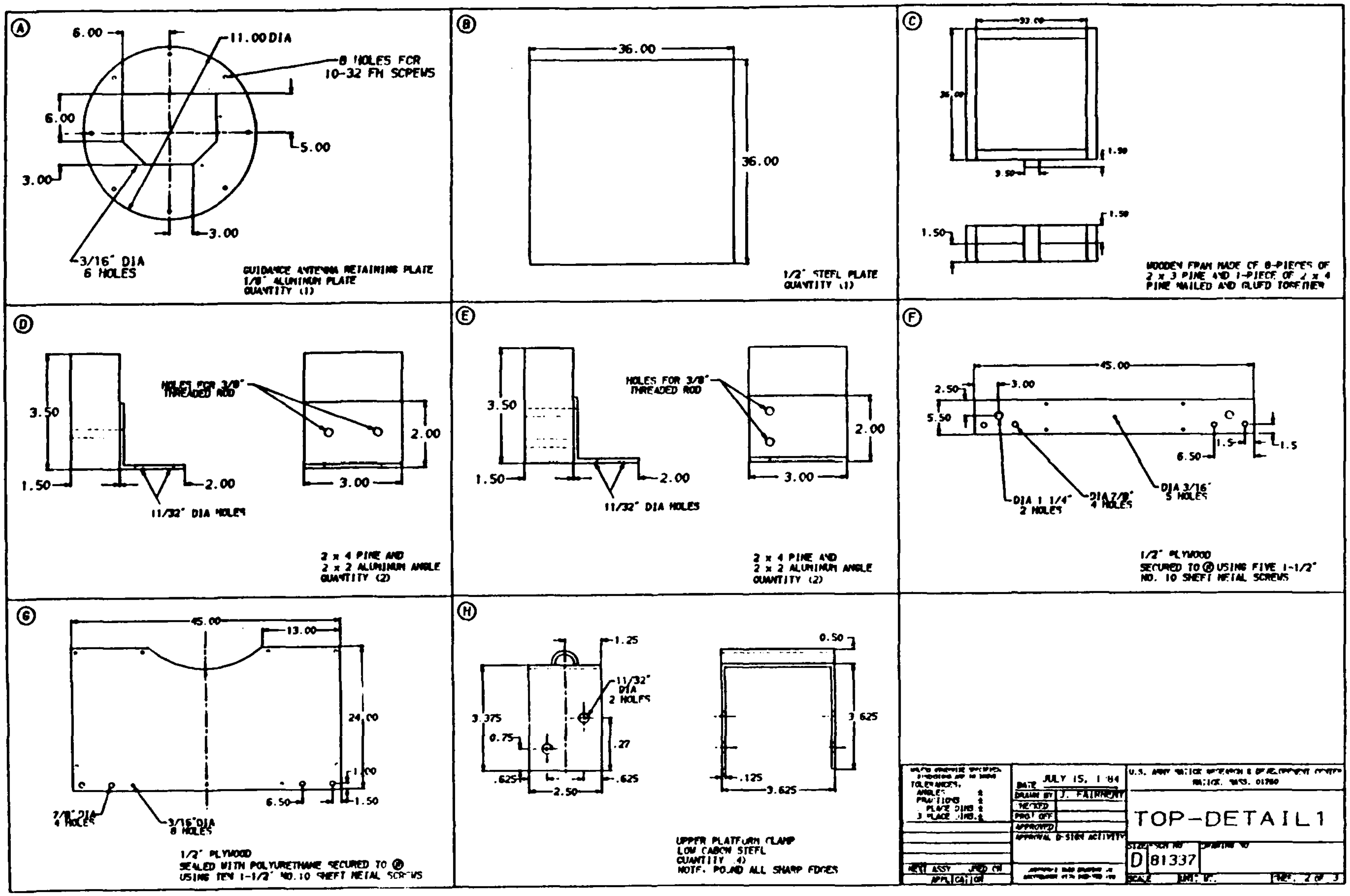

Figure 16. TOP-DETAIL 1.

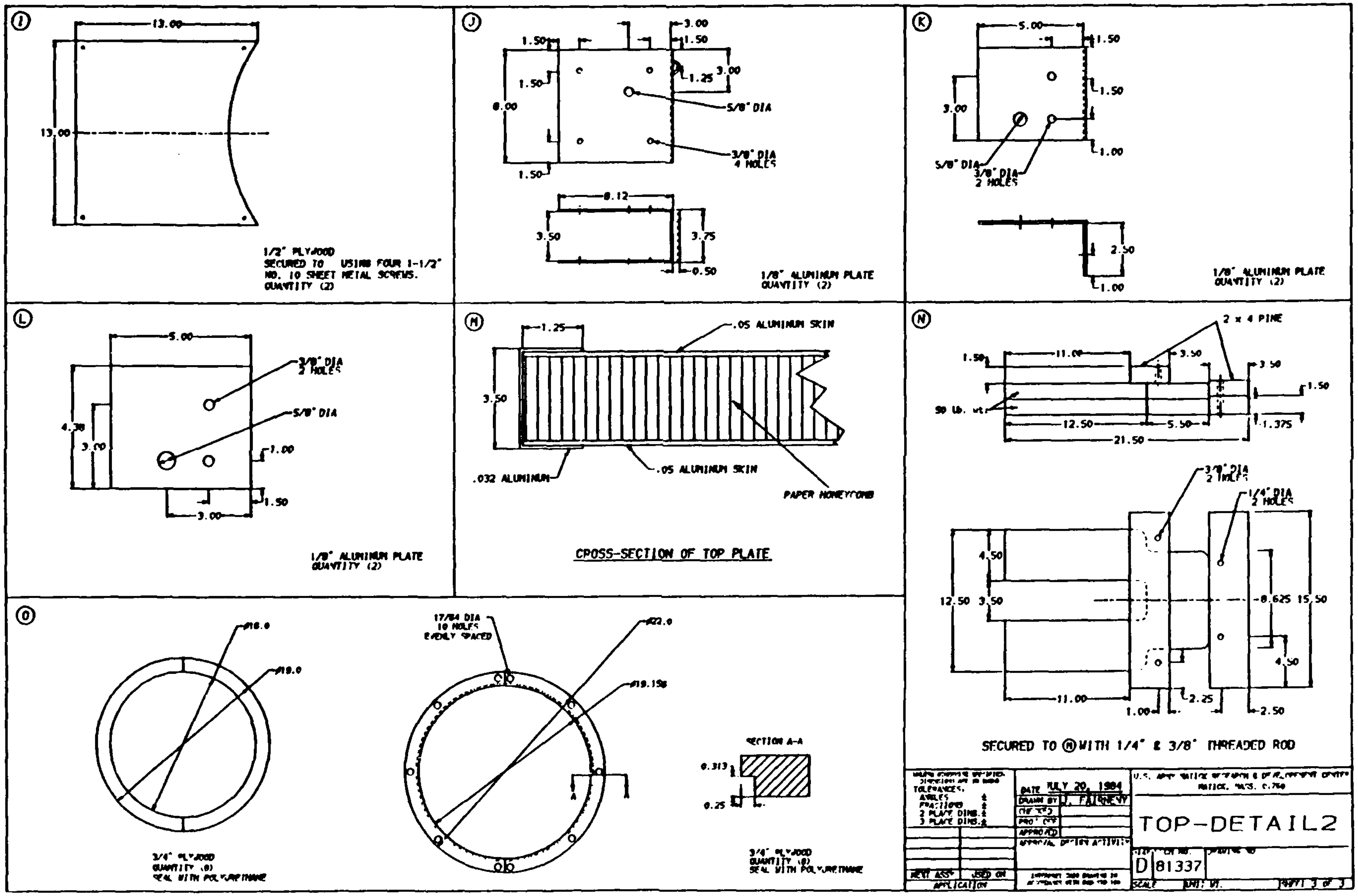

Figure 17. TOP-DETAIL 2.

material used weighed 1.19 kg/m^2 (35 oz/yd^2) and was 0.99 mm (0.039 in) thick (material #16177). The bags were constructed in the tentage shop at Natick RD&E Center. The airbags were sewn as open-ended cylinders to simplify the fabrication task as much as possible. A 3.17 mm (1/8-in) DIA bead was sewn at either end of the bag. The beads extended completely around the bag circumference and were used to secure the bag to the top and bottom plates. The two 25.4 mm (1-in) tubular nylon straps sewn to the outside of the bag were used to inhibit stretching of the bag material. A hoop made of 12.7-mm (1/2-in) DIA nylon rod was mounted on the interior of the bag. The hoop was slightly less than 0.483 m (19 in) across and was oriented parallel to the bag ends. It was secured in place, equidistant from either end, with duct tape. The purpose of the hoop was to insure that at the moment of ground impact the walls of the airbags had not collapsed inward and reduced the volume of the airbags.

Natick RD&E Center tests of the Reeves Brothers' bag material revealed the following. Breakage occurred at 3.278×10^7 N/m^2 (4755 lbf/in^2) with 18.71% elongation.[8] This corresponds to 32470 N/m (185.4 lbf/in) for a material thickness of 0.99 mm (0.039 in). During the simulation runs the maximum pressure encountered was 1.80×10^5 Pa (1.78 atm). Using the following formula the hoop stress was found.

$$\text{Hoop stress (lbf/in)} = \frac{(P - 1)\ PaD}{24}$$

where

Pa = atmospheric pressure

P = (bag pressure)/(atmospheric pressure)

D = bag diameter in feet

$$\text{Hoop stress} = \frac{(1.78 - 1)\ (2116.8)\ (1.583)}{24}\ \frac{(4.4482\ \text{N})}{1\ \text{lbf}}\ \frac{(39.37\ \text{in})}{1\ \text{m}}$$

$$= 19071\ \text{N/m}\ (108\ \text{lbf/in})$$

Comparison of the calculated hoop stress with the ultimate strength of the Reeves Brothers' material indicated that the airbags would not burst. This assumed that the airbag pressure was predicted with reasonable accuracy.

The top plate was constructed using material salvaged from a rigid wall shelter. A section of wall was cut to the 1.14-m x 1.82-m size and the edges covered as shown in Fig. 17, TOP DETAIL 2. Sections of 12.7 mm (1/2-in) plywood were secured to the lower surface of the plate to provide a surface for attaching the airbags. Two concentric rings per airbag were attached to the plywood. The rings are shown in Fig. 15, TOP PLATE and Fig. 17, TOP DETAIL 2. The outer ring is removable. These rings clamp down around the bead sewn into the airbag ends and secure the airbag to the top plate. The sections of 12.7-mm (1/2-in) plywood and the concentric rings were expertly fabricated in the Carpenter's Shop at Natick RD&E Center (see Fig. 18).

The bottom plate was constructed entirely at the Carpenter's Shop at Natick RD&E Center. A 9.5-mm (3/8-in) thick sheet of polypropylene was used for the bottom surface. A framework of 2 x 3 and 2 x 4 clear knotless Douglas-fir was used to provide rigidity. The airbags were secured using a method similar to that used for the top plate. Concentric rings were used to secure the airbags to the 12.7-mm (1/2-in) plywood plates, but the plates were not attached directly to the polypropylene. Instead, they were mounted on the framework made by the 2 x

3 fir (see Fig. 19). This allowed the orifice arrangement shown in Fig. 10, SECTIONS, to be used. In this arrangement, air from each airbag flows through a large hole in the plywood plate, into a box-shaped chamber and is then vented to the atmosphere through four orifice holes. It was assumed that the chamber would act as a stagnation chamber, however the validity of this assumption was not verified. Limited space required that four small orifice holes be used, rather than one large hole. This arrangement differed considerably from the one modeled in LAND3. In the program, the air does not flow through an intermediate chamber, but instead is vented directly to the atmosphere through one large orifice hole. The effect of the box-shaped chamber and additional orifice holes on actual airbag performance was unknown. It was assumed that frictional losses would be greater with four orifice holes. To avoid possible overpressurization of the airbags, the total orifice area of the four orifice holes was made approximately 10% greater than the area of the one large hole modeled in LAND3. The existence of the box-shaped chamber made an exact determination of the correct orifice size difficult. Therefore, it was decided to plan the AGARP testing so that the orifice size could be optimized during the initial test drops.

Appendix F details the methods used to arrive at the final bump stop heights and impact surface areas. The framework of 2 x 3 fir and the hardware used for airbag attachment limited the space available for the bump stops. The bump stops were constructed from 25.4-mm (1-in) thick pieces of Scott 900-8 and Scott 900-4 foam. The foam was arranged in layers (the pieces were stacked one on top of the other)

Figure 18. Attachment of concentric rings to top plate.

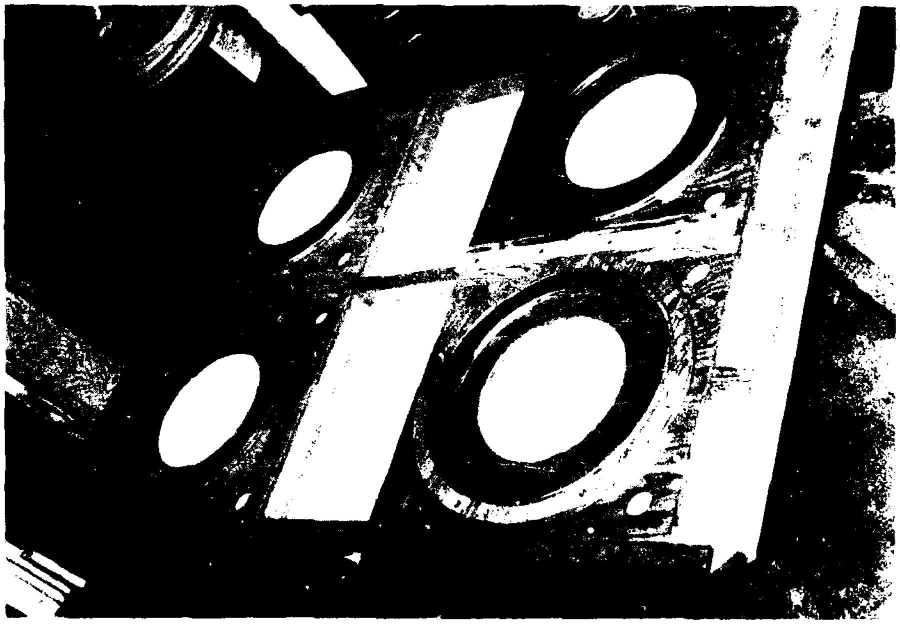

Figure 19. Attachment of concentric rings to bottom plate.

and glued together. The bump stop configurations shown in Fig. 12, DETAIL1 (B) and (D) were mounted at the front and rear ends of the bottom plate. These two configurations utilized two layers of Scott 900-4 foam on top and five layers of Scott 900-8 foam underneath. These bump stops were intended to be the primary bump stops The bump stops shown in Fig. 12, DETAIL1 (C) were mounted in the middle of the bottom plate (see figure 10, SECTIONS). These bump stops were intended as secondary bump stops, to be used only if those at the front and rear ends of the platform crushed too much or did not come into contact with the top plate. The middle bump stops were fabricated using five layers of Scott 900-8 foam. All bump stops, front, rear, and middle were glued to 12.7-mm (1/2-in) thick pieces of plywood. The plywood was clamped to the bottom plate using the brackets shown in Fig. 14, DETAIL3 (O) and (R).

The material used for the straps was 25.44-mm (1-in) tubular nylon, which has a breaking strength of 4000 lb.[9] The side strap arrangement was similar to configuration 2 shown in Fig. 2. The attachment points were not exactly a distance of L/4 apart; however, the variation was not more than 50.8 mm (2 in). The two straps restraining forward motion of the top plate were kept parallel. Four end diagonal (two at each end of the platform) and four vertical straps (one at each corner) were used. The attachment to the bottom plate was done by first drilling a 9.5-mm (3/8-in) diameter holes, in the fir frame-work. A short length of 25.4-mm (1-in) tubular nylon was passed through the hole and tied into a loop. The restraining straps were then tied to these loops. No metal was used. The restraining straps were secured to the top plate in a similar manner.

The loops of 1" tubular nylon were passed through the brackets shown in Fig. 17, TOP DETAIL2 (J) (for the front attachment points), (K) (for the rear attachment points and Fig. 16, TOP DETAIL1 (H) (for the middle attachment points). The restraining straps were then tied to these loops. The loops at the front and rear corners of both the top and bottom plates had three straps tied to them, one vertical strap, one end diagonal strap and one side diagonal strap.

Weights that simulated the guidance package and servo mechanism to be used during actual airdrops were attached to the top plate. (see Fig. 15, TOP PLATE (B) (C) - (M)). The guidance package was simulated by a 0.914-m x 0.914-m x 0.013-m (3-ft x 3-ft x 1/2-in) steel plate (B) mounted on a frame (C) constructed of 2 x 3 pine. The frame held the plate 0.127 m (5 in) above the surface of the top plate; the approximate height of the guidance package c.g. The plate was secured to the frame using four aircraft tie down straps and the frame was attached to the top plate using the brackets shown in Fig. 16, TOP DETAIL1 (D) and (E). The servo mechanism was simulated using two 22.7-kg (50-lbm) weights stacked, one on top of the other (TOP PLATE (M)). These weights were secured in place using threaded rod which passed completely through the top plate (see Fig. 17, TOP PLATE - DETAIL2 (M)). The result was a c.g. slightly lower than that of the servo-mechanism but which had approximately the same position in the horizontal plane. This mounting arrangement offset the top plate c.g. slightly more than 75 mm (3 in) to the rear of the geometric center. The overall platform c.g. (airbags extended) was about 75 mm (3 in) to the rear of the platform geometric center.

Four large eye bolts (15.9-mm (5/8-in) DIA - 25.4-mm (1-in) eye) were bolted to the top plate, one at each of the corners. The bolts passed vertically through the plate. Slings for lifting the platform were attached to these bolts. The assembled platform without all the restraining straps attached is shown in Fig. 20.

Instrumentation

During the course of constructing the AGARP, pressure transducers were installed in two of the four airbags. One transducer was attached to the plywood plate which forms the upper surface of the front right airbag. The transducer was positioned on the centerline of the airbag. The other transducer was installed in the left rear airbag in the same manner. The transducers were Honeywell Miniature Solid State Pressure Transducers type 135PC15AIL (0-30 psia). (see Fig. 21)

When construction of the platform was complete, four Microswitch model BZ-2RW-Z2 contact switches were attached to the bottom plate. Two switches were mounted directly to the bottom plate, one at the right (starboard) front corner and one at the left (port) rear corner. These switches were used to monitor ground contact of the bottom plate. The remaining two contact switches were mounted on the bump stops to indicate when the top plate hit the bump stops. One switch was mounted on the right front (starboard) bump stop, the other on the left (port) rear bump stop.

A total of three Entran D20 (0-50 g) accelerometers were used on the AGARP. One accelerometer was glued to the top plate above the approximate center of the right (starboard) front airbag. It was oriented to monitor accelerations in the vertical direction. The other two

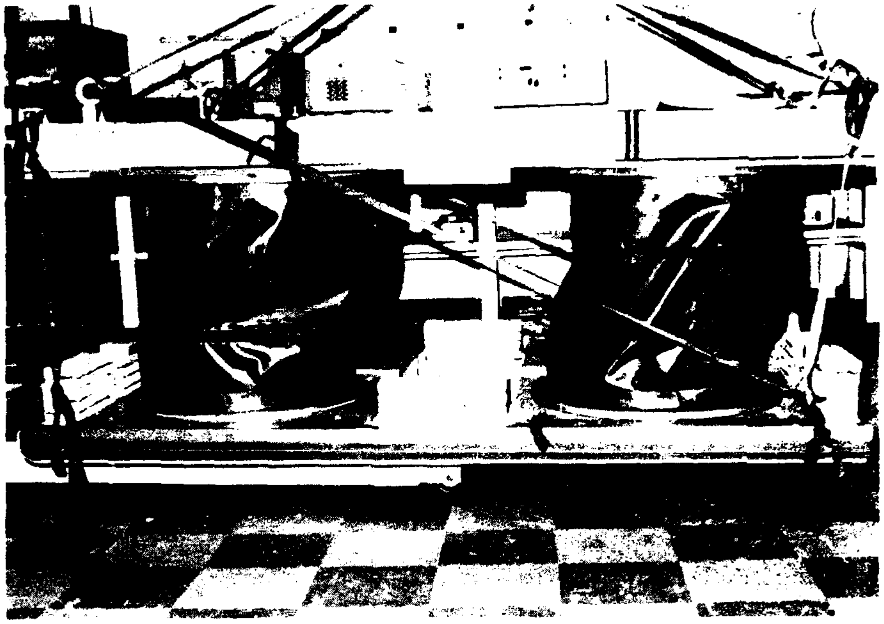

Figure 20. AGARP without full complement of restraining straps.

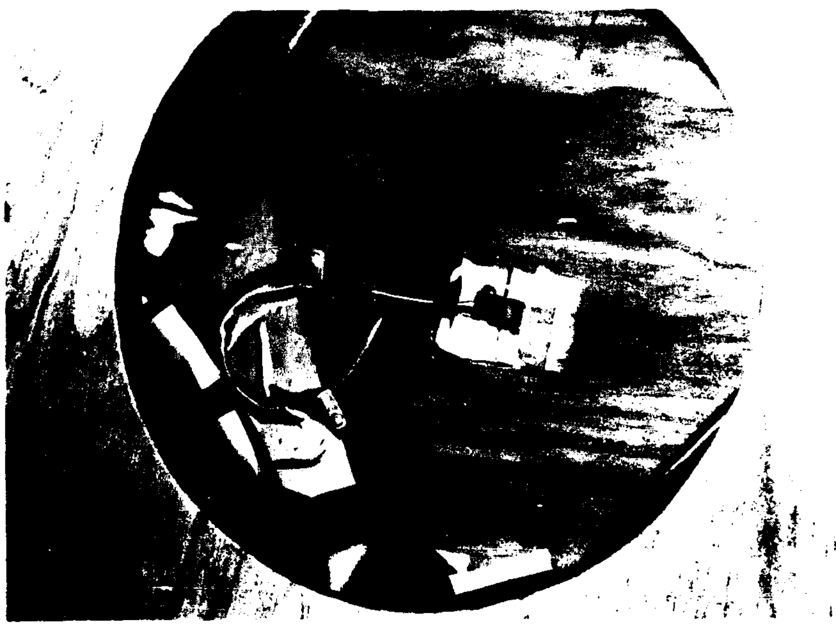

Figure 21. Mounted pressure transducers.

accelerometers were mounted on the simulated guidance package. They were positioned almost directly over the c.g. of the top plate. One of these accelerometers was oriented to monitor vertical accelerations, the other was oriented to monitor accelerations in the fore-aft directions.

Additional instrumentation included two Transducers Inc. 2000-lb load cells. These load cells were connected to two of the restraining straps on the port side of the platform. A Honeywell Model 1858 17-channel Visicorder was used to record the data from the instrumentation. A Wollensak Fastax high speed, 16-mm motion picture camera was used to film some of the testing.

TEST PLAN AND PROCEDURES

The testing of the airbag landing system had two objectives. One was to provide experimental data that could be compared to the output of the computer program, LAND3, and thus give an indication of the accuracy of the program. The other objective of the testing was to verify that the AGARP would perform adequately under conditions that were similar to those encountered during actual airdrops. Adequate performance was defined as:

(a) no damage to payload or platform

(b) total accelerations at the top plate below 15 G (combined vertical and fore-aft acceleration)

(c) limited relative motion between the upper and lower plates (preventing airbag damage)

(d) strap forces below strap break strength.

The test plan is included in Tables 5 and 6. Since there was some uncertainty about the accuracy of the program, LAND3 (particularly with respect to orifice sizes), the drops were arranged so that the severity of the impact conditions increased in a step-by-step manner. The original test plan specified that twelve drops be performed. The drops were divided into two groups of six.

The first group of six drops (Table 5) consisted of vertical drops--the platform hit the ground with only a vertical velocity component. The intent of these drops was to optimize the orifice size and to verify that individual bags would perform adequately during a pitched and/or rolled impact. If the orifices were too small the internal pressure of the bags could become excessively high. If the orifices were too large the bags would not pressurize enough.[10] By using a step-by-step approach, either problem would become evident before the worst case impact conditions were reached. Once the optimum orifice size was found, the platform's behavior during pitched and/or rolled impacts could be investigated. During this type of impact, the bags on the side of the platform that hit the ground first are the first to pressurize. They reach higher pressures and account for most of the acceleration of the top plate.

The second group of drops (Table 6) consisted of swinging drops, which gave the platform both vertical and horizontal velocities at ground impact. The intent of these drops was to simulate conditions that might exist during actual airdrop. These drops would provide the opportunity to verify that the straps did restrict the relative motion of the two plates, that the airbags performed adequately with the

TABLE 5. TEST PLAN FOR VERTICAL DROPS OF AGARP

Drop Number	Desired Impact Velocity (m/s) Vertical	Horizontal	Release Ht. (m)	Orientation at Impact* Pitch	Roll	Yaw	Orifice Size (# holes-area)
1V	3.0	0.0	0.46	0^o	0^o	0^o	4 - 0.00713 m^2
2V	4.5	0.0	1.03	0^o	0^o	0^o	Adjusted according to results of previous drop
3V	6.0	0.0	1.83	0	0	0	Adjusted according to results of previous drop
4V	6.0	0.0	1.83	+10	0	0	As determined above
5V	6.0	0.0	1.83	0	+10	0	As determined above
6V	6.0	0.0	1.83	+10	+10	0	As determined above

*positive pitch: nose down
positive roll: roll right

TABLE 6. TEST PLAN FOR SWINGING DROPS OF AGARP

Drop Number	Desired Impact Velocity (m/s) Vertical	Horizontal	Release Ht. (m)	Orientation at Impact* Pitch	Roll	Yaw	Orifice Size (# holes-area)
1H	3.0	5.2	2.26	0	0	0	As determined previously
2H	4.5	7.8	4.39	0	0	0	As determined previously
3H	6.0	10.4	7.44	0	0	0	As determined previously
4H	6.0	10.4	7.44	-10^{o}	0	0	As determined previously
5H	6.0	10.4	7.44	$+10^{o}$	0	0	As determined previously
6H	6.0	10.4	7.44	0	10^{o}	0	As determined previously

* positive pitch: nose down
positive roll: roll right

relative motion that did occur, and that the accelerations of the top plate were not excessive. These tests followed a pattern similar to that of the vertical drops. First the impact velocities were increased in steps to gradually increase the severity of the impact. Once the maximum impact velocities were reached, the platform's behavior during a pitched or rolled impact could be investigated.

The test drops were all conducted outdoors in the far left field of the EM recreational baseball field at Natick RD&E Center. The impact surface was hard-packed earth covered with grass. The procedure used varied depending on type of drop. The platform, prior to a vertical drop, is shown in Fig. 22. The procedures for the vertical impact velocity drops were as listed below.

(a) Clear impact area of rocks, debris, etc.

(b) Check for proper operation of all transducers and contact switches. Electrically zero-position all transducer outputs while platform is still on the ground.

(c) Adjust suspension slings for zero pitch, zero roll orientation of platform.

(d) Attach suspension slings to crane hook. Raise platform approximately 0.5 m above the ground (measured from bottom plate). Check that restraining straps are not loose, platform offset is correct, airbags are undamaged. Lower platform and release suspension slings.

(e) Adjust suspension slings for proper release orientation.

(f) Attach release mechanism to crane hook. Attach suspension slings to the release mechanism. Raise platform approximately 0.5 m

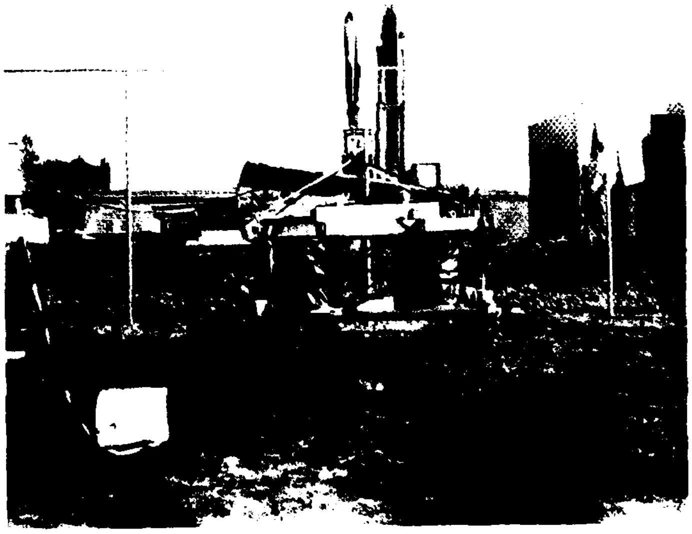

Figure 22. AGARP prior to vertical drop.

above the ground and check orientation of the top plate with a carpenter's level and/or Angle Finder. If the orientation is not correct, lower the platform; readjust the slings and repeat the procedure.

(g) Align high-speed camera, if it is being used.

(h) Attach height determining line to bottom plate and raise the platform to the release height.

(i) Remove height determining line; steady platform.

(j) Start camera and data recorder 2 or 3 seconds before platform release.

(k) Release platform.

(l) Raise the platform and inspect airbags and platform for damage.

(m) Repeat (a) to (l) for next drop.

The procedures for the swinging drops were as follows:

(a) Attach 7.62-m (25-ft) length of six-ply Type XXVI nylon strap, Test strength - (15,000 lb)/ply[11] to the hook on the first crane. Raise hook to the farthest extent possible. Adjust height and position of the crane boom so that when the platform is attached to the six-ply nylon strap, via its suspension lines, ground impact will occur as shown in Fig. 23.

(b) Set up background grid and attach to outfield fence, such that ground impact of the platform occurs while the platform is in front of the grid.

(Steps a & b were extremely time-consuming and were done as few times as possible. As long as the setup remained satisfactory, it was left in place for consecutive drops.

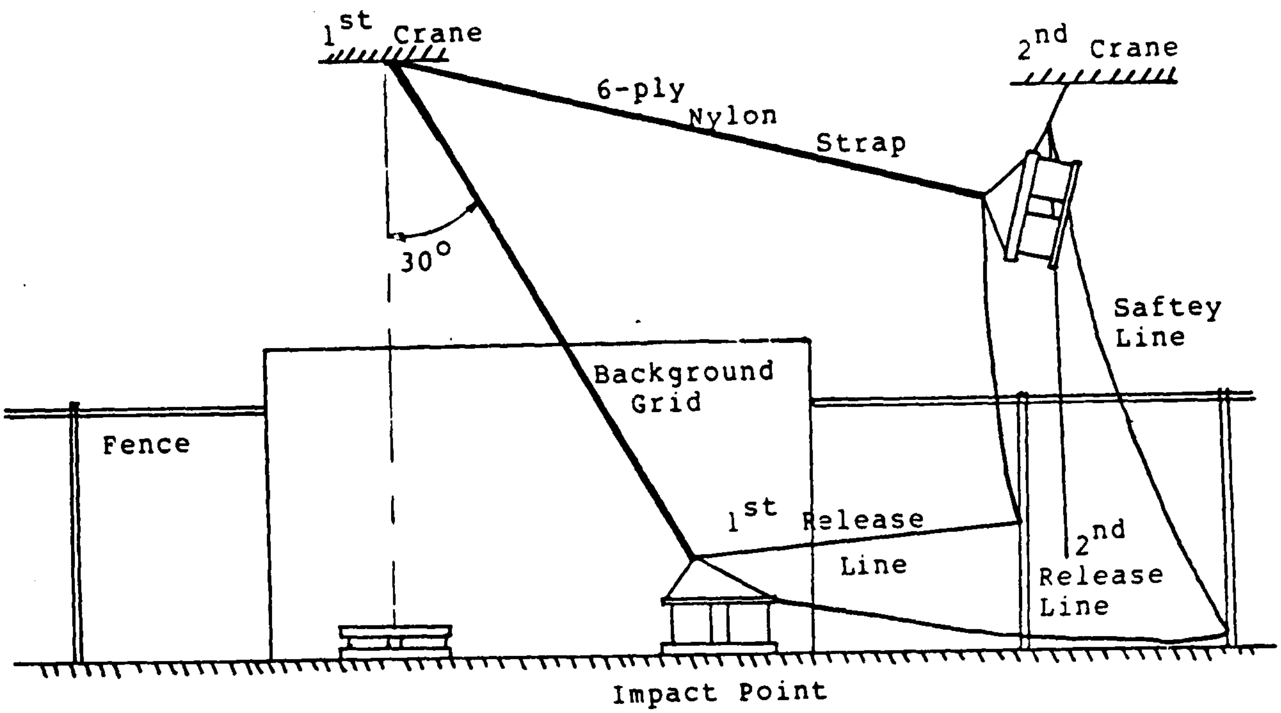

Figure 23. Swinging drop test setup.

(c) Align high-speed camera. Record distance from the background grid.

(d) Check for proper operation of all transducers and contact switches. Electrically zero-position all transducer outputs while the platform is on the ground.

(e) Adjust suspension slings for zero pitch, zero roll platform orientation.

(f) Attach suspension slings to second crane. Raise the platform approximately 0.5 m above the ground (measured from the bottom plate). Check that restraining straps are tight, platform offset is correct, and airbags are undamaged. Lower platform.

(g) Adjust suspension slings for proper release orientation. Attach suspension slings to second crane or forklift and raise platform approximately 0.5 m above the ground. Check orientation of the top

plate using a carpenter's level and/or Angle finder. If orientation is not correct, lower the platform, readjust the suspension slings, and repeat the procedure. Lower the platform, and release the slings when complete.

(h) Attach release mechanism to the six-ply nylon strap suspended from the first crane. Attach suspension lines to the release mechanism. Attach one and of first release line to the release mechanism.

(i) Attach a Type XXVI nylon strap (1-ply) to the rear eyebolts on the top plate. Attach a second release mechanism to the free end of the nylon strap. Attach the release mechanism to the hook of the second crane. Attach one end of the second release line to the release mechanism.

(j) Attach a line to the instrumentation cabling. This line is used to hold the cables out of the path of the swinging platform.

(k) Attach safety line; one end to the rear eyebolts on the top plate, the other end to the outfield fence. This line prevents the platform from sliding to the point where the instrumentation cables are damaged.

(l) Attach height-determining line to the bottom plate.

(m) Using the second crane, lift and pull the platform to its release height and position. The six-ply nylon strap should be tight.

(n) Remove height-determining line.

(o) Set up strobe light in the field of view of the high speed camera.

(p) Attach the free end of the first release line to the outfield

fence. This line should cause the suspension lines to be released just after ground impact of the platform.

(q) Start the camera and data recorder 2 or 3 seconds before the platform is released.

(r) Release the platform using the second release line.

(s) Raise the platform and inspect the airbags and platform for damage.

(t) Repeat (a) to (s) for the next drop.

The platform prior to release is shown in Fig. 24. Fig. 25 shows the platform after impact on drop 3H I.

Figure 24. AGARP prior to swinging drop.

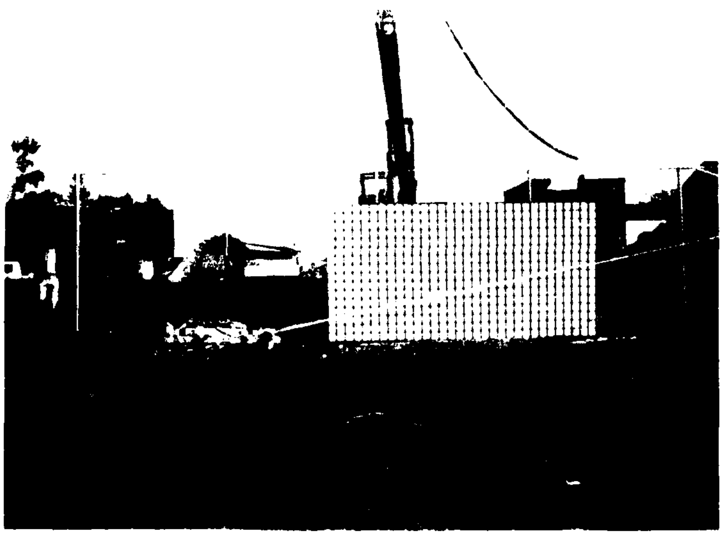

Figure 25. AGARP after drop 3H I impact.

TEST RESULTS

Summary

The testing of the AGARP took place between 7 November 1984 and 28 November 1984. A total of twenty-six test drops were performed. Only twelve drops were called for in the test plan; however, a number of drops were repeated either to determine the correct airbag orifice size or because instrumentation problems resulted in unreadable or unusable data. Table 7 summarizes the data for all twenty-six drops.

The drop numbering system used in Table 7 was based on that used for the test plan. Roman numerals were added to the drop number to indicate if the drop was the initial drop or a repeated drop. Table 7 shows the peak values sensed by the two airbag pressure transducers, the three accelerometers, and the two load cells.

The two pressure transducers were located in the right (starboard) front and left (port) rear airbags. The maximum pressures sensed by these transducers are listed under "Peak Gage Pressure". There was no instrumentation in the other two airbags. Typically, peak pressures were reached in 0.1 seconds or less. The airbags usually remained pressurized for 0.15 to 0.20 seconds.

The maximum accelerations sensed by the three accelerometers are listed in the columns "X c.g.", "Z c.g.", and "Z front", which appear under the heading "Peak Acceleration". The values listed under "X c.g." are from the accelerometer which was oriented to monitor fore/aft accelerations mounted above the c.g. of the top plate. The notations "1st", "2nd", and "3rd" are used to distinguish between the peaks of consecutive acceleration pulses. These peaks were caused by the airbags, the bump stops, and/or the

TABLE 7. SUMMARY OF TEST RESULTS

Drop Date	Drop No.	Desired Impact Velocity Vert (m/s)	Desired Impact Velocity Horz (m/s)	Desired Impact Orientation[a] Roll (deg)	Desired Impact Orientation[a] Pitch (deg)	Desired Impact Orientation[a] Yaw (deg)	Orifice Area (m^2)	Peak Gage Pressure Left Rear (Pa x 10^5)	Peak Gage Pressure Front Right (Pa x 10^5)	Peak Acceleration X c.g. Pulse	Peak Acceleration X c.g. Acc (G)	Peak Acceleration Z c.g. Pulse	Peak Acceleration Z c.g. Acc (G)	Z Front Pulse	Z Front Acc (G)	Strap Forces Strap 1 (N)	Strap Forces Strap 2 (N)	Comments
11/7/84	IVI	3	0	0	0	0	.00713	1.23	1.11	1st	-	Airbag	-	Airbag	1.88	-	-	
										2nd	-	Bump 1	-	Bump 1	9.88			
											-	Bump 2	-	Bump 2	2.66			
	2VI	4.5	0	0	0	0	.00713	1.62	1.41	1st	-	Airbag	-	Airbag	4.00	-	-	
										2nd	-	Bump 1	-	Bump 1	12.44			
											-	Bump 2	-	Bump 2	2.33			
	3VI	6.0	0	0	0	0	.00713	2.63	2.12	1st	-	Airbag	-	Airbag	6.92	-	-	
										2nd	-	Bump 1	-	Bump 1	15.66			
											-	Bump 2	-	Bump 2	2.85			
	2VII	4.5	0	0	0	0	.00623	1.92	1.62	1st	-	Airbag	-	Airbag	4.72	-	-	
										2nd	-	Bump 1	-	Bump 1	10.00			
											-	Bump 2	-	Bump 2	1.75			
	2VIII	4.5	0	0	0	0	.00534	2.22	1.92	1st	-	Airbag	-	Airbag	5.00	-	-	
										2nd	-	Bump 1	-	Bump 1	6.00			
											-	Bump 2	-	Bump 2	.70			
	3VII	6.0	0	0	0	0		3.03	2.63	1st	-	Airbag	-	Airbag	7.80	-	-	
										2nd	-	Bump 1	-	Bump 1	6.20			
											-	Bump 2	-	Bump 2	.40			

[a] positive pitch - nose down
positive roll - roll right (starboard)

[b] data not readable

[c] no data

[d] drop aborted

[e] spike goes to 12+G

TABLE 7. SUMMARY OF TEST RESULTS (Continued)

Drop Date	Drop No.	Desired Impact Velocity Vert (m/s)	Desired Impact Velocity Horz (m/s)	Desired Impact Orientation[a] Roll (deg)	Desired Impact Orientation[a] Pitch (deg)	Desired Impact Orientation[a] Yaw (deg)	Orifice Area (m^2)	Peak Gage Pressure Left Rear (Pa x 10^5)	Peak Gage Pressure Front Right (Pa x 10^5)	Peak Acceleration X c.g. Pulse	Peak Acceleration X c.g. Acc (G)	Peak Acceleration Z c.g. Pulse	Peak Acceleration Z c.g. Acc (G)	Peak Acceleration Z Front Pulse	Peak Acceleration Z Front Acc (G)	Strap Forces Strap 1 (N)	Strap Forces Strap 2 (N)	Comments
11/8/84	3VIII	6.0	0	0	0	0		b		1st	b	Airbag	b	Airbag	b	-	-	
										2nd		Bump 1		Bump 1				
												Bump 2		Bump 2				
	3VIV	6.0	0	0	0	0		2.83	2.63	1st	1.5	Airbag	8.00	Airbag	7.60	-	-	
										2nd		Bump 1	2.10	Bump 1	4.40			
												Bump 2	.80	Bump 2	.30			
	4VI	6.0	0	0	-10	0		2.63	2.42	1st	b	Airbag	b	Airbag	b	-	-	
										2nd		Bump 1		Bump 1				
												Bump 2		Bump 2				
	4VII	6.0	0	0	-10	0		2.73	2.73	1st	b	Airbag	b	Airbag	b	-	-	
										2nd		Bump 1		Bump 1				
												Bump 2		Bump 2				
	5VI	6.0	0	-10	0	0		2.42	2.83	1st	b	Airbag	b	Airbag	b	-	-	
										2nd		Bump 1		Bump 1				
												Bump 2		Bump 2				
	6VI	6.0	0	-10	+10	0	.00634	3.84	2.73	1st	b	Airbag	b	Airbag	b	-	-	
										2nd		Bump 1		Bump 1				
												Bump 2		Bump 2				

[a] positive pitch - nose down
positive roll - roll right (starboard)

[b] data not readable

[c] no data

[d] drop aborted

[e] spike goes to 12+G

TABLE 7. SUMMARY OF TEST RESULTS (Continued)

Drop Date	Drop No.	Desired Impact Velocity Vert (m/s)	Desired Impact Velocity Horz (m/s)	Desired[a] Impact Orientation Roll (deg)	Desired[a] Impact Orientation Pitch (deg)	Desired[a] Impact Orientation Yaw (deg)	Orifice Area (m^2)	Peak Gage Pressure Left Rear (Pa x 10^5)	Peak Gage Pressure Front Right (Pa x 10^5)	X c.g. Pulse	X c.g. Acc (G)	Peak Acceleration Z c.g. Pulse	Peak Acceleration Z c.g. Acc (G)	Z Front Pulse	Z Front Acc (G)	Strap Forces Strap 1 (N)	Strap Forces Strap 2 (N)	Comments
11/9/84	4VIII	6.0	0	0	+10	0		2.73	2.83	1st	1.10	Airbag	9.60	Airbag	8.60	448	0	
										2nd	.80	Bump 1	5.40	Bump 1	8.50			
												Bump 2	.90	Bump 2	.80			
	5VII	6.0	0	+10	0	0		3.03	2.83	1st	+.5/-.5	Airbag	14.60	Airbag	7.00	623	0	Simultaneous
										2nd	-2.5/+1.0	Bump 1		Bump 1	11.60			Airbag & Bump
												Bump 2		Bump 2	1.0			Stop Pulses
	6VII	6.0	0	-10	+10	0		4.04	2.63	1st	+1.5/-1.0	Airbag	12.00	Airbag	10.40	0	0	Simultaneous
										2nd	-.95	Bump 1		Bump 1	9.80			Airbag & Bump
												Bump 2		Bump 2	1.00			Stop Pulses
	3VV	6.0	0	0	0	0		2.63	2.32	1st	-.6/+1.7	Airbag	8.10	Airbag	8.20	712	0	
										2nd		Bump 1	2.30	Bump 1	4.60			
												Bump 2	.90	Bump 2	1.20			
11/15/84	1HI	3.0	5.2	0	0	0		c	c	1st	c	Airbag	c	Airbag	c			
										2nd		Bump 1		Bump 1				
												Bump 2		Bump 2				
	1HII	3.0	5.2	0	0	0		.81	.81	1st	.50	Airbag	3.10	Airbag	1.80	511	267	
										2nd	3.00	Bump 1	3.30	Bump 1	6.20			
												Bump 2	.40	Bump 2	.50			

[a]positive pitch - nose down
positive roll - roll right (starboard)

[b]data not readable

[c]no data

[d]drop aborted

[e]spike goes to 12+G

TABLE 7. SUMMARY OF TEST RESULTS (Continued)

Drop Date	Drop No.	Desired Impact Velocity Vert (m/s)	Desired Impact Velocity Horz (m/s)	Desired Impact Orientation[a] Roll (deg)	Desired Impact Orientation[a] Pitch (deg)	Desired Impact Orientation[a] Yaw (deg)	Orifice Area (m^2)	Peak Gage Pressure Left Rear (Pa x 10^5)	Peak Gage Pressure Front Right (Pa x 10^5)	Peak Acceleration X c.g. Pulse	Peak Acceleration X c.g. Acc (G)	Peak Acceleration Z c.g. Pulse	Peak Acceleration Z c.g. Acc (G)	Peak Acceleration Z Front Pulse	Peak Acceleration Z Front Acc (G)	Strap Forces Strap 1 (N)	Strap Forces Strap 2 (N)	Comments
11/21/84	1HII	3.0	5.2	0	0	0		1.01	.81	1st	-.40	Airbag	1.20	Airbag	1.70	0	245	
										2nd	2.0	Bump 1	3.20	Bump 1	6.00			
												Bump 2	.60	Bump 2	.70			
	2HI	4.5	7.8	0	0	0		d	d	1st	d	Airbag	d	Airbag	d	-	-	
										2nd		Bump 1		Bump 1				
												Bump 2		Bump 2				
	2HII	4.5	7.8	0	0	0		1.82	1.11	1st	1.00	Airbag	4.40	Airbag	3.20	178	222	
										2nd	1.80	Bump 1	4.50	Bump 1	4.50			
										3rd	.90	Bump 2	1.20	Bump 2	1.00			
11/26/84	2HIII	4.5	7.8	0	0	0		1.77	1.16	1st	.70	Airbag	4.20	Airbag	3.60	222	0	
										2nd	1.20	Bump 1	3.00	Bump 1	3.80			
										3rd	.60	Bump 2	.50	Bump 2	-.20			
	3HI	6.0	10.4	0	0	0	.00534	3.03	2.12	1st	.9	Airbag	8.20	Airbag	6.10	890	222	
										2nd	4.2/-2.4	Bump 1	2.60	Bump 1	5.00			
												Bump 2	0.0	Bump 2	.50			

[a]positive pitch - nose down
positive roll - roll right (starboard)

[b]data not readable

[c]no data

[d]drop aborted

[e]spike goes to 12+G

TABLE 7. SUMMARY OF TEST RESULTS (Continued)

Drop Date	Drop No.	Desired Impact Velocity Vert (m/s)	Desired Impact Velocity Horz (m/s)	Desired Impact Orientation[a] Roll (deg)	Desired Impact Orientation[a] Pitch (deg)	Desired Impact Orientation[a] Yaw (deg)	Orifice Area (m^2)	Peak Gage Pressure Left Rear ($Pa \times 10^5$)	Peak Gage Pressure Front Right ($Pa \times 10^5$)	Peak Acceleration X c.g. Pulse	Peak Acceleration X c.g. Acc (G)	Peak Acceleration Z c.g. Pulse	Peak Acceleration Z c.g. Acc (G)	Peak Acceleration Z Front Pulse	Peak Acceleration Z Front Acc (G)	Strap Forces Strap 1 (N)	Strap Forces Strap 2 (N)	Comments
11/28/84	5HI	6.0	10.4	0	-10	0	.00534	4.04	4.34	1st	4.80	Airbag	20.60	Airbag	22.00	222	222	Simultaneous
										2nd		Bump 1		Bump 1				Airbag &
											2.0	Bump 2	2.20	Bump 2	2.00			Bump Stop
																		Pulses
	4HI	6.0	10.4	0	+10	0	.00534	2.12	2.32	1st	.50	Airbag	8.10	Airbag	8.50	667	0	
										2nd	1.40	Bump 1	4.40	Bump 1	4.80			
												Bump 2	1.00	Bump 2	1.00			
	6HI	6.0	10.4	+10	0	0	.00534	2.32	2.12	1st	1.00	Airbag	6.80[e]	Airbag	8.00		311	
										2nd		Bump 1	4.20	Bump 1	6.60			
												Bump 2	1.60	Bump 2	0			

[a]positive pitch - nose down
positive roll - roll right (starboard)

[b]data not readable

[c]no data

[d]drop aborted

[e]spike goes t› 12+G

restraining straps. The values listed under "Z c.g." and "Z front" are from the two accelerometers oriented to monitor vertical accelerations--one mounted above the top plate c.g., the other above the right front airbag. The notations "airbag", "bump 1", and "bump 2" are used to distinguish between the peak acceleration pulse due to the airbags and the peaks of consecutive acceleration pulses due to the bump stops. During most of the drops the acceleration pulses caused by the airbags occurred first and had the largest magnitude. The pulses due to the bump stops occurred after the airbag pulses. The first acceleration pulse caused by the bump stops always had a larger magnitude than the pulses that followed. Generally, there was approximately a 0.075-sec. separation between acceleration peaks (see Fig. 26). On drops 5VII, 6VII and 5HI the first acceleration peak due to the bump stops and the airbags occurred simultaneously; no distinction could be made between the two.

On all of the drops conducted, the data traces produced by the accelerometers showed significant oscillations. The frequency of the oscillations was relatively constant, 60-80 cycle/sec. The oscillations occurred immediately after platform release, during airbag pressurization and between bump stop impacts. Vibration of the top plate was the probable cause, as the oscillations only occurred when the top plate was not in contact with a solid object.

In an attempt to gain some insight into the cause of the vibration, the natural frequencies of the top plate were investigated. This investigation was intended only as a "quick look" to determine if the vertical/rotation motions of the top plate exhibited natural frequencies similar to the vibration frequency. In the analysis the bottom was assumed to be resting

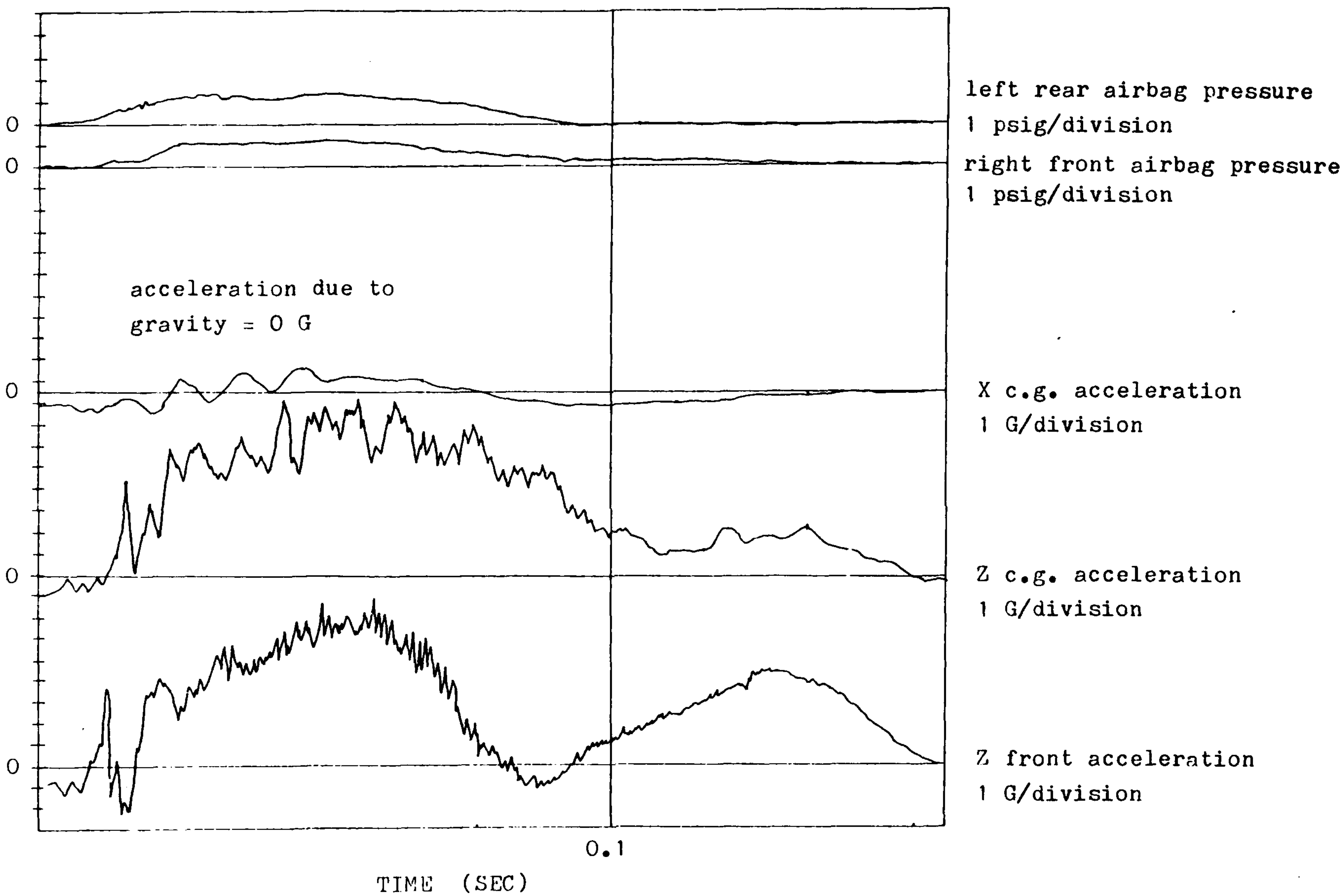

Figure 26. Drop 3V V partial Visicorder data trace.

on the ground. The top plate was restricted to vertical motion and/or rotation about its c.g. (either pitch or roll, each was considered separately). The airbags were modeled as simple springs and the restraining straps were ignored. Thus, the problem was reduced to a degree-of-freedom problem. The results of the analysis did not show any correspondence between these frequencies and the 60-80 cycle/sec vibrations that occurred on the Visicorder data traces.

The maximum forces sensed by the load cells mounted on two of the port side restraining straps are listed under "Strap 1" and "Strap 2". The instrumented straps are shown in Fig. 27. The load cells were used on drops 4V III through 6H I.

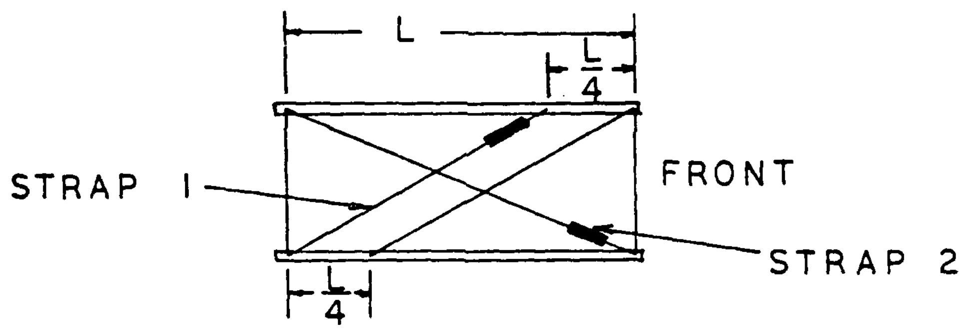

Figure 27. Load cell placement.

Prior to drop 4V III, the wire leads for the load cells were connected to the two contact switches that monitored ground impact of the bottom plate. These two contact switches were disconnected because they added a considerable amount of clutter to the data recordings -- on occasion making it difficult to interpret the data. The switches were not essential, because the accelerometers gave an adequate indication of ground impact. The two contact switches mounted on the bump stops remained connected during all of the drops.

Throughout the testing, the AGARP suffered no significant damage. However, several minor problems were noticed. The hoops inside the airbags slipped a little and were no longer parallel to the airbag ends. The top plate had been allowed to rest on the bump stop for extended periods of time and caused the bump stops to show a small amount of deformation. Towards the end of testing a small nick, 6.35 mm (1/4 in) long, was noticed in the right rear airbag. It did not penetrate completely through the airbag and was not repaired.

The Visicorder used for recording the test data had only nine working data channels. If more data channels had been available, an attempt would have been made to use additional instrumentation: load cells, accelerometers, and pressure transducers.

Orifice Sizing

The purpose of the initial six test drops was to determine the optimum airbag orifice size. The previously mentioned uncertainties in orifice sizing (see CONSTRUCTION) necessitated that the orifice size be determined experimentally. The first six drops were all vertical drops with the platform parallel to the ground at impact. This type of impact results in no strap forces being exerted and the airbags acting without any outside disturbances.

The results of these tests showed that the four orifice holes provided an excessively large orifice area; $0.00713 m^2$ ($11.04 in^2$). The orifice area did not allow a buildup of airbag pressures. As a result, airbag induced accelerations were low. The airbags dissipated only a small amount of the top plate's kinetic energy, and bump stop impact occurred while the top plate was still moving downward at a substantial velocity. The high impact

velocity caused the bump stop induced accelerations to be two to four times greater than those caused by the airbags. The airbag induced accelerations should have been greater than those caused by the bump stops; to produce higher airbag induced acceleration, the orifice area was reduced. Precut pieces of 9.52-mm (3/8-in) thick polypropylene were used to cover one-half of one of the four orifice holes provided for each airbag. Total orifice area was reduced to 0.00623 m^2 (9.66 in^2), approximately equal to the LAND3 predicted optimum orifice area. This modification produced only slightly improved performance. Bump stop induced accelerations were still twice those caused by the airbags. The total orifice area was reduced to 0.00534 m^2 (8.28 in^2) by completely covering one of the four orifice holes provided for each of the airbags. This represented a 25% reduction of the original orifice area and a 16% reduction of the computer predicted optimum orifice area. The result was higher airbag pressures and greatly improved platform performance. The improvement can be seen in the results from drops 3V II. During this drop, ground impact occurred at the maximum vertical velocity expected during actual airdrop. The airbag induced accelerations were greater than those caused by the bump stops. Bump stop induced accelerations were below 10 G. Further reduction of the orifice area was not investigated as the 0.00534 m^2 (8.28 in^2) provided very satisfactory performance.

Maximum Velocity Drops

The remainder of the test drops were used to determine the suitability of the platform for airdrop and to obtain experimental data, which could be compared to data produced by the computer program LAND3. The determination of the platform's suitability for airdrop was based on the evaluation of

eight maximum velocity drops. During the maximum velocity drops, the platform impacted the ground at either the vertical or the combined vertical and horizontal velocity it would have during an actual airdrop. The drops used for the evaluation included the four maximum velocity vertical drops for which complete data recordings were available, drops 3V V, 4V III, 5V II, and 6V II, and the last four swinging drops, drops 3H I, 4H I, 5H I, and 6H I. The last three drops; drops 4H I, 5H I, and 6H I, were selected for comparison with the output from LAND3. These drops were selected because they were representative of actual airdrop conditions and high-speed film was available on all three.

The four maximum velocity vertical drops, 3V V, 4V III, 5V II, and 6V II represented four different impact conditions: flat, nose pitched down 10^{0}, rolled 10^{0}, and nose pitched down 10^{0} with 10^{0} of roll. The four swinging drops, 3H I, 4H I, 5H I, and 6H I were intended to have the following impact conditions: flat, nose pitched down 10^{0}, nose pitched up 10^{0}, and rolled right (starboard) 10^{0}.

During these eight drops it became obvious the four airbags did not begin to pressurize at the same time. Impact conditions and the platform physical characteristics caused the airbags on one side of the platform to begin to pressurize immediately after ground impact and delayed pressurization of the airbags on the opposite side of the platform. When and how much the airbags pressurized was a critical factor in attaining satisfactory platform performance.

On some drops the delay in pressurization of the airbags on one side of the platform was excessive and had an adverse effect on platform performance. A long delay resulted in airbags reaching peak pressures on

one side of the platform, while on the opposite side, bump stop impact was occurring. The effect of the airbag and bump stop forces was additive and caused excessively high accelerations.

During flat impacts, drops 3V V and 3H I, pressurization of the front airbags was delayed until after pressurization of the rear airbag had begun. Delay in pressurization of the front airbags was caused by the unsymmetrical weight distribution of the top plate. The top plate c.g. was slightly more than 76 mm (3 in) to the rear of the geometric center. The rear airbags must decelerate a greater portion of the top plate mass and therefore crush faster and pressurize sooner. The delay in airbag pressurization during this type of impact did not adversely affect platform performance.

During angled impacts, drops 4V III, 5V II, 6V II, 4H I, 5H I, and 6H I, the airbags on the side of the platform that impacted the ground first began to pressurize first. Pressurization of the airbags on the opposite side of the platform was delayed. Delay in pressurization appears to have had at least two causes. The most obvious and probably most significant was the impact angle itself. The airbags are forced to compress when the bottom plate hits the ground. On an angled impact one side of the bottom plate hits the ground first and the airbags on that side begin to pressurize first. The airbags on the opposite side do not begin to pressurize until the part of the bottom plate which is beneath them, impacts the ground. Time is required for the bottom plate to rotate enough for this to occur. The greater the impact angle, the greater the amount of rotation required, and the longer the delay in airbag pressurization.

A second cause for delay in airbag pressurization during angled impacts was airbag volume reduction without a corresponding buildup of pressure.

The mechanism by which this occurred is shown in Fig. 28. Impact occurs on the near side, and bag 2 begins to pressurize. Since airbag 2 has already begun to pressurize, any additional volume reduction will result in an increase in pressure. Airbag 1 does not begin to pressurize during the initial ground impact. The ground and airbag 2 act to rotate the bottom plate towards the ground at a faster rate than the top plate. The difference in rotational rates tends to keep the far side of airbag 1 extended and to compress the side nearest to the impacting edge. At the same time the top plate is also moving in the direction of arrow, A, further deforming airbag 1. These motions occur before the far side of the bottom plate has hit the ground. The result is that the volume of airbag 1 is reduced at a rate which does not cause the airbag to pressurize. At approximately the time the far edge of the bottom plate comes into contact with the ground, the rate of volume change in airbag 1 reaches a level which can cause pressurization of the airbag. However, the amount of air available for pressurization of airbag 1 is less than was available at the initial ground impact. In addition, the fabric on the near side of airbag 1 is loose and must expand outward prior to any pressure increase, wasting part of the compression stroke. The end result is that there is a decrease in the energy dissipating capability of the airbag, and there is a delay in airbag pressurization. The amount of airbag deformation and the delay in pressurization of the airbags increases as the impact angle increases. High-speed film and visicorder data showed that the process illustrated in Fig. 28 did occur on drop 5H I and that the platform performance was adversely affected. This may also have occurred on drops 6V II and 5V II, but high-speed film which could confirm this was not available. On drops 4V

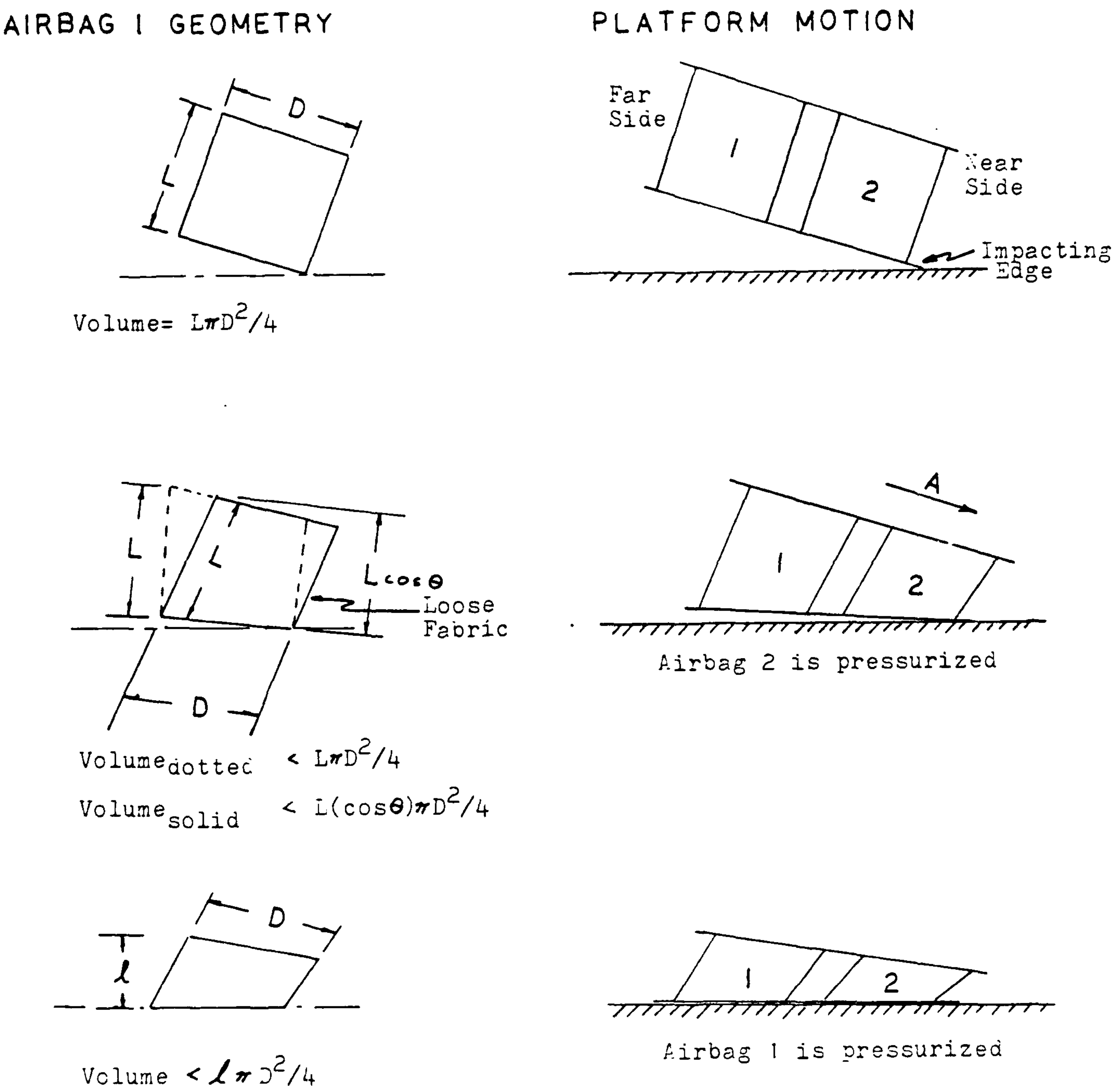

Figure 28. Airbag volume reduction during ground impact.

III, 4H I and 6H I the impact angle and airbag deformation did not adversely affect platform performance.

Table 8 shows the delay in airbag pressurization which occurred during the maximum velocity drops. It can be seen from this table that the flat impacts approached simultaneous airbag pressurization. It can also be seen that during the angled impacts, the delay in pressurization of the airbags farthest from the side of the platform that impacted first increased as the impact angle increased. Table 9 shows the maximum accelerations measured by the two accelerometers mounted above the c.g. of the top plate that result in the maximum combined acceleration. The table lists the fore/aft accelerations, "X c.g."; the vertical accelerations, "Z c.g."; and the combined total, "$((X\ c.g.)^2 + (Z\ c.g.)^2)^{\frac{1}{2}}$". There was no accelerometer to measure accelerations in the port/starboard directions, so the total accelerations for drops 6V II and 6H I were probably higher than is indicated by the table. A more detailed discussion of the eight maximum velocity drops is given below.

Drop 3V V (flat) and 4V III (10^0 nose down) produced the most favorable results of the four vertical drops. In both cases airbag pressures were below 3.03×10^5 Pa (3.0 psig) and vertical accelerations were below 10 G. Examination of the Visicorder data traces showed that the airbag induced acceleration pulses occurred before the acceleration pulses caused by the bump stops (see Fig. 26). On drop 3V V the rear airbags pressurized first, because of the rearward offset

TABLE 8. DELAY IN AIRBAG PRESSURIZATION AFTER GROUND IMPACT

Drop	Impact	Bag	Delay (sec)	Drop	Impact	Bag	Delay (sec)
3V V	Flat	Rear Left	0.006	3HI	Flat	Rear Left	0.008
		Front Right	0.012			Front Right	0.012
4V III	10° Nose Down	Rear Left	0.022	4HI	3.6° Nose Down	Rear Left	0.012
		Front Right	0.006			Front Right	0.003
5V II	10° Roll Right	Rear Left	0.044	5HI	16.1° Nose Up	Rear Left	0.009
		Front Right	0.005			Front Right	0.059
6V II	10° Nose Down	Rear Left	0.025	6HI	6.6° Roll Right	Rear Left	0.014
	10° Roll Left	Front Right	0.031		1.7° Nose Up	Front Right	0.009

TABLE 9. PEAK ACCELERATIONS FOR MAXIMUM COMBINED ACCELERATION

Drop	Orientation	X c.g. (G)	Z c.g. (G)	$[(X\ c.g.)^2 + (Z\ c.g.)^2]^{\frac{1}{2}}$
3V V	Flat	0.0	8.4	8.4
4V III	10° Nose DN	0.3	9.6	9.6
5V II	10° Nose UP	2.5	14.6	14.8
6V II	10° Nose DN 10° Roll LT	0.3	12.0	12.0
3H I	Flat	0.5	8.2	8.2
4H I	3.6° Nose DN	0.4	8.1	8.1
5H I (Z c.g. Spike)	16.1° Nose UP	3.0	20.6	20.8
5H I (Avg. Peak)	16.1° Nose UP	3.2	16.7	17.0
6H I (Z c.g. Spike)	6.6° Roll RT 1.7° Nose UP	1.2	12.0	12.1
6H I (Avg. Peak)	6.6° Roll RT 1.7° Nose UP	2.8	6.8	7.3

of the top plate c.g. However, the delay was small and had a negligible effect on platform performance. On drop 4V III the delay in pressurization of the rear airbags was kept to a minimum by two factors. The side diagonal straps had been tightened so that the top plate was offset 5.08 cm (2 in) behind the bottom plate. The nose down impact tended to cause the top plate to move forward, but the straps restraining it were already under tension and only a limited amount of top plate forward motion was possible. The motion that did occur only caused the airbags to move towards a more cylindrical shape. In addition, the rearward placement of the top plate c.g. tended to shorten the delay in pressurization of the rear airbags. As a result, platform performance during this drop was satisfactory. It should also be noted that although the Strap 1 forces recorded on drop 4V III were less than those recorded on drop 3V V, the drop 4V III forces were of a much longer duration.

Drops 5V II (10° left roll) and 6V II (10° nose down, 10° left roll) produced results that were not as satisfactory as those for drops 3V V and 4V III. On both drops vertical accelerations in excess of 10G were recorded. Examination of the Visicorder data traces showed that on drop 5V II the "Z c.g." accelerometer sensed an acceleration pulse that exceeded 10 G for 0.040 sec, and the "Z front" accelerometer sensed a pulse which exceeded 10 G for 0.015 sec (see Fig. 29). On drop 6V II the "Z c.g." and "Z front" accelerometers sensed acceleration pulses that exceeded 10 G for 0.034 sec and less than 0.001 sec,

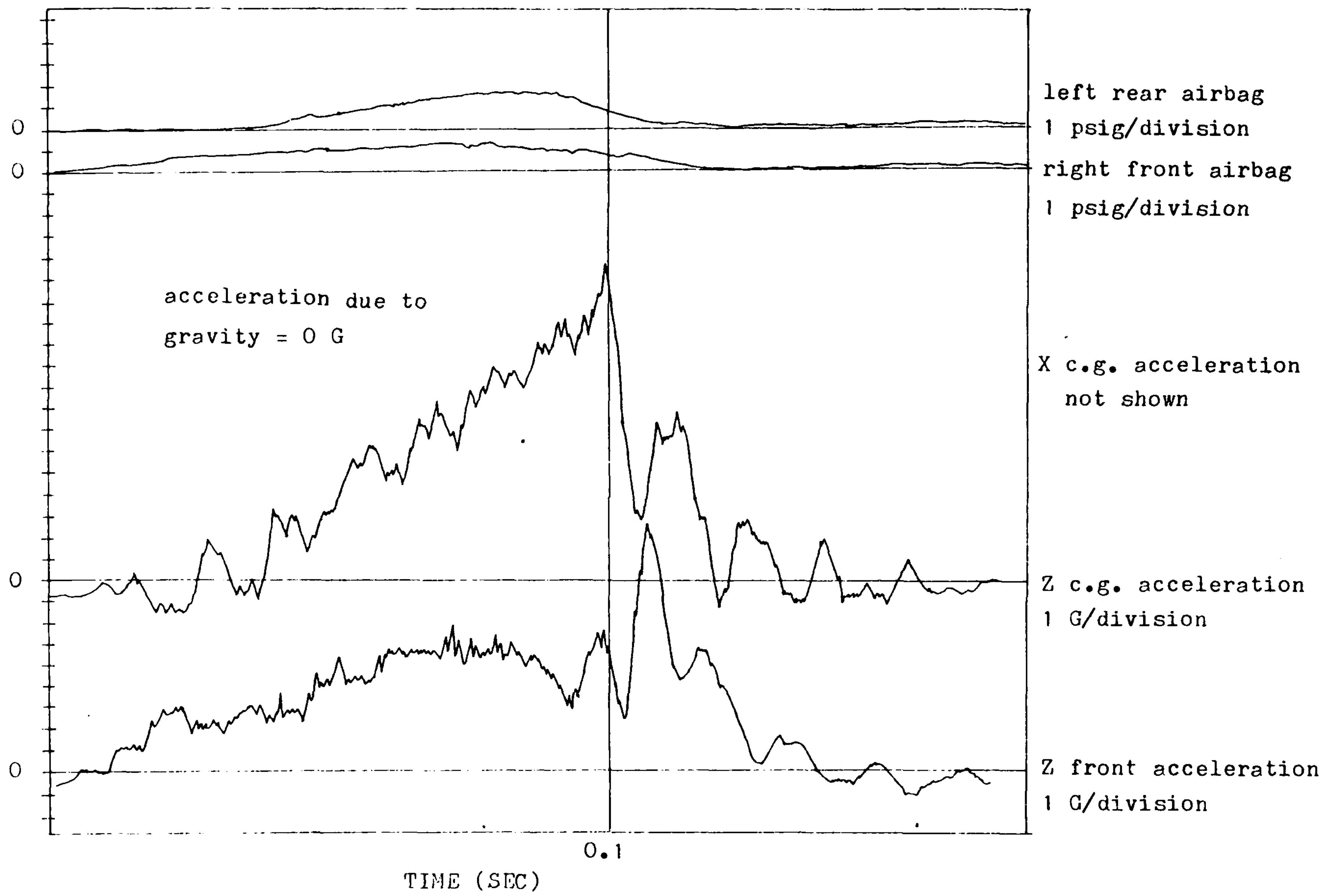

Figure 29. Drop 5V II partial Visicorder data trace.

respectively (see Fig. 30). On both drops, 5V II and 6V II, the "Z c.g." acceleration traces showed no separation between the airbag induced acceleration pulses and the bump stop induced acceleration pulses. The two pulses occurred almost simultaneously, resulting in vertical accelerations of greater than 10 G. On these two drops, delay in pressurization of the airbags--on the side of the platform opposite the one which impacted first--appears to be the reason for the less satisfactory platform performance. Both of the impacts occurred with the platform in a rolled orientation. At ground impact the top plate moved to one side rather than forward or backward. On drop 5V II the final position of the top plate relative to the bottom plate was 0.22 m (8.5 in) at the front end and 0.28 m (11.0 in) at the rear end. On drop 6V II the top plate displacement at the front and rear ends was 0.216 m (8.5 in) and 0.222 m (8.75 in) respectively. The end diagonal straps, those which restrain sideways motion, were intended to be under a slight amount of tension, but they may have actually been slack at ground impact. If the straps allowed the two plates to move in a manner similar to that shown in Fig. 28, it would account for some of the delay in pressurization of the airbags. Another factor to be considered is that the c.g. of the top plate was offset to the rear, not the side. Therefore, weight distribution did not play a part in the rotation of the top plate about the roll axis. Unlike drop 4V III, placement of the top plate c.g. did not shorten the delay in pressurization of the opposite side airbags.

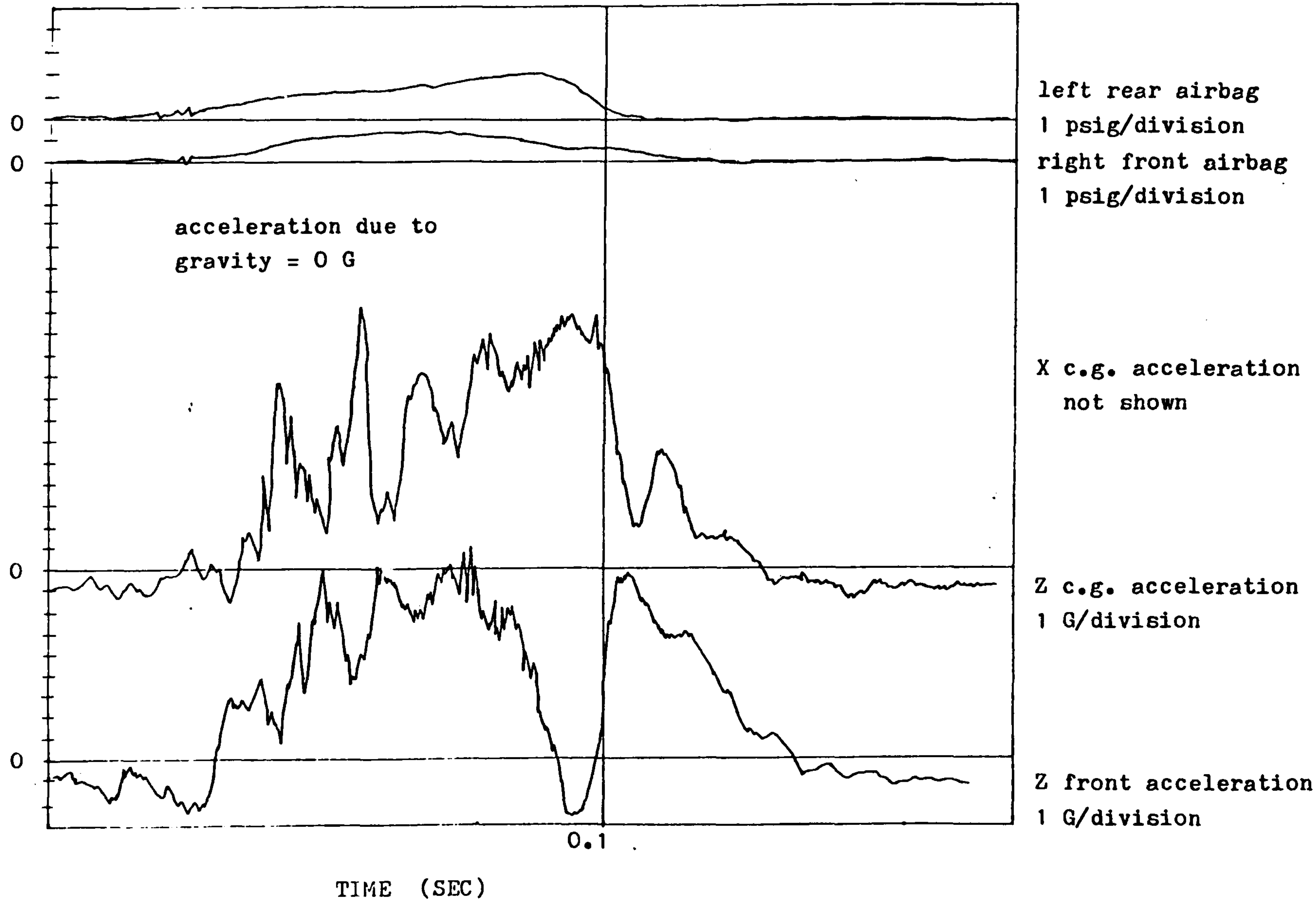

Figure 30. Drop 6V II partial Visicorder data trace.

Note that the side diagonal strap forces, the straps which restrain forward/rearward motion, were somewhat inconsistent for these two drops. The forces for the roll only impact, drop 5V II, were higher than those for the roll and pitch impact, drop 6V II. This is the opposite of what should have occurred. It suggests that either load relief, through knot slippage, occurred at the restraining strap tie-off points, or that the uninstrumented straps were tighter than the instrumented straps and took most of the load. This type of data inconsistency occurred a number of times during the testing.

The four maximum velocity, swinging drops were intended to have the following impact orientations: Drop 3H I--flat, Drop 4H I--10° nose pitch down, Drop 5H I--10° nose pitch up, and Drop 6H I--10° right (starboard) roll. All four drops were intended to have impact velocities of 10 m/s (32.8 ft/s) horizontal and 6 m/s (19.2 ft/s) vertical. The complexity of the experimental setup made attaining exactly these impact conditions almost impossible. However, the actual impact conditions provided useful data.

During the swinging drops, it became obvious that the friction coefficient between the ground and the bottom plate was very low. The friction force was so low that a safety line had to be rigged to the rear of the platform to arrest platform slide before the instrumentation cables were damaged. Review of the high-speed film showed that the deceleration caused by friction corresponded to a friction coefficient of less than 0.1. Various sources list the coefficient of

friction for polypropylene, the lower surface of the bottom plate, as ranging from 0.08 to 0.13, depending upon the opposing material.[12,13] The low friction coefficient was at least partially responsible for the low side strap forces recorded during the swinging drops. There was only a small retarding force exerted on the bottom plate, and as a result its velocity and position remained similar to those of the top plate, and the straps were not subjected to high tension levels. A less smooth impact surface than the one used (a baseball outfield) would result in higher strap forces.

Drops 3H I, 4H I, and 6H I showed the most satisfactory results. The high-speed motion picture film of Drop 3H I did not show the platform just prior to impact, so it was not possible to determine the impact velocities. The film did show a flat impact with almost no motion of the plates relative to one another. The Visicorder data traces showed the airbags beginning to pressurize almost immediately after impact. The airbag and bump-stop induced acceleration pulses were well separated (see Fig. 31). Accelerations were all below 10 G. The AGARP performed exactly as intended.

A review of the high-speed film of Drop 4H I showed the platform orientation and velocity at ground impact were 3.6° nose pitch down, 9.2 m/s (30.2 ft/s) horizontal velocity, and 6.1 m/s (20.0 ft/s) vertical velocity. The Visicorder pressure and acceleration traces were similar to those for Drop 3H I. The major difference was in the strap forces recorded. On Drop 3H I a single spike of 890N (200 lb)

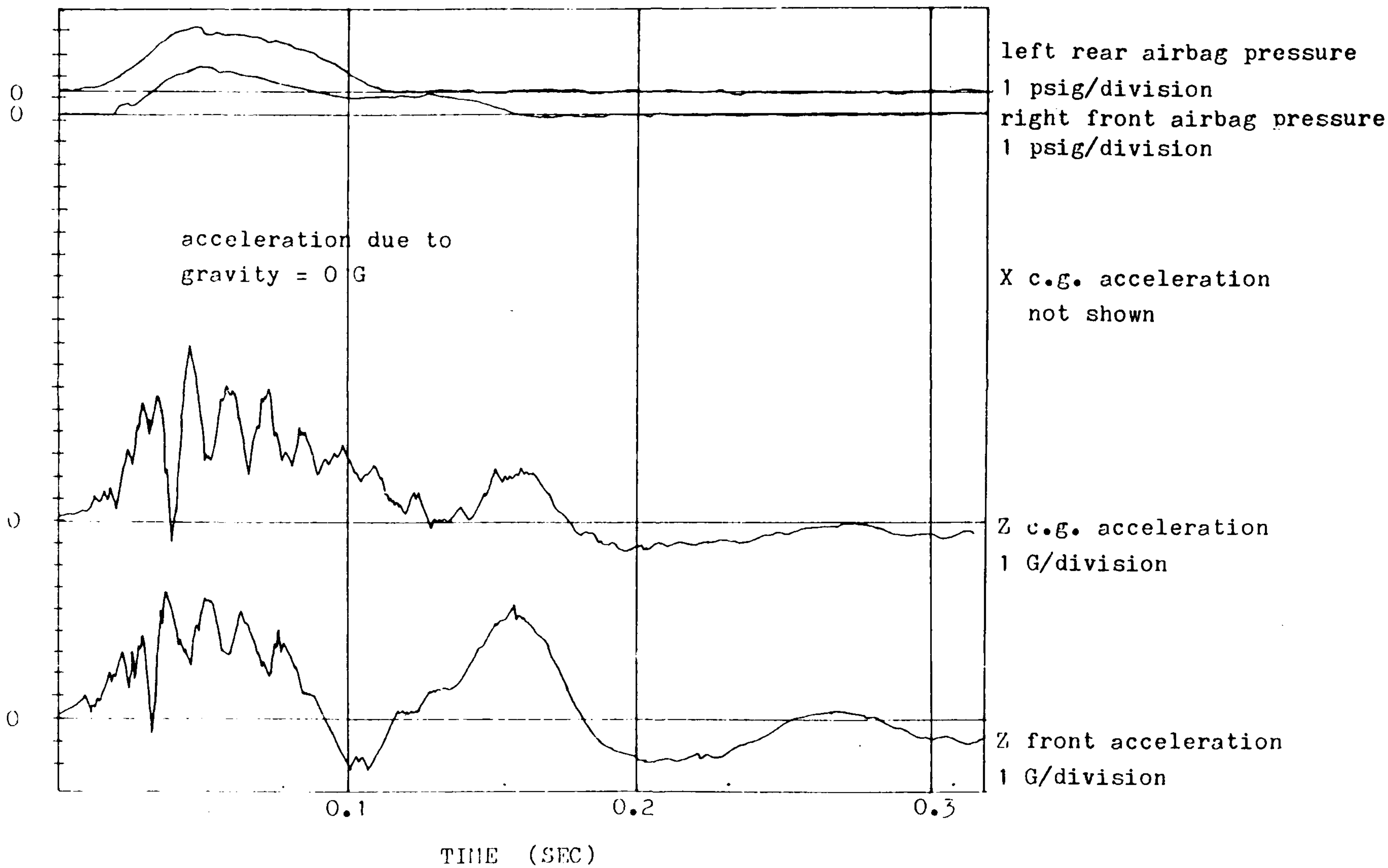

Figure 31. Drop 3H 1 partial Visicorder data trace.

was sensed by the load cell on strap 1. During Drop 4H I this strap exerted forces that peaked at 667 N (150 lb) but which were of significant duration--approximately 0.1 sec. This would be expected from a nose down impact. The overall platform performance was good. The low impact angle was probably responsible for the overall similarity to Drop 3H I.

On Drop 6H I, high speed film showed the impact conditions to be 6.6^{0} right (starboard) roll, 1.7^{0} nose pitch up, 8.85 m/s (29.04 ft/s) horizontal velocity and 6.01 m/s (20.7 ft/s) vertical velocity. This was a roll impact similar to Drops 5V II and 6V II; therefore, prior to performing the drop, the end diagonal straps were checked to make sure they would not be loose at ground impact. This was done to eliminate the large relative motion that occurred on those two drops. Review of the Visicorder data traces showed that the airbags began to pressurize shortly after ground impact and that the airbag and bump stop acceleration pulses were well separated (see Fig. 32). Generally, the acceleration pulses were below 10 G. However, on both the "Z c.g." and "Z front" acceleration traces there was one spike that exceeded 10 G. The duration of the spikes was less than 0.005 sec. These spikes appeared to be the result of the top plate vibrations mentioned at the beginning of this section. The roll impact angle on this drop (6.6^{0}) was less than that for the vertical drops (10^{0}) and probably contributed to the better overall performance.

Drop 5H I yielded the least satisfactory results. The high speed

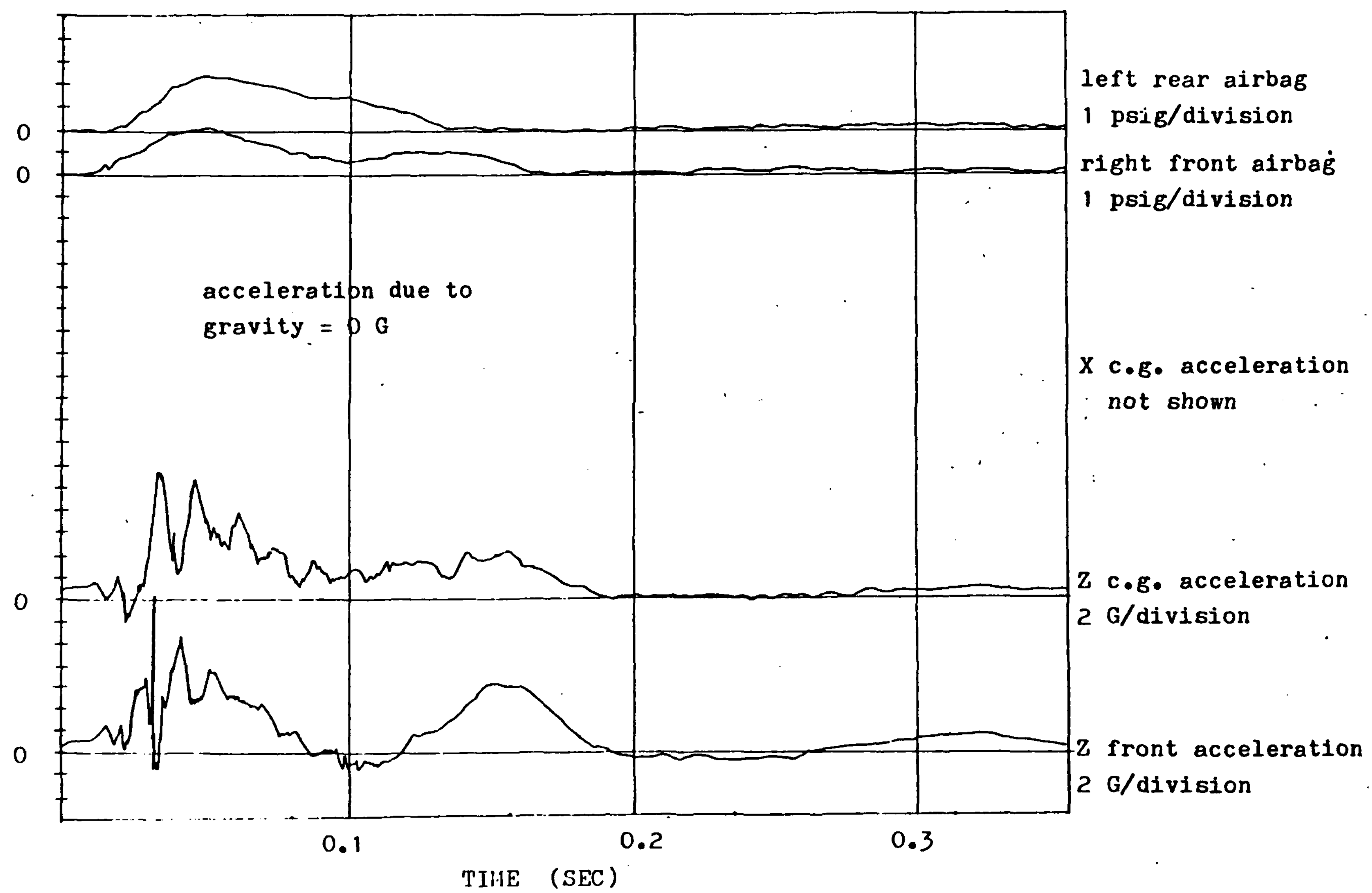

Figure 32. Drop 6H I partial Visicorder data trace.

film of the drop revealed that the impact conditions were 16.1^{o} nose pitch up, 8.4 m/s (27.56 ft/s) horizontal velocity and 6.4 m/s (21.0 ft/s) vertical velocity. The pitch angle was the cause of the less than satisfactory performance, this angle exceeded the design limit by 6.1^{o}. Review of the Visicorder data traces showed that there was a difference of 0.05 sec between the start of pressurization of the rear airbags and the start of pressurization of the front airbags. The airbag and bump stop induced acceleration pulses occurred almost simultaneously and resulted in vertical acceleration spikes of greater than 20 G (see Fig. 33). The duration of the acceleration pulses in excess of 10 G were 0.050 sec and 0.0375 sec for the "Z c.g." and "Z front" accelerometers, respectively. The high-speed film showed that airbag crush occurred as depicted in Fig. 28. The rearward offset c.g. in all likelihood tended to increase the relative motion of the two plates, further increasing the delay in pressurization of the front airbags. The results of this drop could not be considered satisfactory; however, the impact angle was greater than what is normally expected during actual airdrops.

Experiment vs Computer

The experimental data obtained from drops 4H I, 5H I, and 6H I was used for comparison with the output from LAND3. These drops were selected because the impact conditions were similar to conditions that might occur during actual airdrops. In addition, usable high-speed film was available on all three drops.

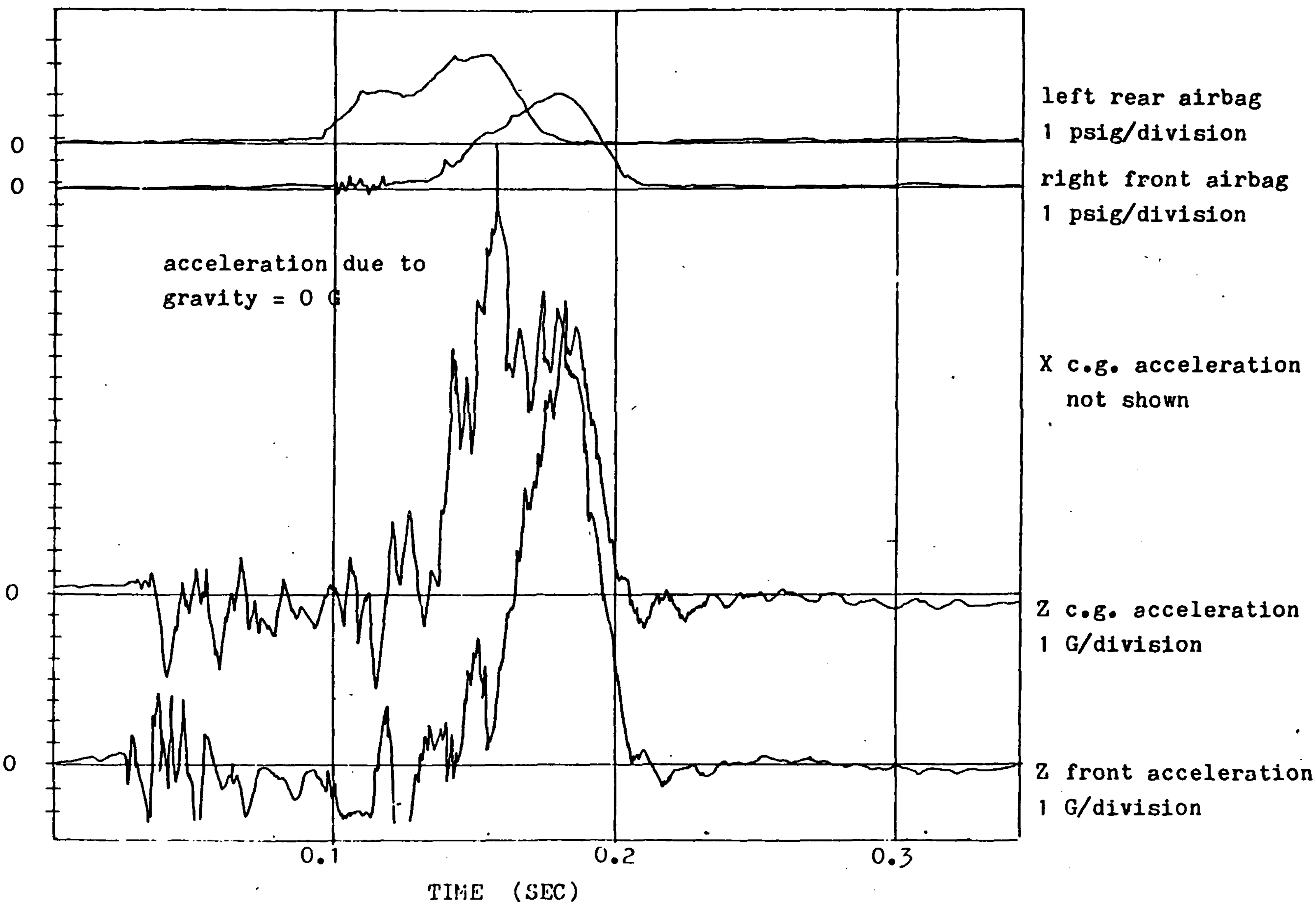

Figure 33. Drop 511 I partial Visicorder data trace.

Experimental data for the comparison was obtained from high-speed film and from Visicorder data traces. The high-speed film was analyzed using a NAC Inc., Film Motion Analyzer linked to a Prime computer. This allowed platform position data to be manipulated in order to obtain the following parameters versus time.

(a) height of the center of the top plate above the ground

(b) vertical velocity of the center of the top plate

(c) horizontal velocity of the center of the top plate

(d) top plate pitch

(e) top plate roll (drop 6H I only).

A combination of averaging and linear regression techniques were used in the calculation of these parameters. The resulting data points were plotted, and a best fit curve was drawn through them. These plots were then digitized and stored on computer tape. The vertical acceleration of the top plate c.g., as well as the airbag pressure data were also digitized and stored on computer tape. This information was taken directly from the Visicorder data traces.

The computer data required for the comparison was obtained by making additional runs of the computer program, LAND3. The initial conditions used for these computer runs were the same as the impact conditions for the three selected test drops. Four computer runs were made for each of the three impact conditions. Each run utilized a different orifice area. The orifice areas used were:

(a) 0.00534 m^2 (8.28 in^2) - the actual AGARP orifice area

(b) 0.00636 m^2 (9.86 in^2) - 19% greater than the AGARP orifice area

(c) 0.00709 m^2 (10.99 in^2) - 33% greater than the AGARP orifice area

(d) 0.00785 m^2 (12.17 in^2) - 47% greater than the AGARP orifice area.

The extra computer runs were made to determine if changing the LAND3 orifice area would yield better agreement between the experimental results and the computer output. The data from each run was stored for latter comparison with the experimental data.

The comparison of the two data sets was made by plotting the experimental data and the LAND3 computer output data on the same graph for each one of the four orifice sizes. A selection of representative graphs for drops 4H I, 5H I, and 6H I are shown in Appendix G. Examination of all the graphs made for the three drops revealed a number of points:

(1) Given a particular parameter, the plots of the experimental and the computed results usually had similar shapes.

(2) The computed initial airbag pressure peaks and the experimental initial airbag pressure peaks occurred at the same time, despite changes to the LAND3 orifice size. The only case where a difference existed was the front airbags on drop 5H I. The experimental data showed a delay in reaching the peak pressure, which the computer program did not predict (see Fig. G-22). This delay was possibly due to the airbag deformation discussed previously (see Fig. 28). The computer program does not model all aspects of this deformation process.

(3) The computed initial acceleration peaks and the experiment initial acceleration peaks occurred at the same time despite changes to the orifice size. Secondary peaks (i.e. bump stop impacts) did not always show a similar correspondence.

(4) The computed data and the experimental data did not show good agreement when the actual AGARP orifice area was used in LAND3. When the actual AGARP orifice area was used in LAND3, the computer program predicted maximum top plate accelerations and airbag pressures which were greater than the experimentally obtained accelerations and pressures. LAND3 also predicted changes in top plate height and vertical velocity, which were less than the experimentally obtained changes in height and vertical velocity--top plate vertical accelerations and the maximum airbag pressures being over-predicted, and the change in the top plate height and vertical velocity being under-predicted. In addition, the computer program did not correctly predict the magnitudes or times of occurrence of the secondary

pressure and acceleration peaks.

(5) Improved agreement between the experimental data and the computer predictions resulted when either the 0.00709 m^2 (10.99 in^2) or the 0.00785 m^2 (12.17 in^2) orifice areas were used in LAND3. The orifice area yielding the best results depended on the drop simulated and the parameter being considered.

(6) Generally, the computer prediction of the top plate height and vertical velocity showed good agreement with the experimental data when the 0.00709 m^2 (10.99 in^2) orifice area was used. The agreement was best prior to bump stop impact, as the computer predicted a larger bump stop rebound than actually occurred. The 0.00785 m^2 (12.17 in^2) orifice area usually yielded the best airbag pressure predictions. The computer prediction of the airbag pressure on the side of the platform impacting the ground first had the highest accuracy. Despite the increased orifice area, LAND3 usually did not accurately predict the pressure in the airbags farthest from the edge that impacted first. Pressures computed by LAND3 were greater than the actual pressures. *If the inaccuracies in the pressure predictions were* great enough, the predicted acceleration would also be greater than the actual experimental values. Proper selection of the LAND3 orifice also resulted in the secondary airbag pressure peaks occurring at the same time in both the experimental results and the computer predictions.

(7) LAND3 consistently predicted a greater maximum pitch angle of the top plate than actually occurred during the tests. The difference between the experimental and the computed pitch curves was possibly the result of the inaccurately predicted airbag pressures. Drop 5H I illustrates the relationship. Drop 5H I showed the best pressure predictions and also showed correspondingly good pitch predictions.

(8) The horizontal velocity showed the least dependence on LAND3 orifice area. The differences in the horizontal velocity curves were probably induced by errors in analyzing the high-speed film. The film was not always of the highest resolution, making exact identification of the required reference points difficult. Also, the nature of the calculation and curve fitting process probably induced some errors.

(9) It was not possible to compare computed restraining strap tension to the actual strap tensions, as the experimental data was unreliable. Tension in the straps can affect airbag crush rate and airbag pressure. However, due to a lack of data it is impossible to state whether or not the strap tension is responsible for the difference between the computed and actual airbag pressures.

(10) In general, as the accuracy of the airbag pressure prediction increased, the overall accuracy of the entire simulation also increased. However, accurate pressure prediction required that the orifice area used in LAND3 be significantly greater than the actual AGARP orifice area.

IMPROVEMENTS - AGARP

A review of the AGARP test results showed that a number of changes could be made to improve platform performance. A change in the method of attaching the restraining straps is the only modification that could be considered necessary before the AGARP is airdropped.

During the AGARP testing, the restraining straps were tied to the top and bottom plates. It was often difficult to tie the straps so that they were all under a slight amount of tension at ground impact. In addition, there was some evidence that the knots used to tie the straps slipped on occasion. The combination of these two factors could cause the motion of one plate with respect to the other to be excessive. An alternative method of attaching the straps is shown in Figure 34.

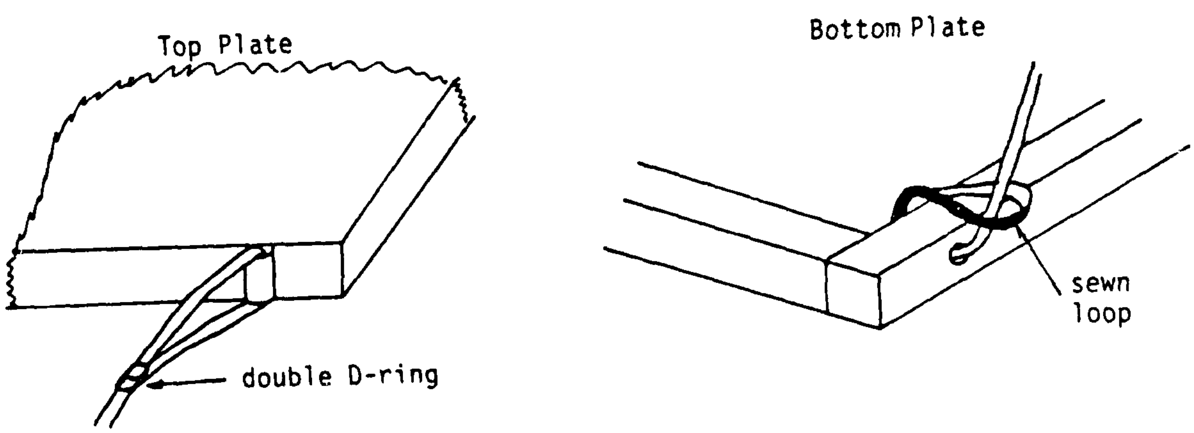

Figure 34. Improved method of restraining strap attachment.

The above arrangement does not require the use of metal on the bottom plate, eliminates knot slippage, and makes strap length adjustment relatively easy.

Currently, the AGARP airbag orifices are simple unobstructed circular holes. This is not the most efficient arrangement. When the airbag collapses part of the compression stroke is used to expand the bag to its maximum extent, then an additional part of the stroke is used to build up pressure in the bag;[14] a large portion of the compression stroke is used before the airbag begins to decelerate the payload. If the airbag is deformed prior to impact or before any significant buildup in pressure occurs, airbag volume will decrease without a corresponding increase in pressure. As a result, the airbag will pressurize after using a greater portion of the compression stroke than if it had remained undeformed. The reason for these problems is that the open orifice holes allow air to escape from the airbags as soon as any airbag deformation occurs; the volume of air that escapes is not available for airbag pressurization. The obvious solution is to stop the air from escaping until a predetermined pressure is reached, or even better, pressurize the bag before it impacts the ground. Pre-pressurizing the airbags would add incredible complexity to the AGARP. Spring loaded orifice hole covers, however, would be a relatively simple modification. Initially, a spring loaded orifice cover would completely cover the orifice hole, blocking any air from escaping. The volume of air inside the bag would not

decrease, much less of the compression stroke would be used in pressurizing the airbag and pressurization of the airbag would take less time. Once the pressure inside the airbag exerted enough force on the orifice cover to overcome the spring force, the cover would open allowing air to escape and the impact energy to be dissipated.[15] The one drawback is that a one-way valve must be provided for airbag inflation. This type of modification would probably have the greatest effect on platform performance during impacts that occurred with the platform at an angle to the ground. The orifices would keep all the air inside the airbags and any deformations would only serve to increase the airbag pressure.

One final improvement to the AGARP could be made by changing the method of securing the nylon hoops inside the airbags. Currently, duct tape is used for this purpose, which is only a temporary solution. One alternative method is to sew small fabric loops to the inside airbag walls and then pass the hoops through them.

LAND3

There are several aspects of the computer program LAND3 which could be modified to increase the accuracy of the simulation. The parts which could be improved are: orifice model and orifice discharge coefficient, calculation of bump stop deflection and energy dissipation, and calculation of airbag volume change.

A comparison of the experimental data and the computer predicted data showed that LAND3 generally predicted pressures greater than the

actual pressures. The use of a LAND3 orifice, which is larger than the actual AGARP orifice, was required to attain agreement between the experimental results and the computer output. Two factors, the orifice model and the orifice discharge coefficient, could have contributed to this discrepancy. The LAND3 orifice model does not duplicate the actual AGARP orifice. LAND3 models one large orifice and direct venting of air to the atmosphere, whereas in the AGARP three orifice holes are used and the air passes through an intermediate chamber before being vented to the atmosphere. The orifice discharge coefficient was experimentally obtained by A. C. Browning for airbags which vent directly to the atmosphere. The discharge coefficient is a function of airbag pressure.[16]

Modification of the orifice model to incorporate the AGARP intermediate chamber would be a complicated process if the chamber does not act as a reservoir. The behavior of the air inside the chamber is an unknown. An alternative approach would be to modify the discharge coefficient. Currently the coefficient is

$$Cd = 0.9 - 0.3/P$$

where

$$P = \frac{\text{Airbag Pressure}}{\text{Atmospheric Pressure}}$$

Perhaps by decreasing the value of 0.3 greater accuracy in the pressure prediction can be obtained, and the need to model the intermediate chamber can be eliminated. The exact change could be determined through trial and error. Modeling of additional orifice holes would

be a relatively simple task.

The bump stop model in LAND3, dissipates less energy than the actual bump stops, and as a result predicts larger top plate rebounds. This problem can be traced to the original bump stop modeling process outlined in Appendix F. Only the deflection part of the curve shown in Fig. F-4 was linearized and inserted into LAND3. The rebound part of the curve was not modeled. Modeling this part of the curve would increase the accuracy of the bump stop model.

One other problem with the current bump stop model is that horizontal motion of the two plates relative to one another is ignored. As a result, the top plate always hits the bump stops, when in fact the relative motion of the two plates may be sufficient for the bump stops to be missed. A method of determining if the top plate actually contacted the bump stops would also improve the accuracy of the bump stop model.

The LAND3 model used for airbag compression and volume change could also be improved upon. Currently, the model does not take into account all aspects of the type of airbag crush shown in Fig. 29. Neither the horizontal motion of the two plates nor the wrinkling of the airbag fabric is modeled. If the wrinkling of the airbag fabric is ignored, it is relatively simple to calculate the change in airbag volume due to the horizontal motion of the plates. However, if the wrinkling is taken into account, the problem becomes extremely complicated. Since these two factors only have a significant effect when

large magnitudes (high angle impacts) are involved, it would probably not be worthwhile to attempt to model the wrinkling of the airbag fabric. If the wrinkling is not modeled, inclusion in the model of the volume change due to the horizontal motion of the plates could probably be accomplished in an acceptable amount of time.

CONCLUSIONS - AGARP

The AGARP demonstrated the ability to dissipate, in a controlled manner, the kinetic energy associated with the landing of a gliding airdrop platform. The results of the test drops indicate that the AGARP should perform well during actual airdrops. A typical ground impact, occurring with less than 10^{0} of platform rotation and with approximately 10 m/s horizontal velocity and 6 m/s vertical velocity, will result in combined total accelerations at the top plate c.g. of less than 15 G and quite possibly less than 10 G. This performance is dependent upon the platform restraining straps being properly rigged and may not be possible if the impact surface is extremely uneven.

Platform rotations of greater than 10^{0} at ground impact will probably result in high accelerations. High impact angles will cause the airbags nearest the impacting edge of the platform to pressurize first. There will, in turn, be a delay in pressurization of the airbags farthest from the impacting edge. As a result the airbags farthest from the impacting edge of the platform will still be exerting significant acceleration forces when the top plate impacts the bump stops nearest the impacting edge of the platform. The effect is additive, the airbag and bump stop forces combine to cause high accelerations. Spring loaded orifice covers may substantially alleviate this problem. Improperly rigged restraining straps can also result in high accelerations. If the straps are loose at ground impact, excessive motion of one plate with respect to the other can occur. The motion of the two

plates could deform the airbags in a manner that adversely affects the energy dissipating capabilities of the airbags. The current method of attaching the restraining straps requires considerable time and effort to assure that all the straps will be under a small amount of tension at ground impact. The alternative method of attaching the straps outlined in the "Improvements" section of this paper would make correct sizing and securing of the straps a much simpler task. Spring loaded orifices would also help to alleviate this problem by preventing air from escaping the airbags during deformations that occur prior to airbag pressurization.

The horizontal forces resulting from bottom plate contact with the ground can be a critical factor in platform performance. These forces retard the sliding motion of the bottom plate and cause the restraining straps to exert forces on the top plate. Restraining strap forces cause most of the horizontal accelerations of the top plate. High retardation forces will cause high top plate accelerations. The horizontal forces exerted on the bottom of the AGARP were not large. This was because the lower surface of the AGARP bottom plate is made of polypropylene, a material with a low friction coefficient. Therefore, on a reasonably smooth surface, this platform will slide extremely well and low horizontal accelerations will result. This was confirmed during the testing. All of the test drops were performed on a baseball outfield, an ideal impact surface; as a result, top plate horizontal accelerations were low. It can probably be assumed that as

impact surface roughness and unevenness increases, the retardation forces on the bottom plate will also increase. Forces seen during impact test on the Natick baseball field were of a small magnitude; for high platform accelerations to occur, the increase in retardation forces would have to be significant.

Although this investigation of the AGARP performance characteristics provided a great deal of useful data, not all aspects of the AGARP's performance were investigated. The platform was not tested with different payload weights, c.g. placements, impact surfaces or an extensive variety of impact orientations. These are areas that merit further investigation, as each one could have an effect on how the platform performs. In addition, nothing has been stated about scaling up AGARP up to a full-size platform. Such a platform would have a greater number of airbags for impact energy dissipation. An increased number of airbags and the larger platform size would probably negate some of the effects of the offset c.g., but further testing would have to be done before any definite statement could be made.

LAND3

LAND3 proved capable of predicting some aspects of the AGARP performance quite well, but also demonstrated deficiencies in predicting other aspects of the platform's performance. In its current form, LAND3 will accurately predict the times of the airbag pressure peaks and the top plate acceleration peaks. After the initial bump stop impact, the accuracy of these predictions will decrease. LAND3

will not always accurately predict the maximum airbag pressures; in general, it will overpredict the pressures. As a result, the top plate height, vertical velocity, and maximum accelerations are not predicted with the highest level of accuracy. The prediction of maximum accelerations are the most susceptible to overpredicted pressures. The top plate height and vertical velocity are the least susceptible. In addition, the bump stop rebound is usually overpredicted by LAND3. There were insufficient data to definitively evaluate how well the strap forces were predicted by the program.

Improved airbag pressure, top plate acceleration, vertical velocity, and height predictions can be obtained if the orifice area used in LAND3 is greater than the actual AGARP orifice area. An increase of 33% above the AGARP orifice area yielded the best LAND3 predictions of the top plate height and vertical velocity. An increase of 47% generally yielded the best LAND3 predictions of top plate accelerations and airbag pressures, although depending on the impact conditions, some of the predicted airbag pressures were still greater than the actual airbag pressures.

Modifications to various elements of the LAND3 program would probably eliminate some if not all of the above mentioned inaccuracies. As mentioned in the "Improvements" section of this paper, a more complete model of the bump stop deflection and corresponding rebound, would improve post bump stop impact predictions made by LAND3. An improved airbag crush model and refined orifice discharge coefficient would result in more accurate top plate acceleration and airbag pressure predictions.

LIST OF REFERENCES

1. Goodrick, Thomas, GLIDE*TFG.LAND Computer Program, ETD, AMED U.S. Army NRDEC, 1979.

2. Browning, A.C., A Theoretical Approach to Airbag Shock Absorber Design (England), Technical Note ME 369, Royal Aircraft Establishment, Farnborough, England, Feb 1963 pp 31-34.

3. Browning, A.C., pp 18, 19.

4. Tomcsack, Stephen L., Decelerator Bag Study, Goodyear Tire and Rubber Co., Akron, Ohio. Special Products Development Department, June 1960 p 25.

5. Bekker, M.G., Introduction to Terrain Vehicle Systems. The University of Michigan Press, Ann Arbor, Michigan, pp 80-90, pp 100-120.

6. Nykvist, William, Unpublished notes on soil deformation, ETD, AMED, U.S. Army NRDEC, Jan 1983.

7. Rosato, Nicholas, Unpublished notes on coefficients of friction for plywood, ETD, AMED, U.S. Army NRDEC, May 1982.

8. Rosato, Nicholas, Unpublished notes on tensile strength of various rubberized fabrics, ETD, AMED, U.S. Army NRDEC, August 1984.

9. Military Specification, Webbing, Textile, Aeromatic Polyanide, High Temperature Resistant, and Nylon, Tubular, MIL-W-81528, April 26, 1967.

10. Tomcsak, Stephen L. p 8.

11. Military Specification, MIL-W-4088J, Webbing Textile, Woven Nylon, December 7, 1984.

12. Baer, Eric, Engineering Design for Plastics. Reinhold Publishing Corp. (Chapman & Hall Ltd, London), 1964 p 736.

13. Bartenev, G.M., V.V. Laurentev, Friction and Wear of Polymers. Translated by D.B. Payne, Elsevier Scientific Publishing Co., NY, 1981 p 81.

14. Tomcsak, Stephen L., p 12.

15. Browning, A.C., p 15.

16. Browning, A.C., p 6.

17. Browning, A.C., p 31-34.

18. Mustin, Gordon S., Theory and Practice of Cushion Design. Shock and Vibration Center, United States Department of Defense, 1968. Special Projects Consultant Inc. p 72, 95.

19. Mustin, Gordon S., p 75.

20. Hilyard, N.C., Mechanics of Cellular Plastics, Macmillan Publishing Co., Inc. NY, 1982 pp 190-191.

This document reports research undertaken at the US Army Natick Research, Development and Engineering Center and has been assigned No. NATICK/TR-87/[illegible] in the series of reports approved for publication.

APPENDIX A

LAND3

Input Variables

APPENDIX A

LAND3 INPUT VARIABLES

Computer Request	Variable Description (Name)
TOP PLATE:	
MASS,	Mass of top plate, including payload, servos guidance mechanism, etc. (TFMS)
INX,	Mass moment of inertia (X-axis) of top plate (TFINX)
INY,	Mass moment of inertia (Y-axis) of top plate (TFINY)
INZ,	Mass moment of inertia (Z-axis) of top plate (TFINZ)
XCG	Distance from top plate X-c.g. to top plate geometric center: measured along X-axis, forward = positive, rearward = negative (XCG)
BOTTOM PLATE:	
MASS,	Mass of bottom plate (BFMS)
INX,	Mass moment of inertia (X-axis) of bottom plate (BFINX)
INY,	Mass moment of inertia (Y-axis) of bottom plate (BFINY)
INZ,	Mass moment of inertia (Z-axis) of bottom plate (BFINZ)
XCG,	Distance from bottom plate Y-c.g. to bottom plate geometric center: measured along X-axis, forward = positive, rearward = negative (XCGB)
XPF,	Distance from top plate c.g. to front attachment points of the end diagonal and vertical straps: measured along X-axis, positive number (XPF)

Computer Request	Variable Description (Name)
XPFB,	Distance from bottom plate c.g. to front attachment points of the end diagonal and vertical straps: measured along X-axis, positive number (XPFB)
XPR,	Distance from top plate c.g. to rear attachment points of the end diagonal and vertical straps: measured along X-axis, negative number (XPR)
XPRB,	Distance from bottom plate c.g. to rear attachment points of end diagonal and vertical straps: measured along X-axis, negative number (XPRB)
YP,	One-half the width of the top plate (YP)
YPB,	One-half the width of the bottom plate (YPB)
ZP,	Distance from top plate c.g. to the bottom of the top plate: measured along Z-axis, negative number (ZP)
HTP,	Distance from top plate c.g. to the top of the top plate: measured along Z-axis, positive number. Not used in calculation, can be arbitrary (HTP)
BUMPER PAD HT.	Height of bump stops (HPAD)
LENGTH/2,	One-half the length of the top plate (TL)
LENGTH B/2,	One-half the length of the bottom plate (BL)
XPANEL,	For computational purposes the top plate is divided into panels. The panels are of equal length and span the width of the plate. There are two airbags for each panel. XPANEL is the length of each panel (XPN)
XPANEL B,	Same as XPANEL, except for bottom plate (XPNB)
NUMBER OF PANELS (2-4)	Number of panels that make up the top and bottom plates, equals one-half the number of airbags desired: 2 panels--4 airbags minimum, 4 panels--8 airbags maximum (NPN)

Computer Request	Variable Description (Name)
BAG DIAMETER,	Airbag diameter--all bags have the same diameter (DB)
ORIFICE DIAMETER,	Airbag orifice diameter--all bags have the same orifice diameter (DO)
BAG HEIGHT	Airbag height--all airbags have the same height (HBO)
HOW MANY STRAPS FOR SIDE? (4 - max)	Number of side diagonal straps on each side of the platform: four straps maximum (NUMSID)
OFFSET OF BOTTOM PLATE	Initial displacement, X-direction, of bottom plate geometric center relative to top plate geometric center: forward = positive, rearward = negative (OFFSET)
ENTER XB(I), XT(I) FOR STRAP ---ENTER ONLY LEFT SIDE	The side strap arrangement of the left and right side of the platform is assumed symmetrical. Left side LEFT SIDE straps are odd numbered, right side straps are even numbered. XB: distance from bottom plate c.g. to bottom plate attachment point (XB(I)) XT: distance from top plate c.g. to top plate attachment point of same strap (XT(I)) Attachment point forward of c.g. = positive number, rearward of c.g. = negative number
STRAP BREAK STRENGTH	Force value selected from Force vs % Elongation graph for the strap material selected. Used along with a corresponding % Elongation value (see below) to calculate a value for strap stiffness (BREAK)
K1G,	Spring constant used to describe ground stiffness (FK1G)
K2G,	Damping coefficient used to describe the ground damping (FK2G)
ELONG-V,	Percent elongation of the vertical straps (ELONGV)
PLIES-V,	Number of plies of material used for vertical straps (PLYSV)

Computer Request	Variable Description (Name)
ELONG-E,	Percent elongation of the diagonal end straps (ELONG E)
PLIES-E,	Number of plies of material used for diagonal end straps (PLYSE)
ELONG-S,	Percent elongation of the side diagonal straps (ELONGS)
PLIES-S	Number of plies of strap material used for the side straps (PLYSS)
DO YOU WANT DAMPING IN THE SLINGS? (0,1)	Input of 0 selects the option of modeling the straps without damping. Any other input will select the option of modeling the straps with damping (DAMPS)
INPUT % OF CRITICAL DESIRED	Sets the damping coefficient of the straps input percentage of the critical damping. Critical damping is calculated automatically by the program and is based on the previously calculated strap stiffness and one-half the mass of the top plate (PCRIT)
MU1,	Ground friction coefficient, X-direction, of edge that digs into ground (FMU1)
MU2,	Ground friction coefficient, X-direction, of edge that does not dig into ground (FMU2)
MU3,	Ground friction coefficient, Y-direction, of edge that digs into ground (FMU3)
MU4,	Ground friction coefficient, Y-direction, of edge that does not dig into ground (FMU4)
TBRAK	Time limit on use of ground friction coefficient of edge that does dig into ground. After limit is exceeded all coefficients are set equal to those used for the edges that do not dig into ground (TBRAK)
BU1,	Bump stop friction coefficient, X-direction (FBU1)

Computer-Request	Variable Description (Name)
BU2,	Bump stop friction coefficient, Y-direction (FBU2)
LANDING NO:	Arbitrary number assigned to computer run by user for reference purposes (ILAND)
ENTER X, Y, Z	Initial position of top plate c.g. defined by X, Y and Z coordinates in the inertial coordinate system. If Z is set so that the airbags are not fully extended at the beginning of the computer run, Z will be redefined so that the bottom plate just touches the ground (X, Y, Z)
VEL COMP: VX=, VY=, VZ=	Initial velocities of the top plate c.g. defined by X, Y and Z velocity components in the inertial coordinate system (XD, YD, ZD)
ORIENTATION: PH=, TH=, SI=	Initial orientation of the top plate defined by roll (PH), pitch (TH) and yaw (SI) rotations in the inertial coordinate system (PH, TH, SI)
ROT VEL COMP: PHD=, THD=, SID=	Initial rotation rates of the top plate defined by roll (PHD), pitch (THD) and yaw (SID) rates in the inertial coordinate system (PHD, THD, SID)
ENTER TILT OF X AXIS	Not modified from original Thomas Goodrick program and is not usable, input value of zero (TILT)
ENTER DTP,	Used along with NLOD and NCAL to calculate the iteration time step, DTC DTO = DTP/NLOD DTC = DTO/NCAL (DTP)
NLOD,	Number of data points calculated in the interval between display of line drawing of platform (NLOD)
NCAL,	Number of iterations made for each data point (NCAL)

Computer Request	Variable Description (Name)
DO YOU WANT RETROS? (0,1)	Input of 0 selects option of not modeling retro rockets, any other input selects option of modeling retro rockets. Not modified from original Thomas Goodrick program. Only input of 0 works (KTHR)
DISPLAY TOTAL TOP SLING FORCES (0) DISPLAY TOTAL BOTTOM SLING FORCES (1)	Allows the choice of assigning either the strap forces at the corners of the top plate or the strap forces at the corners of the bottom plate to output arrays. Only top (0) or bottom (1) forces may be chosen, not both (STRAP)
PAD HT (0) BQ, GEX, GBY, GBZ (1)	Allows the choice of assigning either the heights of the four bump stops or the bottom plate pitch rate (BQ) and c.g. acceleration in X (GBX), Y (GBY) and Z (GBZ) inertial directions to output arrays. Only bump stop height (0) or pitch rate and c.g. acceleration (1) may be chosen, not both (CHZ)
VERT VELOCITY OF TOP CORNERS (0) BPH, BTH, BSI, BP (1)	Allows the choice of assigning either the inertial Z-velocity component of the top plate corners or the bottom plate roll (BPH), pitch (BTH), yaw (BSI) and roll acceleration (BP) to output arrays. Only the velocity of the top plate corners (0) or the bottom plate orientation and roll acceleration (1) may be chosen, not both (CH2)
SEND HT, VV, HV, P, PR, PRES, ACC TO DATA FILE? (0,1)	Input of 1 selects option of sending the numerical values of top plate height, vertical velocity, horizontal velocity, pitch, pitch rate, airbag pressure and two vertical accelerations and the corresponding times to preselected data files numbered 1 through 16.
STD TARGET (0) NEW TARGET (1)	Allows the choice of either standard landing area, L-shaped with 50 ft. obstacle (0) or a new landing area, defined by the user (1) (ITAR)

Computer Request	Variable Description (Name)
X FACTOR, Y FACTOR,	Scaling factors for width and height of the line drawing of platform impact (FX, FY)
XVU, YVU, ZVU	X, Y and Z coordinates, in the inertial coordinate system, of the view point used for the line drawings of the platform impact (XVU, YVU, ZVU)

APPENDIX B

LAND3

Program Listing

GLIDE*TFG(1).LAND3

```
      COMPILER(DIAG=3)
      COMMON D11,D12,D13,D21,D22,D23,D31,D32,D33,
     +      BD11,BD12,BD13,BD21,BD22,BD23,BD31,BD32,BD33,
     +      PH,TH,SI,BTH,BPH,BSI,TAR(6,120),CAR(6,46),
     +      AOUT(86,373),AOT(373),TOUT(373),IIAZ
      DIMENSION TOT(373),XA(373),YA(373)
      DIMENSION RE(8),ICUR(7)
      DIMENSION XSB(20),YSB(20),ZSB(20),XVB(20),YVB(20),
     +          ZVB(20),XST(20),YST(20),ZST(20),XVT(20),
     +          YVT(20),ZVT(20)
      DIMENSION BDEX(4),BDEY(4),BDEZ(4),TDEX(4),
     +          TDEY(4),TDEZ(4),BVXB(4),BVYB(4),BVZB(4),
     +          TVXT(4),TVYT(4),TVZT(4),FGXB(4),FGYB(4),
     +          FGZB(4),BFAB(12),TFAB(12),PCOMP(12),HBAG(12),
     +          TPDX(4),TPDY(4),TPDZ(4),BPDX(4),BPDY(4),
     +          BPDZ(4)
      DIMENSION XT(20),YT(20),ZT(20),XB(20),YB(20),ZB(20),
     +          UT(20),VT(20),ZDT(20),UB(20),VB(20),ZDB(20)
      DIMENSION DES(4),VS(4),BFCX(4),BFCY(4),
     +          BFCZ(4),TFCX(4),TFCY(4),TFCZ(4),BCRL(4),
     +          BCRM(4),BCRN(4),TCRL(4),TCRM(4),TCRN(4),
     +          BFIZ(12),TFIZ(12),BIRL(12),BIRM(12),TIRL(12),
     +          TIRM(12),ZBC(4),TSTRAP(4),BSTRAP(4)
      DIMENSION BSXB(8),BSYB(8),BSZB(8),TSXT(8),TSYT(8),
     +          TSZT(8),SS(8),SDIS(8),FK1S(8),FK2S(8),
     +          BSRL(8),BSRM(8),BSRN(8),TSRL(8),TSRM(8),TSRN(8)
   49 CONTINUE
      CALL TARCAR
      N=28
      NTAR=N
C
      CALL INITT(30)
      CALL ANMODE
C
C     INPUT PLATFORM,AIRBAG AND STRAPS DATA
C
      PRINT 2001
      READ 2,TFMS,TFINX,TFINY,TFINZ,XCG
     +     ,BFMS,BFINX,BFINY,BFINZ,XCGB
      PRINT 2002
      READ 2,XPF,XPR,XPFB,XPRB,YP,YPB,ZP,
     +     HTP,HPAD
      PRINT 2006
      READ 2,TL,BL,XPN,XPNB,NPN
      NAB=2*NPN
      NP=NAB+4
      PRINT 2003
      READ 2,DB,DO,HBO
C
C     SIDE STRAP COORDINATES
C
      PRINT 2013
      READ 2,NUMSID,OFFSET
      OFFSET=OFFSET+(XCG-XCGB)
      I=NP+1
      J=NP+2
```

```
      K=1
      DO 5001 ISN=1,NUMSID
      PRINT 2014,K
      READ 2,XB(I),XT(I)
      YB(I)=YPB
      ZB(I)=0
      YT(I)=YP
      ZT(I)=ZP
      XB(J)=XB(I)
      YB(J)=-YPB
      ZB(J)=0
      XT(J)=XT(I)
      YT(J)=-YP
      ZT(J)=ZP
      K=K+2
      I=I+2
      J=J+2
 5001 CONTINUE
C
C     STRAP SPRING CONSTANTS
C
      PRINT 2015
      READ 2,BREAK
      PRINT 2004
      READ 2,FK1G,FK2G,ELONGV,PLYSV,ELONGE,PLYSE,
     +      ELONGS,PLYSS
       FK1V=PLYSV*BREAK/ELONGV/SQRT(HBO**2+(YP-YPB)**2
     +    +((OFFSET+XPFB)-XPF)**2)
       FK1VR=PLYSV*BREAK/ELONGV/SQRT(HBO**2+(YP-YPB)**2
     +    +((OFFSET+XPRB)-XPR)**2)
       FK1DE=PLYSE*BREAK/ELONGE/SQRT(HBO**2+(YP+YPB)**2
     +    +((OFFSET+XPFB)-XPF)**2)
       FK1DER=PLYSE*BREAK/ELONGE/SQRT(HBO**2+(YP+YPB)**2
     +    +((OFFSET+XPRB)-XPR)**2)
       DO 5002 I=1,NUMSID
       J=NP+(2*I-1)
       SDIS(I)=SQRT(((OFFSET+XB(J))-XT(J))**2+(YB(J)-YT(J))**2+
     +    HBO**2)
       FK1S(I)=PLYSS*BREAK/ELONGS/SDIS(I)
 5002 CONTINUE
      PRINT 2010,FK1DE,FK1DER,FK1V,FK1VR,FK1S(1),FK1S(2),
     +      FK1S(3),FK1S(4)
C
C     STRAP DAMPING COEFFICIENTS
C
      PRINT 2008
      READ 2,DAMPS
      IF(DAMPS.EQ.0)GO TO 222
       PRINT 2011
       READ 2,PCRIT
       FK2DE=PCRIT*SQRT(4*TFMS*FK1DE/2)
       FK2DER=PCRIT*SQRT(4*TFMS*FK1DER/2)
       FK2V=PCRIT*SQRT(4*TFMS*FK1V/2)
       FK2VR=PCRIT*SQRT(4*TFMS*FK1VR/2)
       DO 5003 I=1,NUMSID
       FK2S(I)=PCRIT*SQRT(4*TFMS*FK1S(I)/2)
 5003 CONTINUE
```

```
      PRINT 2009,FK2DE,FK2DER,FK2V,FK2VR,FK2S(1),FK2S(2),
     +      FK2S(3),FK2S(4)
  222 IF(DAMPS.EQ.1)GO TO 221
       FK2DE=0.0
       FK2V=0.0
       DO 5004 I=1,NUMSID
       FK2S(I)=0.0
 5004 CONTINUE
  221 CONTINUE
C
C     GROUND AND BUMPER FRICTION COEFF.
C
      PRINT 2005
      READ 2,FMU1,FMU2,FMU3,FMU4,TBRAK
      PRINT 2012
      READ 2,FBU1,FBU2
C
C     CARGO AND TOP PLATE ARRAY
C
      DO 2050 J=1,14
      IF(CAR(1,J).GT.O) CAR(1,J)=TL+XCG
      IF(CAR(4,J).GT.O) CAR(4,J)=TL+XCG
      IF(CAR(1,J).LT.O) CAR(1,J)=-TL+XCG
      IF(CAR(4,J).LT.O) CAR(4,J)=-TL+XCG
      CAR(2,J)=CAR(2,J)+YP
      CAR(5,J)=CAR(5,J)+YP
      IF(CAR(3,J).EQ.O) CAR(3,J)=ZP
      IF(CAR(3,J).EQ.1) CAR(3,J)=ZP+HTP
      IF(CAR(6,J).EQ.O) CAR(6,J)=ZP
      IF(CAR(6,J).EQ.1) CAR(6,J)=ZP+HTP
 2050 CONTINUE
C
C     BOTTOM PLATE ARRAY
C
      L=14
      DO 2051 J=1,4
      L=L+1
      IF(CAR(1,L).GT.O) CAR(1,L)=BL+XCGB
      IF(CAR(4,L).GT.O) CAR(4,L)=BL+XCGB
      IF(CAR(1,L).LT.O) CAR(1,L)=-BL+XCGB
      IF(CAR(4,L).LT.O) CAR(4,L)=-BL+XCGB
      CAR(2,L)=CAR(2,L)+YPB
      CAR(5,L)=CAR(5,L)+YPB
      CAR(3,L)=0.0
      CAR(6,L)=0.0
 2051 CONTINUE
C
C     INITIALIZE AIRBAG DATA
C
      DT=1.0
      WORK=.000001
      PI=3.1416
      G=9.8
      GMA=1.4
      CK=0.08
      PS=1.894
      PATM=101325.0
```

```
      EK1=(2*GMA)/(GMA-1)
      E1=0.2858
      E2=1/GMA
      E3=(GMA+1)/(2*GMA)
      AO=PI*(DO**2)/4
      AB=PI*(DB**2)/4
      QOUT=AO*340.2787/(AB*SQRT(GMA))
      DO 2053 I=5,NP
      PCOMP(I)=PATM
 2053 CONTINUE
      TOUT(2)=0
      DTO=0.2
      TOUT(3)=0.0
C
C     POSITION AND ORIENTATION DATA
C
 50   PRINT 1
      READ 2,ILAND
      PRINT 1036
      READ 2,X,Y,Z
      PRINT 3
      READ 2,XD,YD,ZD
      PRINT 4
      READ 2,PH,TH,SI
      PRINT 5
      READ 2,PHD,THD,SID
      PRINT 17
      READ 2,TILT
      TILT=TILT*0.01745
      XDT=XD*COS(TILT)+ZD*SIN(TILT)
      ZD=ZD*COS(TILT)-XD*SIN(TILT)
      XD=XDT
      BXD=XD
      BYD=YD
      BZD=ZD
      BPHD=PHD
      BTHD=THD
      BSID=SID
      TH=TH*PI/180.0
      SI=SI*PI/180.0
      PH=PH*PI/180.0
      BTH=TH
      BSI=SI
      BPH=PH
      P=PHD-SID*SIN(TH)
      Q=THD*COS(PH)+SID*(COS(TH)*SIN(PH))
      R=SID*(COS(TH)*COS(PH))-THD*SIN(PH)
      BP=P
      BQ=Q
      BR=R
      XA(2)=X
      YA(2)=Y
      CALL COSINE
      TX=X+ZP*D13
      TY=Y+ZP*D23
      TZ=Z+ZP*D33
      BX=X+OFFSET*D11+(ZP-HBO)*D13
```

```
      BY=Y+OFFSET*D21+(ZP-HBO)*D23
      BZ=Z+OFFSET*D31+(ZP-HBO)*D33
C
C     PLATFORM COORDINATE VALUES
C
      XT(1)=XPF
      XT(2)=XT(1)
      YT(1)=YP
      YT(2)=-YT(1)
      XB(1)=XPFB
      XB(2)=XB(1)
      YB(1)=YPB
      YB(2)=-YB(1)
      XT(3)=XPR
      XT(4)=XT(3)
      YT(3)=YP
      YT(4)=-YT(3)
      XB(3)=XPRB
      XB(4)=XB(3)
      YB(3)=YPB
      YB(4)=-YB(3)
      NP=NAB+4
      DO 2052 I=1,NP
      ZT(I)=ZP
 2052 ZB(I)=0.0
      PNT=NPN+2
      IPNT=PNT
      KK=0
      DO 4004 IPN=1,IPNT
      I=(IPN*2-1)
      J=I+1
      IF(IPN.LE.2)GO TO 4003
      KK=KK+1
      XT(I)=(TL+XCG)+0.5*XPN-(KK*XPN)
      XT(J)=XT(I)
      XB(I)=(BL+XCGB)+0.5*XPNB-(KK*XPNB)
      XB(J)=XB(I)
      YT(I)=YP/2
      YT(J)=-YT(I)
      YB(I)=YPB/2
      YB(J)=-YB(I)
 4003 CONTINUE
 4004 CONTINUE
C
C      STRAP AND AIRBAG ARRAYS
C
C \\\\\\\\\\\\\\\\\\\VERTICAL STRAPS
      DO 2054 JP=1,4
      ILC=18+JP
      CAR(1,ILC)=XT(JP)
      CAR(2,ILC)=YT(JP)
      CAR(3,ILC)=ZT(JP)
      CAR(4,ILC)=XB(JP)
      CAR(5,ILC)=YB(JP)
      CAR(6,ILC)=ZB(JP)
 2054 CONTINUE
C
```

```
      J=1
      K=2
      IK=0
      IJ=0
C
C \\\\\\\\\\\\\\\\\\DIAG END STRAPS
      DO 2056 I=1,2
      IK=IK+1
      ILC1=22+IK
      CAR(1,ILC1)=XT(K)
      CAR(2,ILC1)=YT(K)
      CAR(3,ILC1)=ZT(K)
      CAR(4,ILC1)=XB(K-1)
      CAR(5,ILC1)=YB(K-1)
      CAR(6,ILC1)=ZB(K-1)
      K=K+2
C
      IJ=IK+2
      ILC2=22+IJ
      CAR(1,ILC2)=XT(J)
      CAR(2,ILC2)=YT(J)
      CAR(3,ILC2)=ZT(J)
      CAR(4,ILC2)=XB(J+1)
      CAR(5,ILC2)=YB(J+1)
      CAR(6,ILC2)=ZB(J+1)
      J=J+2
 2056 CONTINUE
C
C \\\\\\\\\\\\\\\\SIDE STRAPS
      NASTRA=2*NUMSID
      DO 2058 IN=1,NASTRA
      ILC3=26+IN
      M=NP+IN
      CAR(1,ILC3)=XT(M)
      CAR(2,ILC3)=YT(M)
      CAR(3,ILC3)=ZT(M)
      CAR(4,ILC3)=XB(M)
      CAR(5,ILC3)=YB(M)
      CAR(6,ILC3)=ZB(M)
 2058 CONTINUE
C
C     TIMING
C
      PRINT 1007
      READ 2,DTP,NLOD,NCAL
      DTO=DTP/NLOD
      DTC=DTO/NCAL
      PRINT 1008,DTO,DTC
C
C     RETROS
C
      PRINT 1028
      READ 2,KTHR
      IF(KTHR.EQ.0) GO TO 1521
      PRINT 1029
      READ 2,ZTH,THR1,THR2,BTIM1,BTIM2
 1521 CONTINUE
```

```
C
C     OUTPUT ARRAY CHOICES
C
      PRINT 2007
      READ 2,STRAP
      PRINT 2016
      READ 2,CH2
      PRINT 2017
      READ 2,CH3
      PRINT 2018
      READ 2,CH4
C
C     DISPLAY: TARGET CHANGES,DATA,VISUALS
C
      IT=2
      T=O
C
C         TARGET ARRAY
C
      PRINT 8
      READ 2,ITAR
      IF(ITAR.EQ.O) GO TO 499
      PRINT 9
      READ 2,N
      NTAR=N
497   PRINT 10
      READ 2,(RE(II),II=1,8)
      IL=RE(1)
      IC=RE(8)
      DO 498 II=2,7
      IIT=II-1
498   TAR(IIT,IL)=RE(II)
      GO TO (497,499),IC
499   CONTINUE
      PRINT 11
      READ 2,FX,FY,XVU,YVU,ZVU
      HOLD=O
      DO 500 J=1,20
      TAR(1,J)=FX*TAR(1,J)
      TAR(4,J)=FX*TAR(4,J)
      TAR(2,J)=FY*TAR(2,J)
      TAR(5,J)=FY*TAR(5,J)
500   CONTINUE
502   CONTINUE
      CALL TINPUT(M)
      CALL ERASE
C
C          OUTPUT DATA
C
      CALL COSINE
      ZIN=O
      DO 55 I=1,4
      ZKK=BZ+D31*XB(I)+D32*YB(I)
      IF(ZKK.LT.ZIN)ZIN=ZKK
55    CONTINUE
      IF(ZIN.GE.O)GO TO [illegible]
      BZ=-ZIN+BZ
```

```
      TZ=-ZIN+TZ
      Z=+ZIN+Z
56    CONTINUE
      AOUT(1,2)=Z
      AOUT(2,2)=PH*180/PI
      AOUT(3,2)=TH*180/PI
      AOUT(4,2)=SI*180/PI
      AOUT(5,2)=XD*COS(SI)+YD*SIN(SI)
      AOUT(6,2)=YD*COS(SI)-XD*SIN(SI)
      AOUT(7,2)=ZD
      AOUT(8,2)=P*180/PI
      AOUT(9,2)=Q*180/PI
      AOUT(10,2)=R*180/PI
      AOUT(20,2)=BZ
      AOUT(21,2)=BPH*180/PI
      AOUT(22,2)=BTH*180/PI
      AOUT(23,2)=BSI*180/PI
      AOUT(24,2)=BXD*COS(BSI)+BYD*SIN(BSI)
      AOUT(25,2)=BYD*COS(BSI)-BXD*SIN(BSI)
      AOUT(26,2)=BZD
      AOUT(27,2)=BP*180/PI
      AOUT(28,2)=BQ*180/PI
      AOUT(29,2)=TPDZ(1)
      TEKIN=TFMS*(XD**2+YD**2+ZD**2)+TFINX*P+TFINY*Q+TFINZ*R
      BEKIN=BFMS*(BXD**2+BYD**2+BZD**2)+BFINX*BP+BFINY*BQ+BFINZ*BR
      TEKINO=TEKIN/2
      BEKINO=BEKIN/2
C     AOUT(17,2)=TEKINO
      AOUT(19,2)=TEKINO
C     AOUT(36,2)=BEKINO
      AOUT(38,2)=BEKINO
60    CONTINUE
C
C     SET UP FOR DISPLAY
C
      CALL SWINDO(100,800,100,600)
      CALL DWINDO(-1.,1.,-0.25,1.25)
      CALL MOVABS(100,100)
      CALL DRWABS(100,700)
      CALL DRWABS(900,700)
      CALL DRWABS(900,100)
      CALL DRWABS(100,100)
      CALL HOME
      CALL ANMODE
      IF(HOLD.GT.1)GO TO 820
      PRINT 1035,ILAND,T
      PRINT 6,X,Y,Z,BX,BY,BZ
      PRINT 1002,AOUT(5,IT),AOUT(6,IT),ZD,AOUT(24,IT),
     +        AOUT(25,IT),BZD
      PRINT 1004,AOUT(2,IT),AOUT(3,IT)
     +        ,AOUT(21,IT),AOUT(22,IT)
      PRINT 1003,AOUT(14,IT),AOUT(15,IT),AOUT(16,IT)
     +        ,TRMC,TRMI
820   CONTINUE
      IF(HOLD.GT.0)GO TO 800
      SI2Y=Y-YVU
      SI2X=X-XVU
```

```
      SI2=ATAN2(SI2Y,SI2X)
  800 CONTINUE
      HOLD=HOLD-1.0
      IF(HOLD.LT.O)HOLD=O
      CALL COSINE
C
C          DISPLAY ARRAYS
C
      XEW=O
      YEW=O
      DO 2064 I=1,4
      ZBC(I)=BZ+BD31*XB(I)+BD32*YB(I)
      J=19+2*I
      J1=J+1
      TUCH=O
      IF(ZBC(I).GT.O) GO TO 2063
      XEW=BX+BD11*XB(I)+BD12*YB(I)
      YEW=BY+BD21*XB(I)+BD22*YB(I)
      TUCH=1
 2063 CONTINUE
      TAR(1,J)=TUCH*(XEW-O.25)
      TAR(2,J)=TUCH*YEW
      TAR(4,J)=TUCH*(XEW+O.25)
      TAR(5,J)=TUCH*YEW
      TAR(1,J1)=TUCH*XEW
      TAR(2,J1)=TUCH*(YEW-O.25)
      TAR(4,J1)=TUCH*XEW
      TAR(5,J1)=TUCH*(YEW+O.25)
 2064 CONTINUE
      ICR=26+NASTRA
      DO 59 I=1,ICR
      LT=NTAR+I
      IF((I.GT.14).AND.(I.LT.19))GO TO 600
      TAR(1,LT)=X+D11*CAR(1,I)+D12*CAR(2,I)+D13*CAR(3,I)
      TAR(2,LT)=Y+D21*CAR(1,I)+D22*CAR(2,I)+D23*CAR(3,I)
      TAR(3,LT)=Z+D31*CAR(1,I)+D32*CAR(2 I)+D33*CAR(3,I)
      IF(I.GT.18)GO TO 602
      TAR(4,LT)=X+D11*CAR(4,I)+D12*CAR(5,I)+D13*CAR(6,I)
      TAR(5,LT)=Y+D21*CAR(4,I)+D22*CAR(5,I)+D23*CAR(6,I)
      TAR(6,LT)=Z+D31*CAR(4,I)+D32*CAR(5,I)+D33*CAR(6,I)
      GO TO 59
  600 TAR(1,LT)=BX+BD11*CAR(1,I)+BD12*CAR(2,I)+BD13*CAR(3,I)
      TAR(2,LT)=BY+BD21*CAR(1,I)+BD22*CAR(2,I)+BD23*CAR(3,I)
      TAR(3,LT)=BZ+BD31*CAR(1,I)+BD32*CAR(2,I)+BD33*CAR(3,I)
  602 TAR(4,LT)=BX+BD11*CAR(4,I)+BD12*CAR(5,I)+BD13*CAR(6,I)
      TAR(5,LT)=BY+BD21*CAR(4,I)+BD22*CAR(5,I)+BD23*CAR(6,I)
      TAR(6,LT)=BZ+BD31*CAR(4,I)+BD32*CAR(5,I)+BD33*CAR(6,I)
   59 CONTINUE
C
C          DISPLAY CALCULATIONS
C
      N=NTAR+ICR
      DO 66 IL=1,N
      XDIF1=TAR(1,IL)-XVU
      YDIF1=TAR(2,IL)-YVU
      ZDIF1=TAR(3,IL)-ZVU
      XDIF2=TAR(4,IL)-XVU
```

```
      YDIF2=TAR(5,IL)-YVU
      ZDIF2=TAR(6,IL)-ZVU
      B1=SQRT(XDIF1**2+YDIF1**2)
      B2=SQRT(XDIF2**2+YDIF2**2)
      ALP=ATAN2(YDIF1,XDIF1)
      BET1=SI2-ALP
      ALP=ATAN2(YDIF2,XDIF2)
      BET2=SI2-ALP
      D1=B1*COS(BET1)
      D2=B2*COS(BET2)
      IF(D1.GE.1.0 .AND. D2.GE.1.0)GO TO 63
      IF(D1.LT.1.0 .AND. D2.LT.1.0)GO TO 66
      IF(D1.GE.1.0) GO TO 61
      XP1=TAN(BET2)
      YP1=ZDIF2/(B2*COS(BET2))
      A=B2*COS(BET2)-B1*COS(BET1)
      A=(B1*SIN(BET1)-B2*SIN(BET2))/A
      XP2=B2*(SIN(BET2)+A*COS(BET2))-A
      YP2=(ZDIF1-ZDIF2)*(B2*COS(BET2)-1)
      YP2=YP2/(B2*COS(BET2)-B1*COS(BET1))
      YP2=YP2+ZDIF2
      GO TO 64
61    XP1=TAN(BET1)
      YP1=ZDIF1/(B1*COS(BET1))
      A=B1*COS(BET1)-B2*COS(BET2)
      A=(B2*SIN(BET2)-B1*SIN(BET1))/A
      XP2=B1*(SIN(BET1)+A*COS(BET1))-A
      YP2=(ZDIF2-ZDIF1)*(B1*COS(BET1)-1)
      YP2=YP2/(B1*COS(BET1)-B2*COS(BET2))
      YP2=YP2+ZDIF1
      GO TO 64
63    XP1=TAN(BET1)
      XP2=TAN(BET2)
      YP1=ZDIF1/(B1*COS(BET1))
      YP2=ZDIF2/(B2*COS(BET2))
64    CONTINUE
      CALL MOVEA(XP1,YP1)
      CALL DRAWA(XP2,YP2)
66    CONTINUE
C
      CALL ANMODE
      CALL BELL
      CALL TINPUT(M)
      IF(M.EQ.49)GO TO 74
      PRINT 1005
      IF(M.EQ.50) GO TO 100
      GO TO 73
74    PRINT 1010
      READ 2,XVU,YVU,ZVU,HOLD
      IF(HOLD.GT.0)CALL ERASE
      IF(HOLD.EQ.0)GO TO 73
      SI2Y=Y-YVU+YD*HOLD/2
      SI2X=X-XVU+XD*HOLD/2
      SI2=ATAN2(SI2Y,SI2X)
73    CONTINUE
C
C      START FORCE CALCULATION CYCLE
```

```
C
      DO 1055 ILOD=1,NLOD
      DO 1050 ICAL=1,NCAL
      CALL COSINE
      U=XD*D11+YD*D21+ZD*D31
      V=XD*D12+YD*D22+ZD*D32
      VW=XD*D13+YD*D23+ZD*D33
      BU=BXD*BD11+BYD*BD21+BZD*BD31
      BV=BXD*BD12+BYD*BD22+BZD*BD32
      BVW=BXD*BD13+BYD*BD23+BZD*BD33
C     FORCE CALCULATIONS
      IF(T.GT.TBRAK) FMU1=FMU2
      IF(T.GT.TBRAK) FMU3=FMU4
      ZDIF=Z+ZP
      IF(ZDIF.GT.ZTH) GO TO 1360
      IF(THTIM.LT.BTIM1) THR=THR1+THR2
      IF(THTIM.GE.BTIM1) THR=THR2
      IF(THTIM.GE.BTIM2) THR=0
      IF(THR.NE.0) FMS=FMS
      THTIM=THTIM+DTC
 1360 CONTINUE
C
      NPTS=NP+NASTRA
      DO 1374 I=1,NPTS
C
C     POSITION AND VELOCITY TOP PLATE COORD. RELATIVE TO GROUND
C
      XST(I)=TX+D11*XT(I)+D12*YT(I)
      YST(I)=TY+D21*XT(I)+D22*YT(I)
      ZST(I)=TZ+D31*XT(I)+D32*YT(I)
      UT(I)=U-YT(I)*R
      VT(I)=V+XT(I)*R
      ZDT(I)=VW-XT(I)*Q+YT(I)*P
      XVT(I)=D11*UT(I)+D12*VT(I)+D13*ZDT(I)
      YVT(I)=D21*UT(I)+D22*VT(I)+D23*ZDT(I)
      ZVT(I)=D31*UT(I)+D32*VT(I)+D33*ZDT(I)
C
C     POSITION AND VELOCITY BOTTOM PLATE COORD. RELATIVE TO GROUND
C
      XSB(I)=BX+BD11*XB(I)+BD12*YB(I)
      YSB(I)=BY+BD21*XB(I)+BD22*YB(I)
      ZSB(I)=BZ+BD31*XB(I)+BD32*YB(I)
      UB(I)=BU-YB(I)*BR
      VB(I)=BV+XB(I)*BR
      ZDB(I)=BVW-XB(I)*BQ+YB(I)*BP
      XVB(I)=BD11*UB(I)+BD12*VB(I)+BD13*ZDB(I)
      YVB(I)=BD21*UB(I)+BD22*VB(I)+BD23*ZDB(I)
      ZVB(I)=BD31*UB(I)+BD32*VB(I)+BD33*ZDB(I)
 1374 CONTINUE
C
C     FORCES AT CORNERS
C
      J=1
      K=2
      DO 1376 I=1,2
C
C
```

```
C          DIAGONAL END STRAPS (TOP LEFT TO BOTTOM RIGHT)
C
      DE12=SQRT((XSB(K-1)-XST(K))**2+(YSB(K-1)-YST(K))**2
     +     +(ZSB(K-1)-ZST(K))**2)
      IF(K.EQ.4)GO TO 7000
      DDE=SQRT(HBO**2+(YP+YPB)**2+((XPFB+OFFSET)-XPF)**2)
      FDE1=FK1DE*(DE12-DDE)
 7000 IF(K.EQ.2)GO TO 7001
      DDE=SQRT(HBO**2+(YP+YPB)**2+((XPRB+OFFSET)-XPR)**2)
      FDE1=FK1DER*(DE12-DDE)
 7001 IF(DE12.LE.DDE)FDE1=0.0
      SDE12X=FDE1*(XST(K)-XSB(K-1))/DE12
      SDE12Y=FDE1*(YST(K)-YSB(K-1))/DE12
      SDE12Z=FDE1*(ZST(K)-ZSB(K-1))/DE12
      DDE12X=FK2DE*(XVT(K)-XVB(K-1))
      DDE12Y=FK2DE*(YVT(K)-YVB(K-1))
      DDE12Z=FK2DE*(ZVT(K)-ZVB(K-1))
      IF(SDE12X.EQ.0.0)DDE12X=0.0
      IF(SDE12Y.EQ.0.0)DDE12Y=0.0
      IF(SDE12Z.EQ.0.0)DDE12Z=0.0
      FDE1XB=SDE12X+DDE12X
      FDE1YB=SDE12Y+DDE12Y
      FDE1ZB=SDE12Z+DDE12Z
      FDE1XT=-FDE1XB
      FDE1YT=-FDE1YB
      FDE1ZT=-FDE1ZB
C
      BDEX(K-1)=BD11*FDE1XB+BD21*FDE1YB+BD31*FDE1ZB
      BDEY(K-1)=BD12*FDE1XB+BD22*FDE1YB+BD32*FDE1ZB
      BDEZ(K-1)=BD13*FDE1XB+BD23*FDE1YB+BD33*FDE1ZB
      TDEX(K)=D11*FDE1XT+D21*FDE1YT+D31*FDE1ZT
      TDEY(K)=D12*FDE1XT+D22*FDE1YT+D32*FDE1ZT
      TDEZ(K)=D13*FDE1XT+D23*FDE1YT+D33*FDE1ZT
      DES(K-1)=SQRT(FDE1XB**2+FDE1YB**2+FDE1ZB**2)
      K=K+2
C
C          DIAGONAL END STRAPS (TOP RIGHT TO BOTTOM LEFT)
C
      DE21=SQRT((XSB(J+1)-XST(J))**2+(YSB(J+1)-YST(J))**2
     +     +(ZSB(J+1)-ZST(J))**2)
      IF(J.EQ.3)GO TO 7002
      DDE=SQRT(HBO**2+(YP+YPB)**2+((XPFB+OFFSET)-XPF)**2)
      FDE2=FK1DE*(DE21-DDE)
 7002 IF(J.EQ.1)GO TO 7003
      DDE=SQRT(HBO**2+(YP+YPB)**2+((XPRB+OFFSET)-XPR)**2)
      FDE2=FK1DER*(DE21-DDE)
 7003 IF(DE21.LE.DDE)FDE2=0.0
      SDE21X=FDE2*(XST(J)-XSB(J+1))/DE21
      SDE21Y=FDE2*(YST(J)-YSB(J+1))/DE21
      SDE21Z=FDE2*(ZST(J)-ZSB(J+1))/DE21
      DDE21X=FK2DE*(XVT(J)-XVB(J+1))
      DDE21Y=FK2DE*(YVT(J)-YVB(J+1))
      DDE21Z=FK2DE*(ZVT(J)-ZVB(J+1))
      IF(SDE21X.EQ.0.0)DDE21X=0.0
      IF(SDE21Y.EQ.0.0)DDE21Y=0.0
      IF(SDE21Z.EQ.0.0)DDE21Z=0.0
      FDE2XB=SDE21X+DDE21X
```

```
      FDE2YB=SDE21Y+DDE21Y
      FDE2ZB=SDE21Z+DDE21Z
      FDE2XT=-FDE2XB
      FDE2YT=-FDE2YB
      FDE2ZT=-FDE2ZB
C
      BDEX(J+1)=BD11*FDE2XB+BD21*FDE2YB+BD31*FDE2ZB
      BDEY(J+1)=BD12*FDE2XB+BD22*FDE2YB+BD32*FDE2ZB
      BDEZ(J+1)=BD13*FDE2XB+BD23*FDE2YB+BD33*FDE2ZB
      TDEX(J)=D11*FDE2XT+D21*FDE2YT+D31*FDE2ZT
      TDEY(J)=D12*FDE2XT+D22*FDE2YT+D32*FDE2ZT
      TDEZ(J)=D13*FDE2XT+D23*FDE2YT+D33*FDE2ZT
      DES(J+1)=SQRT(FDE2XB**2+FDE2YB**2+FDE2ZB**2)
      J=J+2
 1376 CONTINUE
C
      DO 1378 I=1,4
C
C           VERTICAL STRAPS
C
      DV=SQRT((XSB(I)-XST(I))**2+(YSB(I)-YST(I))**2
     +     +(ZSB(I)-ZST(I))**2)
      IF(I.GT.2)GO TO 8000
      DDV=SQRT(HBO**2+(YP-YPB)**2+((XPFB+OFFSET)-XPF)**2)
      FVS=FK1V*(DV-DDV)
 8000 IF(I.LT.3)GO TO 8001
      DDV=SQRT(HBO**2+(YP-YPB)**2+((XPRB+OFFSET)-XPR)**2)
      FVS=FK1VR*(DV-DDV)
 8001 IF(DV.LE.DDV)FVS=0.0
      VSX=FVS*(XST(I)-XSB(I))/DV
      VSY=FVS*(YST(I)-YSB(I))/DV
      VSZ=FVS*(ZST(I)-ZSB(I))/DV
      VDX=FK2V*(XVT(I)-XVB(I))
      VDY=FK2V*(YVT(I)-YVB(I))
      VDZ=FK2V*(ZVT(I)-ZVB(I))
      IF(VSX.EQ.0.0)VDX=0.0
      IF(VSY.EQ.0.0)VDY=0.0
      IF(VSZ.EQ.0.0)VDZ=0.0
      FVXB=VSX+VDX
      FVYB=VSY+VDY
      FVZB=VSZ+VDZ
      FVXT=-FVXB
      FVYT=-FVYB
      FVZT=-FVZB
C
      BVXB(I)=BD11*FVXB+BD21*FVYB+BD31*FVZB
      BVYB(I)=BD12*FVXB+BD22*FVYB+BD32*FVZB
      BVZB(I)=BD13*FVXB+BD23*FVYB+BD33*FVZB
      TVXT(I)=D11*FVXT+D21*FVYT+D31*FVZT
      TVYT(I)=D12*FVXT+D22*FVYT+D32*FVZT
      TVZT(I)=D13*FVXT+D23*FVYT+D33*FVZT
      VS(I)=SQRT(FVXB**2+FVYB**2+FVZB**2)
C
C           GROUND/CORNER
C
      FMUX=0.0
      FDAMP=FK2G
```

```
      IF(ZVB(I).GT.0.0)FDAMP=0.0
      FG=FK1G*(0.0-ZSB(I))-FDAMP*ZVB(I)
      IF(ZSB(I).GT.0.0)FG=0.0
      IF(FG.LT.0.0)FG=0.0
C                                   FRICTION
      IF((UB(I).GT.-0.001).AND.(UB(I).LT.0.001))GO TO 380
      TUB=UB(I)*XB(I)/(ABS(UB(I))*ABS(XB(I)))
      IF(TUB.GT.0)FMUX=-FMU1
      IF(TUB.LT.0)FMUX=-FMU2
380   FMUY=0.0
      IF((VB(I).GT.-0.001).AND.(VB(I).LT.0.001))GO TO 382
      TVB=VB(I)*YB(I)/(ABS(VB(I))*ABS(YB(I)))
      IF(TVB.GT.0)FMUY=-FMU3
      IF(TVB.LT.0)FMUY=-FMU4
382   XDUB=BD11*UB(I)
      YDUB=BD21*UB(I)
      VDBU=SQRT(XDUB**2+YDUB**2)
      XDVB=BD12*VB(I)
      YDVB=BD22*VB(I)
      VDBV=SQRT(XDVB**2+YDVB**2)
      IF(VDBU.LT.0.005)FMUX=0
      IF(VDBV.LT.0.005)FMUY=0
      FFX=(FMUX*XDUB/VDBU+FMUY*XDVB/VDBV)
      FFY=(FMUX*YDUB/VDBU+FMUY*YDVB/VDBV)
      FSZ=FG/(BD13*FFX+BD23*FFY+BD33)
C
      FGXB(I)=FSZ*(BD11*FFX+BD21*FFY+BD31)
      FGYB(I)=FSZ*(BD12*FFX+BD22*FFY+BD32)
      FGZB(I)=FG
C     FXI=FFX*FG
C     FYI=FFY*FG
C     FGXB(I)=FXI*BD11+FYI*BD21+FG*BD31
C     FGYB(I)=FXI*BD12+FYI*BD22+FG*BD32
C     FGZB(I)=FXI*BD13+FYI*BD23+FG*BD33
C
C           BUMPER PAD
C
      FBUX=-FBU1
      FBUY=-FBU2
      UU=0
      VV=0
      PAD1=0.75*HPAD
      PAD2=0.625*HPAD
      PAD3=0.5625*HPAD
      PAD4=0.5*HPAD
      FSPAD1=80032
      FSPAD2=97720
      FSPAD3=142202
      FSPAD4=195440
      FSPAD5=1646008
      CR1=2*SQRT(TFMS*FSPAD1)
      CR2=2*SQRT(TFMS*FSPAD2)
      CR3=2*SQRT(TFMS*FSPAD3)
      CR4=2*SQRT(TFMS*FSPAD4)
      CR5=2*SQRT(TFMS*FSPAD5)
      CRSPAD=ZST(I)-ZSB(I)
      VELPAD=ZVT(I)-ZVB(I)
```

```
C
      IF(CRSPAD.GE.PAD1)GO TO 5501
      IF((CRSPAD.LT.PAD1).AND.(CRSPAD.GE.PAD2))GO TO 5502
      IF((CRSPAD.LT.PAD2).AND.(CRSPAD.GE.PAD3))GO TO 5503
      IF((CRSPAD.LT.PAD3).AND.(CRSPAD.GE.PAD4))GO TO 5504
      IF(CRSPAD.LT.PAD4)GO TO 5505
5501  FSPAD=FSPAD1
      FDPAD=0.025*CR1
      GO TO 5506
5502  FSPAD=FSPAD2
      FDPAD=0.05*CR2
      GO TO 5506
5503  FSPAD=FSPAD3
      FDPAD=0.1*CR3
      GO TO 5506
5504  FSPAD=FSPAD4
      FDPAD=0.2*CR4
      GO TO 5506
5505  FSPAD=FSPAD5
      FDPAD=0.1*CR5
5506  CONTINUE
C
      IF(VELPAD.GT.0.0)FDPAD=0.0
      FPAD=FSPAD*(HPAD-CRSPAD)-FDPAD*VELPAD
      IF(CRSPAD.GT.HPAD)FPAD=0.0
      IF(FPAD.LT.0.0)FPAD=0.0
C                                       FRICTION
      IF((UB(I).GT.-0.001).AND.(UB(I).LT.0.001))UU=UU+1
      IF((UT(I).GT.-0.001).AND.(UT(I).LT.0.001))UU=UU+1
      IF(UU.EQ.2)FBUX=0.0
      IF((VB(I).GT.-0.001).AND.(VB(I).LT.0.001))VV=VV+1
      IF((VT(I).GT.-0.001).AND.(VT(I).LT.0.001))VV=VV+1
      IF(VV.EQ.2)FBUY=0.0
      XDUB=(D11*UT(I))-(BD11*UB(I))
      YDUB=(D21*UT(I))-(BD21*UB(I))
      VDBU=SQRT(XDUB**2+YDUB**2)
      XDVB=(D12*VT(I))-(BD12*VB(I))
      YDVB=(D22*VT(I))-(BD22*VB(I))
      VDBV=SQRT(XDVB**2+YDVB**2)
      IF(VDBU.LT.0.005)FBUX=0
      IF(VDBV.LT.0.005)FBUY=0
      FFX=(FBUX*XDUB/VDBU+FBUY*XDVB/VDBV)
      FFY=(FBUX*YDUB/VDBU+FBUY*YDVB/VDBV)
      TFSZ=FPAD*D33/(D13*FFX+D23*FFY+D33)
      BFSZ=-FPAD*BD33/(BD13*FFX+BD23*FFY+BD33)
C
      TPDX(I)=TFSZ*(D11*FFX+D21*FFY+D31)
      TPDY(I)=TFSZ*(D12*FFX+D22*FFY+D32)
      TPDZ(I)=FPAD*D33
      BPDX(I)=BFSZ*(BD11*FFX+BD21*FFY+BD31)
      BPDY(I)=BFSZ*(BD12*FFX+BD22*FFY+BD32)
      BPDZ(I)=-FPAD*BD33
C     FXI=FFX*FPAD
C     FYI=FFY*FPAD
C     TPDX(I)=FXI*D11+FYI*D21+FPAD*D31
C     TPDY(I)=FXI*D12+FYI*D22+FPAD*D32
C     TPDZ(I)=FXI*D13+FYI*D23+FPAD*D33
```

```
C       BPDX(I)=-FXI*BD11-FYI*BD21-FPAD*BD31
C       BPDY(I)=-FXI*BD12-FYI*BD22-FPAD*BD32
C       BPDZ(I)=-FXI*BD13-FYI*BD23-FPAD*BD33
 1378   CONTINUE
C
C       FORCES AT SIDE STRAPS
C
        DO 5005 NS=1,NASTRA
        I=NP+NS
        LL1=NP+2
        LL2=NP+4
        LL3=NP+6
        LL4=NP+8
        IF(I.LE.LL1)J=1
        IF(I.LE.LL2.AND.I.GT.LL1)J=2
        IF(I.LE.LL3.AND.I.GT.LL2)J=3
        IF(I.LE.LL4.AND.I.GT.LL3)J=4
        DS=SQRT((XSB(I)-XST(I))**2+(YSB(I)-YST(I))**2
       +     +(ZSB(I)-ZST(I))**2)
        FSS=FK1S(J)*(DS-SDIS(J))
        IF(DS.LE.SDIS(J))FSS=0.0
        SSX=FSS*(XST(I)-XSB(I))/DS
        SSY=FSS*(YST(I)-YSB(I))/DS
        SSZ=FSS*(ZST(I)-ZSB(I))/DS
        SDX=FK2S(J)*(XVT(I)-XVB(I))
        SDY=FK2S(J)*(YVT(I)-YVB(I))
        SDZ=FK2S(J)*(ZVT(I)-ZVB(I))
        IF(SSX.EQ.0.0)SDX=0.0
        IF(SSY.EQ.0.0)SDY=0.0
        IF(SSZ.EQ.0.0)SDZ=0.0
        FSXB=SSX+SDX
        FSYB=SSY+SDY
        FSZB=SSZ+SDZ
        FSXT=-FSXB
        FSYT=-FSYB
        FSZT=-FSZB
C
        BSXB(NS)=BD11*FSXB+BD21*FSYB+BD31*FSZB
        BSYB(NS)=BD12*FSXB+BD22*FSYB+BD32*FSZB
        BSZB(NS)=BD13*FSXB+BD23*FSYB+BD33*FSZB
        TSXT(NS)=D11*FSXT+D21*FSYT+D31*FSZT
        TSYT(NS)=D12*FSXT+D22*FSYT+D32*FSZT
        TSZT(NS)=D13*FSXT+D23*FSYT+D33*FSZT
        SS(NS)=SQRT(FSXB**2+FSYB**2+FSZB**2)
 5005   CONTINUE
C
C       FORCES AT INTERIOR POINTS
C
C             AIRBAGS
C
        J=0
        DO 1380 I=5,NP
        AA=0
        BB=0
        CC=0
        AAA=0
        BBB=0
```

```
      CCC=O
      FAB=O
      PP=PCOMP(I)/PATM
      HB=ZST(I)-ZSB(I)
      HBAG(I)=HB
      VTZB=BD13*XVT(I)+BD23*YVT(I)+BD33*ZVT(I)
      VCOMP=VTZB-ZDB(I)
      VCOMP=-VCOMP
      IF(PP.LT.PS)GO TO 384
      AAA=(PS**E1)-1
      BBB=EK1*AAA
      CCC=(SQRT(BBB))*(PP/PS)**E3
      ALPHA=(0.9-(0.3/PS))*CCC
C     ALPHA=PS*(0.9-(0.3/PP))*CCC
      GO TO 386
384   AA=(PP**E1)-1
      BB=EK1*AA
      CC=SQRT(BB)
      ALPHA=(0.9-(0.3/PP))*CC
386   CONTINUE
      BETA=PP**E2
      EPSIL=GMA*PP**E1
      EX=1+CK*(PP-1)
      DPDT1=EX*BETA*VCOMP-ALPHA*QOUT
      DPDT2=(EX/EPSIL+BETA*CK)*HB
      DPDT=DPDT1/DPDT2
      PP=PP+DPDT*DTC
      IF(PP.LT.1)PP=1
      FAB=AB*EX*PATM*(PP-1)
      BFAB(I)=-FAB
      TFAB(I)=FAB
      PCOMP(I)=PP*PATM
1380  CONTINUE
C
C     SUM FORCES AND MOMENTS
C
C           CORNERS
C
      DO 1382 I=1,4
C
      BFCX(I)=BDEX(I)+BVXB(I)+FGXB(I)+BPDX(I)
      BFCY(I)=BDEY(I)+BVYB(I)+FGYB(I)+BPDY(I)
      BFCZ(I)=BDEZ(I)+BVZB(I)+FGZB(I)+BPDZ(I)
      TFCX(I)=TDEX(I)+TVXT(I)+TPDX(I)
      TFCY(I)=TDEY(I)+TVYT(I)+TPDY(I)
      TFCZ(I)=TDEZ(I)+TVZT(I)+TPDZ(I)
C
      SBFCX=BDEX(I)+BVXB(I)
      SBFCY=BDEY(I)+BVYB(I)
      SBFCZ=BDEZ(I)+BVZB(I)
      STFCX=TDEX(I)+TVXT(I)
      STFCY=TDEY(I)+TVYT(I)
      STFCZ=TDEZ(I)+TVZT(I)
      DO 5010 NS=1,NASTRA
      JJ=NP+NS
      IF((XB(JJ).EQ.XB(I)).AND.(YB(JJ).EQ.YB(I)))GO TO 6000
      GO TO 6004
```

```
6000  SBFCX=SBFCX+BSXB(NS)
      SBFCY=SBFCY+BSYB(NS)
      SBFCZ=SBFCZ+BSZB(NS)
6004 IF((XT(JJ).EQ.XT(I)).AND.(YT(JJ).EQ.YT(I)))GO TO 6002
     GO TO 6006
6002  STFCX=STFCX+TSXT(NS)
      STFCY=STFCY+TSYT(NS)
      STFCZ=STFCZ+TSZT(NS)
6006 CONTINUE
5010 CONTINUE
     BSTRAP(I)=SQRT(SBFCX**2+SBFCY**2+SBFCZ**2)
     TSTRAP(I)=SQRT(STFCX**2+STFCY**2+STFCZ**2)
C
     BCRL(I)=BFCZ(I)*YB(I)
     BCRM(I)=-BFCZ(I)*XB(I)
     BCRN(I)=BFCY(I)*XB(I)-BFCX(I)*YB(I)
     TCRL(I)=TFCZ(I)*YT(I)
     TCRM(I)=-TFCZ(I)*XT(I)
     TCRN(I)=TFCY(I)*XT(I)-TFCX(I)*YT(I)
1382 CONTINUE
C
C          INTERIOR POINTS
C
C    J=4
C    K=4
     DO 1384 I=5,NP
C
C    J=J+1
C    K=K+1
C    BFIX(I)=0
C    BFIY(I)=0
     BFIZ(I)=BFAB(I)
C    TFIX(I)=0
C    TFIY(I)=0
     TFIZ(I)=TFAB(I)

     BIRL(I)=BFIZ(I)*YB(I)
     BIRM(I)=-BFIZ(I)*XB(I)
C    BIRN(I)=0
     TIRL(I)=TFIZ(I)*YT(I)
     TIRM(I)=-TFIZ(I)*XT(I)
C    TIRN(I)=0
1384 CONTINUE
C
C          SIDE STRAPS (MOMENTS ONLY)
C
     DO 5011 NS=1,NASTRA
     I=NP+NS
     BSRL(NS)=BSZB(NS)*YB(I)
     BSRM(NS)=-BSZB(NS)*XB(I)
     BSRN(NS)=BSYB(NS)*XB(I)-BSXB(NS)*YB(I)
     TSRL(NS)=TSZT(NS)*YT(I)
     TSRM(NS)=-TSZT(NS)*XT(I)
     TSRN(NS)=TSYT(NS)*XT(I)-TSXT(NS)*YT(I)
5011 CONTINUE
C
C    TOTALS
```

```
C
      BFX1=0
      BFY1=0
      BFZ1=0
      TFX1=0
      TFY1=0
      TFZ1=0
      BRL=0
      BRM=0
      BRN=0
      TRL=0
      TRM=0
      TRN=0
      BFX1C=0
      BFY1C=0
      BFZ1C=0
      TFX1C=0
      TFY1C=0
      TFZ1C=0
      BRLC=0
      BRMC=0
      BRNC=0
      TRLC=0
      TRMC=0
      TRNC=0
      BFX1I=0
      BFY1I=0
      BFZ1I=0
      TFX1I=0
      TFY1I=0
      TFZ1I=0
      BRLI=0
      BRMI=0
      BRNI=0
      TRLI=0
      TRMI=0
      TRNI=0
      BFX1S=0
      BFY1S=0
      BFZ1S=0
      TFX1S=0
      TFY1S=0
      TFZ1S=0
      BRLS=0
      BRMS=0
      BRNS=0
      TRLS=0
      TRMS=0
      TRNS=0
C ///////////////////////////CORNERS
      DO 1386 I=1,4
      BFX1C=BFX1C+BFCX(I)
      BFY1C=BFY1C+BFCY(I)
      BFZ1C=BFZ1C+BFCZ(I)
      TFX1C=TFX1C+TFCX(I)
      TFY1C=TFY1C+TFCY(I)
      TFZ1C=TFZ1C+TFCZ(I)
```

```
C
      BRLC=BRLC+BCRL(I)
      BRMC=BRMC+BCRM(I)
      BRNC=BRNC+BCRN(I)
      TRLC=TRLC+TCRL(I)
      TRMC=TRMC+TCRM(I)
      TRNC=TRNC+TCRN(I)
 1386 CONTINUE
C
C ///////////////////////////INTERIORS
      DO 1388 I=5,NP
C     BFX1I=BFX1I+
C     BFY1I=BFY1I+
      BFZ1I=BFZ1I+BFIZ(I)
C     TFX1I=TFX1I+
C     TFY1I=TFY1I+
      TFZ1I=TFZ1I+TFIZ(I)
C
      BRLI=BRLI+BIRL(I)
      BRMI=BRMI+BIRM(I)
C     BRNI=BRNI+
      TRLI=TRLI+TIRL(I)
      TRMI=TRMI+TIRM(I)
C     TRNI=TRNI+
 1388 CONTINUE
C
C ///////////////////////////SIDES
      DO 5012 NS=1,NASTRA
      BFX1S=BFX1S+BSXB(NS)
      BFY1S=BFY1S+BSYB(NS)
      BFZ1S=BFZ1S+BSZB(NS)
      TFX1S=TFX1S+TSXT(NS)
      TFY1S=TFY1S+TSYT(NS)
      TFZ1S=TFZ1S+TSZT(NS)
C
      BRLS=BRLS+BSRL(NS)
      BRMS=BRMS+BSRM(NS)
      BRNS=BRNS+BSRN(NS)
      TRLS=TRLS+TSRL(NS)
      TRMS=TRMS+TSRM(NS)
      TRNS=TRNS+TSRN(NS)
 5012 CONTINUE
C ///////////////////////////TOTAL
C
      BFX1=BFX1C+BFX1I+BFX1S
      BFY1=BFY1C+BFY1I+BFY1S
      BFZ1=BFZ1C+BFZ1I+BFZ1S
      TFX1=TFX1C+TFX1I+TFX1S
      TFY1=TFY1C+TFY1I+TFY1S
      TFZ1=TFZ1C+TFZ1I+TFZ1S
C
      BRL=BRLC+BRLI+BRLS
      BRM=BRMC+BRMI+BRMS
      BRN=BRNC+BRNI+BRNS
      TRL=TRLC+TRLI+TRLS
      TRM=TRMC+TRMI+TRMS
      TRN=TRNC+TRNI+TRNS
```

```
C
C
C
C     ITERATION CYCLE
C
C           BOTTOM PLATE
C
      BFX=(BFX1)*D11+(BFY1)*D12+(BFZ1)*D13-BFMS*G*SIN(TILT)
      BFY=(BFX1)*D21+(BFY1)*D22+(BFZ1)*D23
      BFZ=(BFX1)*D31+(BFY1)*D32+(BFZ1)*D33-BFMS*G*COS(TILT)
      BPD=(BRL/BFINX)-(BFINZ-BFINY)*BQ*BR/BFINX
      BQD=(BRM/BFINY)-(BFINX-BFINZ)*BP*BR/BFINY
      BRD=(BRN/BFINZ)-(BFINY-BFINX)*BP*BQ/BFINZ
      BPA=BP+BPD*DTC
      BQA=BQ+BQD*DTC
      BRA=BR+BRD*DTC
      BCTH=COS(BTH)
      IF(BCTH.EQ.0) BTH=BTH+0.000001
      BPHDA=BPA+TAN(BTH)*(BQA*SIN(BPH)+BRA*COS(BPH))
      BTHDA=BQA*COS(BPH)-BRA*SIN(BPH)
      BSIDA=(BRA*COS(BPH)+BQA*SIN(BPH))/COS(BTH)
      BPHA=BPH+(BPHD+BPHDA)*DTC/2.0
      BTHA=BTH+(BTHD+BTHDA)*DTC/2.0
      BCTHA=COS(BTHA)
      IF(BCTHA.EQ.0) BTHA=BTHA+0.000001
      BSIA=BSI+(BSIDA+BSID)*DTC/2.0
      BPHDA=BPA+TAN(BTHA)*(BQA*SIN(BPHA)+BRA*COS(BPHA))
      BTHDA=BQA*COS(BPHA)-BRA*SIN(BPHA)
      BSIDA=(BRA*COS(BPHA)+BQA*SIN(BPHA))/COS(BTHA)
      BPH=BPH+(BPHD+BPHDA)*DTC/2.0
      BTH=BTH+(BTHD+BTHDA)*DTC/2.0
      BSI=BSI+(BSID+BSIDA)*DTC/2.0
      BPHD=BPHDA
      BTHD=BTHDA
      BSID=BSIDA
      BXDA=BXD+BFX*DTC/BFMS
      BYDA=BYD+BFY*DTC/BFMS
      BZDA=BZD+BFZ*DTC/BFMS
      BX=BX+(BXD+BXDA)*DTC/2.0
      BY=BY+(BYD+BYDA)*DTC/2.0
      BZ=BZ+(BZD+BZDA)*DTC/2.0
      BEKIN=BFMS*(BXD**2+BYD**2+BZD**2)
      BEKIN=BEKIN+BFINX*BPA**2+BFINY*BQA**2+BFINZ*BRA**2
      BEKINO=BEKIN/2.0
      BWORK=BWORK+(BFX*(BXD+BXDA)+BRL*(BP+BPA))*DTC/2.0
      BWORK=BWORK+(BFY*(BYD+BYDA)+BRM*(BQ+BQA))*DTC/2.0
      BWORK=BWORK+(BFZ*(BZD+BZDA)+BRN*(BR+BRA))*DTC/2.0
      BP=BPA
      BQ=BQA
      BR=BRA
      BXD=BXDA
      BYD=BYDA
      BZD=BZDA
C
C           TOP PLATE
C
C     TFZ1=TFZ1+THR
```

```
      TFX=(TFX1)*D11+(TFY1)*D12+(TFZ1)*D13-TFMS*G*SIN(TILT)
      TFY=(TFX1)*D21+(TFY1)*D22+(TFZ1)*D23
      TFZ=(TFX1)*D31+(TFY1)*D32+(TFZ1)*D33-TFMS*G*COS(TILT)
      PD=(TRL/TFINX)-(TFINZ-TFINY)*Q*R/TFINX
      QD=(TRM/TFINY)-(TFINX-TFINZ)*P*R/TFINY
      RD=(TRN/TFINZ)-(TFINY-TFINX)*P*Q/TFINZ
      PA=P+PD*DTC
      QA=Q+QD*DTC
      RA=R+RD*DTC
      CTH=COS(TH)
      IF(CTH.EQ.O) TH=TH+0.000001
      PHDA=PA+TAN(TH)*(QA*SIN(PH)+RA*COS(PH))
      THDA=QA*COS(PH)-RA*SIN(PH)
      SIDA=(RA*COS(PH)+QA*SIN(PH))/COS(TH)
      PHA=PH+(PHD+PHDA)*DTC/2.0
      THA=TH+(THD+THDA)*DTC/2.0
      CTHA=COS(THA)
      IF(CTHA.EQ.O) THA=THA+0.000001
      SIA=SI+(SIDA+SID)*DTC/2.0
      PHDA=PA+TAN(THA)*(QA*SIN(PHA)+RA*COS(PHA))
      THDA=QA*COS(PHA)-RA*SIN(PHA)
      SIDA=(RA*COS(PHA)+QA*SIN(PHA))/COS(THA)
      PH=PH+(PHD+PHDA)*DTC/2.0
      TH=TH+(THD+THDA)*DTC/2.0
      SI=SI+(SID+SIDA)*DTC/2.0
      PHD=PHDA
      THD=THDA
      SID=SIDA
      XDA=XD+TFX*DTC/TFMS
      YDA=YD+TFY*DTC/TFMS
      ZDA=ZD+TFZ*DTC/TFMS
      X=X+(XD+XDA)*DTC/2.0
      Y=Y+(YD+YDA)*DTC/2.0
      Z=Z+(ZD+ZDA)*DTC/2.0
      TX=TX+(XD+XDA)*DTC/2.0
      TY=TY+(YD+YDA)*DTC/2.0
      TZ=TZ+(ZD+ZDA)*DTC/2.0
      TEKIN=TFMS*(XD**2+YD**2+ZD**2)
      TEKIN=TEKIN+TFINX*PA**2+TFINY*QA**2+TFINZ*RA**2
      TEKINO=TEKIN/2.0
      TWORK=TWORK+(TFX*(XD+XDA)+TRL*(P+PA))*DTC/2.0
      TWORK=TWORK+(TFY*(YD+YDA)+TRM*(Q+QA))*DTC/2.0
      TWORK=TWORK+(TFZ*(ZD+ZDA)+TRN*(R+RA))*DTC/2.0
      P=PA
      Q=QA
      R=RA
      XD=XDA
      YD=YDA
      ZD=ZDA
      T=T+DTC
      WORK=BWORK+TWORK
      EKIN=BEKIN+TEKIN
 1049 CONTINUE
C
C     END OF ITERATION CYCLE
C
 1050 CONTINUE
```

```
C
C     OUTPUT ARRAYS
C
      IT=IT+1
      XA(IT)=X
      YA(IT)=Y
      TOUT(IT)=T
      AOUT(1,IT)=Z
      AOUT(2,IT)=PH*180/PI
      AOUT(3,IT)=TH*180/PI
      AOUT(4,IT)=SI*180/PI
      VH=SQRT(XD**2+YD**2)
      AOUT(5,IT)=XD*COS(SI)+YD*SIN(SI)
      AOUT(6,IT)=YD*COS(SI)-XD*SIN(SI)
      AOUT(7,IT)=ZD
      AOUT(8,IT)=P*180/PI
      AOUT(9,IT)=Q*180/PI
      AOUT(10,IT)=R*180/PI
      AOUT(14,IT)=TFX1/(TFMS*G)
      AOUT(15,IT)=TFY1/(TFMS*G)
      AOUT(16,IT)=TFZ1/(TFMS*G)
      IF(CH3.EQ.0)GO TO 5513
      AOUT(21,IT)=BPH*180/PI
      AOUT(22,IT)=BTH*180/PI
      AOUT(23,IT)=BSI*180/PI
      AOUT(27,IT)=BP*180/PI
5513  IF(CH3.EQ.1)GO TO 5512
      AOUT(21,IT)=ZVT(1)
      AOUT(22,IT)=ZVT(2)
      AOUT(23,IT)=ZVT(3)
      AOUT(27,IT)=ZVT(4)
5512  CONTINUE
      AOUT(11,IT)=PD
      AOUT(12,IT)=QD
      AOUT(13,IT)=RD
      AOUT(20,IT)=BZ
      BVH=SQRT(BXD**2+BYD**2)
      AOUT(24,IT)=BXD*COS(BSI)+BYD*SIN(BSI)
      AOUT(25,IT)=BYD*COS(BSI)-BXD*SIN(BSI)
      AOUT(26,IT)=BZD
      IF(CH2.EQ.1)GO TO 5510
      AOUT(28,IT)=ZST(1)-ZSB(1)
      AOUT(33,IT)=ZST(2)-ZSB(2)
      AOUT(34,IT)=ZST(3)-ZSB(3)
      AOUT(35,IT)=ZST(4)-ZSB(4)
5510  IF(CH2.EQ.0)GO TO 5511
      AOUT(28,IT)=BQ*180/PI
      AOUT(33,IT)=BFX1/(BFMS*G
      AOUT(34,IT)=BFY1/(BFMS*G)
      AOUT(35,IT)=BFZ1/(BFMS*G)
5511  CONTINUE
      AOUT(29,IT)=TPDZ(1)
      AOUT(30,IT)=TPDZ(2)
      AOUT(31,IT)=TPDZ(3)
      AOUT(32,IT)=TPDZ(4)
      IAT=38
      DO 4055 I=1,4
```

```
      IAT1=IAT+I
      AOUT(IAT1,IT)=TPDX(I)
      IAT2=IAT1+4
      AOUT(IAT2,IT)=DES(I)
      IAT3=IAT1+8
      AOUT(IAT3,IT)=VS(I)
      IAT4=IAT1+12
      IF(STRAP.EQ.1)GO TO 250
       AOUT(IAT4,IT)=TSTRAP(I)
  250  IF(STRAP.EQ.0)GO TO 251
       AOUT(IAT4,IT)=BSTRAP(I)
  251 CONTINUE
 4055 CONTINUE
      DO 4060 NS=1,NASTRA
      IST1=54+NS
      AOUT(IST1,IT)=SS(NS)
 4060 CONTINUE
      MM1=0
      MM2=0
      MM3=0
      IBT=62
      MMM=4
      KX=0
      KY=-4
      DO 4056 I=1,8
      KX=KX+1
      KY=KY+1
      MMM=MMM+1
      MM1=MM1+1
      IBT1=IBT+MM1
      AOUT(IBT1,IT)=(PCOMP(MMM)-PATM)+14.7/PATM
      MM2=MM1+8
      IBT2=IBT+MM2
      IF(KX.GT.4)GO TO 4057
      AOUT(IBT2,IT)=XST(KX)-XSB(KX)
 4057 IF(KY.LT.1)GO TO 4058
      AOUT(IBT2,IT)=YST(KY)-YSB(KY)
 4058 CONTINUE
      MM3=MM2+8
      IBT3=IBT+MM3
      AOUT(IBT3,IT)=HBAG(MMM)
 4056 CONTINUE
      AOUT(17,IT)=FGZB(1)
      AOUT(18,IT)=FGZB(2)
      AOUT(19,IT)=TEKINO+TWORK
      AOUT(36,IT)=FGZB(3)
      AOUT(37,IT)=FGZB(4)
      AOUT(38,IT)=BEKINO+BWORK
C     AOUT(39,IT)=WORK
C     AOUT(40,IT)=EKIN/2+WORK
      PHABS=ABS(PH)
      IF(PHABS.GT.1.4) GO TO 100
      THABS=ABS(TH)
      IF(THABS.GT.1.4) GO TO 100
C     END CHECK
 1055 CONTINUE
C
```

```
C     DISPLAY CONTROLS
C
      IF(IT.GE.370) GO TO 100
      IF(HOLD.GT.0)GO TO 60
      CALL ERASE
      GO TO 60
  100 CONTINUE
      CALL ERASE
      CALL ANMODE
      XA(1)=IT
      YA(1)=IT
      CALL BINITT
      CALL CHECK(XA,YA)
      CALL DSPLAY(XA,YA)
      XDZ=TAR(1,3)
      YDZ=TAR(2,3)
      CALL MOVEA(XDZ,YDZ)
      DO 120 I=4,9
      XDZ=TAR(1,I)
      YDZ=TAR(2,I)
      CALL DASHA(XDZ,YDZ,323)
  120 CONTINUE
      CALL TINPUT(M)
      CALL ERASE
      PRINT 2021,IT
 2021 FORMAT('  IT=',I4)
      TOUT(1)=IT
      DO 1060 I=1,86
      AOUT(I,1)=IT
 1060 CONTINUE
      IF(CH4.EQ.0)GOTO 4059
      KT=IT
      IFILE=0
      CALL FILE1(KT,IFILE)
 4059 CONTINUE
 1062 CONTINUE
      CALL HOME
      PRINT 1035,ILAND
      PRINT 1001
      READ 2,NCUR
      READ 2,(ICUR(I),I=1,NCUR)
      CONTINUE
      ISX=900
      ISY=700
 1064 CONTINUE
      AMIN=100000
      AMAX=-100000
      READ 2,TO1,TO2
      IF(TO1.EQ.0)IT1=2
      IF(TO2.EQ.0)IT2=IT
      IF(TO2.EQ.0)GO TO 1117
      DO 1116 I=2,IT
      TO=TOUT(I)
      DTO1=TO1+DTO
      DTO2=TO2-DTO
      IF(TO.GE.TO1.AND.TO.LT.DTO1)IT1=I
 1116 IF(TO.GT.DTO2.AND.TO.LE.TO2)IT2=I
```

```
 1117  CONTINUE
C       PRINT 2022,IT1,IT2
C2022   FORMAT('  IT1=',I4,'  IT2=',I4)
       DO 1118 I=IT1,IT2
       J=I-IT1+2
       TOT(J)=TOUT(I)
C       PRINT 2023,I,J,TOT(J),TOUT(I)
C2023   FORMAT('  I=',I3,'  J=',I3,/,'  TOUT(I)=',F10.3,'  ',F10.3)
 1118  CONTINUE
       TOT(1)=IT2-IT1
       DO 1125 ICV=1,NCUR
       DO 1120 I=IT1,IT2
       AOT(1)=IT2-IT1
       J=I-IT1+2
       IDCV=ICUR(ICV)
       AOT(J)=AOUT(IDCV,I)
C       PRINT 2024,AOT(J)
C2024   FORMAT('  AOT(J)=',F10.3)
 1120  CONTINUE
       CALL MNMX(AOT,AMIN,AMAX)
 1125  CONTINUE
       CALL BINITT
       CALL SLIMX(150,ISX)
       CALL SLIMY(125,ISY)
       CALL DLIMY(AMIN,AMAX)
       IDCV=ICUR(1)
       DO 1130 I=IT1,IT2
       J=I-IT1+2
       AOT(1)=IT2-IT1
 1130  AOT(J)=AOUT(IDCV,I)
       CALL CHECK(TOT,AOT)
       CALL DSPLAY(TOT,AOT)
       IF(NCUR.EQ.1)GO TO 1142
       DO 1140 ICV=2,NCUR
       IDCV=ICUR(ICV)
       DO 1139 I=IT1,IT2
       J=I-IT1+2
       AOT(J)=AOUT(IDCV,I)
       AOT(1)=IT2-IT1
 1139  CONTINUE
       CALL CPLOT(TOT,AOT)
 1140  CONTINUE
 1142  CONTINUE
       CALL TINPUT(M)
 1141  CONTINUE
       CALL ANMODE
       PRINT 7
       READ 2,IK
       CALL ERASE
       IIAZ=14
       REV=PI/180
       IF(IK.EQ.2)GO TO 200
       IF(IK.EQ.3)GO TO 219
       IF(IK.EQ.5)GO TO 220
       IF(IK.EQ.6)GO TO 215
       GO TO 1062
 215   CONTINUE
```

```
      CALL ERASE
      CALL HOME
      PRINT 12,ILAND
      READ 2,X1C,Y1C,Z1C
      READ 2,TO1,TO2
      IF(TO1.EQ.O)IT1=2
      IF(TO2.EQ.O)IT2=IT
      IF(TO2.EQ.O)GO TO 2117
      DO 2116 I=2,IT
      TO=TOUT(I)
      DTO1=TO1+DTO
      DTO2=TO2-DTO
      IF(TO.GE.TO1.AND.TO.LT.DTO1)IT1=I
2116  IF(TO.GT.DTO2.AND.TO.LE.TO2)IT2=I
2117  CONTINUE
      DO 2118 I=IT1,IT2
      J=I-IT1+2
      TOT(J)=TOUT(I)
2118  CONTINUE
      TOT(1)=IT2-IT1
      CALL BINITT
      CALL SLIMY(550,730)
      CALL YDEN(10)
      AOT(1)=IT2-IT1
      DO 216 I=IT1,IT2
      J=I-IT1+2
      AOT(I)=X1C*((AOUT(10,I)*REV)**2+(AOUT(9,I)*REV)**2)
      AOT(I)=AOT(I)-Y1C*AOUT(13,I)+Z1C*AOUT(12,I)
      AOT(I)=AOT(I)/G+AOUT(14,I)
216   CONTINUE
      CALL CHECK(TOT,AOT)
      CALL DSPLAY(TOT,AOT)
      CALL ANMODE
      PRINT 13
      CALL BINITT
      CALL SLIMY(320,500)
      CALL YDEN(10)
      DO 217 I=IT1,IT2
      J=I-IT1+2
      AOT(J)=Y1C*((AOUT(8,I)*REV)**2+(AOUT(10,I)*REV)**2)
      AOT(J)=AOT(J)+X1C*AOUT(13,I)-Z1C*AOUT(11,I)
      AOT(J)=AOT(J)/G+AOUT(15,I)
217   CONTINUE
      CALL CHECK(TOT,AOT)
      CALL DSPLAY(TOT,AOT)
      CALL ANMODE
      PRINT 14
      CALL BINITT
      CALL SLIMY(90,270)
      CALL YDEN(10)
      DO 218 I=IT1,IT2
      J=I-IT1+2
      AOT(J)=Z1C*((AOUT(8,I)*REV)**2+(AOUT(9,I)*REV)**2)
      AOT(J)=AOT(J)-X1C*AOUT(12,I)+Y1C*AOUT(11,I)
      AOT(J)=AOT(J)/G+AOUT(16,I)
218   CONTINUE
      IF(CH4.EQ.O)GOTO 230
```

```
      IIAZ=IIAZ+1
      KT2=IT2
      IFILE=1
      CALL FILE1(KT2,IFILE)
230   CONTINUE
      CALL CHECK(TOT,AOT)
      CALL DSPLAY(TOT,AOT)
      CALL ANMODE
      PRINT 15
      CALL TINPUT(M)
      PRINT 16
      READ 2,IK
      IF(IK.EQ.2)GO TO 200
      IF(IK.EQ.3)GO TO 1141
      IF(IK.EQ.4)GO TO 4319
      GO TO 215
4319  CALL ERASE
      CALL ANMODE
      GO TO 50
219   CONTINUE
      PRINT 1007
      READ 2,DTP,NLOD,NCAL
      GO TO 60
220   CONTINUE
      PRINT 1007
      READ 2,DTP,DTO,DTC
      DO 225 I=1,86
225   AOUT(I,2)=AOUT(I,IT)
      XA(2)=XA(IT)
      YA(2)=YA(IT)
      TOUT(2)=T
      IT=2
      GO TO 60
200   CONTINUE
      CALL FINITT(0,760)
      STOP
1     FORMAT(20X,'      LOONY LANDER'//'  LANDING NO:')
2     FORMAT()
6     FORMAT(' X=',F7.2,' Y=',F7.2,' Z=',F7.2,20X
     +      ,' BX=',F7.2,' BY=',F7.2,' BZ=',F7.2)
7     FORMAT('  RETURN,STOP(2),RESUME(3),DUMP OUT(5),ACCEL(6)')
8     FORMAT('  STD TARGET (O), NEW TARGET (1)')
9     FORMAT('  HOW MANY LINES? (STD N=28)')
10    FORMAT('  IL  X1  Y1  O  X2  Y2  Z2  IC')
11    FORMAT('  X FACTOR, Y FACTOR,XVU,YVU,ZVU')
12    FORMAT('  ENTER CARGO COORDS X,Y,Z & T1-T2',20X,'LANDING:',I8)
13    FORMAT('  ACC X')
14    FORMAT('  ACC Y')
15    FORMAT('  ACC Z')
16    FORMAT('  MORE'/'  STOP(2)'/'  PLOT(3)'/'  NEW(4)')
17    FORMAT('  ENTER TILT OF X AXIS ')
1001  FORMAT('  NUMBER OF CURVES, CURVE ID,T1-T2,')
1002  FORMAT(' VX1=',F7.2,' VY1=',F7.2,' VZ=',F7.2
     +      ,15X,' BVX1=',F7.2,' BVY1=',F7.2,' BVZ=',F7.2)
1003  FORMAT(' ACCX=',F7.3,' ACCY=',F7.3,' ACCZ=',F7.3
     +      ,11X,' TRMC=',F8.3,' TRMI=',F8.3)
1004  FORMAT(' PH=',F7.2,' TH=',F7.2,28X
```

```
     +       ,' BPH=',F7.2,' BTH=',F7.2)
1005  FORMAT('  COMPUTATION RESUMED')
1007  FORMAT('  ENTER DTP,NLOD,NCAL')
1008  FORMAT('  DTO=',F9.6,' DTC=',F9.6)
1010  FORMAT('  SET XVU,YVU,ZVU,HOLD')
1015  FORMAT('  XY PLOT SIZE (900,700)')
1035  FORMAT(25X,'LANDING NO: ',I8,5X,' T='F6.3)
1036  FORMAT('  ENTER X,Y,Z')
4     FORMAT('  ORIENTATION: PH=, TH=, SI=')
3     FORMAT('  VEL COMP: VX=, VY=, VZ=')
5     FORMAT('  ROT VEL COMP: PHD=, THD=, SID=')
1028  FORMAT('  DO YOU WANT RETROS? ( 0,1)')
1029  FORMAT('  ENTER ZTH,THR1, THR2,BTIM1,BTIM2')
2001  FORMAT('  TOP PLATE: MASS,INX,INY,INZ,XCG ',/,
     +'  BOTTOM PLATE: MASS,INX,INY,INZ,XCG')
2002  FORMAT('  XPF,XPR,XPFB,XPRB ',/,
     +'  YP,YPB,ZP,HTP,BUMPER PAD HT.')
2003  FORMAT('  BAG DIAMETER,ORIFICE DIAMETER,BAG HEIGHT')
2004  FORMAT('  K1G,K2G,ELONG-V,#PLIES-V,ELONG-E,#PLIES-E',
     +   ',ELONG-S,#PLIES-S')
2005  FORMAT('  MU1,MU2,MU3,MU4,TBRAK  (GROUND FRICTION)')
2006  FORMAT('  LENGTH/2,LENGTHB/2,XPANEL, XPANELB ',/,
     +'  NUMBER OF PANELS (2-4)')
2007  FORMAT('  DISPLAY TOTAL TOP SLING FORCES, (0)',/,
     +'  DISPLAY TOTAL BOTTOM SLING FORCES, (1)')
2008  FORMAT('  DO YOU WANT DAMPING IN THE SLINGS? (0,1)')
2011  FORMAT('  INPUT % OF CRITICAL DESIRED ')
2009  FORMAT('  FK2DE=',F9.0,'   FK2DER=',F9.0,'   FK2V= ',F9.0
     +,'   FK2VR=',F9.0,/,'  FK2S1=',F9.0,'   FK2S2= ',F9.0
     +,'   FK2S3=',F9.0,'   FK2S4=',F9.0)
2010  FORMAT('  FK1DE=',F9.0,'   FK1DER=',F9.0,'   FK1V= ',F9.0
     +,'   FK1VR=',F9.0,/,'  FK1S1=',F9.0,'   FK1S2= ',F9.0
     +,'   FK1S3=',F9.0,'   FK1S4=',F9.0)
2012  FORMAT('  BU1,BU2     (BUMPER FRICTION)')
2013  FORMAT('  HOW MANY STRAPS PER SIDE? (4-MAX)',/,
     +       '  OFFSET OF BOTTOM PLATE (X-DIREC.)')
2014  FORMAT('  ENTER XB(I),XT(I) FOR STRAP',I3,/,'  RIGHT',
     +'-SIDE EVEN NUMBERED,LEFT-SIDE ODD NUMBERED, SYMETRICAL GEOM.
     +',/,'  ENTER ONLY LEFT SIDE')
2015  FORMAT('  STRAP BREAK STRENGTH')
2016  FORMAT('  PAD HT (0)',/,'  BQ,GBX,GBY,GBZ (1)')
2017  FORMAT('  VERT. VELOCITY OF TOP CORNERS (0)',/,
     +'  BPH,BTH,BSI,BP  (1)')
2018  FORMAT('  SEND HT,VV,HV,P,PR,PRES,ACC TO DATA FILE?',
     +/,'  (0,1)')
2020  FORMAT(2X,F7.5,1X,F9.5)
      END

@PRT,S TFG.TARCAR
```

```
GLIDE*TFG(1).COSINE
        COMPILER(DIAG=3)
        SUBROUTINE COSINE
        COMMON D11,D12,D13,D21,D22,D23,D31,D32,D33,
     +        BD11,BD12,BD13,BD21,BD22,BD23,BD31,BD32,BD33,
     +        PH,TH,SI,BTH,BPH,BSI,TAR(6,120),CAR(6,46),
     +        AOUT(86,373),AOT(373),TOUT(373),IIAZ
        D11=COS(TH)*COS(SI)
        D12=SIN(PH)*SIN(TH)*COS(SI)-COS(PH)*SIN(SI)
        D13=COS(PH)*SIN(TH)*COS(SI)+SIN(PH)*SIN(SI)
        D21=COS(TH)*SIN(SI)
        D22=SIN(PH)*SIN(TH)*SIN(SI)+COS(PH)*COS(SI)
        D23=COS(PH)*SIN(TH)*SIN(SI)-SIN(PH)*COS(SI)
        D31=-SIN(TH)
        D32=SIN(PH)*COS(TH)
        D33=COS(PH)*COS(TH)
        BD11=COS(BTH)*COS(BSI)
        BD12=SIN(BPH)*SIN(BTH)*COS(BSI)-COS(BPH)*SIN(BSI)
        BD13=COS(BPH)*SIN(BTH)*COS(BSI)+SIN(BPH)*SIN(BSI)
        BD21=COS(BTH)*SIN(BSI)
        BD22=SIN(BPH)*SIN(BTH)*SIN(BSI)+COS(BPH)*COS(BSI)
        BD23=COS(BPH)*SIN(BTH)*SIN(BSI)-SIN(BPH)*COS(BSI)
        BD31=-SIN(BTH)
        BD32=SIN(BPH)*COS(BTH)
        BD33=COS(BPH)*COS(BTH)
        RETURN
        END

@PRT,S TFG.FILE1
```

```
GLIDE*TFG(1).FILE1
           COMPILER(DIAG=3)
           SUBROUTINE FILE1(KIT,IIFF)
           COMMON D11,D12,D13,D21,D22,D23,D31,D32,D33,
     +            BD11,BD12,BD13,BD21,BD22,BD23,BD31,BD32,BD33,
     +            PH,TH,SI,BTH,BPH,BSI,TAR(6,120),CAR(6,46),
     +            AOUT(86,373),AOT(373),TOUT(373),IIAZ
           DO 30 I=2,KIT
           IF(IIFF.EQ.1)GOTO 10
           WRITE(7,2020)TOUT(I),AOUT(1,I)
           WRITE(8,2020)TOUT(I),AOUT(7,I)
           WRITE(9,2020)TOUT(I),AOUT(5,I)
           WRITE(10,2020)TOUT(I),AOUT(3,I)
           WRITE(11,2020)TOUT(I),AOUT(9,I)
           WRITE(12,2020)TOUT(I),AOUT(2,I)
           WRITE(13,2020)TOUT(I),AOUT(64,I)
           WRITE(14,2020)TOUT(I),AOUT(65,I)
           GOTO 30
      10   IF(IIAZ.EQ.16)GOTO 20
           WRITE(15,2020)TOUT(I),AOT(I)
           GOTO 30
      20   WRITE(16,2020)TOUT(I),AOT(I)
      30   CONTINUE
           RETURN
    2020   FORMAT(2X,F7.4,1X,F9.5)
           END

@BRKPT PRINT$
```

```
GLIDE*TFG(1).TARCAR
      COMPILER(DIAG=3)
      SUBROUTINE TARCAR
      COMMON D11,D12,D13,D21,D22,D23,D31,D32,D33,
     +       BD11,BD12,BD13,BD21,BD22,BD23,BD31,BD32,BD33,
     +       PH,TH,SI,BTH,BPH,BSI,TAR(6,120),CAR(6,46),
     +       AOUT(86,373),AOT(373),TOUT(373),IIAZ
      DATA (TAR(I,1),I=1,6)/0.,-2000.,0.,0.,2000.,0./
      DATA (TAR(I,2),I=1,6)/-2000.,0.,0.,2000.,0.,0./
      DATA (TAR(I,3),I=1,6)/-30.,-40.,0.,-30.,160.,0./
      DATA (TAR(I,4),I=1,6)/-30.,160.,0.,30.,160.,0./
      DATA (TAR(I,5),I=1,6)/30.,160.,0.,30.,40.,0./
      DATA (TAR(I,6),I=1,6)/30.,40.,0.,90.,40.,0./
      DATA (TAR(I,7),I=1,6)/90.,40.,0.,90.,-40.,0./
      DATA (TAR(I,8),I=1,6)/90.,-40.,0.,-30.,-40.,0./
      DATA (TAR(I,9),I=1,6)/-30.,-40.,15.,-30.,160.,15./
      DATA (TAR(I,10),I=1,6)/-30.,160.,15.,30.,160.,15./
      DATA (TAR(I,11),I=1,6)/30.,160.,15.,30.,40.,15./
      DATA (TAR(I,12),I=1,6)/30.,40.,15.,90.,40.,15./
      DATA (TAR(I,13),I=1,6)/90.,40.,15.,90.,-40.,15./
      DATA (TAR(I,14),I=1,6)/90.,-40.,15.,-30.,-40.,15./
      DATA (TAR(I,15),I=1,6)/-30.,-40.,0.,-30.,-40.,15./
      DATA (TAR(I,16),I=1,6)/-30.,160.,0.,-30.,160.,15./
      DATA (TAR(I,17),I=1,6)/30.,160.,0.,30.,160.,15./
C
      DATA (CAR(I,1),I=1,6)/0.,-1.,0.,1.,-1.,0./
      DATA (CAR(I,2),I=1,6)/1.,-1.,0.,1.,1.,0./
      DATA (CAR(I,3),I=1,6)/1.,1.,0.,0.,1.,0./
      DATA (CAR(I,4),I=1,6)/0.,1.,0.,-1.,1.,0./
      DATA (CAR(I,5),I=1,6)/-1.,1.,0.,-1.,-1.,0./
      DATA (CAR(I,6),I=1,6)/-1.,-1.,0.,0.,-1.,0./
      DATA (CAR(I,7),I=1,6)/0.,-1.,1.,0.,1.,1./
      DATA (CAR(I,8),I=1,6)/0.,1.,1.,-1.,1.,1./
      DATA (CAR(I,9),I=1,6)/-1.,1.,1.,-1.,-1.,1./
      DATA (CAR(I,10),I=1,6)/-1.,-1.,1.,0.,-1.,1./
      DATA (CAR(I,11),I=1,6)/1.,-1.,0.,0.,-1.,1./
      DATA (CAR(I,12),I=1,6)/1.,1.,0.,0.,1.,1./
      DATA (CAR(I,13),I=1,6)/-1.,1.,0.,-1.,1.,1./
      DATA (CAR(I,14),I=1,6)/-1.,-1.,0.,-1.,-1.,1./
C
      DATA (CAR(I,15),I=1,6)/1.,-1.,0.,1.,1.,0./
      DATA (CAR(I,16),I=1,6)/1.,1.,0.,-1.,1.,0./
      DATA (CAR(I,17),I=1,6)/-1.,1.,0.,-1.,-1.,0./
      DATA (CAR(I,18),I=1,6)/-1.,-1.,0.,1.,-1.,0./
      RETURN
      END

@PRT,S TFG.COSINE
```

APPENDIX C

LAND3

Output Variables

APPENDIX C

OUTPUT VARIABLES

(Output is in graphical form - variable vs time)

ID	No.	Variable Name - Description (Units)
1	Z	Height of top plate c.g. above the ground in inertial coordinate system (meters)
2	PH	Roll orientation of top plate in inertial coordinate system (degrees)
3	TH	Pitch orientation of top plate in inertial coordinate system (degrees)
4	SI	Yaw orientation of top plate in inertial coordinate system (degrees)
5	VX1	Velocity component of top plate c.g. in the inertial X-direction (m/s)
6	VY1	Velocity component of top plate c.g. in the inertial Y-direction (m/s)
7	ZD	Velocity component of top plate c.g. in the inertial Z-direction (m/s)
8	P	Roll rate of top plate in inertial coordinate system (rad/s)
9	Q	Pitch rate of top plate in inertial coordinate system (rad/s)
10	R	Yaw rate of top plate in inertial coordinate system (rad/s)
11	PD	dP/dt of top plate in inertial coordinate system (rad/s)
12	QD	dQ/dt of top plate in inertial coordinate system (rad/s)

ID No.		Variable Name - Description (Units)
13	RD	dR/dt of top plate in inertial coordinate system (rad/s)
14	GX	Acceleration of top plate c.g. in the inertial X-direction (G)
15	GY	Acceleration of top plate c.g. in the inertial Y-direction (G)
16	GZ	Acceleration of top plate c.g. in the inertial Z-direction (G)
17	FGZB[1]	Force the ground (spring-damper combination) exerts on the front-left corner of the bottom plate, body Z-direction (N)
18	FGZB[2]	Force the ground exerts on the front-right corner of the bottom plate, body Z-direction (N)
19	TEKINO +TWORK	Top plate kinetic energy plus top plate work (N-m)
20	BZ	Height of bottom plate c.g. above the ground in inertial coordinate system (m)
21	BPH	Roll orientation of bottom plate in inertial coordinate system (degrees)
		or
	ZVT[1]	Velocity component of top plate, front-left corner, in the inertial Z-direction (m/s)
22	BTH	Pitch orientation of bottom plate in inertial coordinate system (degrees)
	or	
	ZVT[2]	Velocity component of top plate, front-right corner, in the inertial Z-direction (m/s)
23	BSI	Yaw orientation of bottom plate in inertial coordinate system (degrees)
	or	
	ZVT[3]	Velocity component of top plate, rear-left corner, in the inertial Z-direction (m/s)

ID No.		Variable Name - Description (Units)
24	BVX1	Velocity component of bottom plate c.g. in the inertial X-direction (m/s)
25	BVY1	Velocity component of bottom plate c.g. in the inertial Y-direction (m/s)
26	BZD	Velocity component of bottom plate c.g. in the inertial Z-direction (m/s)
27	BP	Roll rate of bottom plate in inertial coordinate system (rad/s)
	or	
	ZVT[4]	Velocity component of top plate, rear-right corner, in the inertial Z-direction (m/s)
28	BQ	Pitch rate of bottom plate in inertial coordinate system (rad/s)
	or	
	ZST[1] -ZSB[1]	Z-position of top plate (front-left corner) minus Z-position of bottom plate (front-left corner) (inertial coordinates m)
29	TPDZ[1]	Force the front-left bump stop exerts on the front-left corner of the top plate in the top plate Z-direction (N)
30	TPDZ[2]	Force the front-right bump stop exerts on the front-right corner of the top plate in the top plate Z-direction (N)
31	TPDZ[3]	Force the rear-left bump stop exerts on the rear-left corner of the top plate in the top plate Z-direction (N)
32	TPDZ[4]	Force the rear-right bump stop exerts on the rear-right corner of the top plate in the top plate Z-direction (N)
33	GBX	Acceleration of bottom plate c.g. in the inertial direction (G)
	or	

ID No.	Variable Name	Description (Units)
	ZST[2] ZSB[2]	Z-position of top plate (front-right corner) minus Z-position of bottom plate (front-right corner) (inertial coordinates m)
34	GBY	Acceleration of bottom plate c.g. in the inertial Y-direction (G)
	or	
	ZST[3] ZSB[3]	Z-position of top plate (rear-left corner) minus Z-position of bottom plate (rear-left corner) inertial (coordinates m)
35	GBZ	Acceleration of bottom plate c.g. in the inertial Z-direction (G)
	or	
	ZST[4] Z-ZSB[4]	Z-position of top plate (rear-right corner) minus position of bottom plate (rear-right corner) inertial (coordinates m)
36	FGZB[3]	Force the ground exerts on the rear-left corner of the bottom plate in the bottom plate Z-direction (N)
37	FGZB[4]	Force the ground exerts on the rear-right corner of the bottom plate in the bottom plate Z-direction (N)
38	BEKINO +BWORK	Bottom plate kinetic energy plus bottom plate work (N-m)
39	TPDX[1]	Force (friction) the front-left bump stop exerts on the front-left corner of the top plate in the top plate X-direction (N)
40	TPDX[2]	Force (friction) the front-right bump stop exerts on the top plate, front-right corner in the top plate X-direction (N)
41	TPDX[3]	Force (friction) the rear-left bump stop exerts on the top plate, rear-left corner in the top plate X-direction (N)

ID No.	Variable Name - Description (Units)	
42	TPDX[4]	Force (friction) the rear-right bump stop exerts on the top plate, rear-right corner in the top plate X-direction (N)
43	DES[3]	Tension in the front, bottom left to top right, diagonal end strap (N)
44	DES[2]	Tension in the front, bottom right to top left, diagonal end strap (N)
45	DES[3]	Tension in the rear, bottom left to top right, diagonal end strap (N)
46	DES[4]	Tension in the rear, bottom right to top left, diagonal end strap (N)
47	VS[1]	Tension in the front-left vertical strap (N)
48	VS[2]	Tension in the front-right vertical strap (N)
49	VS[3]	Tension in the rear-left vertical strap (N)
50	VS[4]	Tension in the rear-right vertical strap (N)
51	TSTRAP[1]	Total strap forces exerted on top plate, front-left corner (N)
	or	
	BSTRAP[1]	Total strap forces exerted on bottom plate, front-left corner (N)
52	TSTRAP[2]	Total strap forces exerted on top plate, front-right corner (N)
	or	
	BSTRAP[2]	Total strap forces exerted on bottom plate, front-right corner (N)
53	TSTRAP[3]	Total strap forces exerted on top plate, rear-left corner (N)
	or	
	BSTRAP[3]	Total strap forces exerted on bottom plate, rear-left corner (N)

ID No.	Variable Name - Description (Units)	
54	TSTRAP[4]	Total strap forces exerted on top plate, rear-right corner (N)
	or	
	BSTRAP[4]	Total strap forces exerted on bottom plate, rear-right corner (N)
55	SS[1]	Tension in side diagonal strap number 1, left side (N)
56	SS[2]	Tension in side diagonal strap number 2, right side (N)
57	SS[3]	Tension in side diagonal strap number 3, left side (N)
58	SS[4]	Tension in side diagonal strap number 4, right side (N)
59	SS[5]	Tension in side diagonal strap number 5, left side (N)
60	SS[6]	Tension in side diagonal strap number 6, right side (N)
61	SS[7]	Tension in side diagonal strap number 7, left side (N)
62	SS[8]	Tension in side diagonal strap number 8, right side (N)
63	PCOMP[1]	Pressure in airbag number 1, left side (Atm)
64	PCOMP[2]	Pressure in airbag number 2, right side (Atm)
65	PCOMP[3]	Pressure in airbag number 3, left side (Atm)
66	PCOMP[4]	Pressure in airbag number 4, right side (Atm)
67	PCOMP[5]	Pressure in airbag number 5, left side (Atm)
68	PCOMP[6]	Pressure in airbag number 6, right side (Atm)
69	PCOMP[7]	Pressure in airbag number 7, left side (Atm)
70	PCOMP[8]	Pressure in airbag number 8, right side (Atm)

ID No.		Variable Name - Description (Units)
71	XST[1]	X-position of top plate (front-left corner) minus X-position of bottom plate (front-left corner) (inertial coordinates m)
72	XST[2] XSB[3]	X-position of top plate (front-right corner) minus X-position of bottom plate (front-right corner) (inertial coordinates m)
73	XST[3] XSB[3]	X-position of top plate (rear-left corner) minus X-position of bottom plate (rear-left corner) (inertial coordinates m)
74	XST[4] XSB[4]	X-position of top plate (rear-right corner) minus X-position of bottom plate (rear-right corner) (inertial coordinates m)
75	YST[1] YSB[1]	Y-position of top plate (front-left corner) minus Y-position of bottom plate (front-left corner) (inertial coordinates m)
76	YST[2] YSB[2]	Y-position of top plate (front-right corner) minus Y-position of bottom plate (front-right corner) (inertial coordinates m)
77	YST[3] YSB[3]	Y-position of top plate (rear-left corner) minus Y-position of bottom plate (rear-left corner) (inertial coordinates m)
78	YST[4] YSB[4]	Y-position of top plate (rear-right corner) minus Y-position of bottom plate (rear-right corner) (inertial coordinates m)
79	HBAG[1]	Height of airbag number 1 (m)
80	HBAG[2]	Height of airbag number 2 (m)
81	HBAG[3]	Height of airbag number 3 (m)
82	HBAG[4]	Height of airbag number 4 (m)
83	HBAG[5]	Height of airbag number 5 (m)
84	HBAG[6]	Height of airbag number 6 (m)
85	HBAG[7]	Height of airbag number 7 (m)
86	HBAG[8]	Height of airbag number 8 (m)

APPENDIX D

Preliminary LAND3 Validation

APPENDIX D

Preliminary LAND3 Validation

Validation of the entire program, LAND3 without using actual test results for comparison was not feasible. However, an attempt was made to insure that the predicted performance for the major elements of the program was not obviously wrong.

Two elements of the program, the bump stops and the ground, were modeled as damped springs. Whether or not a damped spring was the best possible representation for these components could only be determined through testing of the completed platform. Whether or not the performance predicted by LAND3 using that model was reasonable was determined through comparison with a second computer program. This program, called BUMP, predicted the behavior of a one degree of freedom, mass/spring/damper system using the exact solution to the equation:

$$m\ddot{x} + b\dot{x} + kx = 0$$

The comparison was made by first selecting part of a LAND3 computer run when either ground impact of the bottom plate or bump stop impact of the top plate was occurring. The ground/bump stop impact conditions and the resultant deflections, accelerations and forces were recorded. The program BUMP was then run using similar impact conditions. The deflections, accelerations and forces predicted by this program were then compared to those predicted by LAND3.

The evaluation of the ground was made by running LAND3 with the initial conditions: zero-roll, zero-pitch, zero-yaw, zero horizontal

velocity, and 6 m/s vertical velocity. The deflection of the ground, the force exerted by the ground on each corner of the bottom plate, and the acceleration of the bottom plate at the c.g. during the initial ground impact were recorded. Next, the program BUMP was run using as input parameters the mass of the bottom plate, the ground impact velocity of 6 m/s, and the same ground spring constant and damping coefficient used in LAND3. The mass of the bottom plate was used because during the initial impact the airbag pressure is still very low and the top plate motion has not yet begun to affect the bottom plate motion. The deflection, exerted force, and acceleration predicted by BUMP were recorded and compared to those predicted by LAND3. The output of the two programs showed good agreement.

The same type of comparison was made to evaluate the accuracy of the bump stop behavior predicted by LAND3. The LAND3 computer run used to evaluate the ground model was used for this comparison as well. During this run the airbags crushed, the top plate hit the bump stops, bounced up, then impacted the bump stops again. The bump stop deflections, exerted forces, and the top plate accelerations occurring during the second impact were recorded. These values were chosen because during the second impact the bottom plate remained on the ground for the entire time. Therefore, its motion could be neglected and the problem remained a one-degree-of-freedom problem. The program BUMP was run using as input parameters the top plate mass, the top plate impact velocity (as obtained from LAND3), and the same bump stop

constants and damping coefficients used in LAND3. The bump stop deflections, bump stop forces, and top plate c.g. accelerations predicted by LAND3 compared well to the values predicted by BUMP.

The platform restraining straps were modeled as simple tension springs in LAND3. Since the spring constant was an input variable, it was a simple matter to compare predicted strap stretch with predicted resultant strap forces. The comparison did not reveal any obvious irregularities. Examination of the output from various computer runs also confirmed that the straps did not exert any forces when the strap lengths computed by LAND3 were less than the original lengths.

Evaluation of the airbag model was limited to comparing the top plate c.g. accelerations to the airbag pressures. The average peak pressure of the four bags was multiplied by the total airbag surface area in contact with the top plate. The result was divided by the top plate mass and evaluated with respect to the peak accelerations of the top plate c.g. Considering the approximations made, agreement was good.

APPENDIX E

Equations for LAND3 Airbag Model

APPENDIX E

Equations For LAND3 Airbag Model

The equations used to model the airbags were developed by A. C. Browning. Browning developed the equations using basic principles of fluid mechanics and thermodynamics. These equations are used in combination with equations describing the motion of the bag ends. Initially, the interior bag pressure is set to atmospheric pressure. Changes in airbag pressure during a time increment, t, are calculated using the bag height and compression rate for that particular time increment. The Browning equations are:

$$\frac{dP}{dt} = \frac{(Ex\ B\ Vy - \alpha\ Q')}{(Ex/\varepsilon' + B\ CK)}\ \frac{1}{h}$$

$$P = P + \left(\frac{dP}{dt}\right)\ t$$

$$F = (AO)(Ex)*(PA)*(P-1)$$

where

$Ex = 1 + Ck\ (P-1)$

$B = P^{\varepsilon 2}$

Vy = compression rate

$\alpha = (0.9 - 0.3/P)\ \sqrt{K1\ (P^{\varepsilon 1} - 1)}$ (subsonic orifice flow, CD $= 0.9 - 0.3/P$)

$\alpha = (0.9 - 0.3/P)\ \sqrt{K1\ (PS^{\varepsilon 1} - 1)}\ (P/PS)$ (supersonic orifice flow, CD $= 0.9 - 0.3/PS$)

$Q' = AO\ (340.28\ m/s)/(AB/\sqrt{\gamma})$ (340.28 m/s = speed of sound)

$\varepsilon' = P$

$CK = 0.25$ (fabric extensibility coefficient)

h = airbag height

P = (bag pressure/atmospheric pressure)

γ = 1.4 (ratio of specific heats of air)

PS = 1.894 (ratio of bag pressure to orifice pressure for supersonic flow)

K1 = $2\gamma/(\gamma-1)$

E1 = $1 - (1/\gamma)$

E2 = $1/\gamma$

E3 = $(\gamma + 1)/2$

A0 = orifice area

AB = bag base area

Browning made the following assumptions:

"The airbag is assumed at all times to be cylindrical, have a height h, cross sectional area AB, an orifice area A0 and the air inside it to be at a pressure p, and density ... the areas AB and A0 are constant." Adiabatic airflow was also assumed because "the bag compression usually takes about 0.2 sec. to occur and this is sufficiently rapid for negligible heat transfer from the air".[17]

APPENDIX F

Bump Stop Analysis

APPENDIX F

Bump Stop Analysis

During ground impact the kinetic energy associated with AGARP's top plate is dissipated primarily by the airbags. However, the airbags do not dissipate all of the kinetic energy and some residual velocity remains after the airbags have deflated. An additional energy dissipating device is needed to eliminate the possibility of damage to the top or bottom plate. In AGARP this device took the form of foam cushions, referred to as bump stops. Polymer foam cushions were chosen because they were both compact and reusable.

Selection and modeling (for use in LAND3) of the foam most suitable for use in the AGARP presented a number of problems. Describing the behavior of polymer cushions is a rather complicated task. The type of loading the polymer cushion is subjected to affects the behavior exhibited by the cushion. The types of loading a cushion may be subjected to are usually divided into three categories; static, dynamic, and impact loading. There are various theories for describing the behavior of polymers subjected to these different loading conditions. In most cases the theories do not yield exact solutions. Static loading is the type of loading most often discussed in the literature and impact loading is discussed the least often.[18] However, there is some indication that the material properties under impact loading are related to those exhibited during static loading.[19,20] The AGARP bump stops are subjected to static loading when the platform is on the ground and the top plate is simply resting on the bump

stops. During the landing of the platform, immediately after the airbags have deflated, the bump stops are subjected to impact loading.

The first step in selecting a bump stop material was to make a general survey of the materials available at Natick RD&E Center. The object of the survey was to determine if any of the available materials appeared to have the required stiffness to absorb the impact of a 220 kg (440 lb) mass as well as good resilence characteristics. Good resilence characteristics were required because the top plate of the platform was to rest on the bump stops prior to being airdropped. The bump stops would be deformed by the weight of the top plate. After deployment of the parachute, the bottom plate falls away from the top plate, removing that weight. The bump stops must return to the original undeformed shape before ground impact, if the impact energy of the top plate is to be absorbed. These two requirements eliminated all but two possible foams. These two foams were Scott 900-8 and Scott 900-4.

Both the Scott 900-8 and Scott 900-4 foams had previously been tested on an impact testing machine at Natick RD&E Center. After examining the data from these tests, it was decided to evaluate the Scott 900-8 foam first. This foam was the stiffer of the two and appeared to be the most suitable. The intent of the evaluation was to develop a model of the foam and then use the model to determine if AGARP bump stops could be constructed using the foam.

A schematic of the impact testing machine used to obtain the data on the Scott 900-8 foam is shown in Figure F-1.

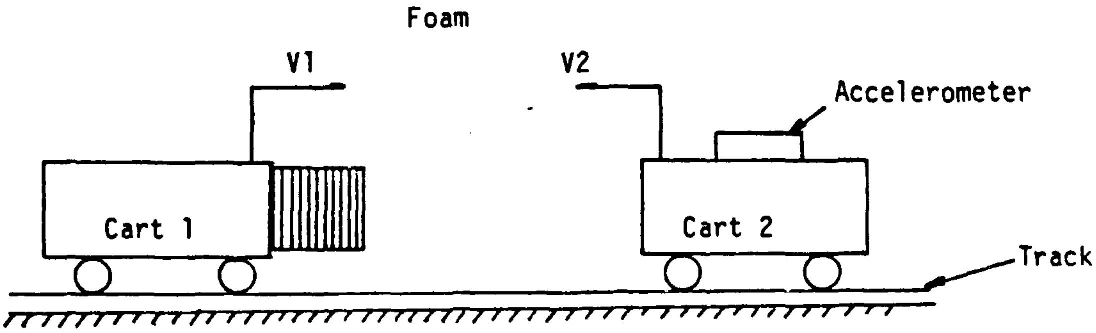

Fig. F-1 Schematic of Impact Testing Machine.

The machine used two carts of equal mass, mounted on a track. The foam was mounted to the front end of one cart and an accelerometer was mounted on the other cart. The two carts were propelled towards each other at equal velocities. The accelerations resulting from the impact were recorded and plotted versus time. This is a two-degree-of-freedom system, a fact which caused a problem in relating the data to design of the bump stops. The top plate impacts the bump stops after the vertical motion of the bottom plate has stopped. The result is a one-degree-of-freedom system similar to that shown in Figure F-2. It was therefore necessary to find a way to equate the two systems, if an accurate evaluation of the foam was to be made.

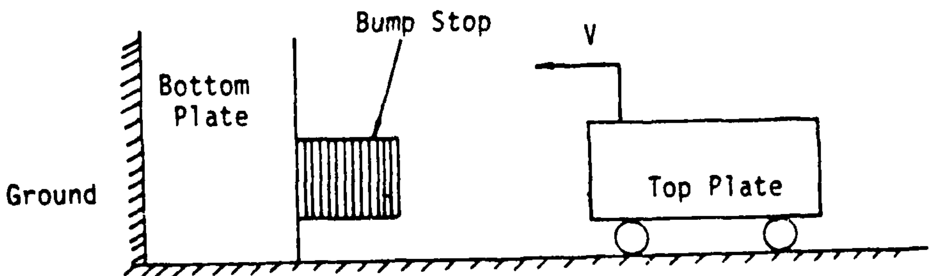

Fig. F-2 Schematic of Top Plate Impact.

In Figure F-3 the two systems are redrawn and relabeled. These two systems are essentially equivalent given the above specified masses and velocities.

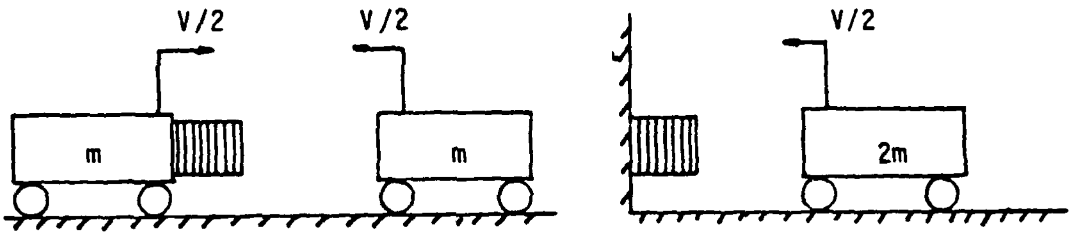

Case 1: Test set-up

Case 2: Actual bump stop use

Fig. F-3 Comparison of Bump Stop Systems.

This is shown by the comparison of kinetic energies and momentums given below:

Case 1: $KE = \frac{1}{2}m\left(\frac{V}{2}\right)^2 + \frac{1}{2}m\left(\frac{V}{2}\right)^2 = \frac{1}{4}mV^2$

$H = m\frac{V}{2} + m\frac{V}{2} = mV$

Case 2: $KE = \frac{1}{2}(2m)\left(\frac{V}{2}\right)^2 = \frac{1}{4}mV^2$

$H = 2m\left(\frac{V}{2}\right) = mV$

since $d(mv) = F\,dt$ or $F = ma$

$$2\,(a_{case\ 2}) = a_{case\ 1}$$

where KE = kinetic energy

H = momentum

m = mass

V = velocity

a = acceleration

When all other parameters are equal, the only difference between the two systems is that in Case 1, the actual test set-up, the acceleration is twice that of Case 2, the actual bump stop usage.

The next step was to develop a computer model of the foam to facilitate design of the bump stops. Towards this end a short computer program, called BUMP, was written. This program obtains the exact solution to the one-degree-of-freedom system which models the actual bump stop usage. This program solved the following equation:

$$m\ddot{x} - c\dot{x} + K x = 0$$

where c = damping coefficient

k = spring constant

m = mass

Input parameters were: initial velocity, initial position, mass, spring constant and damping coefficient. Output parameters were: position, velocity and acceleration. The intent was to use this program to find the proper combination of spring constants and damping coefficients that could be used to simulate the foam behavior under impact lcading.

First, a typical top plate impact velocity was determined by examining the results of previous LAND3 computer runs. Next, the foam test data was reviewed and the data from the test most closely approxmating this impact velocity was selected. The data was linearized by breaking it up into five segments. The segments were chosen based on

percent deflection from the undeformed height. Spring constants were then calculated for each segment, as shown in Fig. F-4.

The program BUMP was utilized to determine the damping coefficients, which, when combined with the above mentioned spring constants, would yield a reasonable foam model. This was a trial and error process. The damping coefficient associated with each segment of the test data was varied until a reasonable match of acceleration and deflection was obtained. The damping coefficient was specified a percent of critical damping. The process started with the first segment, (i.e. zero deflection) and then continued on to the subsequent segments. The points marked with triangles in Fig. F-4 were obtained using the program BUMP and the values for the damping coefficients that yielded the best match of acceleration and deflection. As can be seen from the graph, the result of the entire process was a reasonable model of the 0.305- x 0.305- x 0.305-m (12- x 12- x 12-in) sample used during the impact test. (The sample was made from twelve 25.4-mm (1-in) thick pieces of foam.)

Since a model of the sample was now available, the next objective was to determine if the Scott 900-8 could be used to make bump stops for the AGARP. A height of 0.305 m (12 in) was excessive for use as a bump stop. Therefore, it was necessary to find out how the properties of the foam varied with changes in its original undeformed height. The Instron compression/tension testing machine at Natick RD&E Center was used for this purpose. Individual pieces of foam measuring 0.305 m x 0.305 m x 0.0254 m (12 x 12 x 1 in) were stacked one on top of the

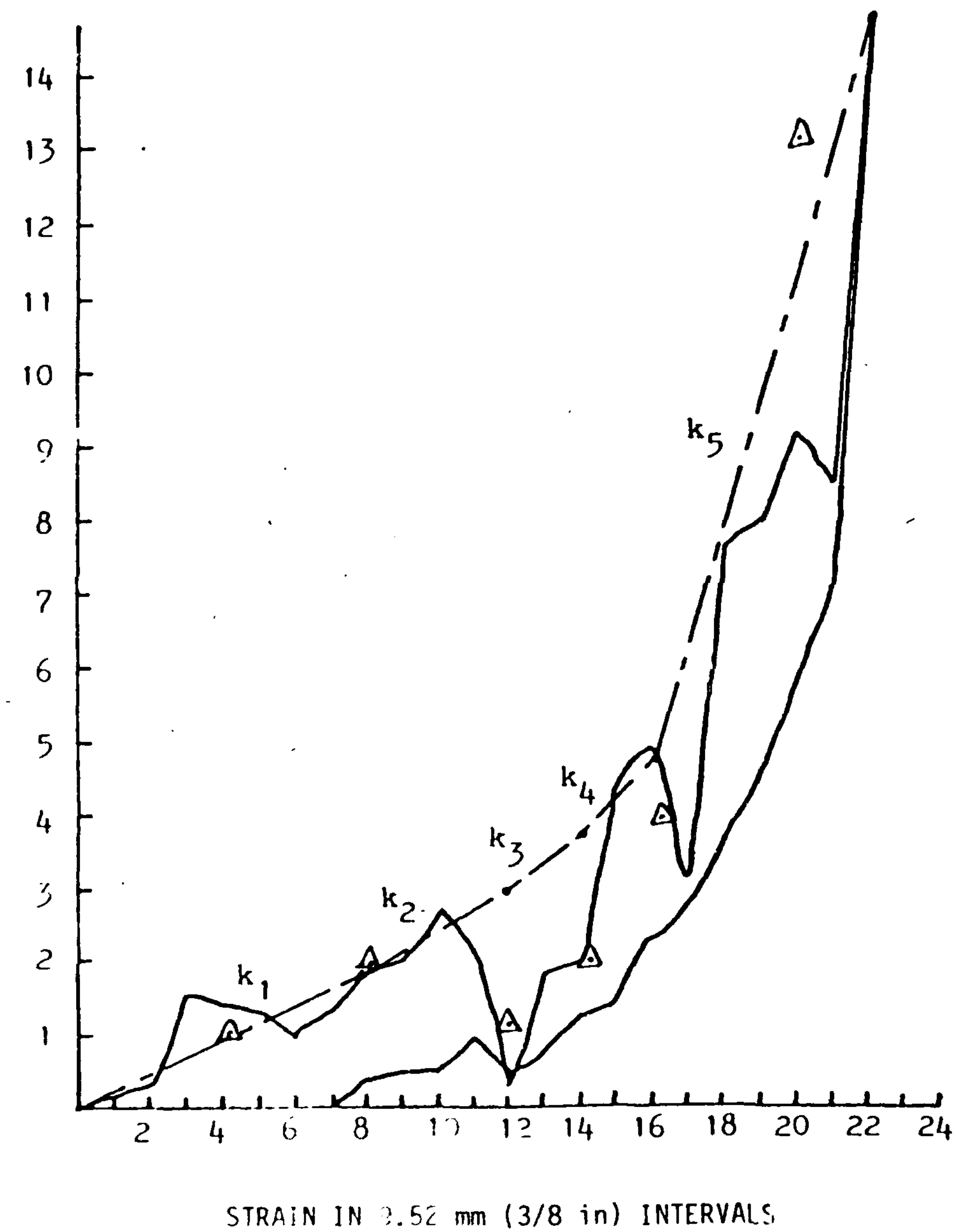

Figure F-4. Impact data for Scott 900-8 foam.

$k_1 = 159924$ N/m
$c_1 = 0.025cr_1$
$k_2 = 195457$ N/m
$c_2 = 0.050cr_2$
$k_3 = 284298$ N/m
$c_3 = 0.100cr_3$
$k_4 = 390880$ N/m
$c_4 = 0.200cr_4$
$k_5 = 1646005$ N/m
$c_5 = 0.100cr_5$

k: spring constant
c: damping coefficient
cr: critical damping

Initial velocity 5.23 m/s

0.304 m x 0.304 m x 0.304 m sample

other to attain heights ranging from 0.076-m (3-in) to 0.305-m (12-in). Sections of 19-mm (3/4-in) plywood were placed on top of and underneath the foam stacks to distribute the load. The machine was set to the maximum compression rate of 200 mm/min (4.23 ft/min), and the various stacks of foam were tested. The machine provided output graphs of load vs deflection. These graphs were linearized and the spring constants calculated for each of the linearized sections. The graph for the 0.152-m (6-in) high stack of foam is shown in Fig. F-5. The results obtained from the Scott 900-8 foam are shown in Table F-1. This table shows that as the height of the stack decreases, the spring constant increases.

At this point in time, the computer study was well under way, and the general dimensions of the platform had been determined with a fair amount of certainty. Bump stops approximately 0.152-m (6-in) in height were considered to be the tallest that could be used and still maintain an acceptable amount of airbag crush. Therefore, the spring constants of the 0.305-m (12-in) and 0.152-m (6-in) stacks of 900-8 foam were compared. This comparison is shown in Table F-2. As can be seen from the table, the stiffness of this foam seems to vary inversely with the height of the foam stack. If it is assumed that stiffness also varies linearly with the surface area to which the load is applied, the following relationship for the stiffness of different size stacks can be written:

$$E = \frac{P/A1}{\Delta L1/L1} \qquad\qquad E = \frac{P/A2}{\Delta L2/L2}$$

$$(1)\quad \frac{P}{\Delta L1} = \frac{EA1}{L1} = K1 \qquad\qquad (2)\quad \frac{P}{\Delta L2} = \frac{EA2}{L2} = K2$$

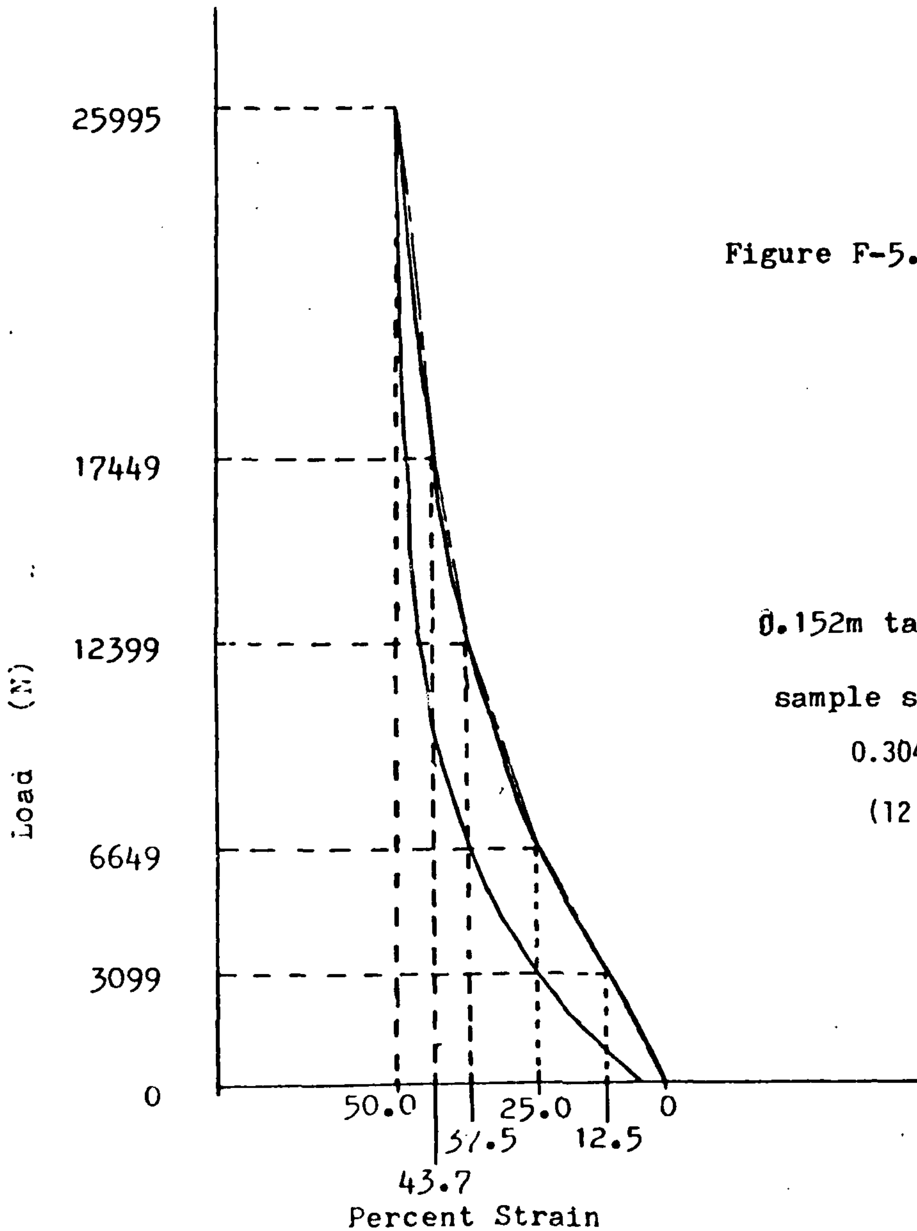

Figure F-5. <u>Compression data for Scott 900-8 foam.</u>

0.152m tall stack of Scott 900-8

sample size:

0.304 m x 0.304 m x 0.152 m

(12 in x 12 in x 6 in)

dividing equation (1) by equation (2)

$$\frac{K1}{K2} = \frac{EA1/L1}{EA2/L2}$$

$$K2 = K1\frac{A2}{A1}\ \frac{L1}{L2}$$

where E = modulus of elasticity

P = applied load

A = area to which load is applied

L = original height of foam stack

Δ L = change in height after the load is applied

K = spring constant

The final bump stop configuration for use in the AGARP was arrived at by trial and error. The above equation along with the previously determined spring constants of the 0.305-x 0.305-x 0.305-m (12-x 12-x 12-in) foam stack and the program BUMP were used to determine a workable bump stop configuration. The final configuration had to fit within the space available on the bottom plate of the AGARP and could not allow more than 0.076 m (3 in) of deflection. Greater amounts of deflection would result in top to bottom plate contact. The trial and error process started with specification of the spring constant. Spring constants were calculated for the same percent deflections as shown in Fig. F-4. The spring constant was changed by varying the impact surface area. Given a particular spring constant, the damping coefficient was determined as a percent of critical damping, using the mass of the top plate. The top plate mass was used because a worst case impact would be one corner of the plate impacting one bump stop.

The previously determined typical top plate impact velocity, the new spring constant, the new damping coefficient and the top plate mass were used as the input parameters for BUMP. The program was then run and the resultant accelerations and deflections were reviewed to determine if the performance objectives had been met. Modifications were made to the spring constant to make up for any performance deficiencies. The final bump stop impact surface area was 0.023 m^2 (36 in^2). A bump stop occupying that much area could be placed at each one of the four corners of 1/2 the bottom plate. The dimensions would be 0.076 x 0.457 x 0.152 m (13 x 18 x 6 in). The spring constants and damping coefficients corresponding to this surface area and height were incorporated into the LAND3 bump stop model. These values were used during the computer runs summarized in Table 4.

After the computer study was completed, but before final fabrication of the bump stops, it was decided to try to reduce bump stop caused accelerations by increasing bump stop deflections. Towards this end the top layer of Scott 900-8 foam was replaced by two layers of Scott 900-4 foam. Given the space restrictions of the bottom plate, the configuration shown in Fig. F-6 was decided upon. Some rough calculations were made to evaluate this configuration. The difference between the combined foam bump stop and the previously evaluated 0.076- x 0.457- x 0.152-m (3- x 18- x 6-in) Scott 900-8 foam bump stop was small. However, the two layers of Scott 900-4 foam on top of the combined foam bump stop would allow more initial deflection and thus

reduce the acceleration peak. It was thought that this would more than make up for the 0.025 m (1 in) of available airbag crush which would be lost by using 0.178-m (7-in) high bump stops.

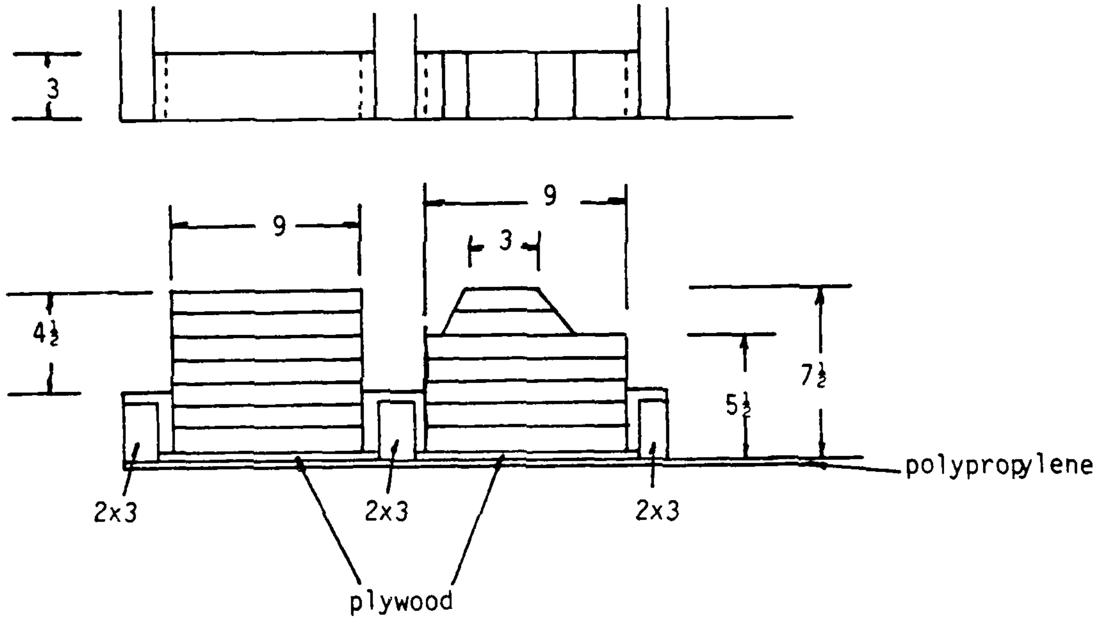

Figure F-6. Combined foam bump stop as used in AGARP.

TABLE F-1. Spring Constants of Scott 900-8 Foam

Original Height	Spring Constant (N/m) for Percent Deflection (N) 0-25.0%	25.0-37.5%	37.5-43.75%	43.75-50.0%	25-50%
12	81,853	134,759	226,682	435,747	232,987
9	113,726	183,724	353,421	622,256	336,819
6	174,530	301,811	530,175	897,203	507,759
3	301,741	503,398	830,463	1,679,717	879,218

TABLE F-2. Comparison of Scott 900-8 Spring Constants

Percent Deflection	Spring Constant (N/m) 0.305-m Stack K12	0.152-m Stack K6	K6 / K12
0-25.00%	81,853	174,530	2.13
25.00-37.50%	134,759	301,811	2.24
37.50-43.75%	226,682	530,175	2.34
43.75-50.00%	435,747	897,203	2.05
25.00-50.00%	232,987	507,759	2.18

APPENDIX G

Plots of

Experimental

versus

LAND3 Data

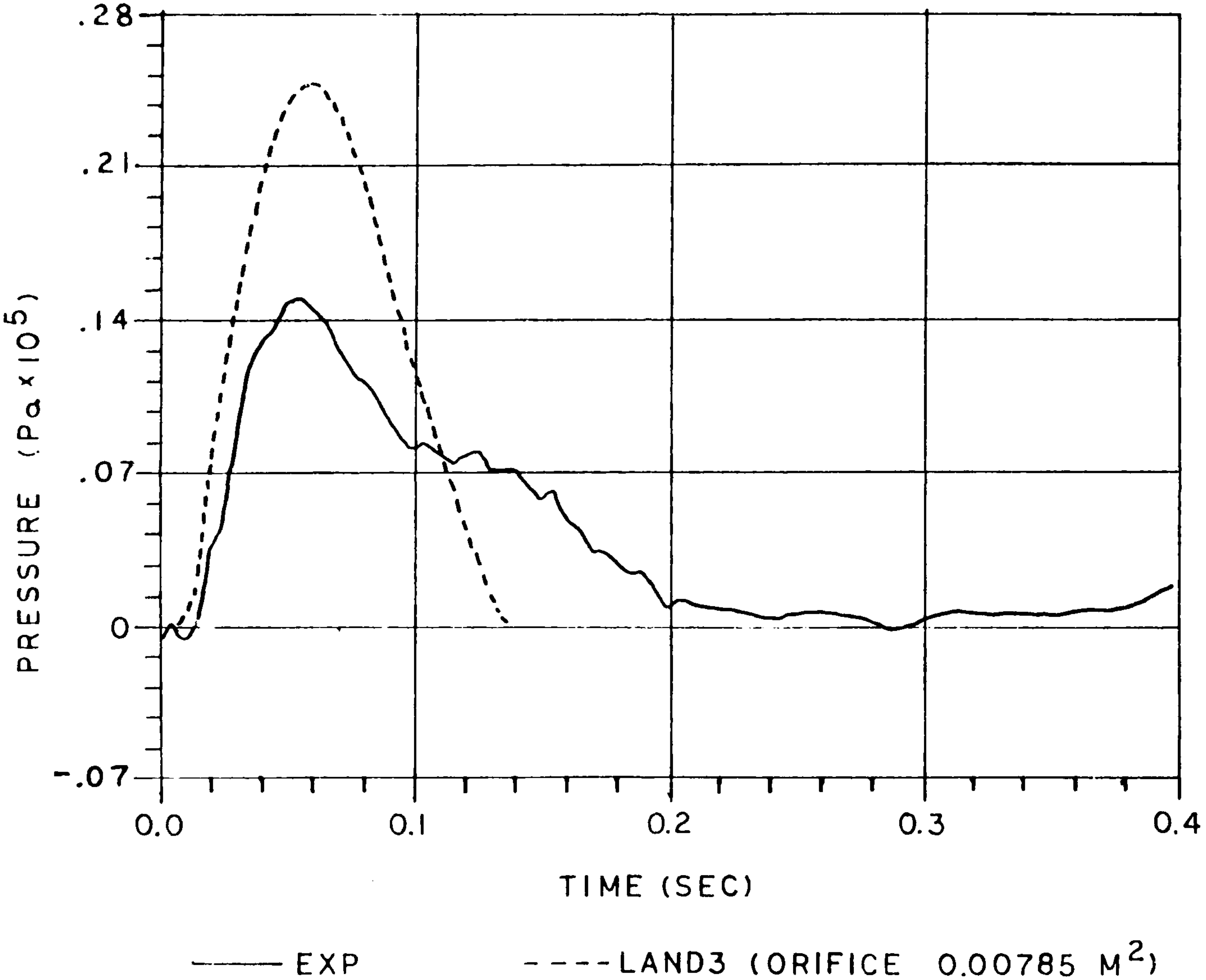

Figure -1. Drop 4H I left rear airbag pressure.

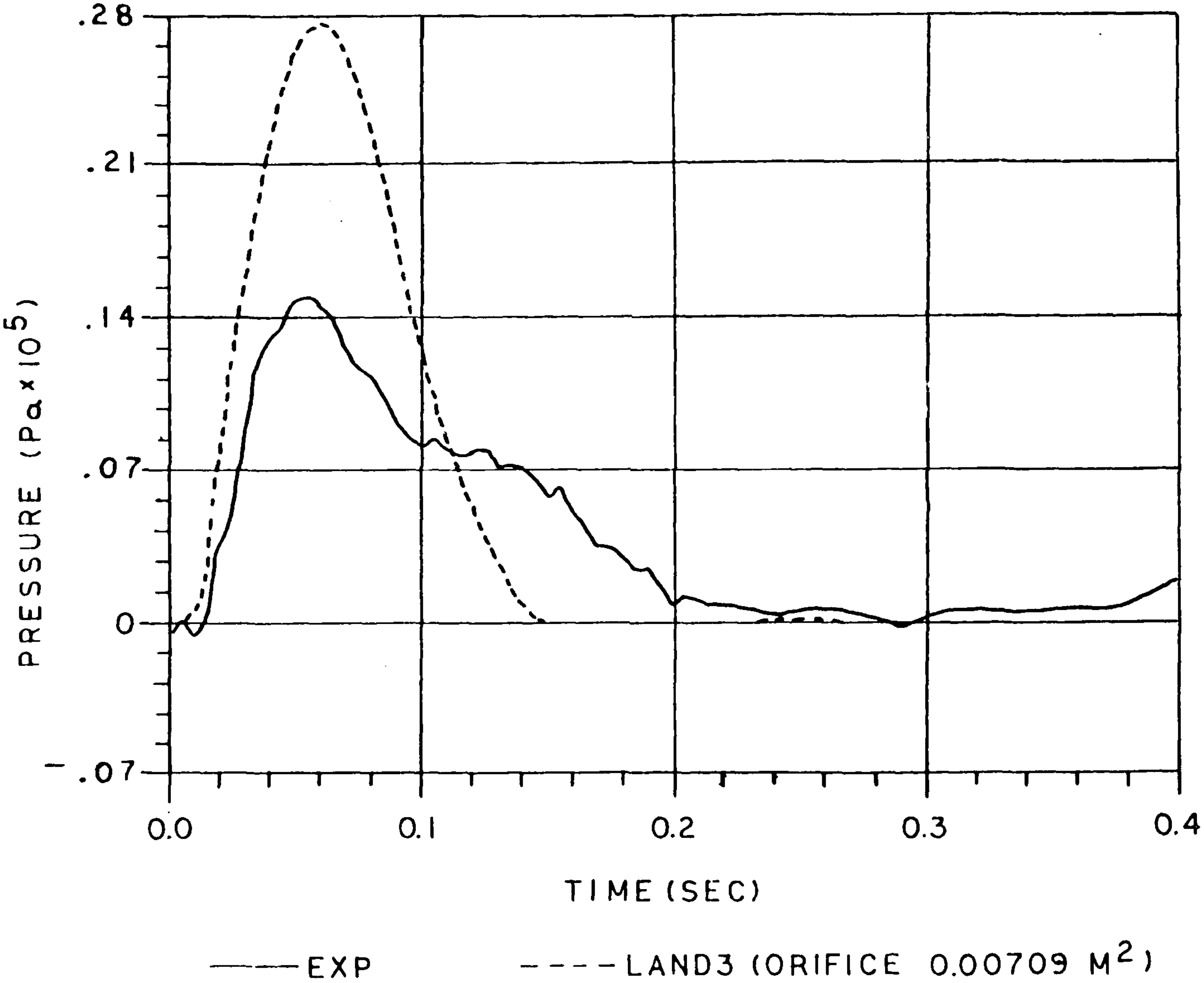

Figure G-2. Drop 4H I left rear airbag pressure.

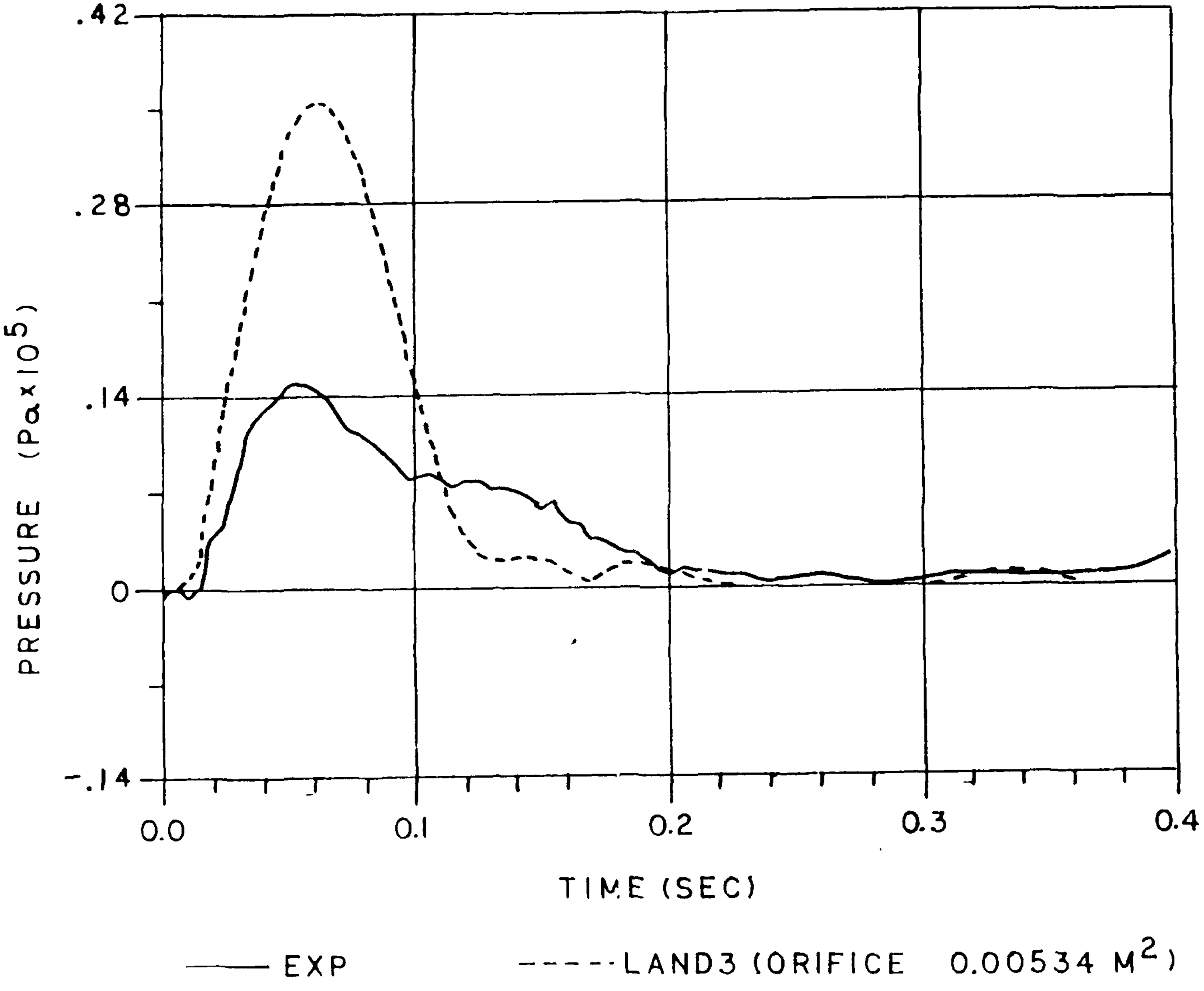

Figure G-3. Drop 4H I left rear airbag pressure.

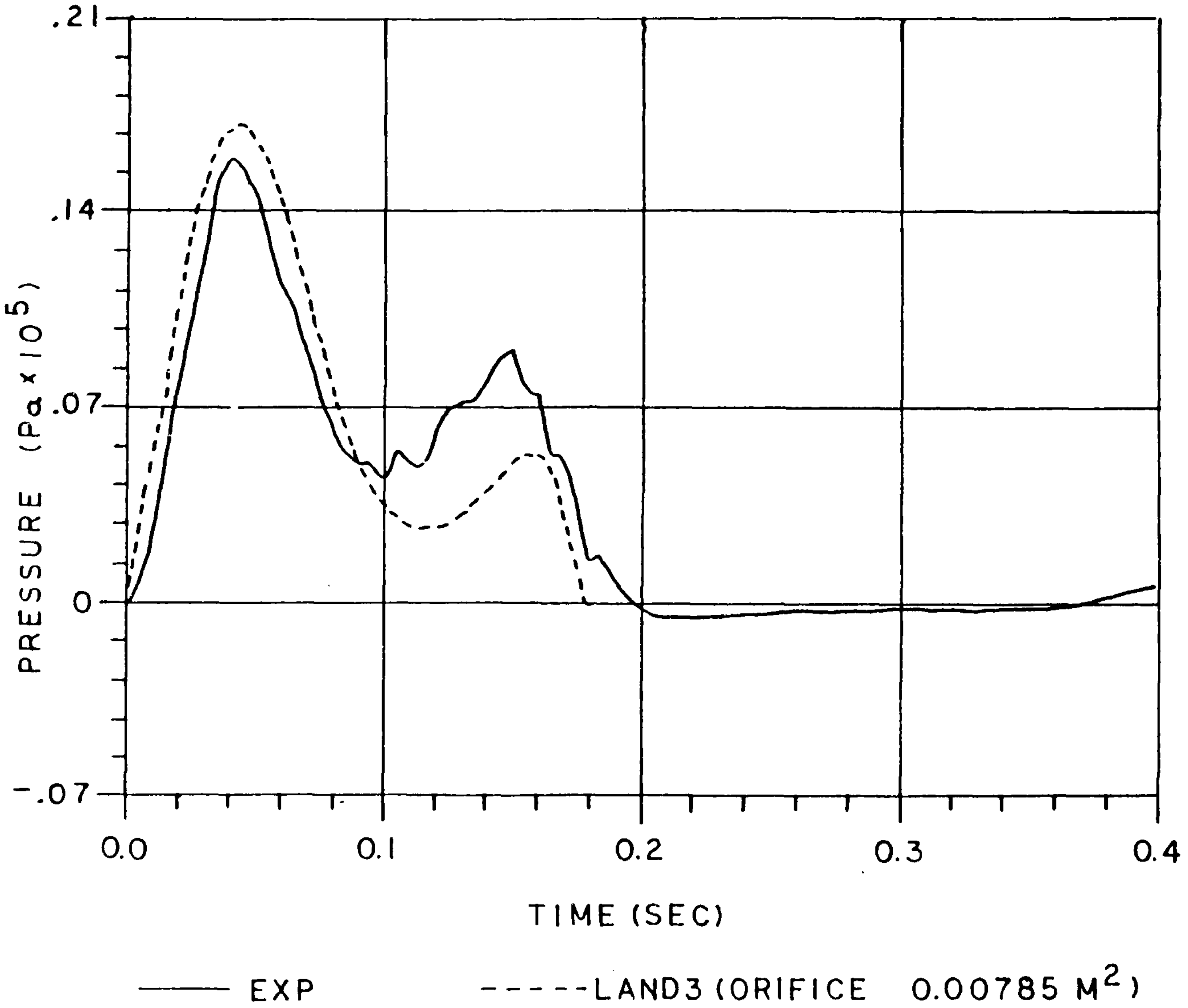

Figure G-4. Drop 4II I right front airbag pressure.

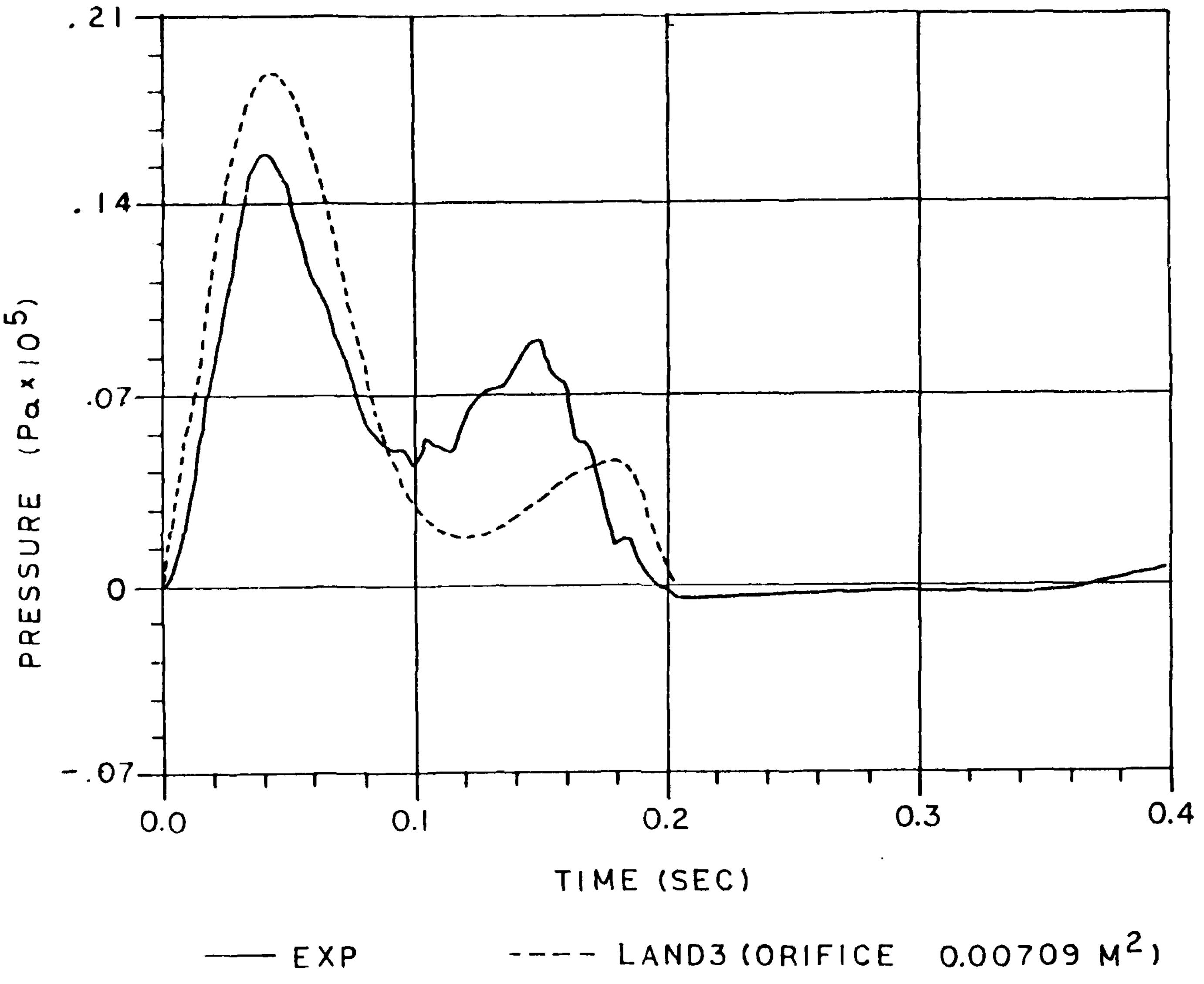

Figure [illegible]-5. Drop 4H I right front airbag pressure.

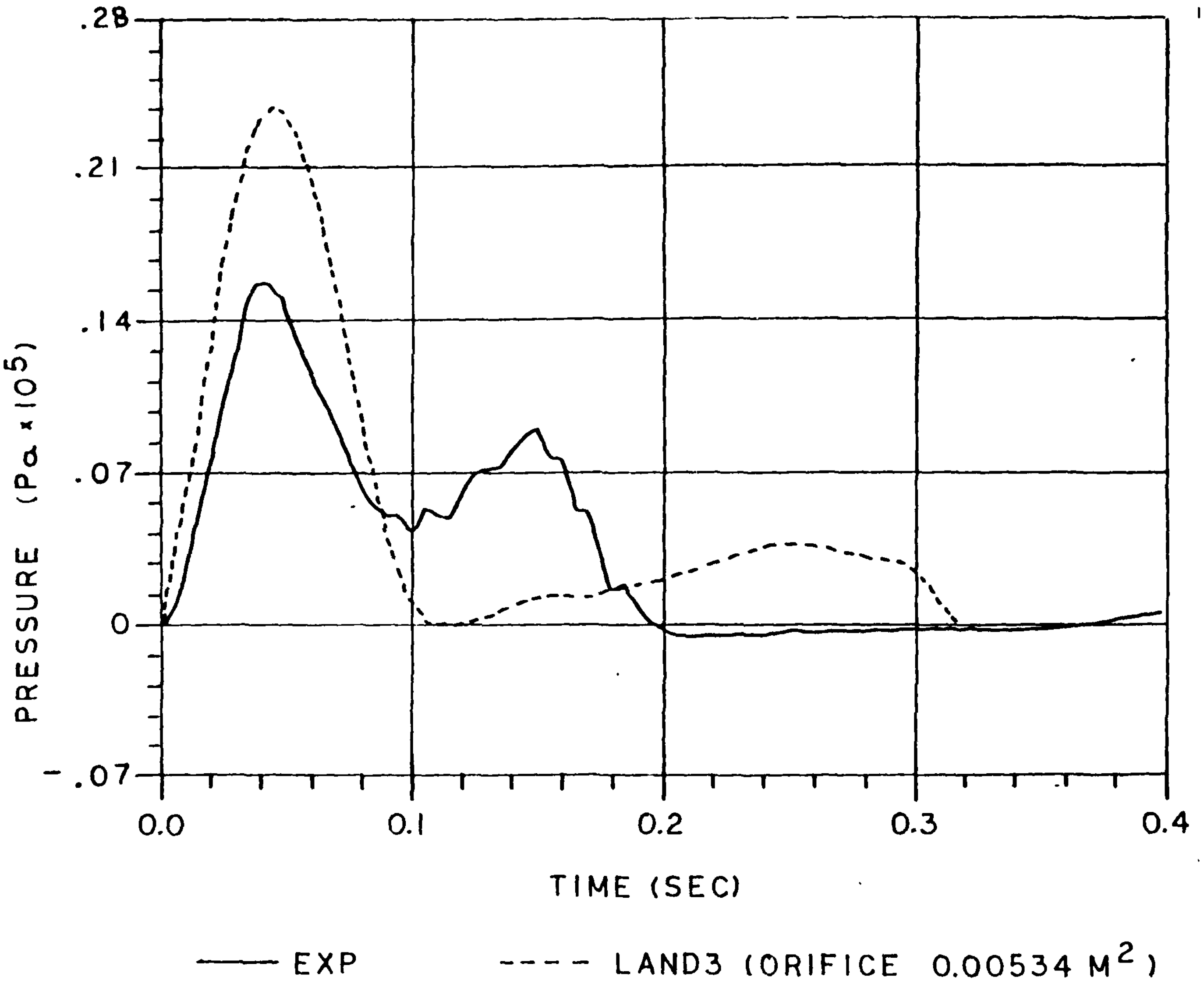

Figure G-6. Drop 4H I right front airbag pressure.

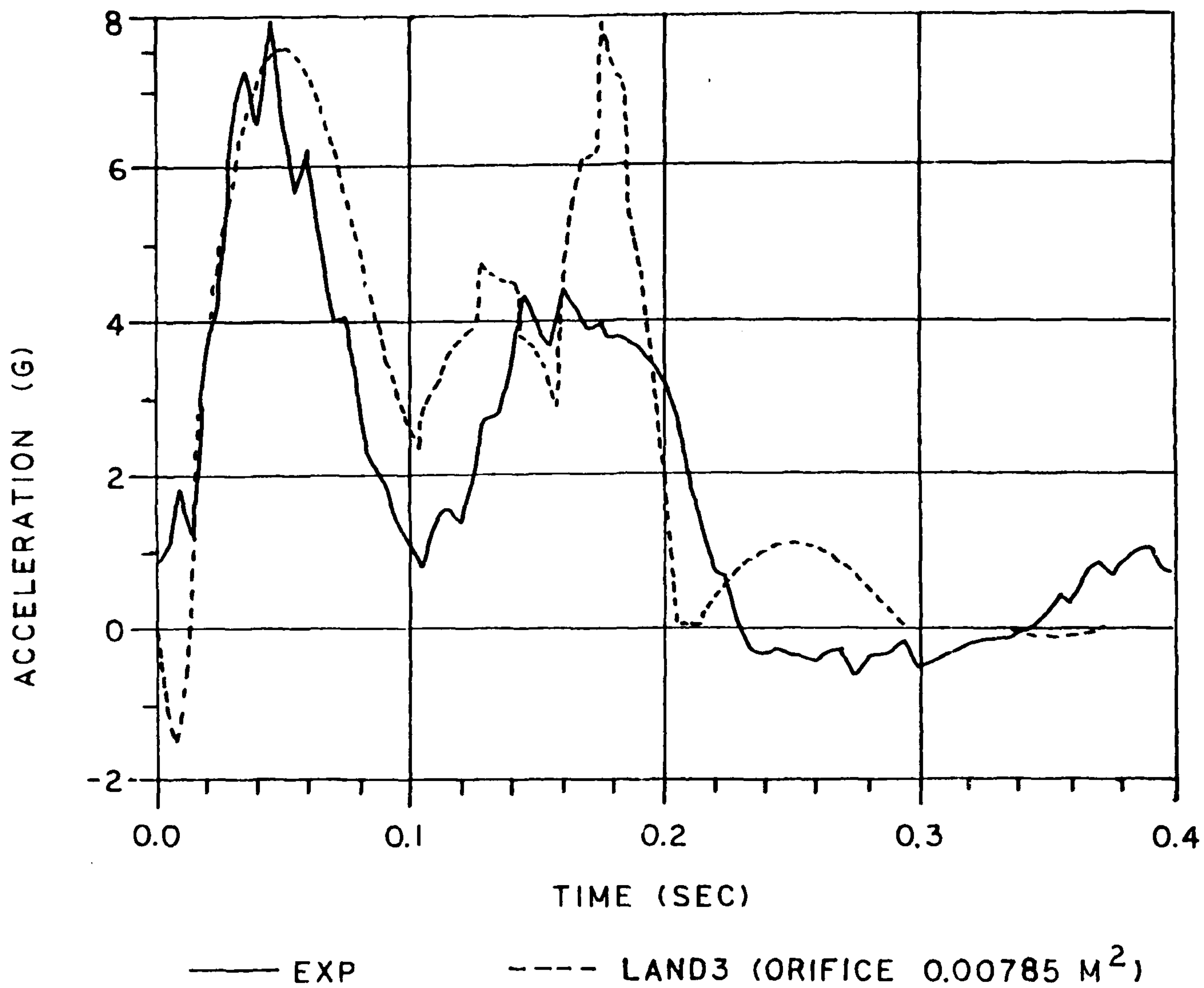

Figure G-7. Drop 4H I top plate vertical acceleration at the c.g..

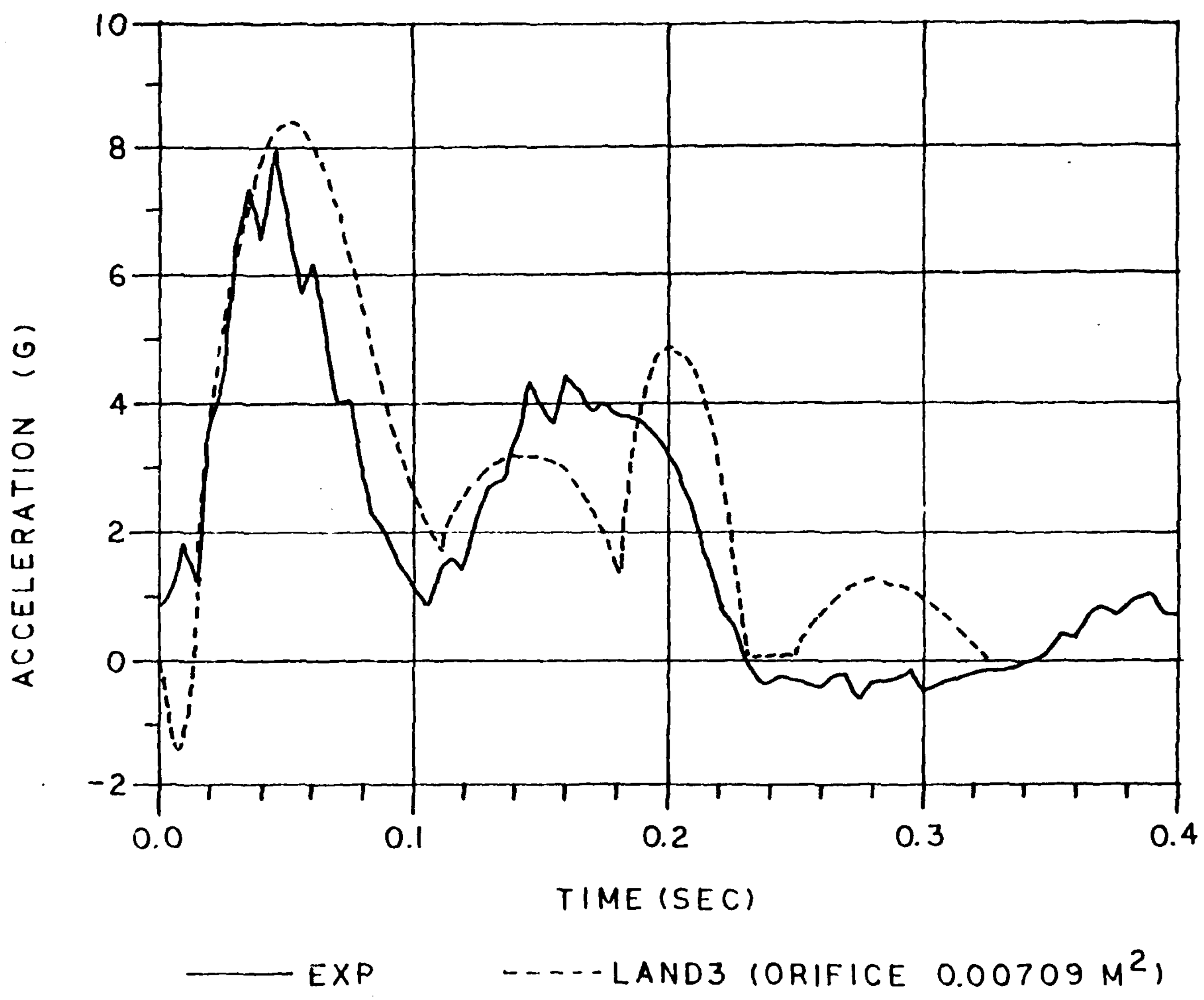

Figure G-8. Drop 4H I top plate vertical acceleration at the c.g..

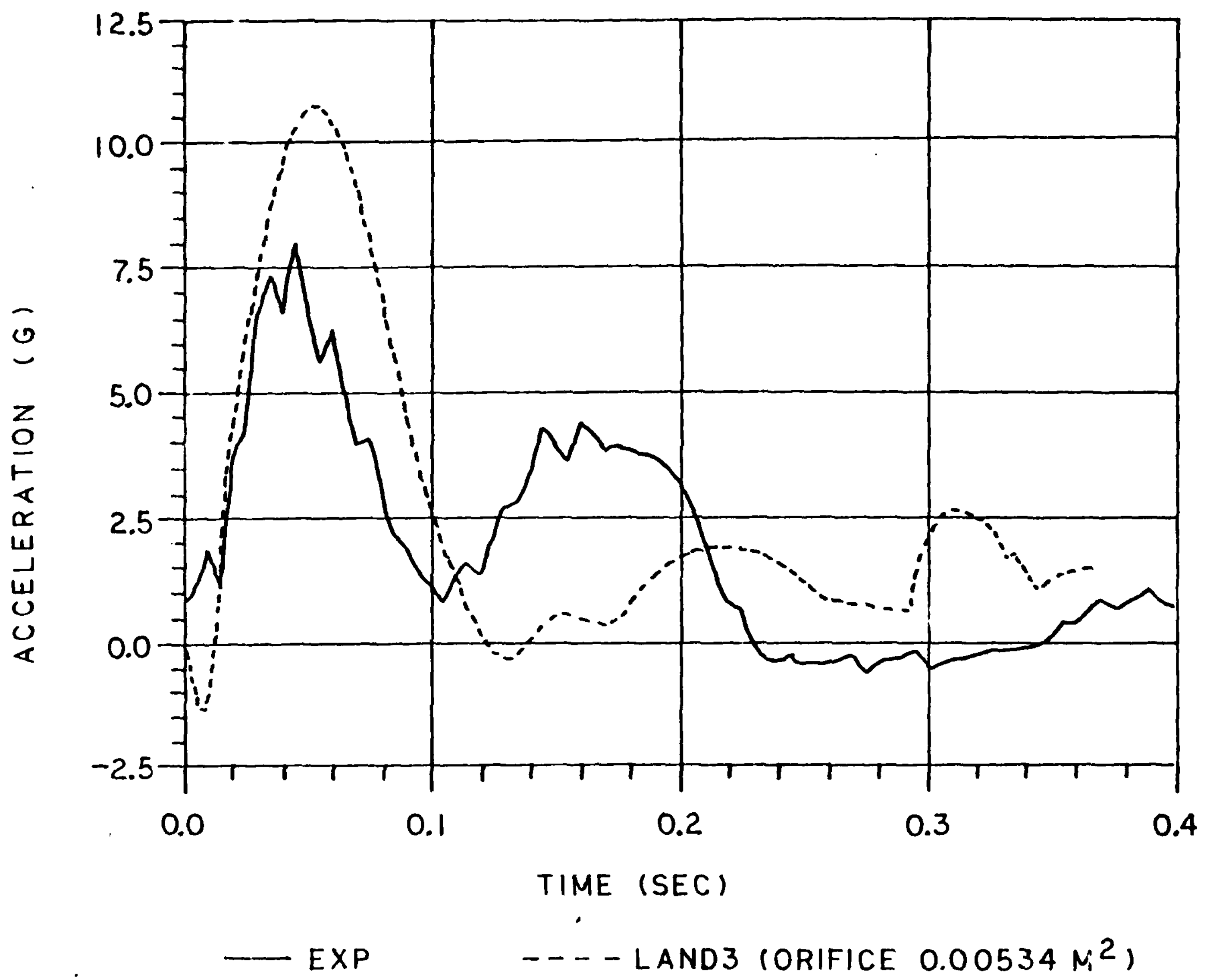

Figure G-9. Drop 4H I top plate vertical acceleration at the c.g..

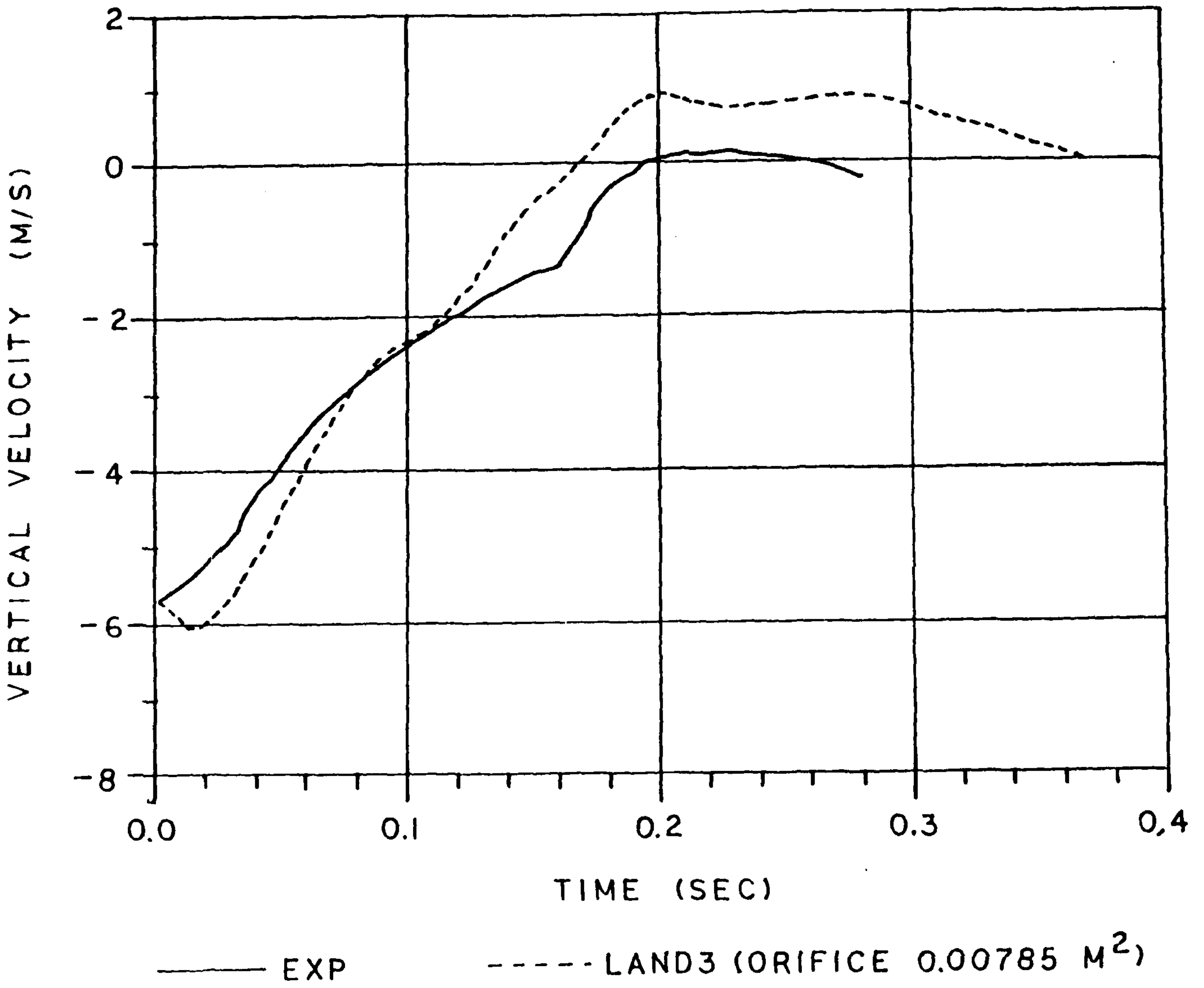

Figure G-10. Drop 4H I top plate vertical velocity.

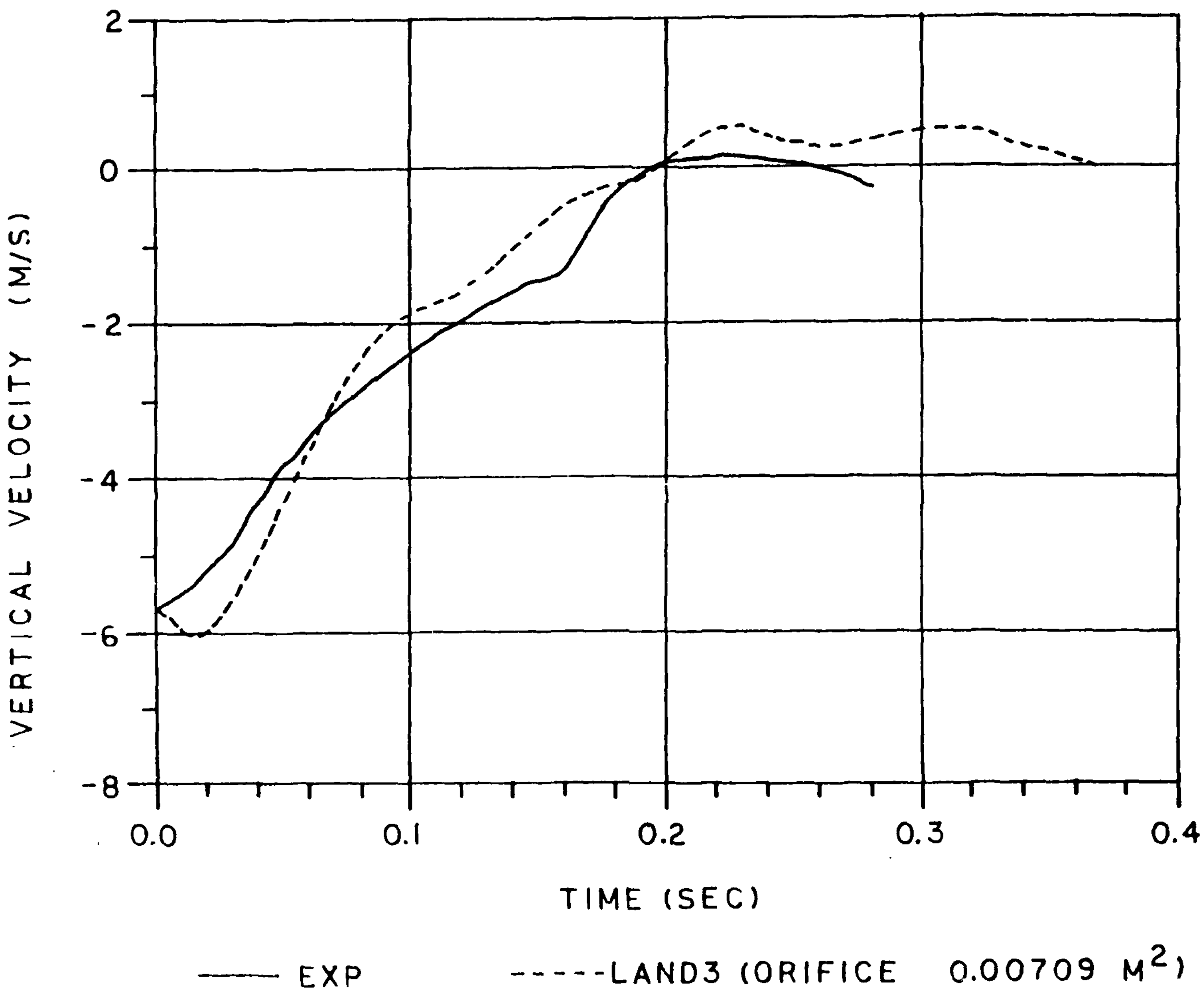

Figure G-11. Drop 4H I top plate vertical velocity.

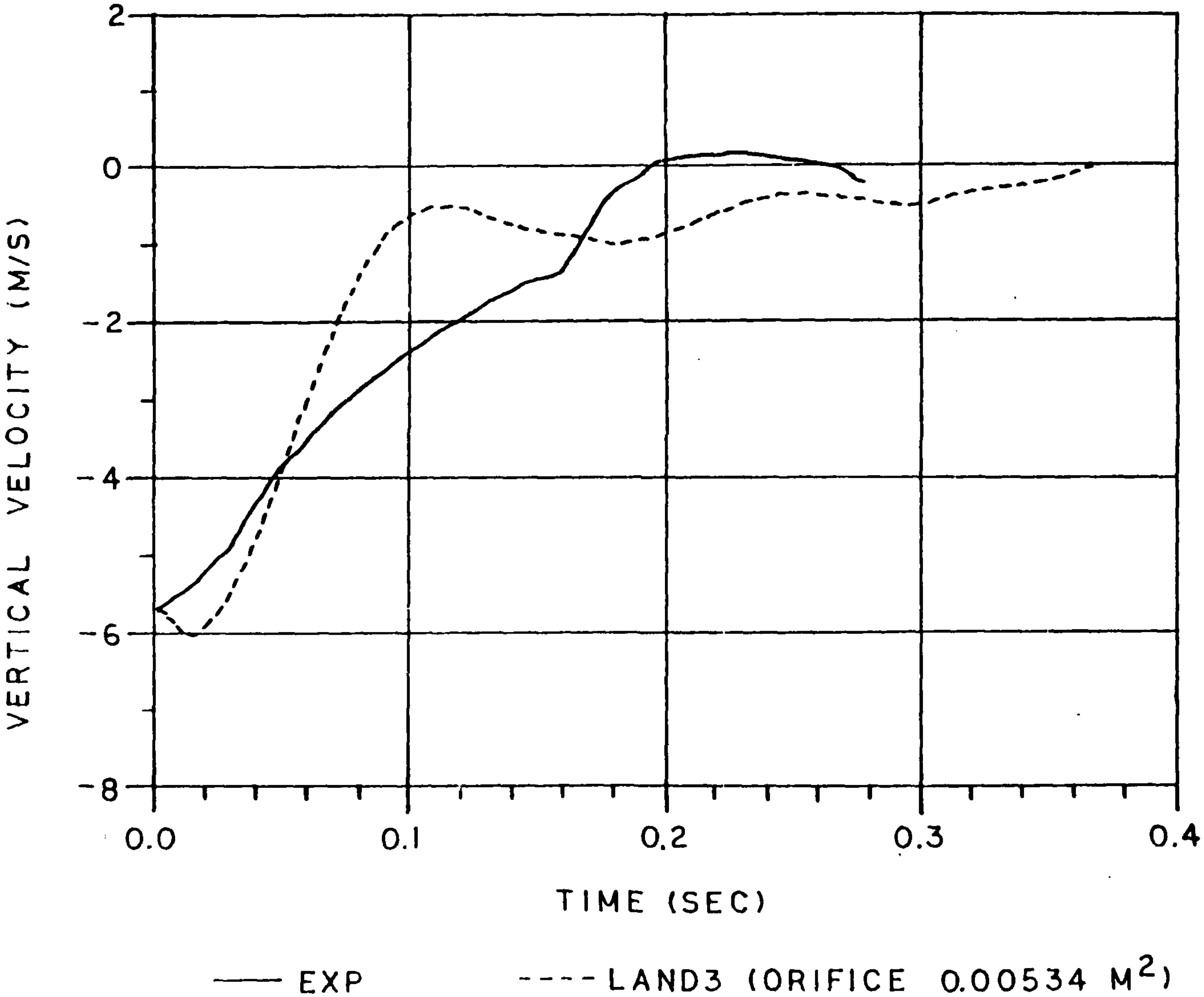

Figure G-12. Drop 4H 1 top plate vertical velocity.

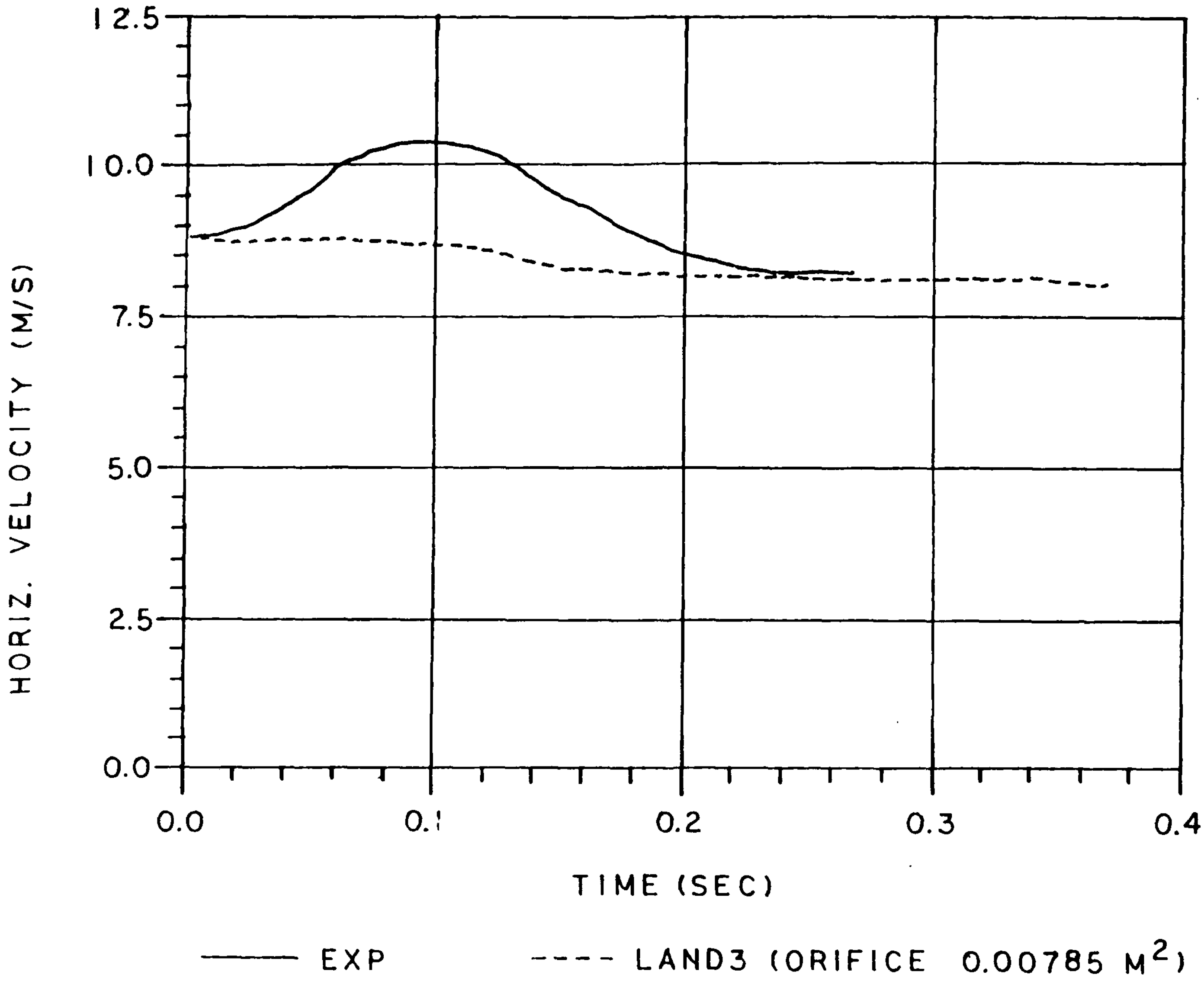

Figure G-13. Drop 4H I top plate horizontal velocity.

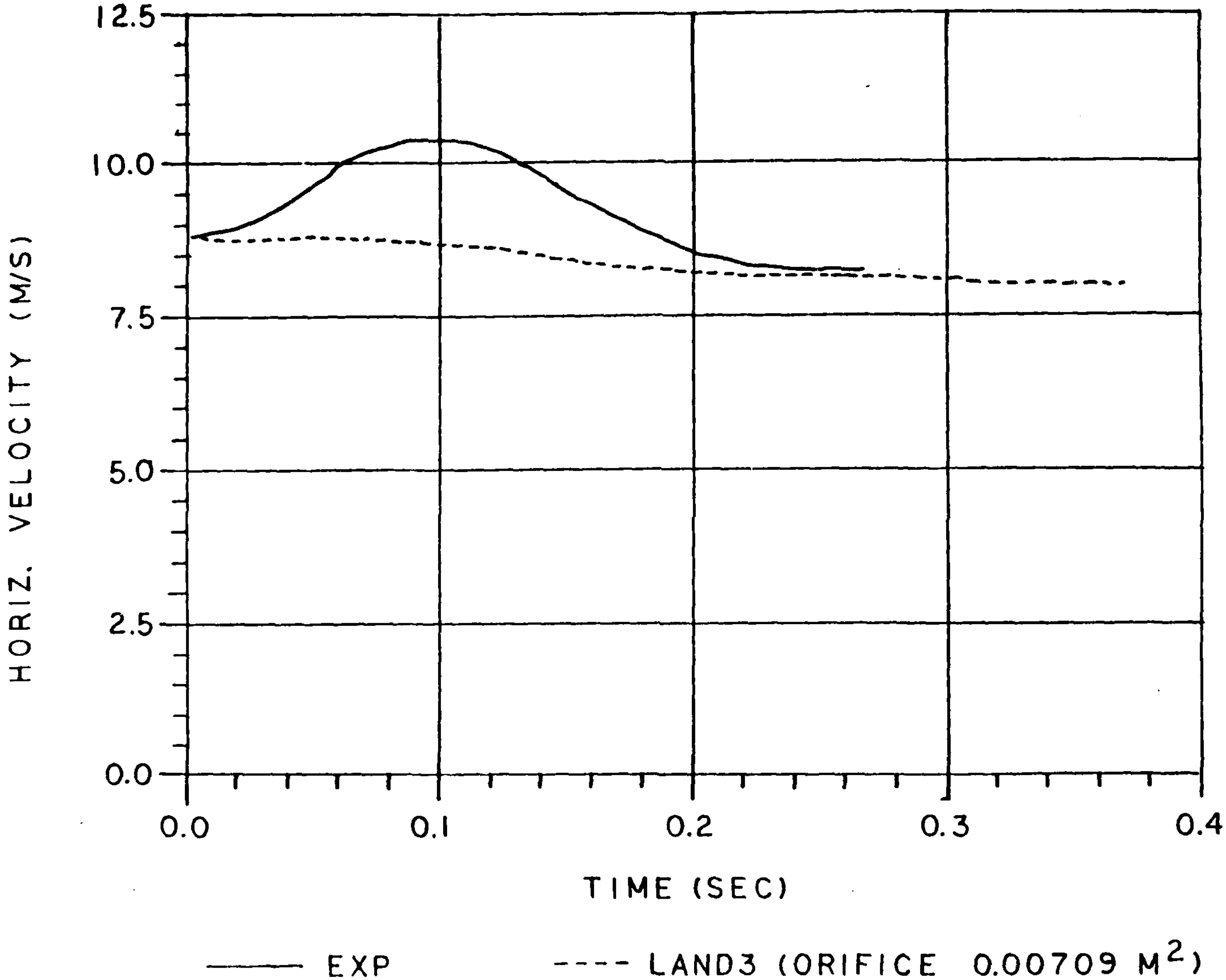

Figure G-14. Drop 4H I top plate horizontal velocity.

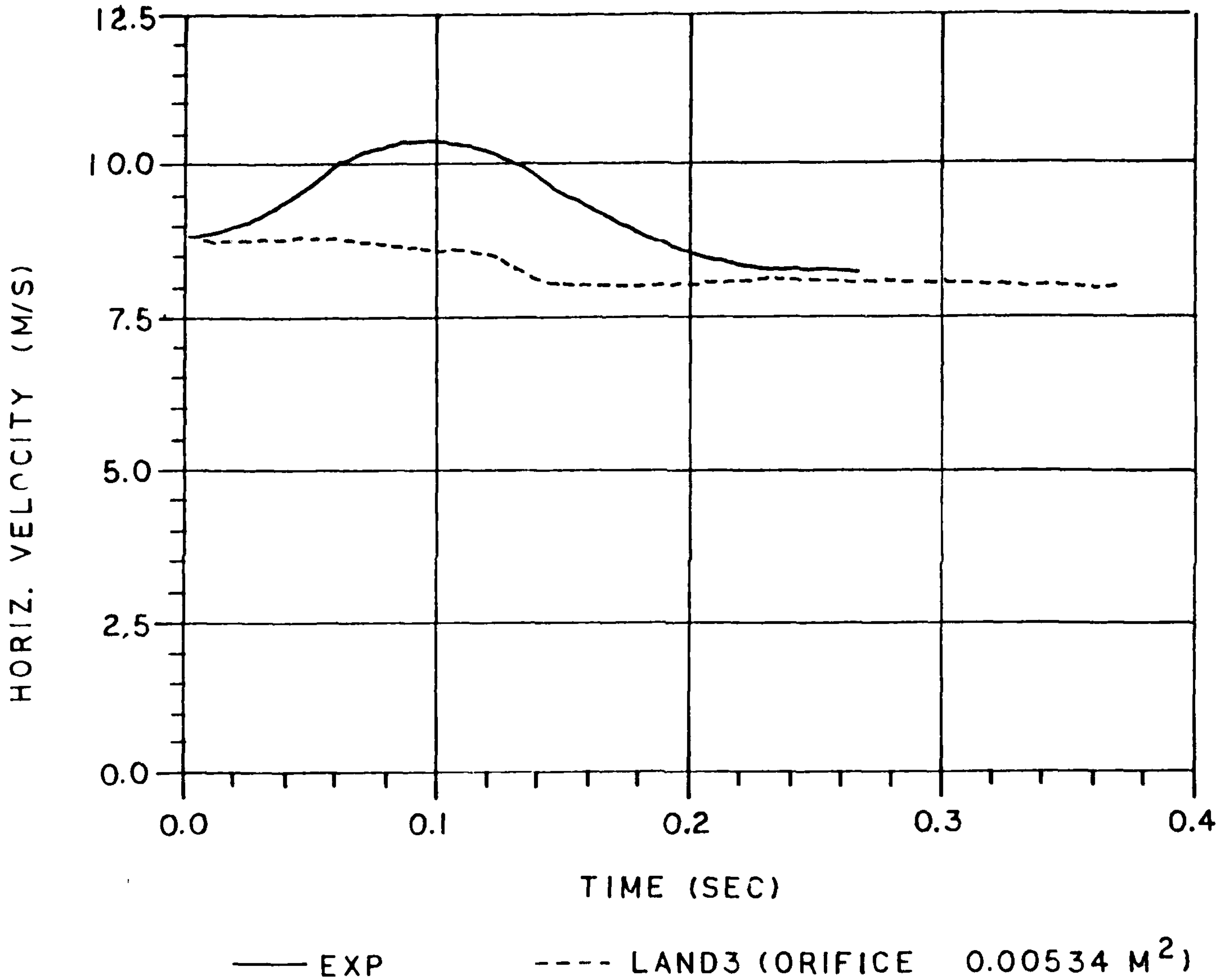

Figure G-15. Drop 411 I top plate horizontal velocity.

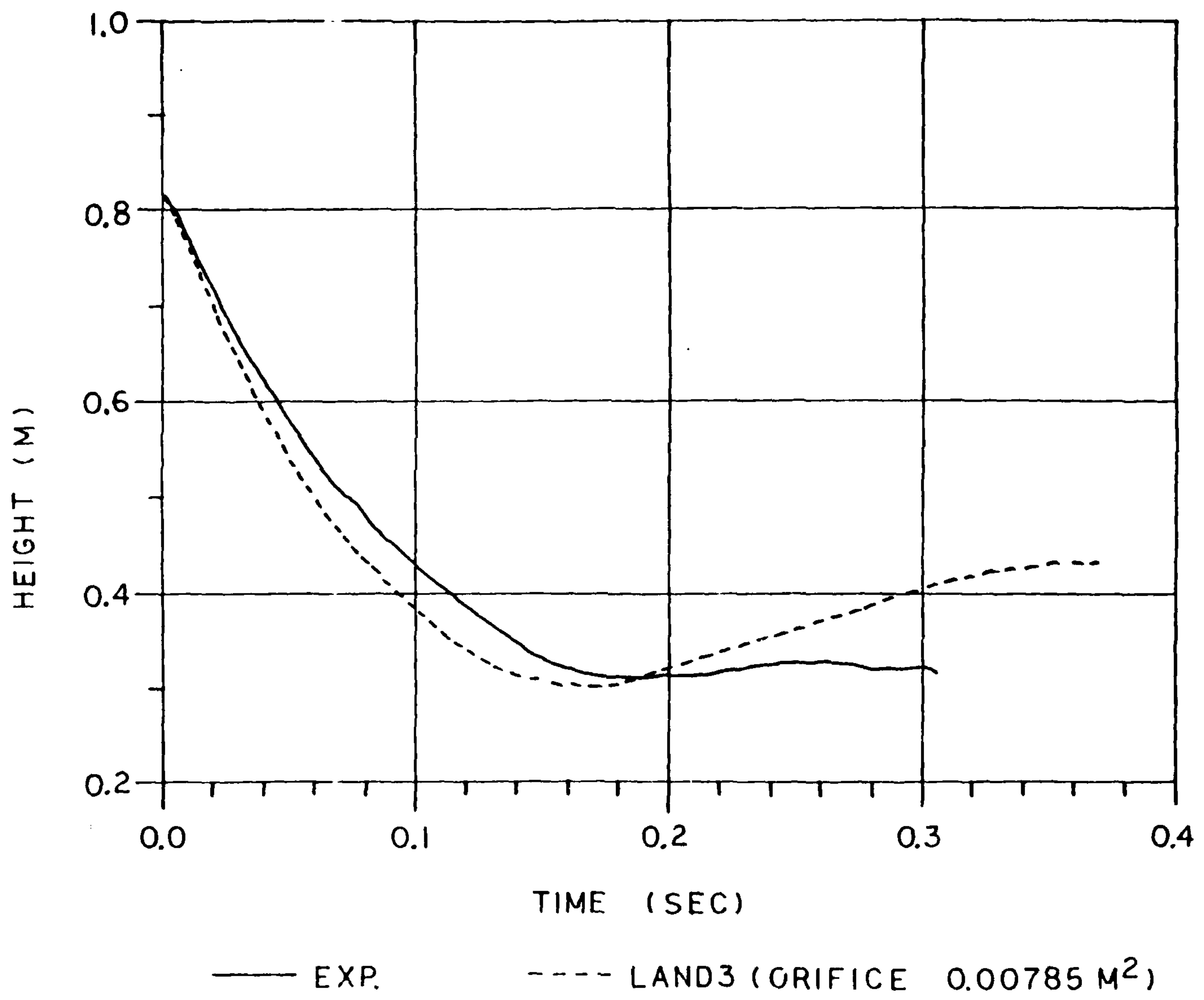

Figure G-16. Drop 4H I top plate height at the c.g..

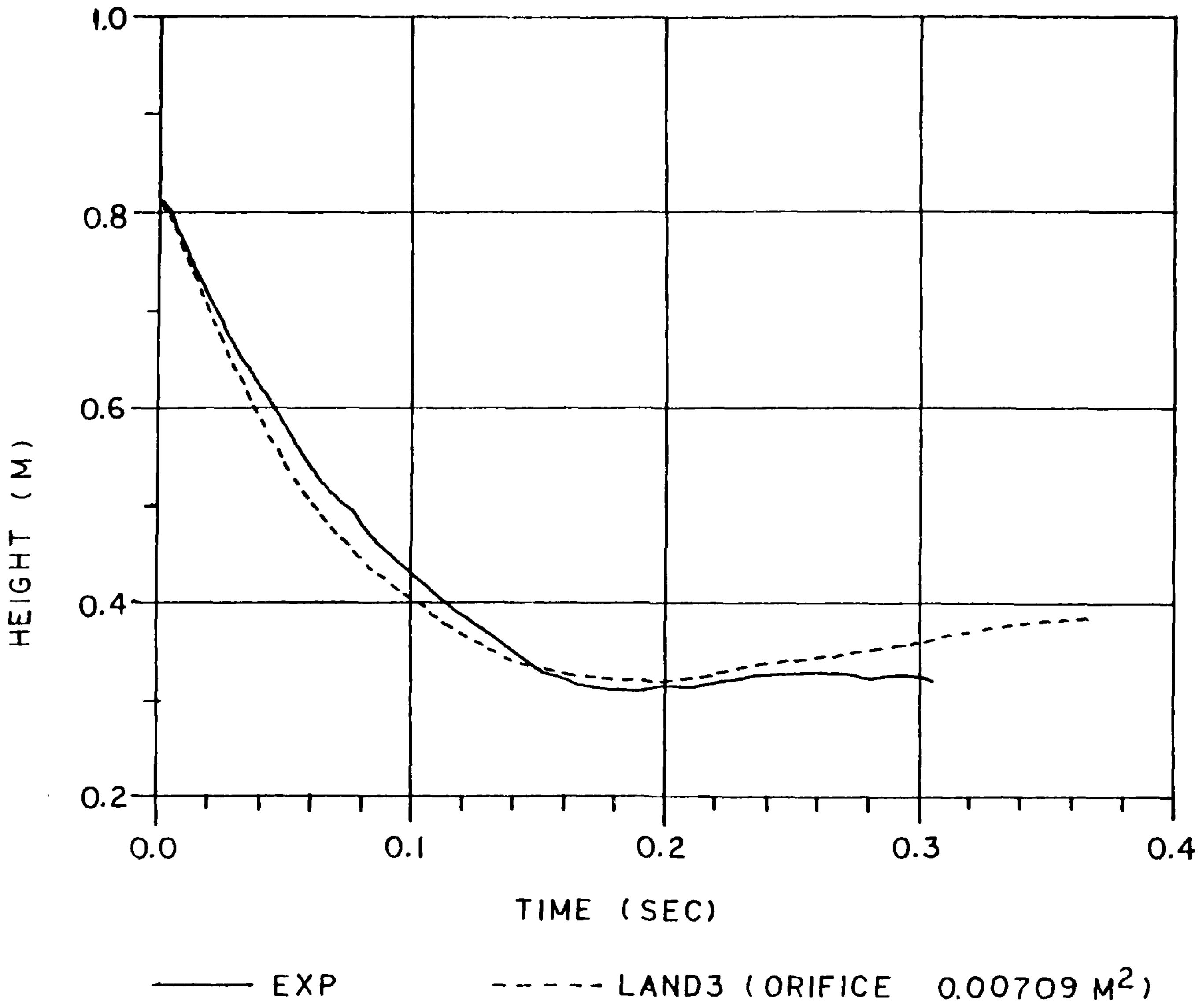

Figure G-17. Drop 4H I top plate height at the c.g..

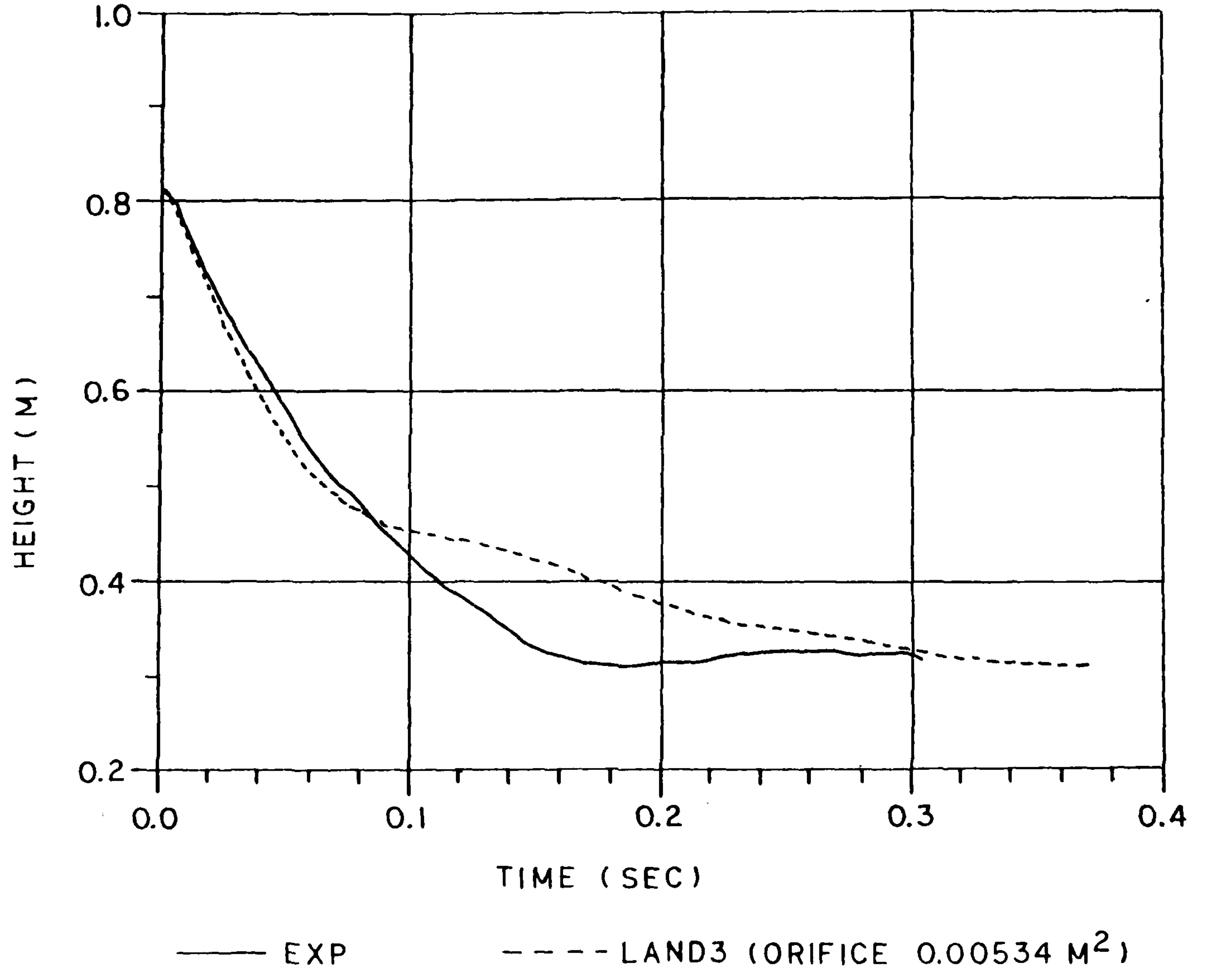

Figure G-18. Drop 4H I top plate height at the c.g..

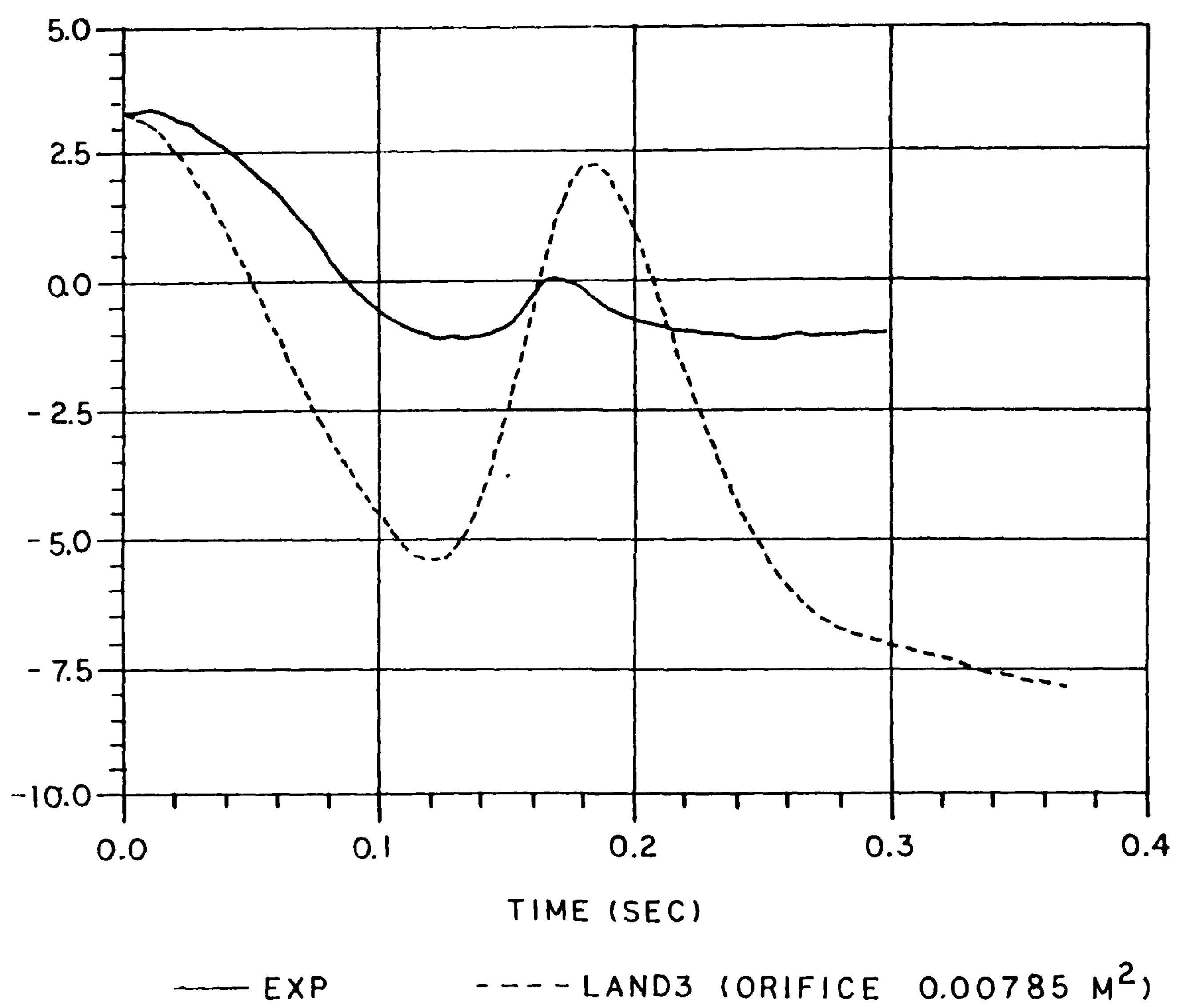

Figure G-19. Drop 4H I top plate pitch.

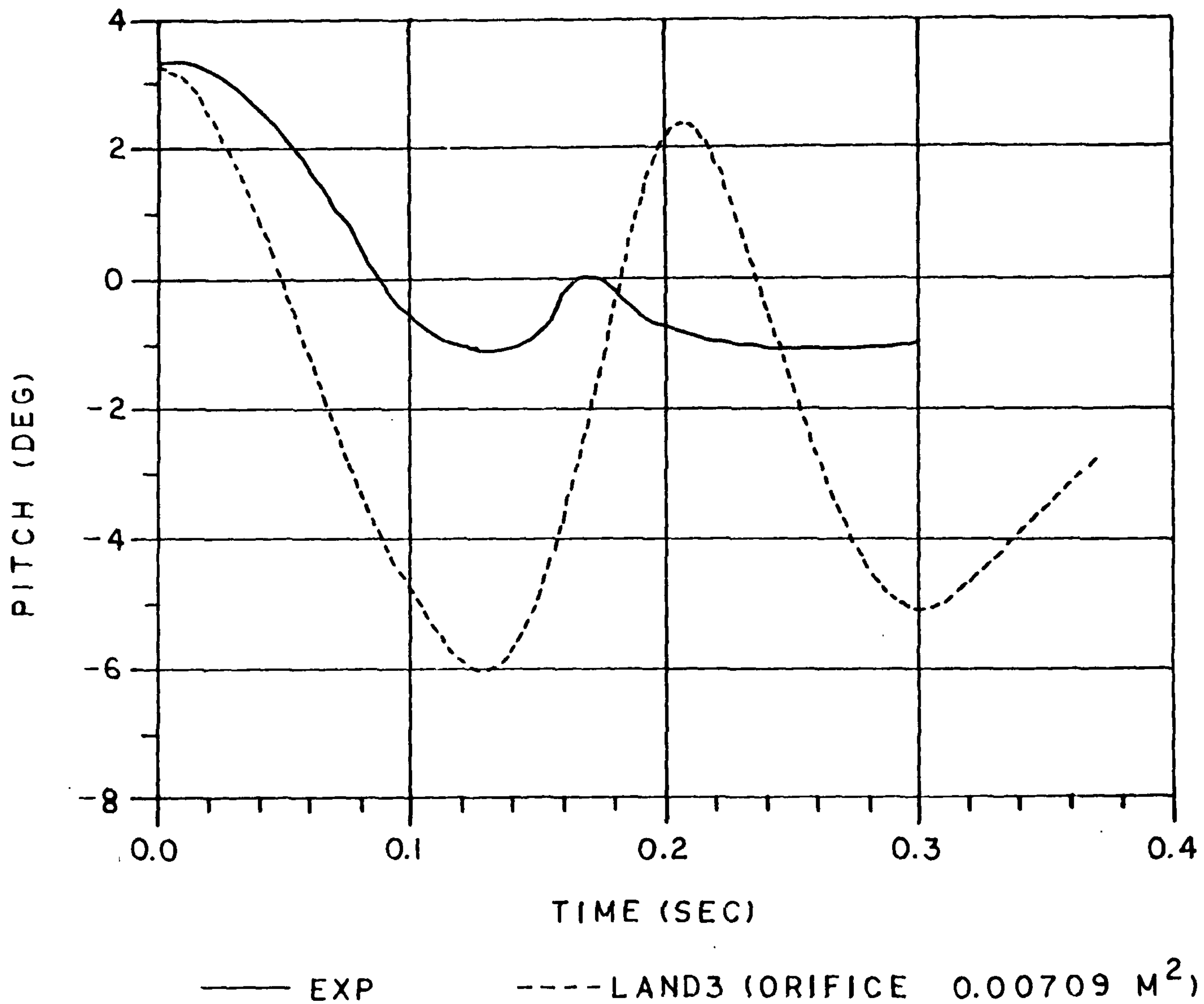

Figure G-20. Drop 4H I top plate pitch.

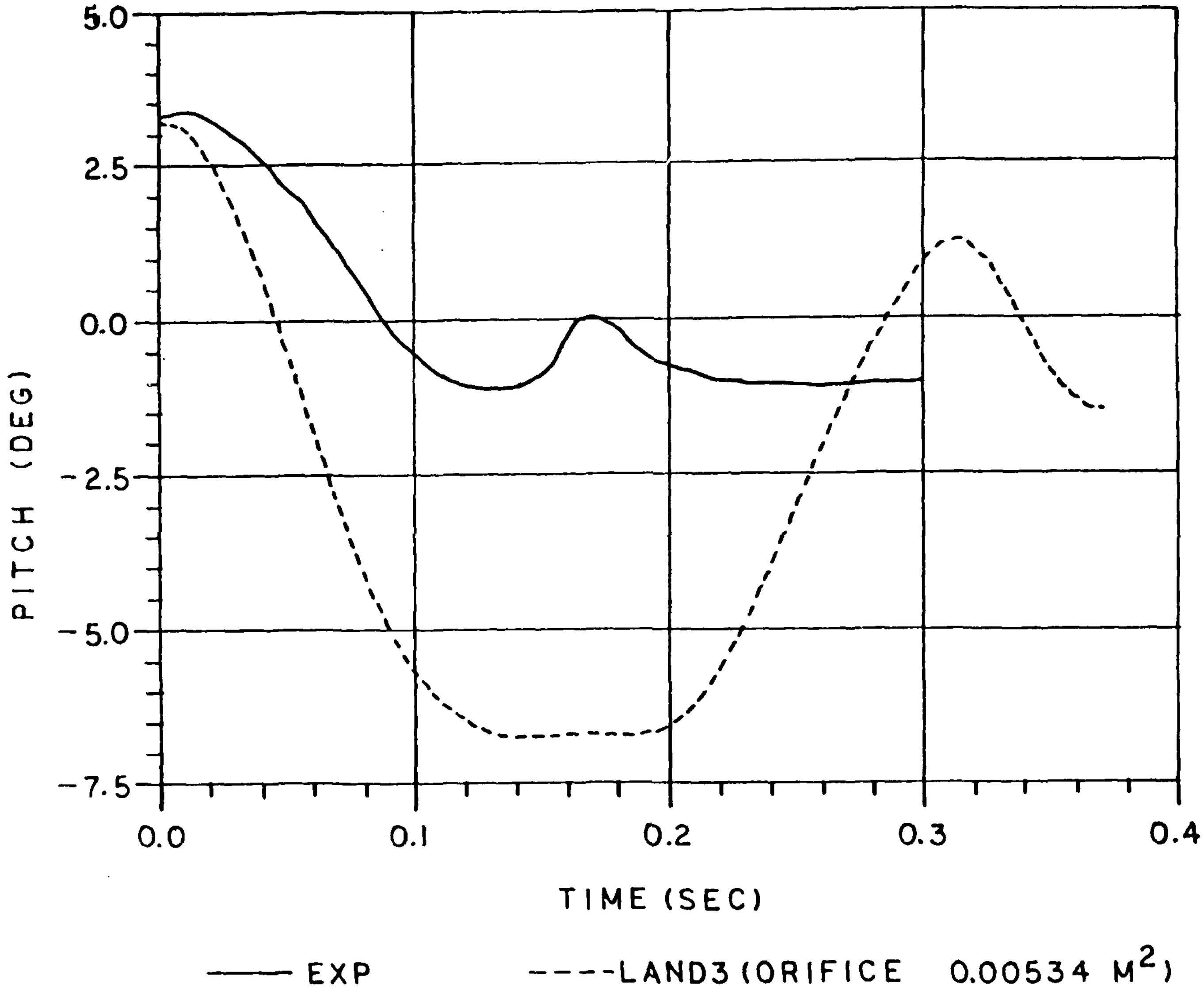

Figure G-21. Drop 4H I top plate pitch.

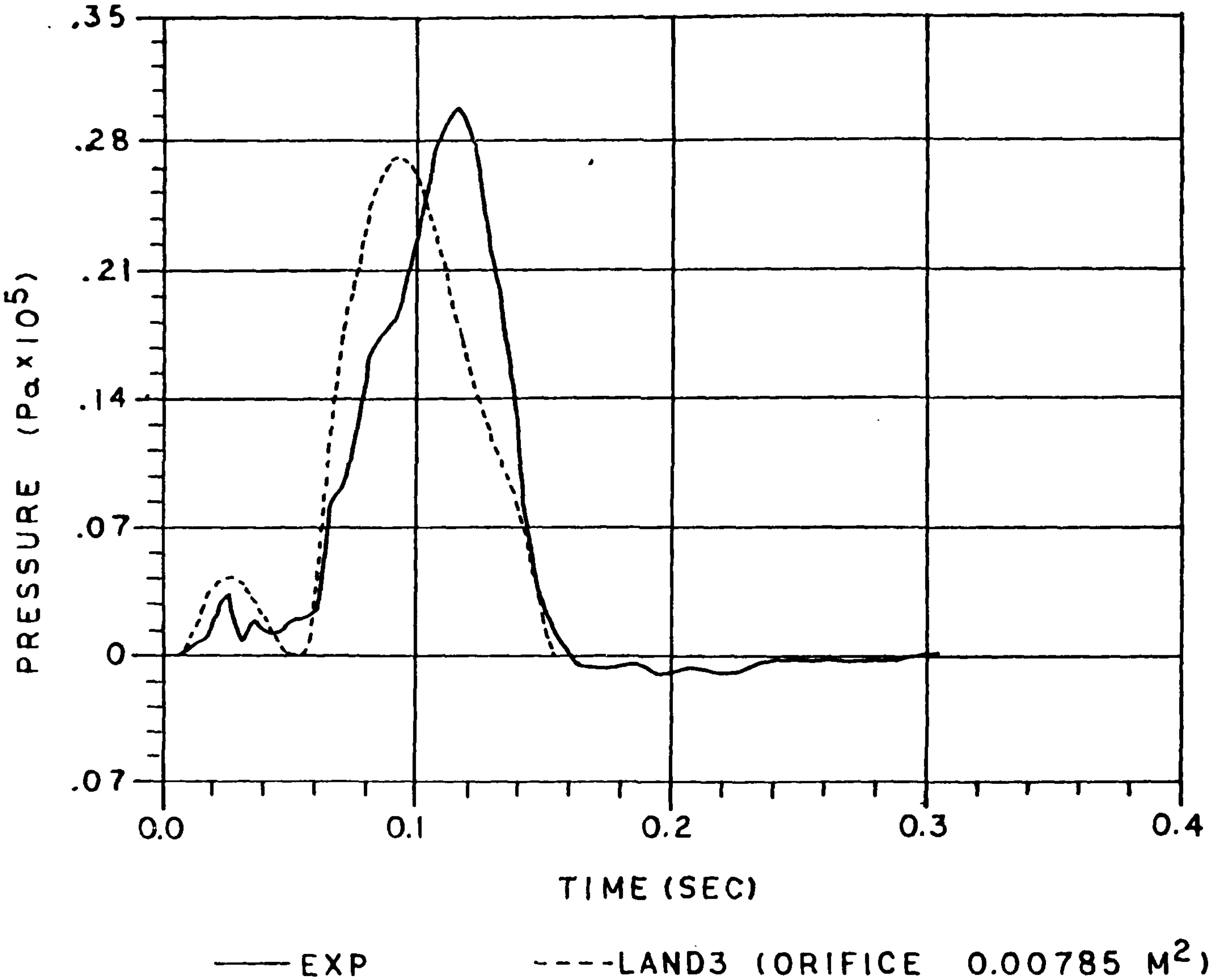

Figure G-22. Drop 5H I right front airbag pressure.

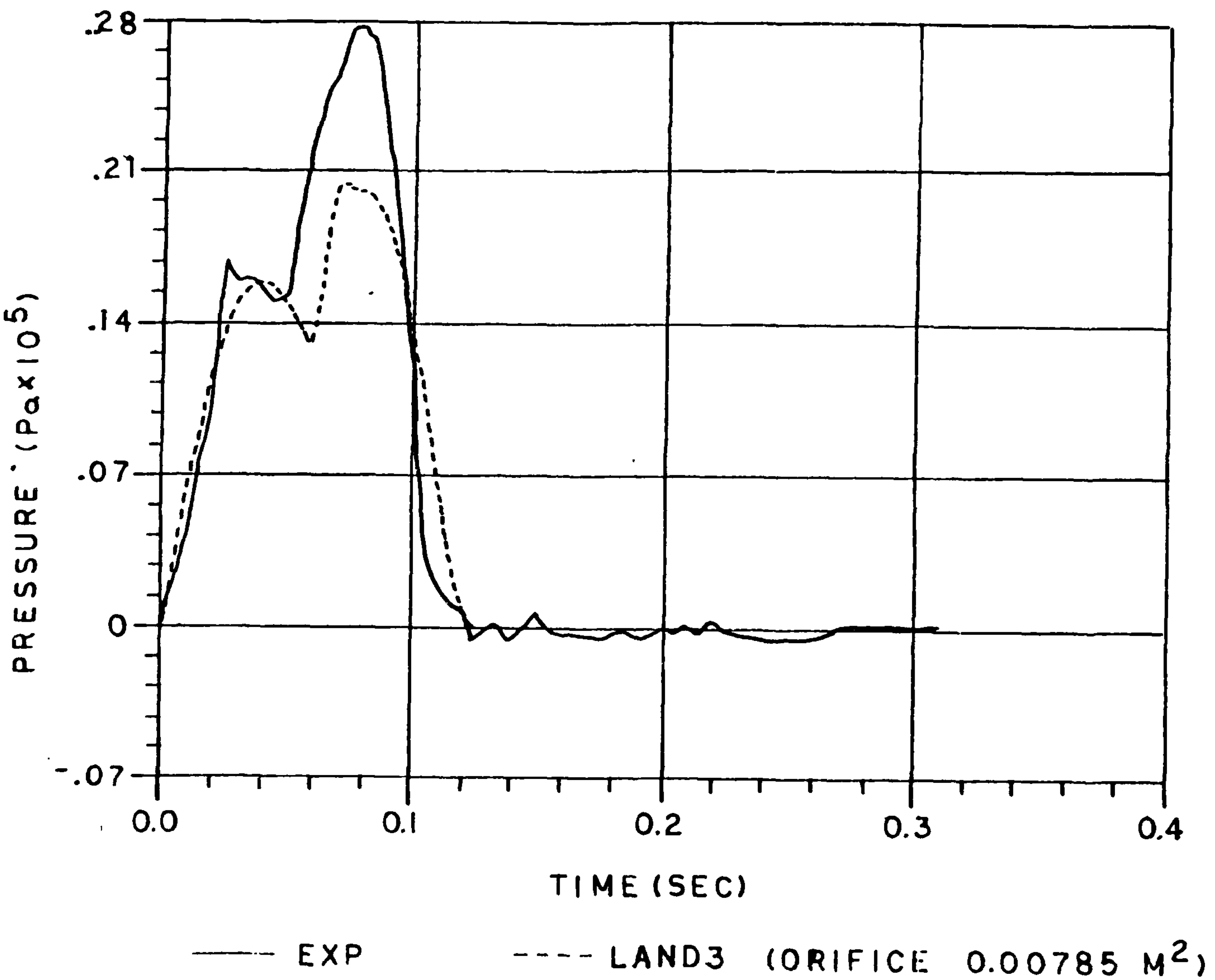

Figure G-23. Drop 5H I left rear airbag pressure.

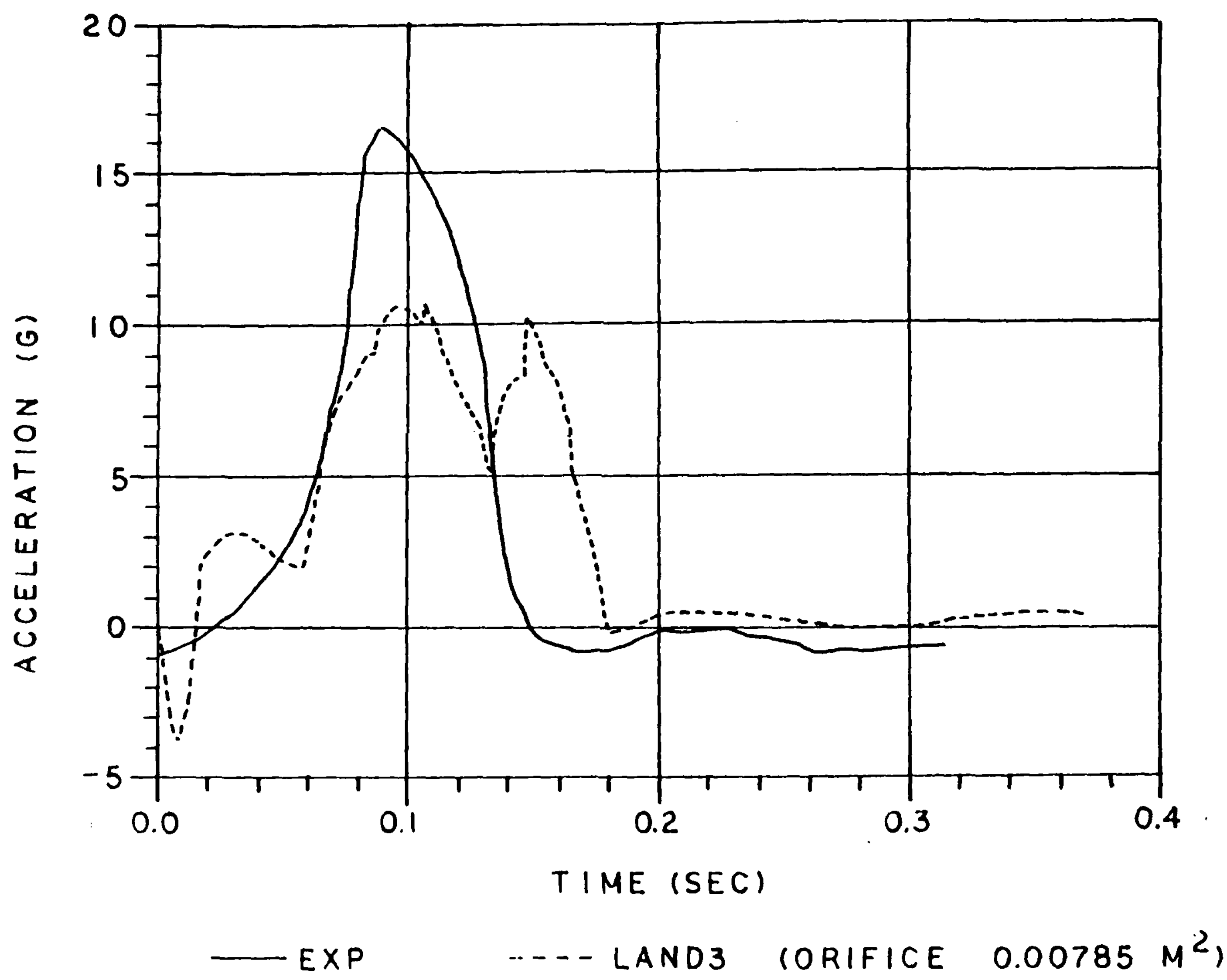

Figure G-24. Drop 5H I top plate acceleration at the c.g..

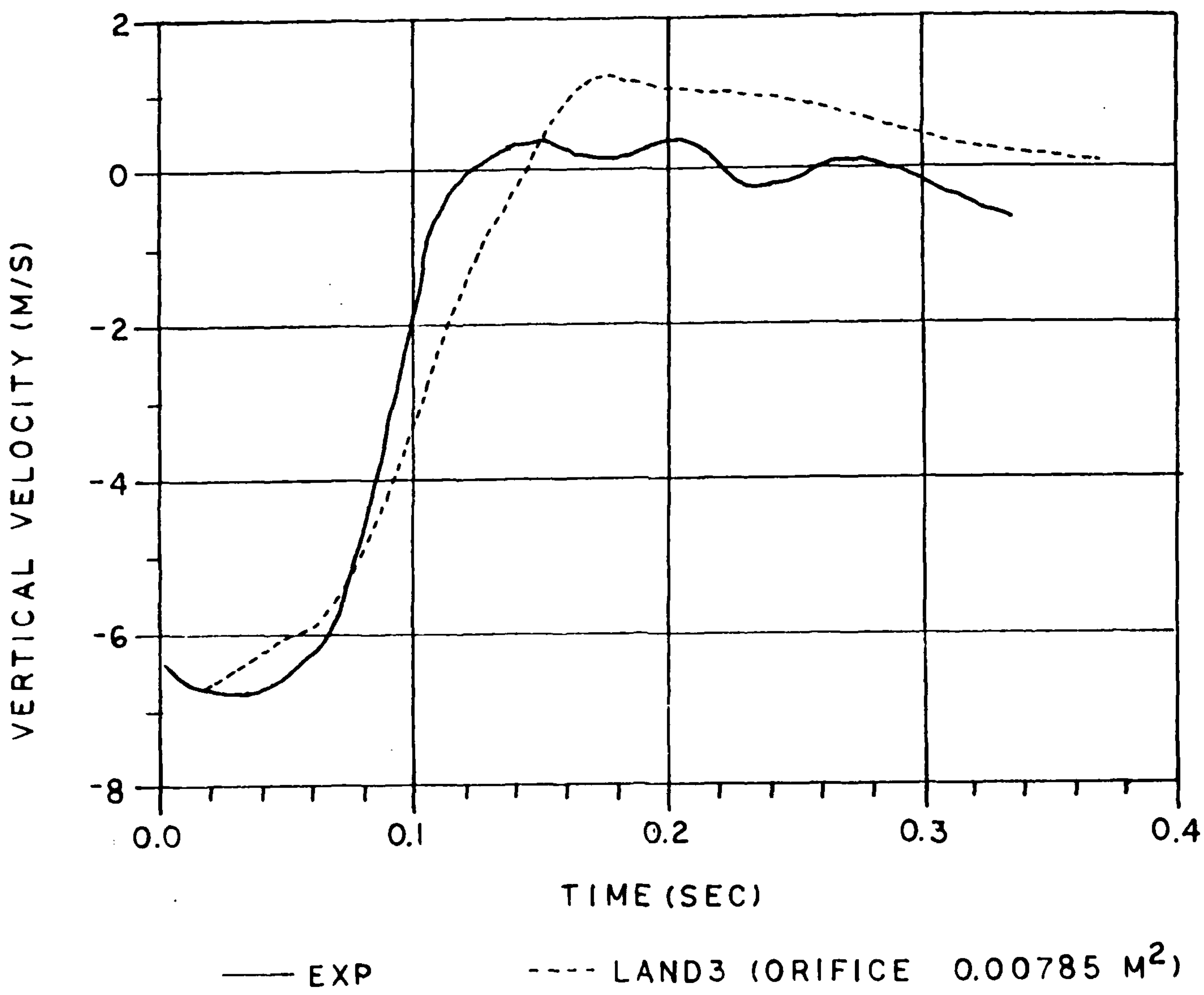

Figure G-25. Drop 5H 1 top plate vertical velocity.

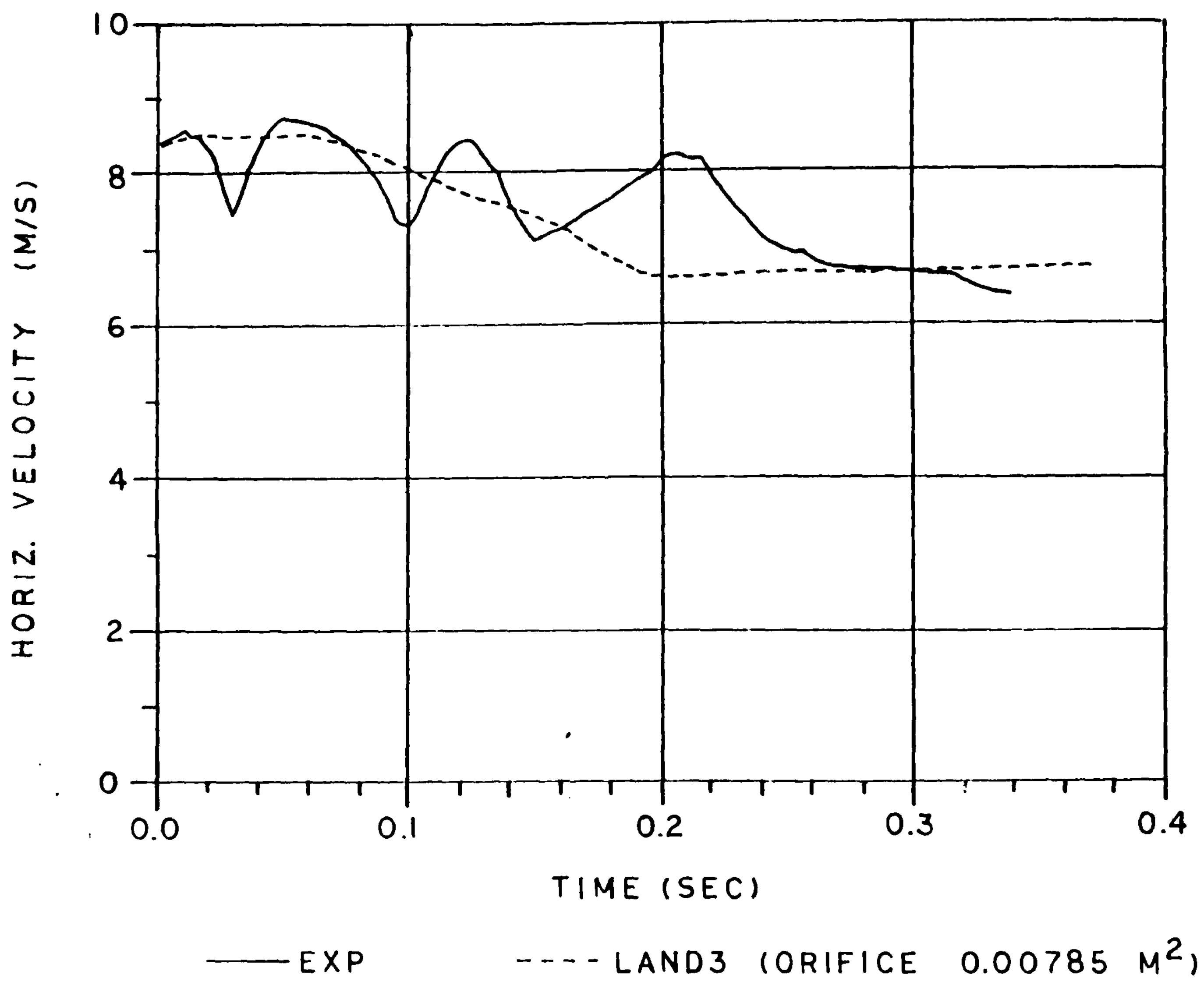

Figure G-26. Drop 5H I top plate horizontal velocity.

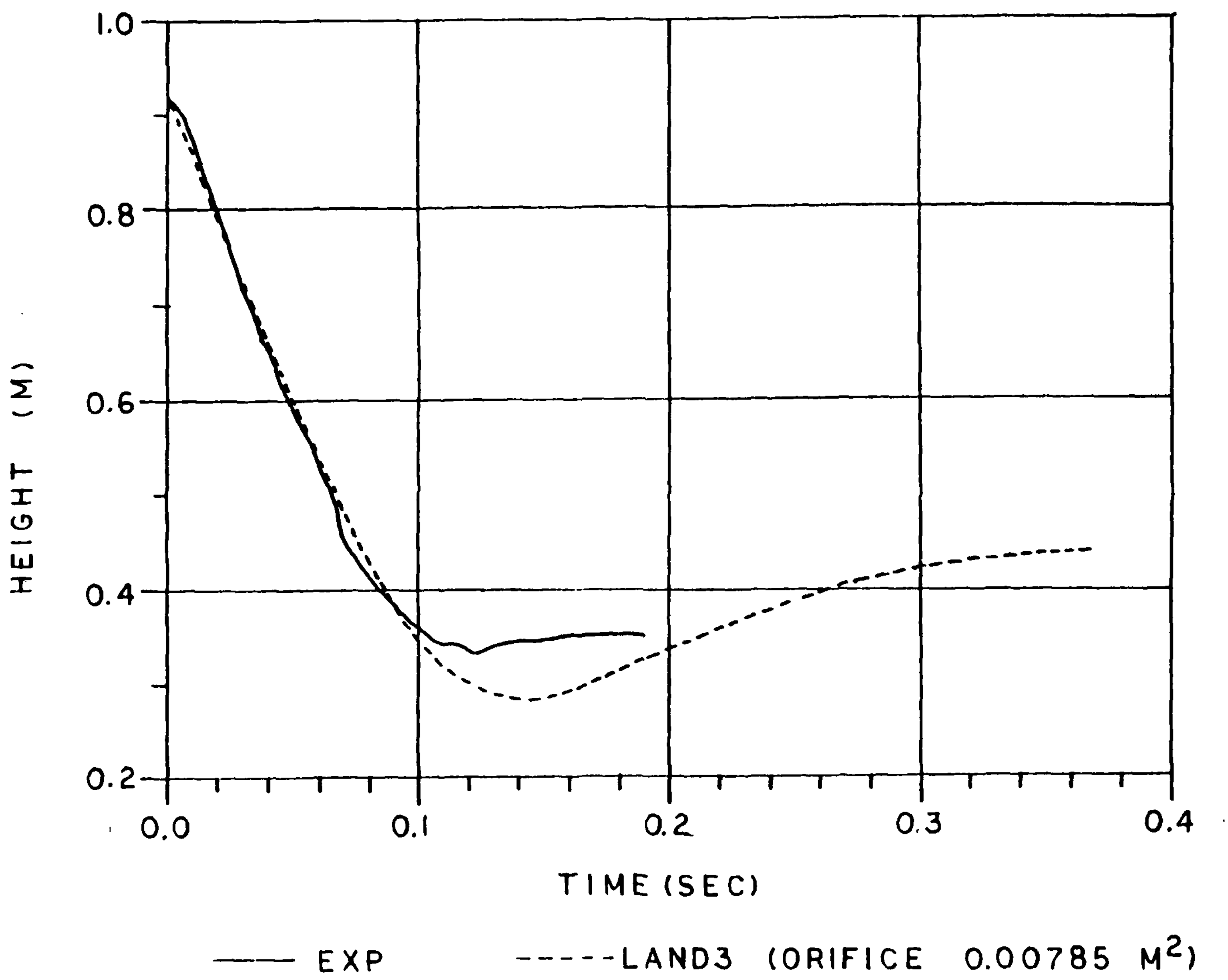

Figure G-27. Drop 5II I top plate height at the c.g..

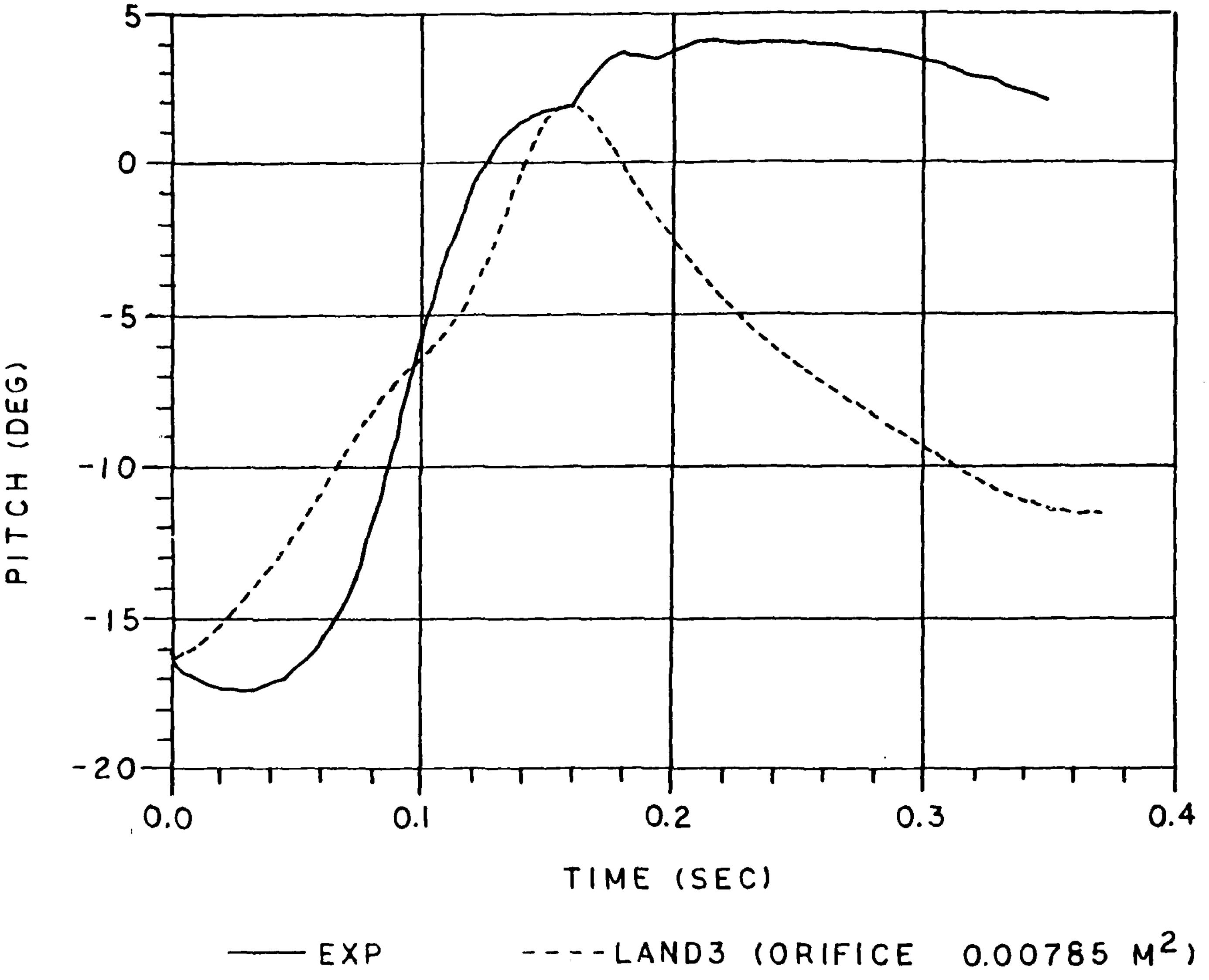

Figure G-28. Drop 5H I top plate pitch.

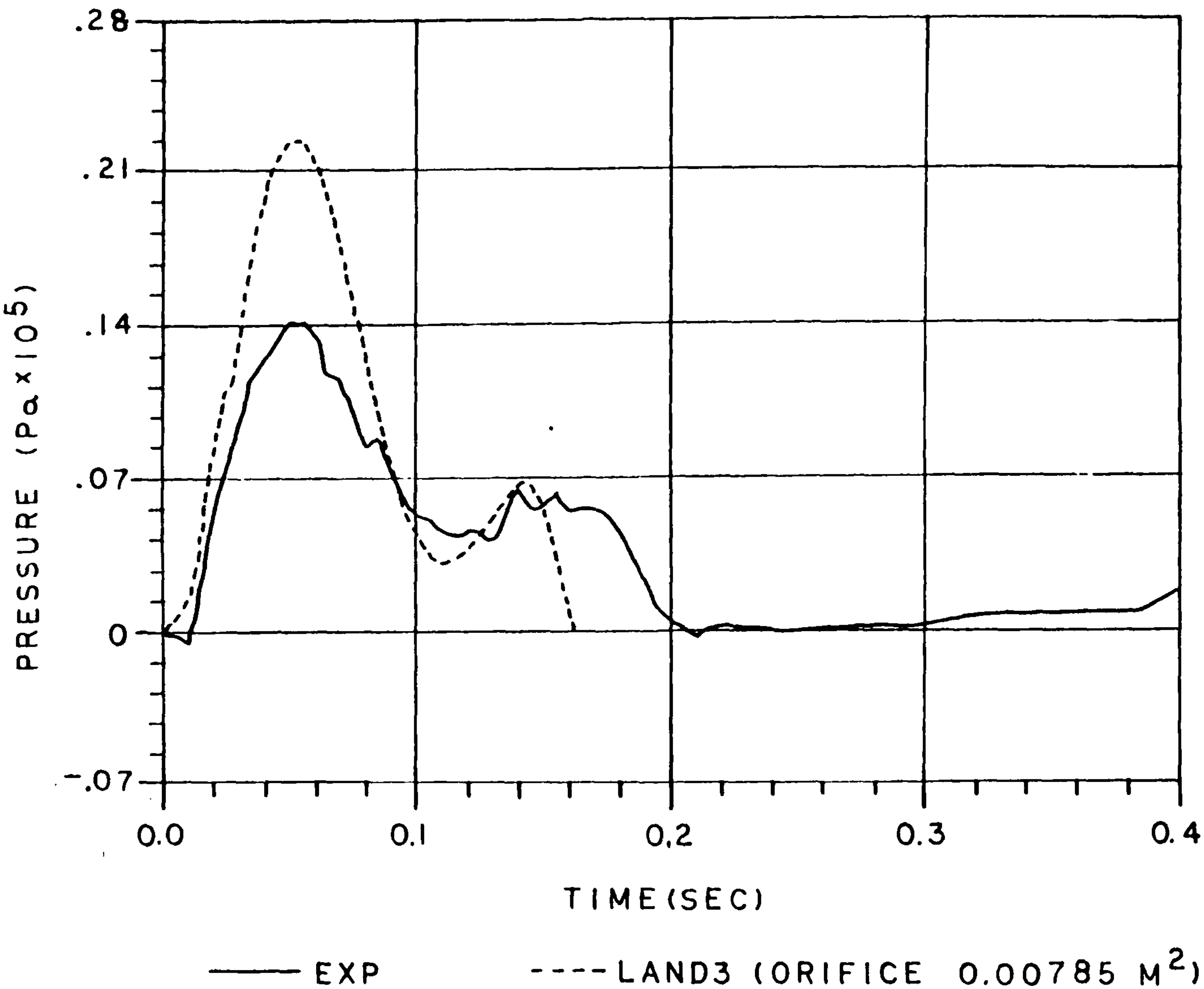

Figure G-29. Drop 6H I right front airbag pressure.

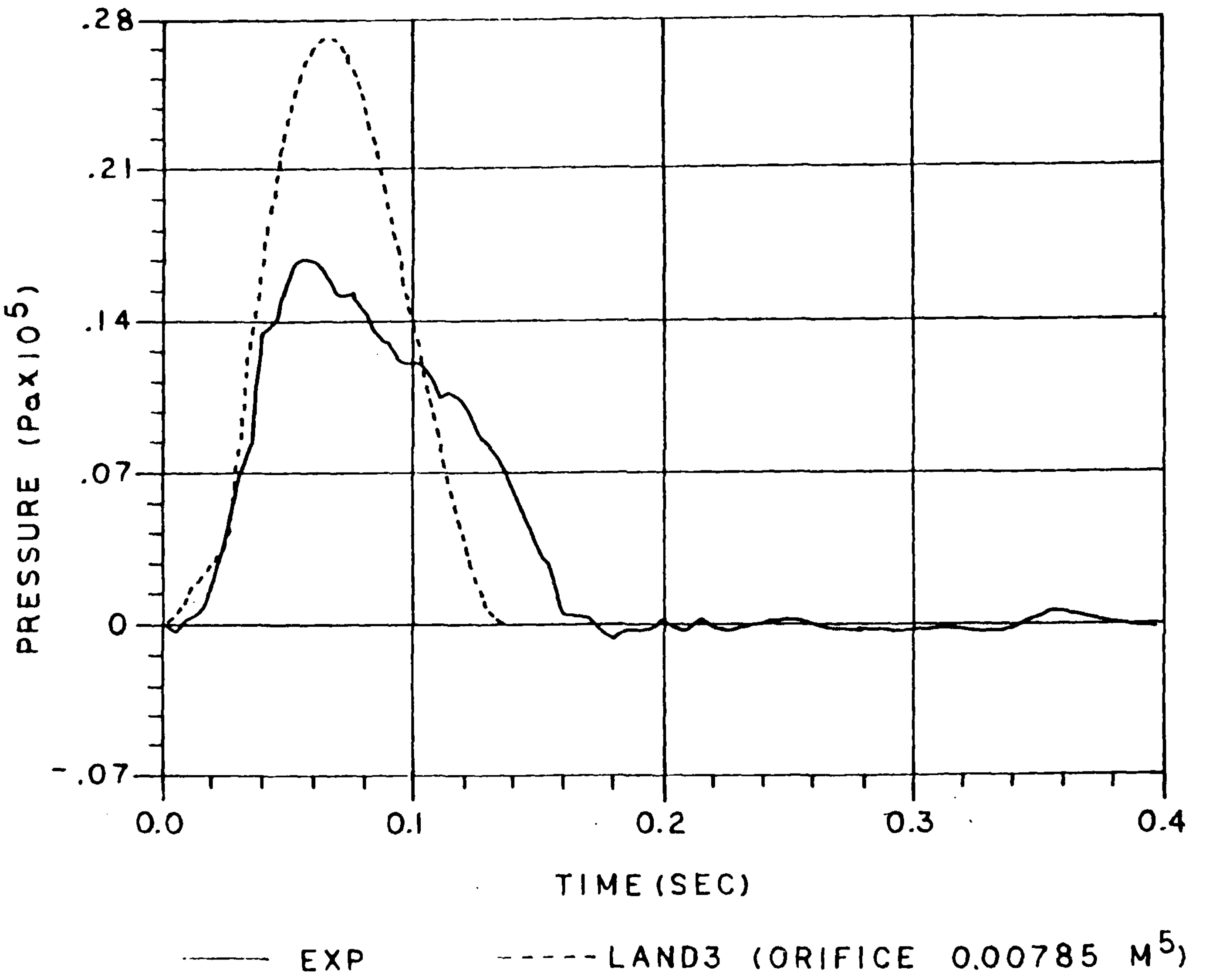

Figure G-30. Drop 6H I left rear airbag pressure.

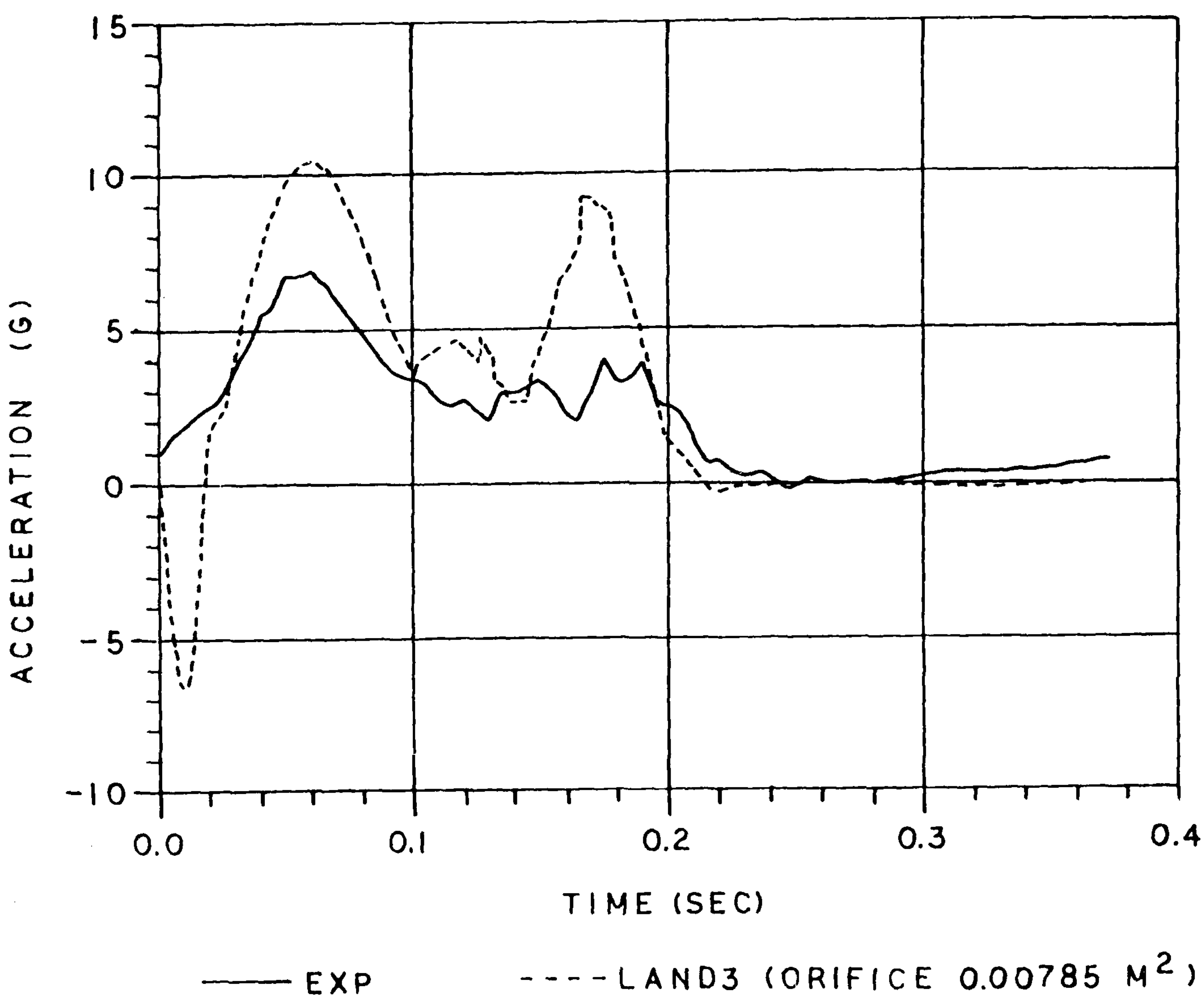

Figure G-31. Drop 6H I top plate acceleration at the c.g..

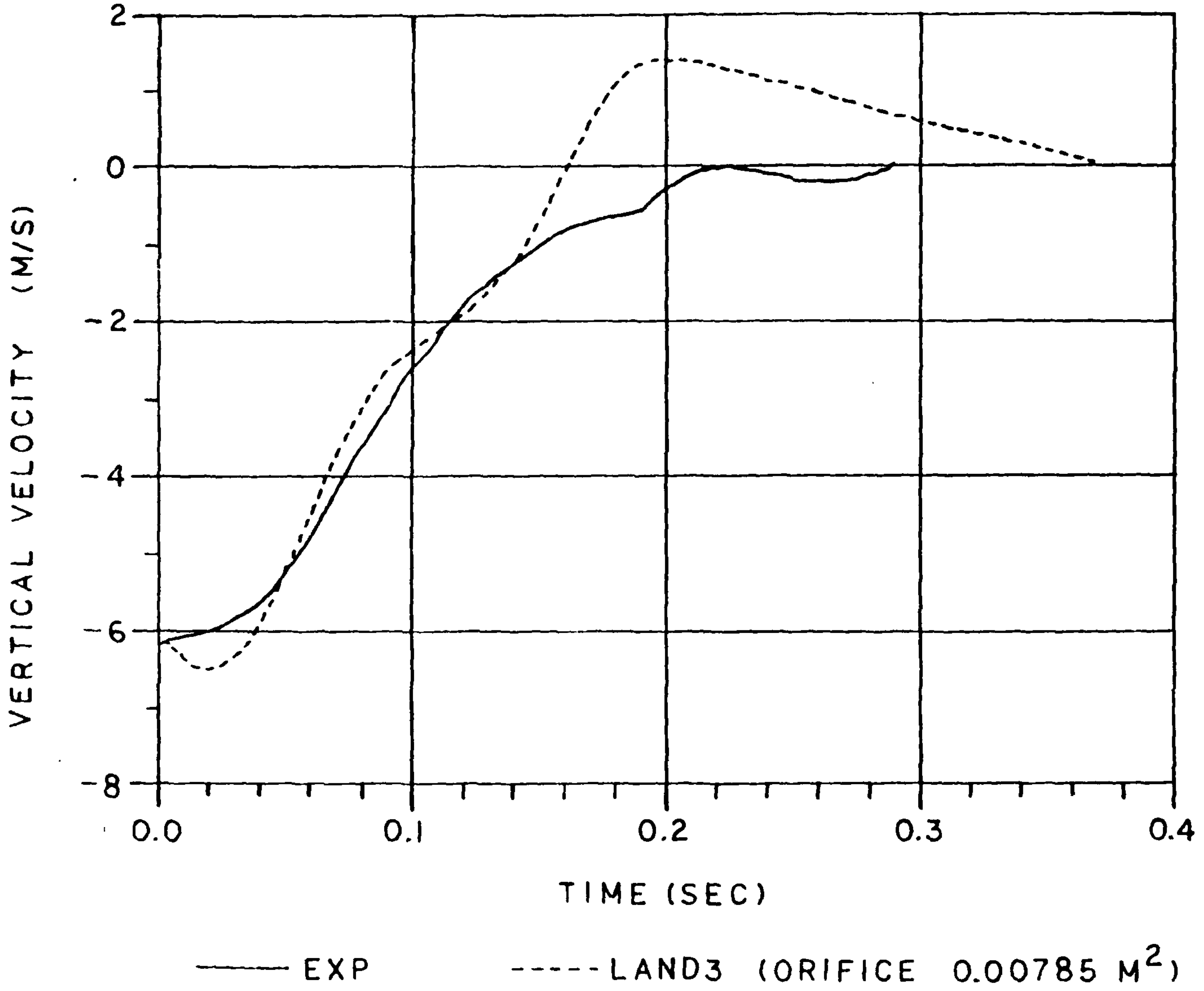

Figure G-32. Drop 6H I top plate vertical velocity.

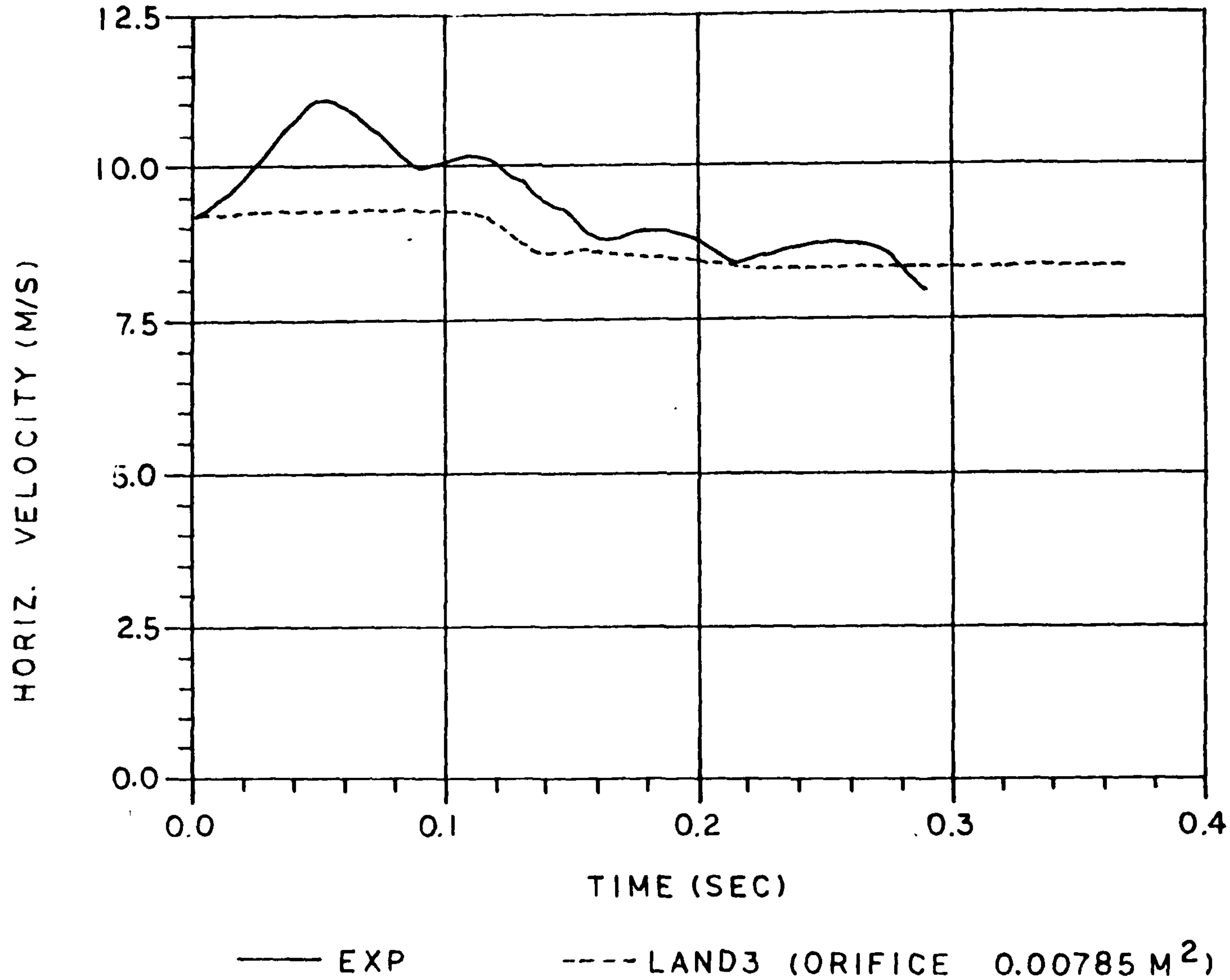

Figure G-33. Drop 6H I top plate horizontal velocity.

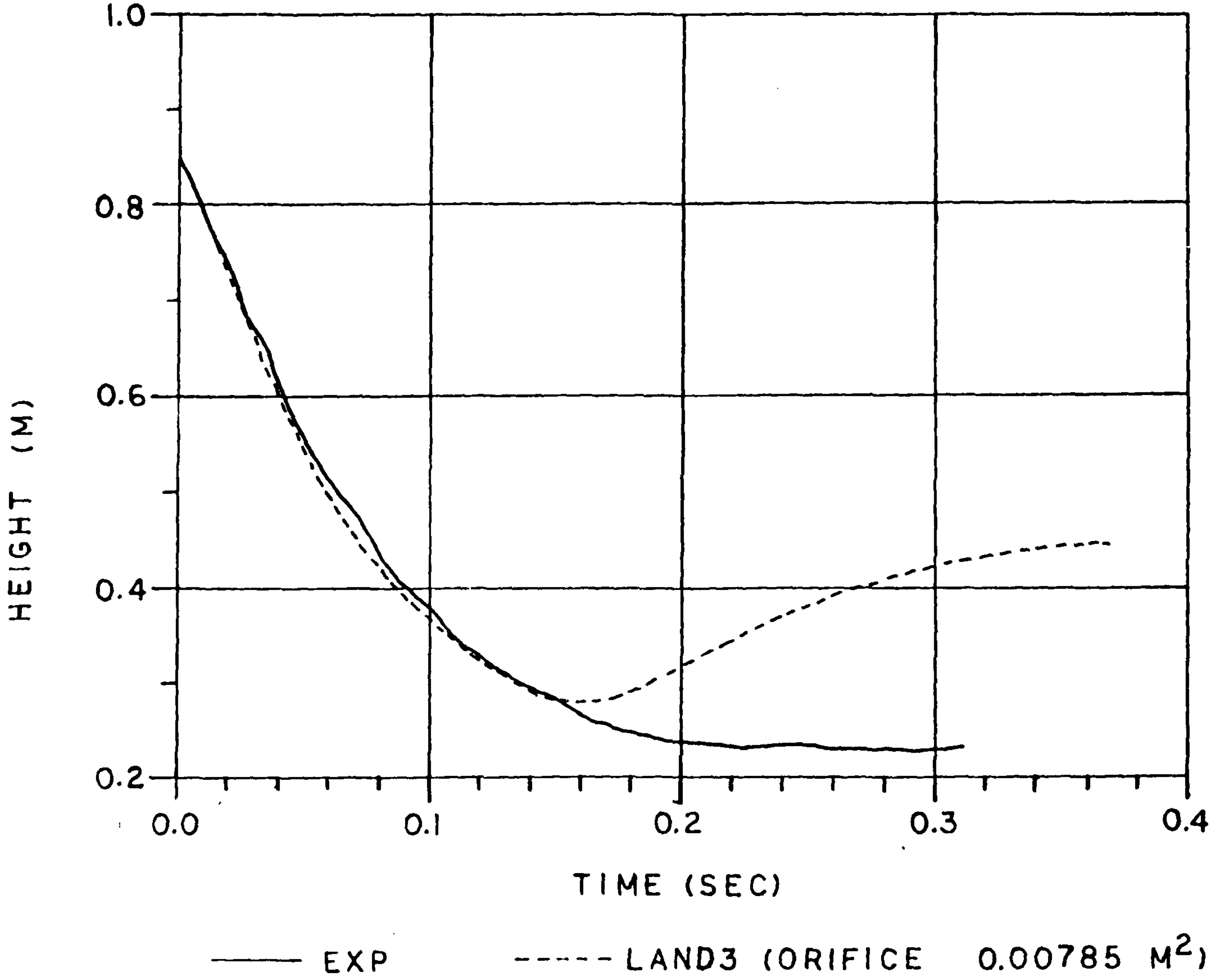

Figure G-34. Drop 6H I top plate height at the c.g..

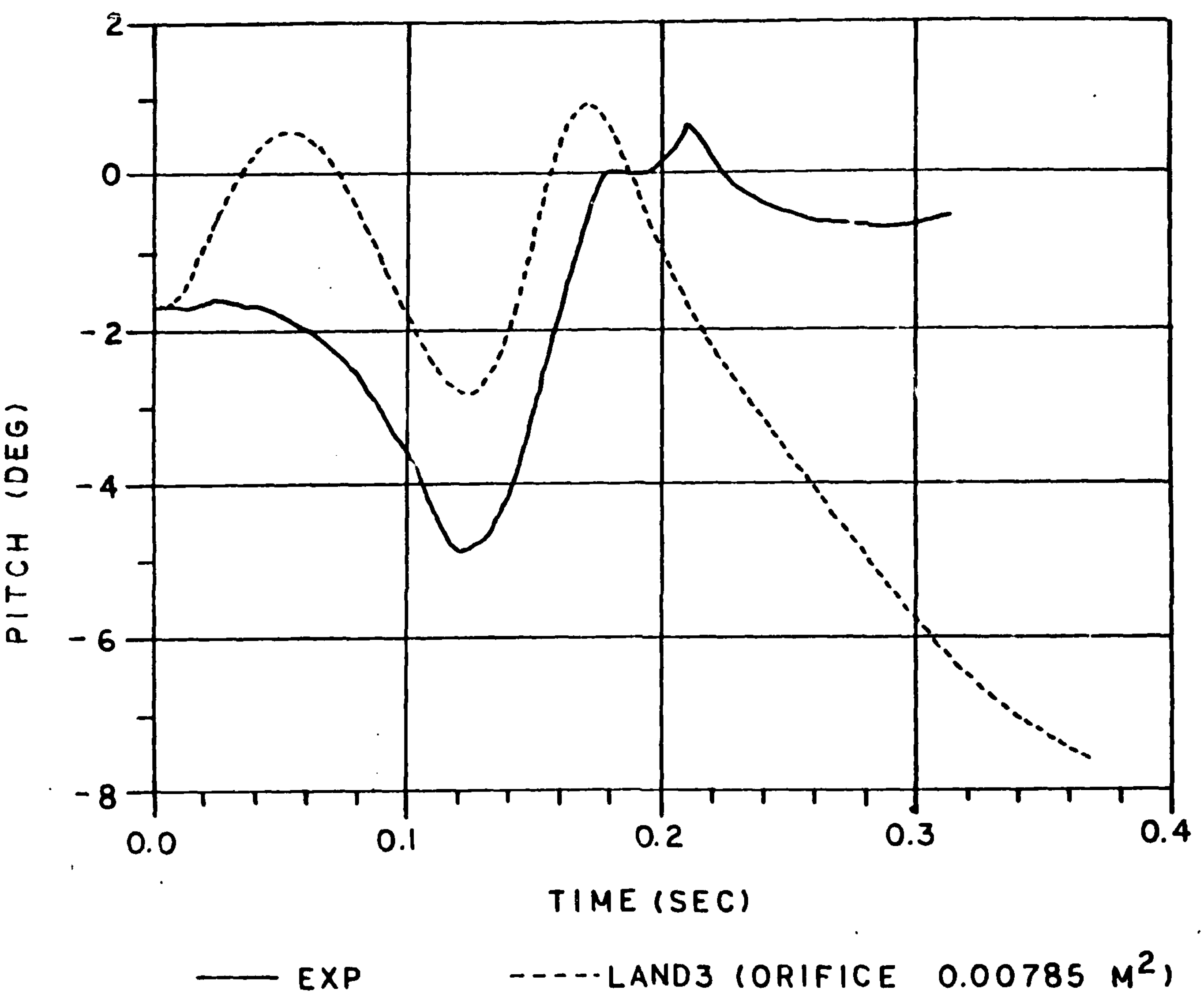

Figure G-35. Drop 611 I top plate pitch.

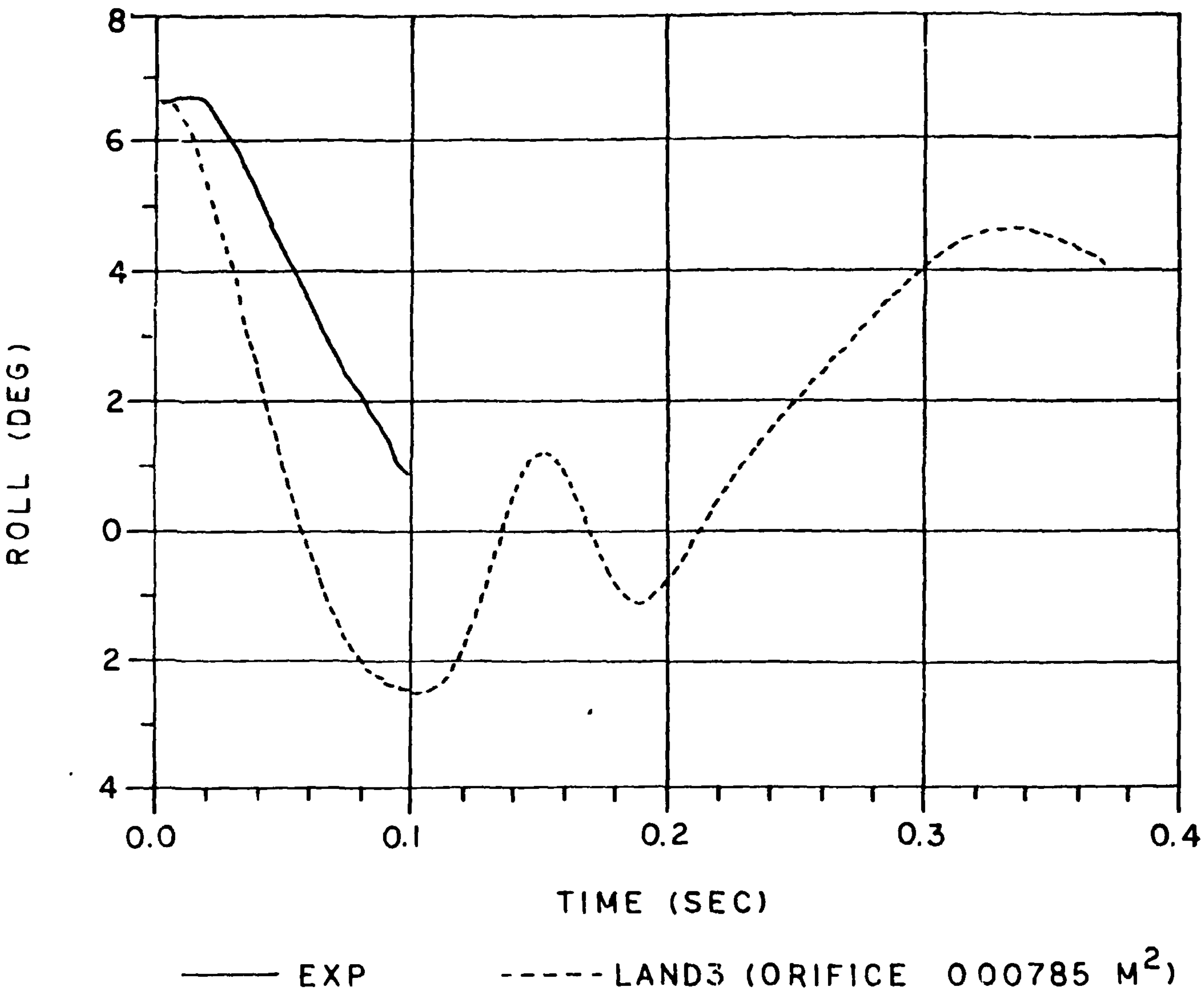

Figure G-36. Drop 6H I top plate roll.